ROLE OF IL-10 AND IL-6 OVEREXPRESSION IN MICROGLIAL CELLS DURING PHYSIOLOGICAL AGING: IMPLICATIONS IN PHAGOCYTOSIS AND NEUROGENESIS

PAULA SÁNCHEZ MOLINA

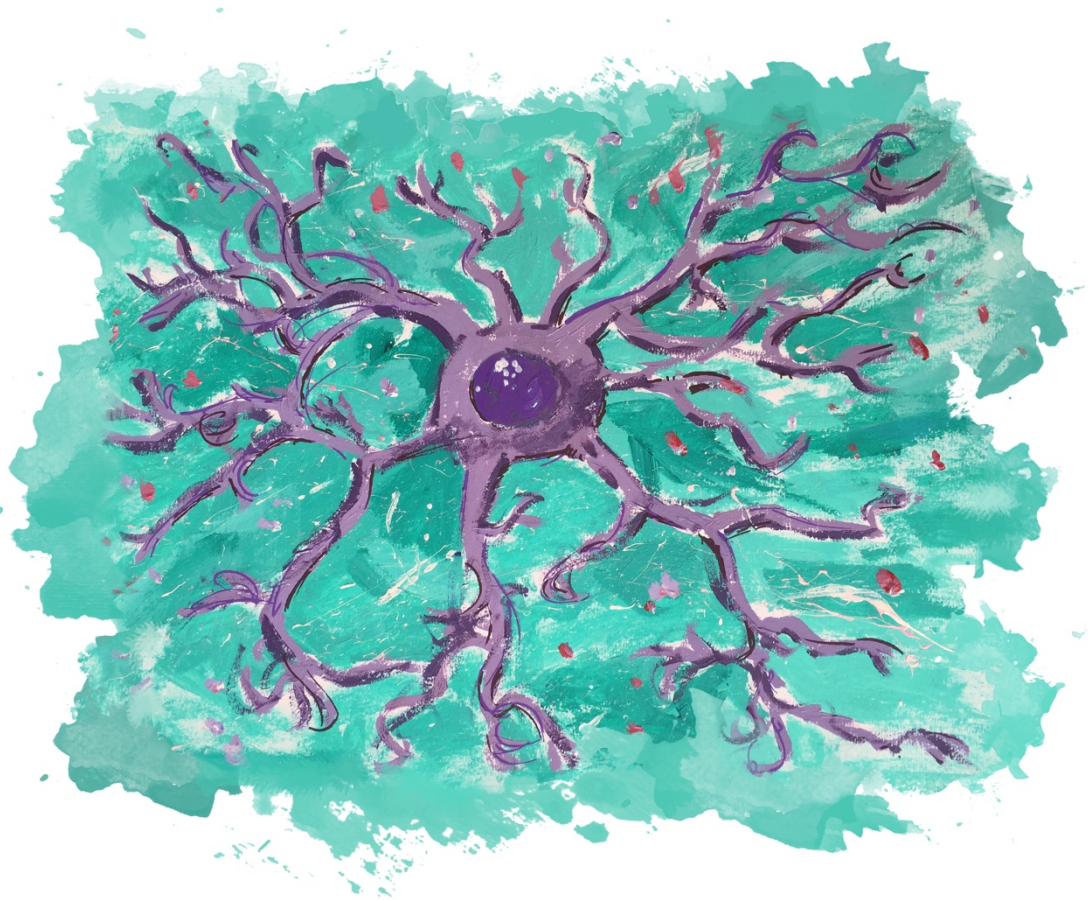PhD Dissertation

Universitat Autònoma
de Barcelona

BARCELONA, 2021

INc
Institut de
Neurociències

UAB

Universitat Autònoma de Barcelona

DEPARTMENT OF CELL BIOLOGY, PHYSIOLOGY AND IMMUNOLOGY

ROLE OF IL-10 AND IL-6 OVEREXPRESSION IN MICROGLIAL CELLS DURING PHYSIOLOGICAL AGING: IMPLICATIONS IN PHAGOCYTOSIS AND NEUROGENESIS

A dissertation to obtain the degree of Doctor in Neuroscience submitted by

PAULA SÁNCHEZ MOLINA

This work has been done at the Medical Histology Unit
of the Faculty of Medicine at the Autonomous University of Barcelona
under the supervision of Dr. Beatriz Almolda.

_____   _____
Dr. Beatriz Almolda   Prof. Bernardo Castellano
Thesis Director   *Thesis Tutor*

_____
Paula Sánchez Molina
PhD Student

BARCELONA, SEPTEMBER 2021

TABLE OF CONTENTS

1. ABBREVIATIONS

Aβ	Amyloid-β
ATP	Adenosine Triphosphate
BDNF	Brain-derived Neurotrophic Factor
CNS	Central Nervous System
DAM	Damage-Associated Microglia
DAMPs	Danger-Associated Molecular Patterns
DG	Dentate Gyrus
EMPs	Erythro-Myeloid Progenitors
GABA	Gamma-Aminobutyric Acid
GAL-3	Galectin-3
GDNF	Glial cell line-Derived Neurotrophic Factor
GFAP	Glial Fibrillary Acidic Protein
GM	Grey Matter
GM-CSF	Granulocyte-Macrophage Colony-Stimulating Factor
IFNγ	Interferon-γ
IGF-1	Insulin-like Growth Factor-1
IL	Interleukin
IL-10R	IL-10 Receptor
IL-6R	IL-6 Receptor
LPS	Lipopolysaccharide
LTP	Long-Term Potentiation
MBP	Myelin Basic Protein
MHC-II	Major Histocompatibility Complex-II
MRI	Magnetic Resonance Imaging
NGF	Nerve Growth Factor
NMDA	N-Methyl-D-Aspartate
NO	Nitric Oxide
NT-3	Neurotrophin-3
NPCs	Neural Stem Cells
OPCs	Oligodendrocyte Precursor Cells
PAM	Proliferating-Associated Microglia
PAMPs	Pathogen-Associated Molecular Patterns
PRRs	Pattern-Recognition Receptors
PS	Phosphatidylserine
ROS	Reactive Oxygen Species
sIL-6R	Soluble IL-6 Receptor
TGFβ	Transforming Growth Factor-β
TLRs	Toll-Like Receptors

TNFα	Tumor Necrosis Factor-α
TREM-2	Triggering Receptor Expressed on Myeloid cells 2
UTP	Uridine-5'-Triphosphate
WAM	White matter-Associated Microglia
WM	White Matter
WT	Wild-Type

2. ABSTRACT

Aging is a time-dependent physiological process that affects to all living organisms. In the central nervous system (CNS) this process is characterized by neuroinflammation and cognitive decline, being the main risk factor for developing neurodegenerative diseases. In this context, microglial cells play a fundamental role as the intrinsic immune cells of the CNS parenchyma. Microglia are continuously surveilling their surrounded microenvironment and they maintain the brain homeostasis regulating physiological and pathological processes. During aging, these cells undergo morphological and phenotypical changes probably due to the environmental modifications produced at this life stage. However, few is known about the influence of these microglial changes on age-related processes like increased load of cellular debris, decreased neurogenesis, synaptic impairments or myelin alterations. If cellular intrinsic factors govern the microglial alterations observed in the aged brain or age-associated environmental factors lead to changes in microglial properties, it is an issue that need to be deeply explored. For this purpose, we investigated the influence of a CNS microenvironment modulated by the chronic overexpression of either IL-10 or IL-6, two different cytokines with traditionally opposite properties that highly regulate microglia cells, on the microglial population during physiological aging. Adult and aged mice with astrocyte-targeted production of IL-10 or IL-6 and their corresponding wild-type (WT) littermates were used in this study. By different behavioral, biochemical and histological approaches, we evaluated physical and cognitive status of mice as well as changes in microglial population and their implication in processes altered during aging like phagocytosis and neurogenesis. No differences in animal survival were observed by chronic IL-10 or IL-6 overproduction. However, animals overexpressing IL-6 developed motor problems with aging. Our results showed that both cytokines induced an increased microglial activation and density along different brain areas of grey matter (GM) and white matter (WM) in adult mice. These changes were also observed by the effect of normal aging mainly in WM areas, suggesting an age-derived myelin damage. Specifically, aged WT mice showed a particular microglial phagocytic phenotype characterized by receptors involved in myelin recognition without changes in their phagocytic capacity of myelin. In addition, a decreased lipid oxidation restricted to highly myelinated areas was detected during aging. Interestingly, while microglial age-related changes were exacerbated in animals overexpressing IL-6, no modifications in the microglial phenotype or density upon aging were observed in animals overexpressing IL-10. However, neither IL-10 nor IL-6 influenced on the reduction of lipid oxidation detected in WM areas. Together with microglial modifications, we observed a negative impact of both cytokines on the hippocampal neurogenesis since adulthood. Whereas IL-6 effect was probably exerted directly on neural precursor cells inhibiting their survival and differentiation, the absence of IL-10 receptor in these cells implied an indirect effect of IL-10 on the neurogenesis regulation. In this sense, microglia-neuron communication, which is involved in neurogenesis, was similarly impaired by both normal aging and IL-10 overexpression. Hippocampal learning and memory impairments developed

usually at advanced ages, were also observed in adult animals overexpressing IL-10. In conclusion, IL-10 and IL-6 chronic overexpression differently impacts on the age-associated microglial responses, does not interfere with the myelin status and reduces the hippocampal neurogenesis during aging.

3. INTRODUCTION

Neuroinflammation is one of the most common hallmarks in neurological disorders as well as in physiological aging. Whereas infiltration of peripheral immune cells depends on the type of pathology, microglial cells, as the intrinsic immune cells of the central nervous system (CNS) parenchyma, are always the first line of defense in any alteration of the CNS homeostasis. These cells are continuously surveying the neural tissue and exerting important functions in physiology and pathology. Changes in the local microenvironment determine the activation of microglia and lead to a wide variety of cellular phenotypes and specialized functions. Thus, during aging, where changes in the microenvironment are produced, microglial cells acquire a special identity towards a pro-inflammatory status. Remarkably, in addition to the beneficial role that microglia usually exert, exacerbation or prolongation of their pro-inflammatory status can result in tissue damage. For that reason, understanding the involvement of the microenvironment in microglial cells modification during physiological aging, it is an issue of relevance in neuroscience with a special interest in the contextualization of age-related neurodegenerative diseases.

3.1. Microglial cells

Microglia are the principal representant of the immune system within the CNS parenchyma. This cellular population was first described by the Spanish researcher Pío del Río-Hortega in 1919, giving name to the "third element" of the neural centers that Santiago Ramón y Cajal previously mentioned (del Río-Hortega, 1919a). In a series of four papers (Sierra et al., 2016), del Río-Hortega recognized the distinctive mesodermal origin of microglia unlike neuroectodermal (del Río-Hortega, 1919c), their morphological changes in pathological situations (del Río-Hortega, 1919b), and their phagocytic capacity (del Río-Hortega, 1919d). However, it was not until 1990 when publications about microglia grew at an exponential rate in Pubmed. One century after their discovery, around 4,000 publications per year about microglia are generated.

3.1.1. Origin and heterogeneity

As already proposed del Río-Hortega, microglia present a different origin from the rest of the nervous system cells. However, the exact source of microglial population has been very difficult to clarify, and to date, it continues being studied. Initially, microglial ontogeny was believed to arise mostly from bone marrow-derived hematopoietic stem cells due to their myeloid lineage (Chan et al., 2007). It was in 2010 when microglial origin was attributed to myeloid precursors derived from the yolk sac, which invade the brain parenchyma through blood vessels between embryonic day 8.5 and 9.5 (Ginhoux et al., 2010). Some years later, it was demonstrated that most tissue-resident macrophages arise from erythro-myeloid progenitors (EMPs) developed in the yolk sac (Hoeffel et al., 2015; Gomez Perdiguero et al., 2015). Interestingly, whereas microglia

are the unique tissue-resident macrophage that derive from early c-Myb⁻ EMPs, the rest of tissue-resident macrophages are derived from late c-Myb⁺ EMPs that first colonize the fetal liver, giving rise to fetal monocytes, and later invade the different tissues (Hoeffel et al., 2015). Like other tissue-resident macrophages, the microglial pool is self-renewed locally by proliferation without infiltration of circulating bone marrow-derived precursors or monocytes in the steady state and even after microglial ablation or some CNS insults (Ajami et al., 2007; Hashimoto et al., 2013; Bruttger et al., 2015; Askew et al., 2017). Nevertheless, the microglial proliferation rate in homeostasis is a controversial issue. It has been assumed that microglia are long-lived cells with a low proliferation rate that usually takes place during inflammatory conditions, indicating that a stable microglial population is maintained throughout life (Lawson et al., 1992). However, other studies have updated this issue showing that microglia are renewed several times by cell proliferation coupled to apoptosis, resulting in a stable but renewed microglial density over a lifetime (Askew et al., 2017; Réu et al., 2017).

The yolk sac-derived origin of microglia confers them a special identity. Thus, engrafted hematopoietic stem cell-derived macrophages in the brain parenchyma acquire a microglia-like signature, but differs from that of microglia in some genes such as *Sall1* and *Gpr56* (Bennet et al., 2018; Cronk et al., 2018; Lund et al., 2018; Shemer et al., 2018). However, microglial identity is not only stablished by their ontogeny, the CNS microenvironment is also an essential factor to confer and maintain the unique microglial signature (Gosselin et al., 2014; Lavin et al., 2014; Bennet et al., 2020). This is demonstrated by studies reporting that cultured microglia undergo dramatic transcriptional changes (Bohlen et al., 2017; Gosselin et al., 2017), which are reverted when cells are transplanted in the brain parenchyma (Bennet et al., 2018).

Moreover, CNS cues differ between cerebral regions and life stages, giving rise to different microglial phenotypes across brain areas and throughout life. The most evident region-specific microglial phenotypes are observed when compared white matter (WM) and grey matter (GM) areas, although microglial properties also differ between determined areas such as basal ganglia, hippocampus, cerebellum and subventricular zone (Lawson et al., 1990; de Haas et al., 2008; Olah et al., 2011; Böttcher et al., 2019; Tan et al., 2020). Microglial population heterogeneity is also observed throughout the lifespan, being the most diverse during developmental stages (Olah et al., 2011; Hammond et al., 2019; Masuda et al., 2019). Interestingly, microglial population in the postnatal brain shares characteristics with that of the aged brain and during disease (Li et al., 2019).

3.1.2. Properties and functions

Microglial cells present specific cellular properties that given them the ability to play key roles in physiological and pathological processes of the CNS (Casano and Peri, 2015; Sierra et al., 2019). In **Figure 1** are listed the main properties and functions attributed nowadays to microglia.
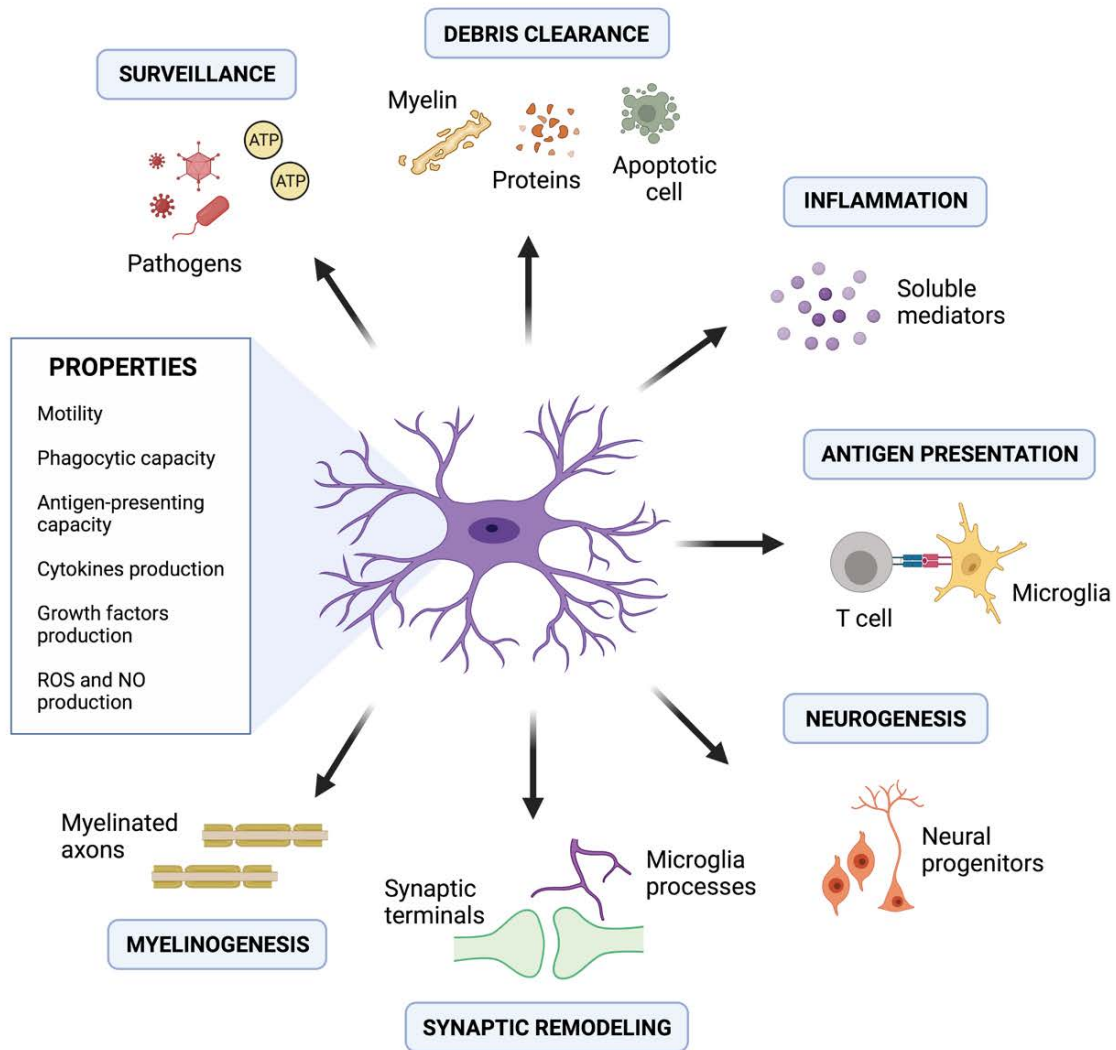
Figure 1. Microglial properties and functions. Arrows indicate the main cellular processes in which microglial cells are involved. Abbreviations: ROS (reactive oxygen species), NO (nitric oxide). *Created by Biorender.com.*

The high motility of their processes and their wide repertoire of proteins for sensing endogenous and exogenous ligands allow microglia to be continuously surveying the brain parenchyma and detect tissue disturbances (Nimmerjahn et al., 2005; Hickman et al., 2013). Thus, after recognition of infection, brain injury or neurodegeneration, microglia play a critical role modulating neuroinflammation thanks to specific cellular properties like their phagocytic capacity and the production of different soluble mediators. Clearance of cellular debris is one of the principal functions that microglia exert after an insult. They can phagocyte exogenous pathogens like viruses and bacteria, disease-associated protein aggregates, myelin debris, and apoptotic cells (Neumann et al., 2009). In addition to phagocyte, microglia can secrete anti-inflammatory cytokines and growth factors to repair the neuronal damage (Streit et al., 2005; Neumann et al., 2009; Duarte Azevedo et al, 2020). Remarkably, when neurons are endangered, microglia are able to detach pre- and post-synaptic terminals to promote neuroprotection in a mechanism

termed "synaptic stripping" (Blinzinger and Kreutzberg, 1968; Trapp et al., 2007). Moreover, after pathogen invasion, microglia usually release toxic factors and pro-inflammatory cytokines to end with the infection. Although microglia represent the cells of the innate immune system in the CNS, they also participate in adaptive immune responses when is required. Thus, microglial cells can communicate with lymphocytes acting like antigen-presenting cells due to their ability to express MHC-II and costimulatory molecules (Almolda et al., 2011). However, it is important to highlight that although microglia play an important role in most neurological diseases, it is not possible to generalize the effect of these cells to all pathological situations but rather they respond in a very precise manner depending on the type, origin and duration of the insult.

In addition to pathology, microglia are equally necessary under physiological conditions where they intervene in several processes, such as vasculogenesis, synaptic remodeling, myelinogenesis and neurogenesis, to maintain the CNS homeostasis. Along life, microglial processes directly monitor synapses participating in their remodeling by phagocytosis of synaptic elements (Wake et al 2009; Tremblay et al., 2010; Wu et al, 2015). Specifically, microglia engulf presynaptic structures instead of entire synapses, which is termed "trogocytosis" (Weinhard et al., 2018). In addition, microglial release of neurotrophic factors like BDNF is essential for a correct synaptic plasticity (Parkhurst et al., 2013). Due to the participation of microglia in synapses, the term "quad-partite" synapse has been introduced (Schafer et al., 2013). Moreover, microglia can modulate neuronal circuits phagocyting stressed-but-viable live neurons, in a mechanism termed "phagoptosis" (Brown and Neher, 2014). Microglia are also implicated in adult neurogenesis through engulfing apoptotic neural precursors cells (Sierra et al., 2010) and modulating the neurogenic niche by the secretion of soluble factors such as growth factors (Lichtenwalner et al., 2001; Scharfman et al., 2005; Battista et al., 2006). Thus, depletion of microglia in the dentate gyrus (DG) inhibits adult neurogenesis due to a reduction of neuroblast survival (Kreisel et al., 2019). On the contrary, microglial secretion of pro-inflammatory cytokines impacts negatively on neurogenesis (Monje et al., 2003; Cacci et al., 2005; Nakanishi et al., 2007; Carpentier and Palmer, 2009). Furthermore, a correct communication between microglia and neurons is necessary for the promotion of newborn cells. Supporting this, it has been shown that modifications of this communication lead to a different microglial activation resulting in adult neurogenesis alterations (Bachstetter et al., 2011; Vukovic et al., 2012; Varnum et al., 2015).

Remarkably, microglial functions acquire a special relevance in critical life stages such as the postnatal development and aging. During brain development, microglia are involved in "synaptic pruning", a process by which inappropriate synaptic connections are eliminated by C1q tagging and subsequent CR3/C3-dependent microglial phagocytosis (Paolicelli et al., 2011; Schafer et al., 2012). At this stage, the number of cortical neural precursor cells is also regulated by microglia limiting the production of new neurons (Cunningham et al., 2013). Similarly, myelinogenesis is modulated by microglial cells at postnatal stages, where a subset of proliferating-associated microglia (PAM) is reported in WM areas (Li et al., 2019). PAM present a specific phagocytic

phenotype involved in the removal of apoptotic oligodendrocytes (Li et al., 2019) and release IGF-1 to promote oligodendrocyte precursor cells (OPCs) survival (Wlodarczyk et al., 2017). During aging, microglial function is especially important to clearance the age-related cellular debris and to modulate the characteristic neurogenesis decline. However, their function is less studied at this life stage and there is controversy whether they exert a detrimental or beneficial role in the aged brain. Microglial features during aging will be described in more detail in the 3.2. section of this Introduction.

3.1.3. Regulation of microglial activation

Microglial activation has been traditionally described as all or nothing, however, these cells are continuously active sensing the surrounded microenvironment with their motile processes to detect possible disturbances in the milieu (Davalos et al., 2005; Nimmerjahn et al., 2005). Part of this active surveillance is based on the communication that microglial cells establish with other cells of the CNS parenchyma, especially with neurons (Biber et al., 2007; Linnartz and Neumann, 2013; Hu et al., 2014).

In homeostatic conditions, neurons present on their surface and/or release "off signals" that interact with microglial receptors (**Figure 2**). These interactions lead to anti-inflammatory signaling pathways that maintain microglia in a homeostatic state (Biber et al., 2007; Linnartz and Neumann, 2013; Hu et al., 2014). The most important ligand-receptor couples that promote inhibitory signaling to microglia are: CX3CL1-CX3CR1 (Cardona et al., 2006), CD200-CD200R (Manich et al., 2018), CD47-SIRPα (Zhang et al., 2015) and CD22-CD45 (Mott et al., 2004). This inhibitory signaling can be also mediated by the neuronal release of trophic factors, such as BDNF, NGF, NT-3 and TGFβ, to the extracellular space (Biber et al., 2007). Neuronal activity is another signal involved in the regulation of microglial function. During development, microglia modulate the neuronal circuits engulfing the less active synapses through the complement cascade (Schafer et al., 2012). Moreover, microglia detect neuronal activity in adulthood showing a prolonged cellular contact through their processes with highly active synapses (Wake et al., 2009) and somas (Li et al., 2013). Neuronal ATP release play an important role in the recognition of this neuronal hyperactivity by microglia (Li et al., 2013; Dissing-Olesen et al., 2014; Eyo et al., 2014; Badimon et al., 2020). Neurotransmitters also provide information about the neuronal activity, being mainly linked to anti-inflammatory signals for microglia (Pocock and Kettenmann, 2007). Although neuron-microglia communication has been quite described in the last years, very few it is known about the dialogue between microglia and other brain resident cells. As an example, the astrocytic release of soluble molecules, such as TGFβ (Schilling et al., 2001; Abutbul et al., 2012), GDNF (Rocha et al., 2012) and GABA (Lee et al., 2011), as well as the nitric oxide (NO) produced by endothelial cells (Katusic and Austin, 2014), are necessary to maintain microglia in a homeostatic state.
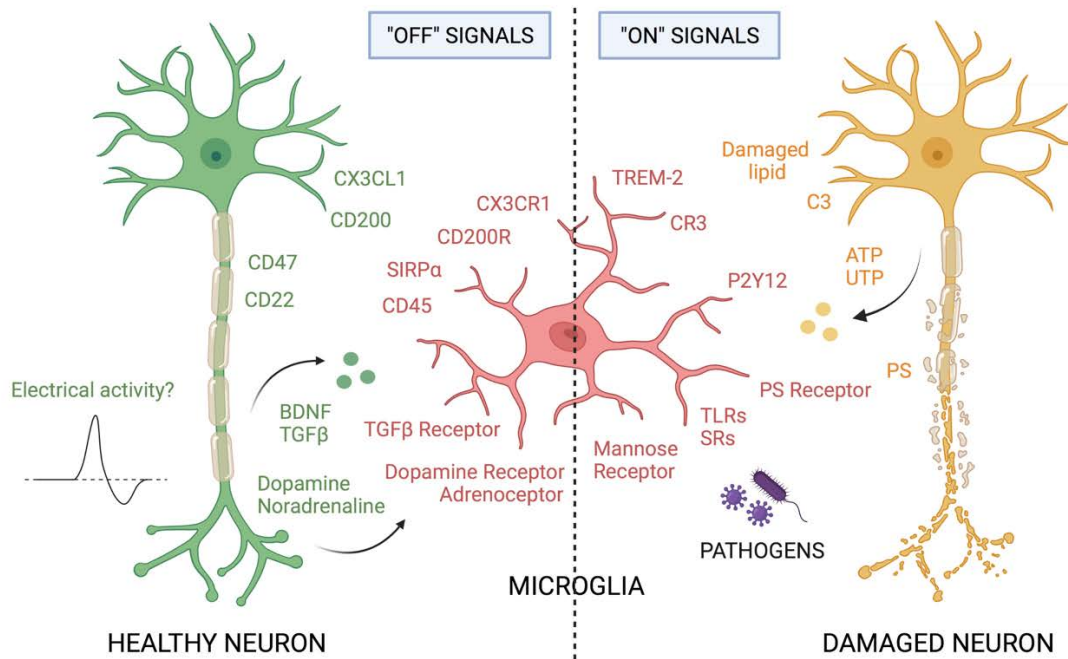
Figure 2. Microglial regulation. Neuronal "off" signals, neuronal "on" signals and microglial receptors are represented in green, yellow and red, respectively. Some molecules present in pathogens also constitute "on" signals. Arrows indicate molecules released by neurons. Abbreviations: BDNF (brain-derived neurotrophic factor), TGFβ (transforming growth factor-β), C3R (complement receptor 3), PS (phosphatidylserine), TLRs (toll-like receptors), SRs (scavenger receptors). *Created by BioRender.com.*

After brain injury or neurodegeneration, the constitutive "off signals" in neurons become altered and microglial responses are triggered. As example, CD47 decrease results in myelin phagocytosis (Zhang et al., 2015). In addition to disturbances of inhibitory signals, damaged neurons can induce the expression of "on signals" leading also to the activation of microglia (**Figure 2**). Thus, microglia recognize "find-me" signals, such as ATP and UTP, through their purinergic receptors and move towards the site of injury (Davalos et al., 2005; Chen et al., 2014; Castellano et al., 2016). Once in the damage site, microglia can recognize endogenous danger-associated molecular patterns (DAMPs) through pattern-recognition receptors (PRRs), such as Toll-like receptors (TLRs), inflammasomes, phosphatidylserine (PS) receptors, complement receptors, scavenger receptors or mannose receptors (Hanisch and Kettenmann, 2007; Palm and Medzhitov, 2009; Lucin and Wyss-Coray, 2009). Moreover, PRRs can also recognize exogenous pathogen-associated molecular patterns (PAMPs), like viruses and bacterial components. Of importance, TREM-2 is one of the main microglial sensors due to the detection of damage-associated lipids, which are present in apoptotic cells, amyloid-beta (Aβ) plaques and myelin debris, among others (Takahashi et al., 2005; Hsieh et al., 2009; Cannon et al., 2012; Wang et al., 2015). Recognition of DAMPs and PAMPs lead to microglial activation that usually is characterized by the release of cytokines and reactive oxygen/nitrogen species, as well as by the expression of molecules involved in antigen presentation. Damage-associated molecules can also act as "eat-me" signals promoting microglial phagocytosis. As example, apoptotic cells

expose PS on their surface leading to microglia engulfment. Moreover, as in the brain development, complement components induce microglial phagocytosis of synapses in pathology (Hong et al., 2016; Shi et al., 2017). Release of cytokines by brain resident or peripheral cells has also an important role regulating microglial responses. Regarding microglial phagocytic activity, pro-inflammatory cytokines, such as TNFα, IFNγ and IL-1β, exert inhibitory effects on fibrillar Aβ phagocytosis (Koenigsknecht-Talboo and Landreth, 2005), whereas IL-6 overexpression increases Aβ plaques clearance (Chakrabarty et al., 2010). On the other hand, TNFα, IFNγ and IL-10 enhance microglial phagocytosis of myelin *in vitro* (Smith, 1999).

In general, the microenvironment composed by cellular and extracellular molecules is critical to the activation and regulation of microglial cells. Thus, disruption of constitutive molecules or the apparition of new ones lead to a wide variety of microglial responses. As is mentioned in 3.1.1. section, microglia diversity is determined by spatial and temporal external cues intervening in their activation. During aging, the milieu is altered and, therefore, microglial cells undergo specific changes.

3.2. Aging

Aging is a time-dependent physiological process that affects to all living organisms. It is characterized by genomic and metabolic changes at the cellular level, such as genomic instability, loss of protein homeostasis, mitochondrial dysfunction, and increase of inflammatory-mediators production, among others (López-Otín et al., 2013) (**Figure 3**).
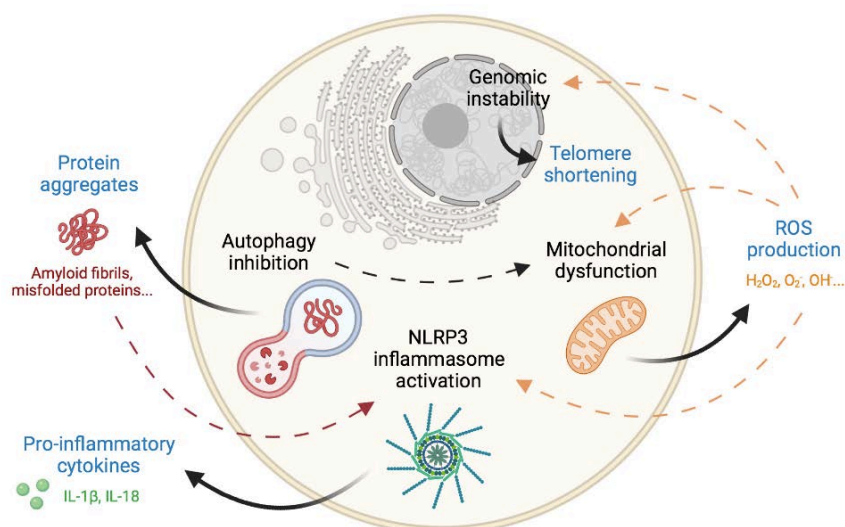
Figure 3. Principal cellular hallmarks of aging. Solid arrows indicate the consequences of altered cellular processes. Dashed arrows indicate the participation of altered cellular processes or their products in the triggering of other cellular alterations. Note that inflammasomes are mainly present in innate immune cells. Abbreviations: ROS (reactive oxygen species). *Created by BioRender.com.*

As consequence, telomere attrition, protein aggregation, increased production of reactive oxygen species (ROS), and a status of mild chronic inflammation denominated "inflammaging" are generated (Harman 1956; Franceschi et al., 2000; Salminen et al., 2012; López-Otín et al., 2013). ROS-production induced by oxidative stress can produce oxidative damage in lipids, proteins and DNA, as well as induce the NLRP3 inflammasome activation (Radak et al., 2011; Salminen et al., 2012). In the CNS, these age-associated cellular changes give place to neuroinflammation and, ultimately, to neurodegeneration and cognitive decline (Halliwell, 1992; Berr et al., 2000; Mrak and Griffin, 2005; Radak et al., 2011).

3.2.1. The aged brain

The brain suffers anatomical modifications during aging. Studies of magnetic resonance imaging (MRI) have revealed a reduction especially in the volume of WM areas (Guttmann et al., 1998; Bartzokis et al., 2003; Hinman and Abraham, 2007), but also in specific brain regions such as the cerebellum, the hippocampus, and the prefrontal cortex (Salat et al., 2004; Raz et al., 2005) during aging.

At the molecular level, the aged brain is characterized by microenvironmental changes produced by an imbalance between pro-inflammatory and anti-inflammatory mediators. The redox status is disturbed presenting reduced levels of endogenous antioxidants (glutathione, glutathione peroxidase, catalase, superoxide dismutase, etc.) and increased levels of ROS (Gupta et al., 1991; Tian et al., 1998; Rodrigues Siqueira et al., 2005; Zhu et al., 2006; Radak et al., 2011). Of special relevance of this imbalance are the cytokines. While pro-inflammatory cytokines, such as IL-6, IL-1β, IFNγ and TNFα, are increased during aging (Ye and Johnson, 1999; Maher et al., 2004; Frank et al., 2006; Campuzano et al., 2009), anti-inflammatory cytokines, such as IL-10 and IL-4, are decreased by age (Ye and Johnson, 2001; Maher et al., 2005; Nolan et al., 2005; Frank et al., 2006). Moreover, the expression of neurotrophic factors is reduced in the aged brain (Lee et al., 2000). The signaling by other anti-inflammatory mediators like corticoids, catecholamines and neurotransmitters may also be impaired during aging. As example, glucocorticoid receptor expression is reduced in the brain of old rats (Bizon et al., 2001; Kasckow et al., 2009; Mizoguchi et al., 2009) and a reduced number of inhibitory GABAergic interneurons has been reported in the hippocampus of aged mice (Gavilán et al., 2007). Thus, downregulation of anti-inflammatory signals together with upregulation of pro-inflammatory signals leads to neuroinflammation in the aged brain. Of note, long-term administration of anti-inflammatory drugs such as aspirin increases longevity in mice (Strong et al., 2008).

Aging-associated neuroinflammation impacts on the different cell populations within the brain. Several studies have shown no differences in the number of neurons during aging, however, these cells undergo a loss of dendrite number and dendritic spines (Pannese, 2011). Moreover, aging drives to a dramatical reduction of neural stem cells in neurogenic niches (Rao et al., 2006; Klempin and Kempermann, 2007). Remarkably, in contrast with the reduced WM volume reported

in aged subjects (Guttmann et al., 1998; Bartzokis et al., 2003; Hinman and Abraham, 2007) as well as the alterations observed in myelin sheets (Safaiyan et al., 2016), the number of oligodendrocytes remains stable along lifetime (Tripathi et al., 2017). On the other hand, astrocytes and microglia increase their cellular density and become activated during aging in a regional-dependent manner. Astrocytes present a more reactive phenotype characterized by increased levels of GFAP, among other molecules, (Wu et al., 2005; Clarke et al., 2018). This increased astrocytic activation has been associated with microenvironmental changes mediated by microglial-secreted molecules (Clarke et al., 2018). As the intrinsic immune cells of the CNS, microglia play an essential role regulating neuroinflammation and can contribute to the cellular changes described in neural populations during aging (Elmore et al., 2018). Moreover, these cells are highly regulated by their surrounding environment, thus, they also undergo changes intimately related to the described pro-inflammatory milieu during aging.

3.2.2. Microglial age-related changes

It is widely known that microglial cells undergo evident changes during normal aging. However, whether these microglial changes are contributors for the inflamed aged brain, or they are consequences of the inflammatory and oxidative microenvironment stablished at advanced ages, it is still an important issue to be determined. Likely, microglia are modified by the specific altered landscape of the aged brain and, at the same time, they participate in this inflammatory status with the production of pro-inflammatory mediators and dysfunction of some relevant functions, such as efficient surveillance and phagocytosis. Thus, a neuroinflammatory loop is created in the CNS during aging. The main phenotypical and functional age-related changes described in microglia are listed in **Figure 4**.

Morphologically, aged microglia present less and shorter processes than adult microglia (Sierra et al., 2007; Damani et al., 2011). In humans, "dystrophic" microglia showing deramification and spheroid formations in their processes has been observed (Streit et al., 2004). Additionally, by live imaging, a decrease of process motility in aged microglia has been demonstrated (Damani et al., 2011). These morphological changes could result in a deficient immunosurveillance of the neural parenchyma during aging. Supporting this notion, in response to laser-induced focal tissue injury, aged microglia failed to increase process motility and presented lower migratory velocity than adult microglia (Damani et al., 2011). Moreover, molecules related to the microglial "sensome" are modified during aging. While receptors that recognize endogenous ligands such as purinergic receptors and Siglech are downregulated, receptors involved in microbe recognition such as TLR2 are upregulated (Letiembre et al., 2007; Hickman et al., 2013). Additionally, microglial communication with neurons is altered during aging. Specifically, neuronal expression of molecules like CD200 (Frank et al., 2006; Lyons et al., 2007; Cox et al., 2012) and CX3CL1 (Lyons et al., 2009; Wynne et al., 2010; Bachstetter et al., 2011; Vukovic et al., 2012) is decreased in aged rodents leading to microglial activation (Jurgens and Johnson, 2012). Thus, infusion of

CX3CL1 in the aged brain attenuates the age-related microglial activation (Lyons et al., 2009; Bachstetter et al., 2011). Although transcriptomical analyses have reported downregulation of homeostatic receptors like CX3CR1 in aged mice (Keren-Shaul et al., 2017; Krasemann et al., 2017), modifications in the expression of microglial molecules involved in neuronal communication are few reported during aging.
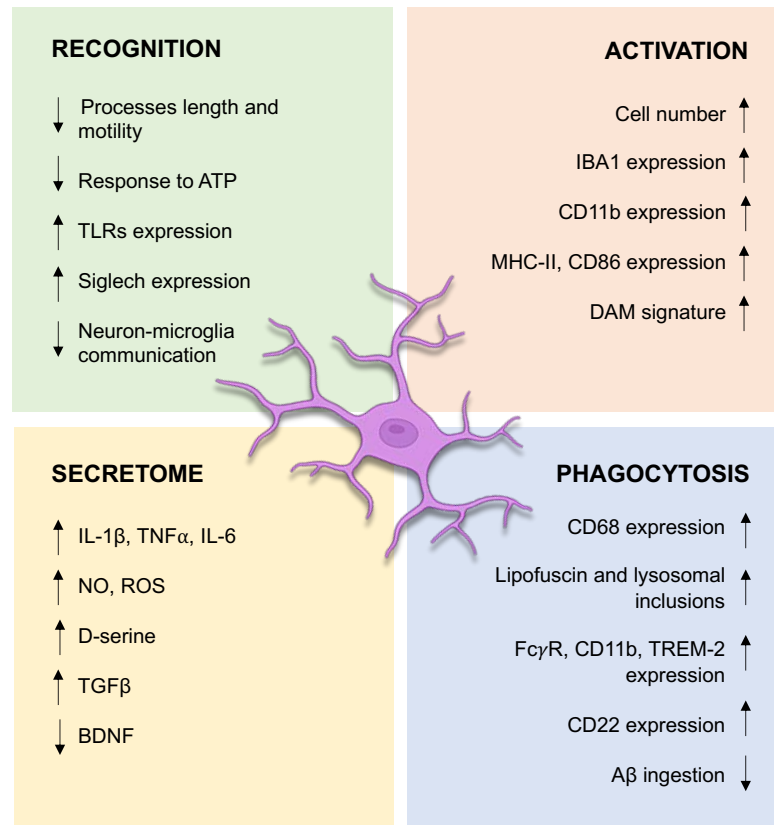
Figure 4. Main age-related phenotypical and functional microglial changes. Abbreviations: TLRs (toll-like receptors), DAM (damage-associated microglia), TNFα (tumor necrosis factor-α), NO (nitric oxide), ROS (reactive oxygen species), TGFβ (transforming growth factor-β), BDNF (brain-derived neurotrophic factor), Aβ (amyloid-β).

Increased microglial cell number, which is associated with activation processes, has been also reported during aging in a local-dependent manner. Importantly, aged microglia are characterized by an activated phenotype with an increased expression of IBA1, MHC-II, CD86, CD11b and TLRs, among others (Perry et al., 1993; Frank et al., 2006; Letiembre et al., 2007; Hwang et al., 2008). Some authors have associated this microglial phenotype with a "primed" state as consequence of different inflammatory stimuli throughout life that will lead to an exaggerated response after a second inflammatory stimuli (Franceschi et al., 2000; Cunningham et al., 2005; Niraula et al., 2017). Supporting this notion, aged microglial response to lipopolysaccharide (LPS) (Xie et al., 2003; Godbout et al., 2005; Sierra et al., 2007) or *Escherichia coli* (Barrientos et al., 2006) stimulation is amplified compared with adult microglial response. Like density, microglial phenotype is altered differently depending on the brain region during aging (Grabert al., 2016).

Indeed, age-related microglial activation is higher in WM areas respect to GM areas, especially in terms of the expression of phagocytosis-associated markers (Sheffield and Berman, 1998; Sloane et al., 1999; Hart et al., 2012; Raj et al., 2017). At the transcriptomic level, a specific damage-associated microglia (DAM) signature has been identified during aging and neurodegeneration, which is characterized by the downregulation of *Cx3cr1*, *Csf1r*, *Tgfbr1*, *Smad3*, *Hexb*, *P2ry12*, *Tmem119* and *Sall1* genes as well as the upregulation of *Apoe*, *Trem2*, *Clec7a*, *Lgals3*, *Itgax*, *Spp1*, *Axl*, and *Ccl2* genes, among others (Keren-Shaul et al., 2017; Krasemann et al., 2017). In this transcriptional profile, most of the characteristic genes are implicated in phagocytosis and lipid metabolism (Keren-Shaul et al., 2017; Deczkowska et al., 2018).

In addition to modifications in phagocytic receptors, aged microglia present lysosomal inclusions that have been associated with an altered phagocytic capacity (Vaughan and Peters, 1974; Tremblay et al., 2012; Safaiyan et al., 2016). Concomitantly, the lysosomal marker CD68 is increased in aged microglia (Perry et al., 1993; Wong et al., 2005). However, the knowledge about microglial functional phagocytosis during aging is poorly studied. Some *ex vivo* studies have reported deficits in Aβ and beads ingestion by aged microglia (Nije et al., 2012; Ritzel et al., 2015). In concordance, Pluvinage et al. recently demonstrated that expression of CD22, a molecule upregulated in aged microglia, inhibits phagocytosis of myelin debris, Aβ oligomers and α-synuclein fibrils (Pluvinage et al., 2019). In this context, it would be of special interest to explore the effect of aging on microglial phagocytic function, especially *in vivo,* due to the accumulation of different substrates to eliminate in the aged brain.

The activated microglial phenotype is accompanied by a differential "secretome" characterized by an increased production of pro-inflammatory cytokines, such as IL-1β, TNFα and IL-6 (Ye and Johnson, 1999; Godbout and Johnson, 2004; Sierra et al., 2007; Nije et al., 2012) as well as the release of NO and ROS (von Bernhardi et al., 2015). D-serine, which potentiates NMDA receptor-dependent excitotoxicity, is also produced by aged microglia (Beltrán-Castillo et al., 2018). A more debatable issue is the secretion of anti-inflammatory cytokines by aged microglia. Specifically, no changes in microglial IL-10 production have been reported upon aging under basal conditions, but an increased production has been showed observed after LPS stimulation (Sierra et al., 2007; Henry et al., 2009). Moreover, the anti-inflammatory TGFβ cytokine is increased by aged microglia (Sierra et al., 2007). On the other hand, BDNF is decreased in microglia during aging (Wu et al., 2020). Of note, microglia from aged brains present less levels of glutathione, an antioxidant molecule, compared with microglia from adult brains (Nije et al., 2012).

3.2.3. Microglial role in age-dependent neurodegeneration

Impaired immunoregulation in the CNS has been pointed as a key factor for developing age-related neurological problems (Corona et al., 2012; Barrientos et al., 2015). As we previously

mentioned, microglial cells exert essential roles modulating processes like neuroinflammation, debris clearance, synaptic plasticity and neurogenesis, which are altered during aging and can contribute to neurodegeneration. Therefore, the changes observed in these cells during aging are proposed to be involved in age-related neurodegeneration (Lucin and Wyss-Coray, 2009; Elmore et al., 2018).

Cellular debris, such as protein aggregates, myelin or apoptotic cells, are accumulated in the aged brain altering the homeostasis of the CNS parenchyma and leading to neuronal toxicity. Microglia, as the main phagocytes of the brain, play a critical role eliminating these products. Thus, alterations in their phagocytic capacity are proposed to lead to an inefficient removal of age-related cellular debris. Specifically, decreased phagocytosis of Aβ peptides has been reported in aged microglia (Nije et al., 2012; Ritzel et al., 2015). Moreover, molecules involved in recognition and degradation of Aβ are decreased in mouse models of Alzheimer's disease during aging (Hickman et al., 2008). Interestingly, restoring microglial phagocytosis in healthy aged mice leads to cognitive function improvement (Pluvinage et al., 2019).

Another feature of brain aging is an altered synaptic plasticity characterized by a reduction in synapses number and a decreased long-term potentiation (LTP), which contributes to age-related learning and memory deficits (Geinisman et al., 1986; Shi et al., 2015). Microglia, through their motile processes, regulate the number of synapses monitoring and engulfing synaptic components (Wake et al., 2009; Tremblay et al., 2010; Ji et al., 2013). However, if the reduced movement of microglial processes or the altered microglial phagocytic capacity reported during aging results in a dysregulation of synaptic activity, it is an unexplored issue. Interestingly, animals deficient of C3 preserve the number of synapses along life (Shi et al., 2015), indicating that microglial complement-mediated phagocytosis is involved in the aberrant loss of synapses during aging as it is observed in mouse models of Alzheimer's disease (Hong et al., 2016; Shi et al., 2017). Secretion of soluble mediators by microglia also interfere in synaptic modulation. Thus, the increased release of D-serine by aged microglia potentiates glutamate-induced excitotoxicity through NMDA receptors and promotes neurodegeneration and cognitive decline (Beltrán-Castillo et al., 2018). Moreover, enhanced IL-1β expression has been associated with the suppression of LTP during aging (Lynch, 1998; Chapman et al., 2010; Frank et al., 2010). Further work to elucidate whether microglial cytokine expression during aging alter synaptic plasticity it would be required.

Importantly, aging is the main factor affecting negatively the process of neurogenesis (Kuhn et al., 1996; Rao et al., 2006; Klempin and Kempermann, 2007). As it has been described in previous sections, microglia play an important role modulating this process throughout life by the secretion of soluble factors and the phagocytosis of apoptotic neural precursors. Since neuroinflammation is detrimental for neurogenesis (Ekdahl et al., 2003; Monje et al., 2003; Carpentier and Palmer, 2009), microglia may affect negatively the formation of newly neurons by the pro-inflammatory

phenotype acquired during aging. However, although microglial phagocytic activity is altered during aging, no changes in the removal of apoptotic neural stem cells have been reported at this life stage (Sierra et al., 2010). On the other hand, the disrupted microglia-neuron dialogue observed during aging has an impact on the process of neurogenesis. Supporting this notion, infusion of CX3CL1 reverses the age-related decrease in neurogenesis (Bachstetter et al., 2011). Moreover, administration of CD200 restores neurogenesis in a mouse model of Alzheimer's disease by suppressing microglial pro-inflammatory activation and increasing phagocytosis (Varnum et al., 2015).

Ultimately, the accumulation of cellular debris, alterations in synaptic plasticity, and the reduction of new hippocampal neurons contribute to the characteristic age-related cognitive decline, pointing aging as the major risk factor for developing neurodegenerative diseases. However, whether microglial changes observed during aging are implicated in the onset or are the response to cognitive decline and disease, it is still a controversial issue. Indeed, as we previously mentioned, microglial cells are highly dependent on their local microenvironment, which is modified during normal aging. Remarkably, among all the molecules that shape the brain milieu, cytokines play a fundamental role in microglial regulation (Colton, 2009; Ramesh et al., 2013).

3.3. Cytokines

Cytokines are an extensive group of small proteins with pleiotropic functions that participate in cellular communication. In a simplistic classification, cytokines are classified in pro- and anti-inflammatory. IL-1β, IL-6, TNFα, IFNγ, IL-12, IL-18 and GM-CSF are related to exert pro-inflammatory actions, whereas IL-4, IL-10, IL-13 and TGFβ are referred to anti-inflammatory properties. Although they are usually produced by immune cells, other cells type from different tissues can also release them. In the CNS, neurons and glial cells are both cytokine producers and receptors (Sei et al., 1995; Vitkovic et al., 2000). Here, one of their main actions is the regulation of neuroinflammatory and neurodegenerative processes (Allan and Rothwell, 2001). During aging, this action is of special interest considering the reported microenvironmental changes towards a pro-inflammatory state in the brain. Several therapeutical approaches have been developed modulating cytokines towards neuroprotective actions. However, *in vivo*, a wide range of effects is observed for these cytokines depending on the route of administration or production, the target cell, the time of exposition and the physiological or pathological condition (Croxford et al., 2001; Ding et al., 2015). Indeed, several studies have described different functions of typical pro-inflammatory cytokines like IL-6, but also of typical anti-inflammatory cytokines like IL-10 in the CNS depending on the experimental design carried out.

3.3.1. Interleukin-10

IL-10 is considered an immunoregulatory cytokine with anti-inflammatory properties in the periphery that appears to resolve inflammatory responses (Moore et al., 2001; Couper et al., 2008). In the CNS, IL-10 is mainly released by astrocytes and microglia after activation (Ledeboer et al., 2002; Park et al., 2007; Lim et al., 2013). This cytokine exerts its effect through the binding to the IL-10 receptor (IL-10R), which triggers signaling cascades mediated by the JAK1/STAT3 pathway (Moore et al., 2001; Hutchins et al., 2013). IL-10R has been reported in astrocytes, microglia, oligodendrocytes, and neurons (Ledeboer et al., 2002; Cannella and Raine, 2004; Zhou et al., 2009; Lim et al., 2013; Norden et al., 2014). However, results from our laboratory show that, in basal conditions, IL-10R is mainly restricted to neurons and astrocytes (Almolda et al., 2015; Recasens et al., 2019). Importantly, several studies have associated IL-10 with a protective role in neurodegenerative diseases such as multiple sclerosis (Bettelli et al., 1998; Cua et al., 2001), Alzheimer's disease (Kiyota et al., 2012) and Parkinson's disease (Arimoto et al., 2007; Schwenkgrub et al., 2013). By contrast, other studies have reported a detrimental role of IL-10 in these pathologies (Canella et al., 1996; Chakrabarty et al., 2015; Guillot-Sestier et al., 2015). Remarkably, the route of IL-10 administration/production is determinant for its actions as it has been shown for experimental autoimmune encepha1lomyelitis (Croxford et al., 2001; Cua et al., 2001), traumatic brain injury (Knoblach and Faden, 1998) or excitotoxic spinal cord injury (Brewer et al., 1999). Interestingly, a recent study has demonstrated that modulation of IL-10R affinity can lead to different actions of the IL-10 signaling (Saxton et al., 2021). In physiological aging, few it is known about the role of this cytokine. Limited literature has reported contradictory results showing a decreased expression of IL-10 (Ye and Johnson, 2001; Frank et al., 2006) or no evidences of changes (Henry et al., 2009) in the aged brain. Regarding the IL-10 production by specific cells, unaltered microglial IL-10 expression has been reported during aging, however, the induction of this cytokine after an inflammatory stimulus such as LPS is increased by aged microglia (Sierra et al., 2007; Henry et al., 2009). Of note, it has been reported that aged astrocytes present a reduced IL-10R expression and responsiveness to IL-10 (Norden et al., 2016).

3.3.2. Interleukin-6

IL-6 is classically considered as a pro-inflammatory cytokine involved in immune activation and sickness behavior, although anti-inflammatory properties have also been attributed to IL-6, pointing it as a pleiotropic cytokine (Schöbitz et al., 1995; Gadient and Otten, 1997; Bluthé et al., 2000; Hunter and Jones, 2015). In the CNS, neurons, glial cells and endothelial cells can produce IL-6 and express the IL-6 receptor (IL-6R) (Schöbitz et al., 1993; Gadient and Otten, 1994; Reyes et al., 1999; Cannella and Raine, 2004; Erta et al., 2012). Interestingly, in addition to the classical IL-6 signaling mediated by the IL-6R located on the cell membrane and coupled to the gp130 receptor subunit, IL-6R exists in a soluble form (sIL-6R) that binds to the ubiquitous gp130 protein

producing an alternative pathway termed trans-signaling (Kishimoto et al., 1995; Rose-John and Neurath 2004). Thus, in the presence of sIL-6R, IL-6 action can be exerted in all the cells. IL-6 has been associated to contribute to major depression (Maes et al., 1993; Dowlati et al., 2010), schizophrenia (Smith et al., 2007; Potvin et al., 2008) and some neurodegenerative diseases like multiple sclerosis (Gijbels et al., 1995; Eugster et al., 1998; Samoilova et al., 1998) and Alzheimer's disease (Hüll et al., 1996). However, other studies have reported that IL-6 overexpression enhances Aβ clearance in animal models of Alzheimer's disease (Chakrabarty et al., 2010) and that IL-6 deficiency exacerbates Huntington's disease phenotype (Wertz et al., 2020). Moreover, a neuroprotective role of IL-6 in Parkinson's disease has been observed (Müller et al., 1998; Bolin et al., 2002). Importantly, physiological aging is associated with high IL-6 levels in the serum (Wei et al., 1992; Ye and Johnson, 1999; Ershler and Keller, 2000; Godbout et al., 2005) and in the brain (Ye and Johnson, 1999; Campuzano et al., 2009). Specifically, brain endothelial cells (Reyes et al., 1999) and glial cells (Xie et al., 2003; Sierra et al., 2007) from aged animals present an increased IL-6 production *in vitro.*

Previous studies from our group have showed that chronic overexpression of either IL-10 or IL-6 restricted to the CNS exerts an important impact on microglial and neuronal population of adult mice, demonstrating again the importance of the microenvironment in microglial function and responses. Specifically, mice with astrocyte-targeted IL-10 overexpression showed a distinctive microglial phenotype characterized by the upregulation of IBA1, CD11b, CD16/32 F4/80, and CD150 (Almolda et al., 2015). Interestingly, these mice also presented alterations in the neuronal population showing lower synaptic excitability and decreased LTP responses in the CA1-CA3 hippocampal area (Almolda et al., 2015). On the other hand, mice with astrocyte-targeted IL-6 overexpression were characterized by microglial activation together with neurodegeneration, learning impairment and reduced hippocampal neurogenesis (Campbell et al., 1993; Heyser et al., 1997; Vallières et al., 2002). Moreover, these animals showed increased levels of inflammatory mediators, such as acute-phase proteins (Campbell et al., 1993), metallothionein-I and -III (Hernández et al., 1997), and complement C3 (Barnum et al., 1996), in some brain areas. In this context, we found very interesting to study whether the changes observed by chronic IL-10 and IL-6 overexpression in adult mice will have an impact on the process of normal aging and specifically on the characteristic microglial phenotype associated to this life stage

4. HYPOTHESIS AND OBJECTIVES

W e hypothesize that changes in the CNS microenvironment by overexpression of specific cytokines will modulate the age-related microglial modifications, impacting on biological processes altered during brain aging such as phagocytosis and neurogenesis.

The general objective of the present doctoral thesis is to evaluate the effect of local and chronic IL-10 and IL-6 overexpression on the principal microglial responses associated to physiological aging.

Specific objectives:

1. To study physical and behavioral general features of aging and the possible modifications induced by chronic and local IL-10 or IL-6 overexpression.
2. To characterize the pattern of microglial activation and especially their phagocytic function along GM and WM areas during normal aging.
3. To investigate putative effects of IL-10 and IL-6 overexpression on the microglial age-related phenotype and especially on their phagocytic capacity.
4. To evaluate the role of microglia in the clearance of aging-derived myelin debris and the implication of IL-10 and IL-6 overexpression.
5. To analyze the impact of microglial cells on aged hippocampal neurogenesis under IL-10 and IL-6 overexpression.

5. SUMMARY OF RESULTS AND DISCUSSION

This doctoral thesis is the compendium of published studies that have been performed to expand the knowledge of microglial role during physiological aging and the influence of microenvironmental modifications in the aged brain. Specifically, we have focused on the effects that local production of IL-10 and IL-6 exert on microglial cells, which are notably altered during aging, and their subsequent impact on two crucial processes modified by the age and extremely regulated by microglia: phagocytosis and neurogenesis.

For this purpose, two mouse transgenic lines on the C57BL/6J background with heterozygous overexpression of either IL-10 or IL-6 under the astrocytic GFAP promoter have been used. These transgenic mice denominated as GFAP-IL10Tg and GFAP-IL6Tg were previously generated and characterized by Almolda et al. (2015) and Campbell et al. (1993), respectively. Animals from both sexes and both genotypes with their corresponding wild-type (WT) littermates were grouped into adult (4-6 months old) and aged (18-24 months old) mice. Attending to the regional heterogeneity of microglial cells, brain regions of GM (cerebral cortex and hippocampus) and WM (corpus callosum and fimbria) areas were analyzed separately to evaluate microglial characteristics. Specifically, the DG was analyzed to study hippocampal neurogenesis.

Most of the results obtained have been published in scientific journals and will be referred in the text as Article 1 (*Sanchez-Molina et al., 2020, Biomolecules 10, 1099*), Article 2 (*Sanchez-Molina et al., 2021, Neurobiology of Aging 105, 280-295*) or Article 3 (*Sanchez-Molina et al., 2021, under review in Brain, Behavior, and Immunity*). These articles are included as Annex I. Additional non-published results of this thesis will be referred as Supplementary Figures, which are included as Annex II.

5.1. General physical and behavioral status

The general status of WT and transgenic animals in adulthood and aging was evaluated. Our observations showed no differences between genotypes in animal survival up to age of 24 months old. Body weight of GFAP-IL10Tg animals was similar to their WT littermates at both ages, however, aged GFAP-IL6Tg mice weighed less than aged WT (**Supp. Figure 1**). A reduced size of animals with overexpression of IL-6 was also reported in adult homozygous GFAP-IL6Tg mice (Campbell et al., 1993). Since IL-6 levels are unmodified in peripheral organs and serum of GFAP-IL6Tg mice (Campbell et al., 1993; Giralt et al., 2013; Recasens et al., 2021), these data indicate that higher or chronic amount of IL-6 restricted to the CNS has a direct impact on the body weight. This effect could be attributed to the "sickness behavior", a phenomenon importantly induced by IL-6 and characterized by a decreased intake of food, among other features (Schöbitz et al., 1995; Bluthé et al., 2000; Dantzer, 2006).

Behavioral analyses were performed in transgenic mice to measure general anxiety and locomotor activity (**Article 3, Supp. Figure 2 and 3**). In the corner test, animals overexpressing IL-10 showed a lower number of corners visited than WT animals in adulthood, indicating an increased neophobia (**Article 3**). This result was also observed by the effect of the age in WT mice. Moreover, aged GFAP-IL10Tg mice presented an increased grooming latency when were placed on the open field apparatus. However, no alterations in general anxiety-like behavior or locomotion, measured by the number of total rearings, the time in the center and the distance traveled during the 5 minutes of the open field test, were observed in GFAP-IL10Tg mice. On the other hand, a similar number of visited corners and a latency of grooming were observed between GFAP-IL6Tg and WT mice at both ages, indicating no alterations in neophobia by IL-6 overexpression. Importantly, while the number of crossings was unchanged by age or genotype, the number of total rearings measured in the open field test was dramatically decreased in GFAP-IL6Tg mice during aging (**Supp. Figure 2**). This result could suggest an increased anxiety in aged mice with IL-6 overexpression, however, the time spent in the center of the open field apparatus was considerably high in these animals. A more likely explanation for the low number of rearings during aging, would be an age-dependent affectation of general locomotion activity in GFAP-IL6Tg mice, which was qualitative observed during the 5 minutes of testing in the open field. In concordance, tremor and ataxia were previously reported in GFAP-IL6Tg mice upon 6 months of age (Campbell et al., 1993). Therefore, we evaluated in detail the motor function of aged GFAP-IL6Tg mice by specific quantitative tests (**Supp. Figure 3**). General sensorimotor features including balance, coordination and muscle function (measured by beam walking test, gait test and rotarod test) were impaired by IL-6 overexpression. Moreover, scoring for cerebellar ataxia (measured by ledge test, hindlimb clasping test, gait test and kyphosis) and Huntington's disease (measured by neurobehavioral and physical assessments) phenotypes were significantly higher in aged GFAP-IL6Tg mice with respect to aged WT mice. In agreement, early IL-6 increase has been reported in motor-related disorders such as ataxias and Huntington's disease (Björkqvist et al., 2008; Olejniczak et al., 2015; Raposo et al., 2017). Since cerebellum and thalamus are two of the main areas implicated in motor control and coordination (Ichinohe et al., 2000; Caligiore et al., 2017), the observed phenotypes in transgenic animals are probably induced by the particular high expression of IL-6 reported in these areas (Campbell et al., 1993; Quintana et al., 2009). In parallel with our study, other authors have demonstrated important cerebellar inflammation and volume loss together with motor problems in aged GFAP-IL6Tg mice (Gyengesi et al., 2019). Therefore, the chronic IL-6 production in particular CNS areas along life could be exacerbating the common motor problems that are usually developed with aging (Richwine et al., 2005) towards a phenotype similar to that of motor-related diseases.

5.2. Cytokines levels in brain and serum

Local microenvironment is a key point in the aged brain, which is characterized by an imbalance between pro-inflammatory and anti-inflammatory mediators (Cornejo and von Bernhardi, 2016).

Thus, in order to evaluate the possible alterations that transgenic mice present in their microenvironment, we analyzed the expression of the principal cytokines modified during aging by Luminex assay (**Article 2 and 3**).

In adulthood, GFAP-IL10Tg and GFAP-IL6Tg mice presented higher IL-10 and IL-6 levels, respectively, than their counterparts WT mice in different brain areas. Interestingly, while overexpression of IL-10 did not induce alterations in the expression of other cytokines beyond IL-10, IL-6 overexpression induced also an increase of cerebral IL-10 levels under basal conditions. These results suggest that chronic overexpression of the pro-inflammatory IL-6 cytokine may be counterbalanced for the promotion of life. Of note, only GFAP-IL10Tg mice showed cytokine modifications in the serum with increased IL-10 levels, pointing to a possible systemic action of this cytokine.

During aging, the IL-10 and IL-6 levels observed in adult mice remained unaltered in different brain areas in all genotypes. These data contrast with a part of the literature reporting an increase of IL-6 levels in some areas of the normal aged brain (Ye and Johnson, 1999; Campuzano et al., 2009). Age could be a determinant factor for differences in the cytokine amount. Thus, while studies reporting increased IL-6 levels were performed in animals around 24 months of age, we used around 21-month-old mice for the biochemical approach. Supporting this hypothesis, a study performed in 3-, 12-, 18- and 24-month-old mice showed no measurable expression of IL-6 in the first three ages, but an increase at 24 months of age (Terao et al., 2002). Additionally, Godbout et al. (2005) showed no differences of IL-6 levels in the brain of 20-24-month-old mice when compared to 3-6-month-old mice. Regarding to IL-6 cell production, some authors have reported an increased production of this cytokine by cultured brain endothelial cells (Reyes et al., 1999) and glial cells (Xie et al., 2003; Sierra et al., 2007; Nije et al., 2012) derived from aged animals. However, it must be considered that cellular cytokine secretion may differ from *in vitro* to *in vivo* conditions. A more robust data is published about increased IL-6 levels in the serum of elderly people and rodents (Wei et al., 1992; Ye and Johnson, 1999; Ershler and Keller, 2000; Godbout et al., 2005), which was also observed by our cytokine analysis. On the other hand, IL-10 dynamic during aging is poorly described with studies showing decreased (Ye and Johnson, 2001; Frank et al., 2006) or equal (Henry et al., 2009) IL-10 levels in the aged brain. In agreement with other authors (Henry et al., 2009), we showed that IL-10 levels in serum were also maintained during aging. Additionally, we measured IL-1β and TNFα as pro-inflammatory cytokines that have been reported to increase at advanced ages (Maher et al., 2004; Campuzano et al., 2009). Nevertheless, our analysis found that the levels of these cytokines were very low or undetectable in all experimental groups, suggesting no important changes in the IL-1β and TNFα production by age or genotype.

In summary, possible differences between GFAP-IL10Tg and WT mice during aging will come given by increased levels of IL-10, whereas differences between GFAP-IL6Tg and WT mice could

be attributed to increased IL-10 and IL-6 levels. In both situations, the transgenic cytokine supply is present since adulthood and remains unchanged until aging despite the reported GFAP increase with age (Nichols et al., 1993; Kohama 1995; Wu et al., 2005).

5.3. Microglial activation and density

Microglial activation has been widely reported in normal aging by several markers (Perry et al., 1993; Sierra et al., 2007; Cornejo and von Bernhardi, 2016). Our results obtained by IBA1 immunostaining showed that, during aging, microglia from WM areas undergo a higher activation than microglia from GM areas (**Article 2**). In addition, morphological changes characterized by the presence of a larger soma and thicker processes were observed in aged microglia through the brain. Since infiltration of peripheral immune cells in the aging brain is very slight, we used PU.1 (a transcription factor of myeloid cells) to evaluate microglial cell density (**Article 2**). The number of PU.1^{+} cells was also upregulated during aging in a regional-dependent manner. Similar to IBA1, microglial cell density increase was higher in WM than in GM areas. Of note, we also observed microglial clusters specifically in WM areas of aged mice. All these results indicate an important microglial proliferation, which is usually associated with inflammatory processes, in WM areas during aging. Remarkably, although MHC-II expression is commonly associated with aging (Perry et al., 1993; Frank et al., 2006), this marker was absent throughout the aged brain in our study. MHC-II is a molecule involved in antigen presentation to T-cells and it usually appears in microglial cells after brain insults (Perry, 1998; Almolda et al., 2011). Along life, animals can suffer different infections leading to MHC-II apparition in the brain, however, it must be considered that experimental mice usually are maintained under sterile conditions. Thus, differences in MHC-II expression in aged mice could be due to the degree of sterility that present their animal's facilities.

In this thesis, we demonstrated that chronic IL-10 or IL-6 overproduction has an impact on microglial activation and density during aging (**Article 2**). Animals with IL-10 overexpression presented higher microglial activation and density than aged WT mice only in GM areas. However, when compared to aged WT animals, IL-6 overexpression exacerbated microglial age-related changes regardless of the cerebral area. As in WT mice, no evidence of MHC-II expression was found in transgenic mice, suggesting no influence of IL-10 or IL-6 overproduction in the microglial antigen-presenting capacity during aging.

Importantly, we showed that both cytokines led to an increased IBA1 immunostaining and PU.1^{+} cells number since adulthood in all the areas studied. However, the number of proliferating microglia in adult GFAP-IL10Tg (Almolda et al., 2015; Recasens et al., 2019) and GFAP-IL6Tg (Recasens et al., 2021) mice was unaltered respect to WT mice. Interestingly, an increased PU.1[+] cell density has been also observed in transgenic mice at early postnatal stages (unpublished results), suggesting a higher entrance of microglial precursors into the brain parenchyma or a higher microglial proliferation during development. Considering that IL-10 has no effect on

microglial proliferation but inhibits microglial apoptosis (Sawada et al., 1999; Strle et al., 2002), GFAP-IL10Tg mice may present an increased microglial density due to a higher microglial survival during postnatal development. On the other hand, IL-6 induces microglial proliferation (Streit et al, 2000; Recasens et al., 2021). This cytokine action could be exerted at early stages leading to the higher microglial density observed in GFAP-IL6Tg mice. Moreover, previous results from our research group have showed an increased number of intraparenchymal monocytes in both transgenic lines, which could also intervene in the higher number of PU.1^{+} cells since postnatal stages (Recasens et al., 2019; Recasens et al., 2021). Since opposite properties regarding microglial activation have been traditionally attributed to IL-10 and IL-6, our observations showing similar effects concerning IBA1 expression on both adult transgenic mice may be unexpected. However, it must be taken into account that most of the effects described for these cytokines have been evaluated following acute exposure. In contrast, here we showed effects produced by chronic production of either IL-10 or IL-6 since the birth, which could be different from short-term effects of these cytokines. Moreover, independently of the cytokine, animals of both transgenic lines presented a disruption of the brain homeostasis since postnatal stages that is maintained throughout the life in a GFAP-dependent manner. Since alterations in the brain parenchyma alert and activate microglia, it could be expected to observe general changes on microglial population by IL-10 or IL-6 overproduction. In addition, we showed that GFAP-IL6Tg mice also present higher IL-10 levels, which could be counterbalancing the IL-6 effect resulting in a similar effect to the observed by IL-10 overproduction. More importantly, here we described a similar microglial activation pattern in transgenic mice under basal conditions during adulthood, however, our previous results demonstrated that after a challenge this pattern differ depending on the cytokine-associated activation. As example, chronic IL-10 or IL-6 overproduction leads to opposite lesion outcome after facial nerve axotomy (Almolda et al., 2014; Villacampa et al., 2015) and perforant pathway transection (Recasens et al., 2019; Recasens et al., 2021). Accordingly, in the present study we observed that the characteristic microglial modifications associated to aging differ between GFAP-IL10Tg and GFAP-IL6Tg animals. While GFAP-IL10Tg mice maintained the same microglial properties throughout life, GFAP-IL6Tg mice increased microglial activation and density upon aging. Thus, in the WM, where the age-related microglial changes are more prominent than in the GM, the effect of aging in WT animals was equal to that observed in GFAP-IL10Tg mice since adulthood. These results indicate that while normal age-related microglial activation and proliferation is observed in GFAP-IL6Tg mice, in GFAP-IL10Tg mice is inhibited. In agreement, previous studies from our group have shown that microglia from GFAP-IL10Tg mice undergo slight changes regarding activation and proliferation after perforant pathway transection (Recasens et al., 2019) and traumatic brain injury (Shanaki, 2020) when compared to lesion-induced changes in microglia from WT mice.

5.4. Microglial phagocytosis

Phagocytosis is a process that takes special relevance during physiological aging. At this life stage, accumulation of cellular debris, such as apoptotic cells, protein aggregates and myelin debris, can lead to inflammation and tissue damage (Mattson and Magnus, 2006). In the brain, microglia are the intrinsic phagocytes in charge of clearing cellular debris (Neumann et al., 2009; Fu et al., 2014) and modifications in this process have been reported during aging (Nije et al., 2012; Ritzel et al., 2015; Safaiyan et al., 2016).

5.4.1. Phagocytic phenotype

A specific transcriptomic signature related to DAM has been identified in neurodegeneration and aging (Keren-Shaul et al., 2017; Krasemann et al., 2017). This signature is characterized by upregulation of genes involved in phagocytosis and lipid metabolism. Some of the most important genes related to phagocytosis that are enhanced in DAM are: *Trem-2, Lgals3* and *Itgax*. Importantly, the induction of this transcriptomic profile is TREM-2-dependent. Our results corroborated the apparition of DAM markers in aged animals, however, in agreement with previous studies (Hart et al., 2012; Raj et al., 2017), differences in their pattern of expression were detected between cerebral areas (**Article 2**). TREM-2 was localized in the microglial soma from GM areas, indicating unfunctional expression, but along the microglial processes in the WM areas. Interestingly, Galectin-3 (encoded by *Lgals3* gene) and CD11c (encoded by *Itgax* gene) were found exclusively in WM areas of aged mice (**Article 2**). TREM-2 is a microglial lipid sensor whose deficiency is linked to Nasu-Hakola disease (Paloneva et al., 2002) and impairments in myelin debris clearance by microglia after pathological demyelination (Poliani et al., 2015; Piccio et al., 2007). Moreover, TREM-2 is a key regulator of cholesterol metabolism derived from myelin phagocytosis (Nugent et al., 2020). In a similar way, Galectin-3 (GAL-3) is a microglial carbohydrate receptor that recognizes myelin debris and is necessary for their phagocytosis (Rotshenker et al., 2008), being induced in demyelination processes (Reichert and Rotshenker, 1999; Hoyos et al., 2014). Additionally, GAL-3 promotes oligodendrocyte differentiation (Pasquini et al., 2011). CD11c^{+} microglia have been also found in demyelinating conditions (Remington et al., 2007; Wlodarczyk et al., 2014) and during postnatal myelinogenesis (Wlodarczyk et al., 2017). Considering the specific expression of TREM-2, GAL-3 and CD11c in WM areas of aged mice and taking into account the role of these receptors in myelin debris recognition, we hypothesized an aging-derived myelin deterioration and the need of a specialized microglia in the recognition and phagocytosis of myelin debris. In parallel with our study, Safaiyan et al. (2021) showed similar results by single cell RNA-sequencing. Safaiyan and collaborators identified a specific transcriptomic profile of aged microglia in WM areas, being dependent of TREM-2 expression and characterized by phagocytic markers. This microglial population, which is different to the already described DAM subset, has been denominated white matter-associated microglia (WAM) and proposed to be engaged in phagocyting age-related degenerated myelin (Safaiyan et al.,

2021). Previous data support this assumption showing an increased number of microglia with internalized myelin fragments during aging (Safaiyan et al., 2016).

In this study, we also demonstrated that chronic modifications in the microenvironment can exert changes in WAM related to aging (**Article 2**), suggesting possible effects on the removal of age-derived myelin damage as we will explain in detail in the 5.5. section. Specifically, similar to microglial activation, we demonstrated that IL-10 overexpression precedes but maintains the microglial phagocytic phenotype upon aging, whereas IL-6 overexpression enhances this phenotype in aged animals.

GFAP-IL10Tg mice presented an early TREM-2 and GAL-3 apparition since adulthood that could suggest an anticipated myelin damage by chronic IL-10 overproduction. Although IL-10 expression is usually associated with improvement of myelin disorders such as experimental autoimmune encephalomyelitis, there are contradictory results depending on its route of administration (Beebe et al., 2002). In support with our hypothesis, transgenic overexpression of IL-10 in neural tissues leads to demyelinating polyneuropathy mediated by macrophage infiltration (Dace et al., 2009). Remarkably, we also observed an increased number of infiltrated macrophages in GFAP-IL10Tg mice (**Article 3**). As we observed for IBA1, TREM-2 and GAL-3 expression was barely modified upon aging in GFAP-IL10Tg mice. Therefore, IL-10 overproduction enhances microglial activation and their phagocytic phenotype in adulthood, but it mitigates the effect of normal aging. In this case, we could again suggest that the microglial response to age-related myelin damage is stopped by IL-10 overproduction. Interestingly, the original concept of microglial "priming" described as an amplified microglial response to a second inflammatory stimulus (Franceschi et al., 2000; Cunningham et al., 2005), it has been recently integrated as a type of microglial "innate immune memory" (Neher and Cunningham, 2019). Depending on the initial stimulus, microglia can become "primed" or "desensitized", leading to a stronger (immune training) or weaker (immune tolerance) response to a second inflammatory insult, respectively (Neher and Cunningham, 2019). Thus, the early induction of age-related microglial markers in mice overexpressing IL-10 may lead to a "desensitized" microglia, which show "tolerant" responses to aging. On the other hand, CD11c expression was absent in GFAP-IL10Tg mice throughout life, indicating that IL-10 overproduction exerts an inhibitory effect on the CD11c population. This is in agreement with results showing that CD11c induction after perforant pathway transection is downregulated by the effect of IL-10 (Recasens et al., 2019). In contrast to the observed under chronic IL-10 overexpression, WAM phenotype in GFAP-IL6Tg mice was slightly visualized during adulthood. During aging, IL-6 overproduction exacerbated TREM-2 and GAL-3 expression especially in the fimbria. The higher activation on aged microglia from GFAP-IL6Tg mice could be attributed to a "primed" microglia induced by IL-6 overexpression since postnatal stages. Indeed, microglial priming has been already reported in the aged brain and IL-6 has been described as a key contributor to this process (Garner et al., 2018; Godbout et al., 2005; Norden and Godbout, 2013). Thus, microglial cells from GFAP-IL6Tg mice could exert

"trained" responses to aging exacerbating their phagocytic phenotype. In agreement, after anterograde axonal injury, GFAP-IL6Tg mice showed higher TREM-2 induction compared to WT mice (Manich et al., 2020). However, TREM-2 is downregulated after retrograde axonal injury (Manich et al., 2020) and cuprizone-induced demyelination (Petković et al., 2016) in GFAP-IL6Tg mice, indicating an injury-dependent control of this receptor. More studies to elucidate the role of IL-10 and IL-6 in phagocytic receptors such as TREM-2 and GAL-3 would be required.

5.4.2. Phagocytic capacity

To deepen in microglial phagocytic activity, we analyzed CD68 expression (**Article 2**), a molecule expressed in lysosomes of phagocytic cells, being upregulated in the digestion process. As previously reported (Perry et al., 1993; Wong et al., 2005), we observed a different lysosomal activity in aged microglia respect to adult determined by increased CD68 expression. Similar to our observations in TREM-2, while in GM areas CD68 was localized in the microglial soma during aging, in WM areas this molecule was homogeneously increased in microglial soma and processes. The observed differences in the CD68 expression pattern between GM and WM reinforce the presence of regional-dependent phagocytic changes in aging. CD68 inclusions observed in GM could be related to an inefficient phagocytic capacity to degrade the lysosomal content as it has been suggested by some authors (Vaughan and Peters, 1974; Mosher and Wyss-Coray, 2014). In contrast, the pattern of CD68 along the microglial processes observed in WM could mean a high and functional phagocytic activity. Interestingly, our results showed that both IL-10 and IL-6 overexpression induced, since adulthood, the same pattern of CD68 expression as the observed in the WM areas of WT aged mice regardless of the cerebral area. This pattern was maintained in aged GFAP-IL10Tg mice and exacerbated in aged GFAP-IL6Tg mice. As result, microglial lysosomal activity in WM areas was unchanged by IL-10 overexpression and increased by IL-6 overexpression during aging.

To evaluate whether the specific WAM phenotype was linked to modifications in the functional microglial phagocytosis, we performed a myelin phagocytosis assay by flow cytometry (**Article 2**). Our results showed that the percentage of microglia able to phagocyte myelin and their individual phagocytic capacity were similar between adult and aged mice. These data argued for the presence of a specific WAM during aging due to a high phagocytic demand rather than to microglial age-related intrinsic changes in their phagocytic capacity. In contrast with our results, decreased phagocytosis of Aβ peptides and fluorescent beads has been reported in aged microglia *ex vivo* (Nije et al., 2012; Ritzel et al., 2015). It would be important to take into account that depending on the product to phagocytose, age-related changes in phagocytosis could be different. Moreover, microglial phagocytic capacity could be different depending on the brain area. In fact, whereas the mentioned works were performed in the whole brain, we studied this feature specifically in microglia from the corpus callosum, where we described distinctive age-related microglial characteristics compared to other brain areas. Thus, this study showed that phagocytic

function of WAM is maintained during aging for myelin products. However, both IL-10 and IL-6 transgenic overexpression led to intrinsic changes in aged microglial cells towards a higher phagocytic capacity when are exposed to myelin *ex vivo* (**Article 2**). In agreement, IL-10 has been reported to stimulate myelin phagocytosis in cell cultures (Smith, 1999) and, although IL-6 effect on myelin phagocytosis has not been reported before to our knowledge, overexpression of IL-6 increases the clearance of Aβ plaques by microglia (Chakrabarty et al., 2010). In contrast to GFAP-IL10Tg mice, the increased microglial phagocytic capacity in GFAP-IL6Tg mice was observed since adulthood.

Taken together, we showed that the specific phagocytic phenotype observed in microglia from WM areas during aging is not clearly correlated with changes in their intrinsic phagocytic capacity. These data suggested that the microglial shift to a phagocytic phenotype in WT mice during aging is dependent on local signals, such as possible myelin damage, instead of an age-related change at the cellular level. On the other hand, chronic IL-10 and IL-6 overexpression exerted intrinsic cellular modifications on microglia increasing their phagocytic capacity of myelin *ex vivo*. Thus, we hypothesized that GFAP-IL10Tg and GFAP-IL6Tg mice could present differences in the clearance of age-related myelin debris when compared with WT mice. To prove that, next we evaluated the relationship between WAM and the presence of possible myelin alterations during aging.

## 5.5. Myelin and lipid status

Cerebral WM lesions are a common feature of elderly people (de Leeuw et al., 2001). Moreover, reduction of WM volume has been widely reported in humans during aging by MRI (Guttmann et al., 1998; Bartzokis et al., 2003; Hinman and Abraham, 2007) and decreased myelin amount has been showed in aged dogs by histological analysis (Chambers et al., 2012). However, a less evident data about age-related WM alterations have been reported in mice until the date. As main finding, Safaiyan et al. (2016) showed extracellular myelin fragments in the optic nerve of aged mice by electron microscopy. Following our finding of a specific phagocytic microglial phenotype in WM areas of aged mice, we tried to clarify the effect of aging on myelin and elucidate whether the observed modifications in microglia by IL-10 or IL-6 overexpression, especially in relation to the phagocytic phenotype, could influence in this issue.

Evaluation of principal protein and lipid composition by MBP and luxol fast blue analysis, respectively, showed a similar staining along the different ages and genotypes, indicating that no evident demyelination is produced during aging in mice (**Article 2**). However, less evident features affecting the integrity or composition of myelin without modifying the total amount could be happening. Due to the rich lipid content of myelin and the upregulation of genes related to lipid metabolism in DAM, we evaluated the lipid status of the aged brain by Fourier-transform infrared microspectroscopy based on synchrotron radiation, a useful and precise methodology to study

tissue biochemical properties (Baker et al., 2014). Before to study biochemical differences by age or cytokines depending on the cerebral area, we performed a comparative study between GM and WM with this method to define physiological parameters in these areas (**Article 1**). In both mouse and human samples, we demonstrated a different infrared profile between brain areas. Specifically, WM showed higher absorbances than GM in the lipid region, indicating a higher amount of this component, although lipid oxidation measured by carbonyl (C=O) and unsaturated olefinic (C=CH) groups was lower than in GM. Moreover, we established a lipid/protein threshold value to discriminate between GM and WM under basal conditions. Values higher than 1.5 for the lipid/protein (CH_2/Amide I) ratio were related to WM areas. Therefore, we proposed that values under 1.5 corresponding to infrared measures from WM areas indicate important tissue biochemical composition alterations. Supporting this, we showed that the corpus callosum of animals treated with cuprizone for 5 weeks, when the major demyelination is reached, presented values lower than 1.5 for this ratio as well as increased values of lipid oxidation when compared with untreated mice (**Supp. Figure 4**). Next, we evaluated possible differences in lipid amount and lipid oxidation due to the effect of the age or the genotype in WT, GFAP-IL10Tg and GFAP-IL6Tg mice (**Article 2**). Contrary to the observed after cuprizone-induced demyelination, the values corresponding to the lipid/protein ratio were within the threshold established for GM and WM in all the groups studied, suggesting an absence of important demyelination by age or genotype. Regarding lipid oxidation, we demonstrated a regional-dependent decrease of carbonyl groups (C=O/CH_2), indicative of a lower oxidation, specifically in WM during aging. This result was in contrast with previous literature reporting increased lipid oxidation in the aged brain (Ando et al., 1990; Leutner et al., 2001; Clausen et al., 2010). The methodology performed in these studies using mainly homogenates of the whole brain in contrast to our tissue non-destructive methodology measuring specific areas of the brain, is probably responsible for the discrepancies in the results. Taking into account the presence of phagocytic microglia in WM areas during aging, a removal of oxidized lipids followed by their renovation could be taken place at this life stage, making difficult to detect lipid oxidation. In agreement, a higher lipid turnover of myelin has been reported in the aged brain (Ando et al., 2003). Interestingly, despite the differences observed in microglia, transgenic overexpression of IL-10 or IL-6 did not influence significantly in the lipid status reported during physiological aging. This was in contrast to the association of high IL-6 levels with lower WM integrity in older individuals (Bettcher et al., 2014) and myelin disorders, such as transverse myelitis (Kaplin et al., 2005) or neuromyelitis optica (Uzawa et al., 2010). Of note, GFAP-IL10Tg mice showed a tendency of higher lipid oxidation than WT mice in adulthood, which could be related with the early apparition of phagocytic receptors such as TREM-2 and GAL-3 in these animals.

In conclusion, although histological changes in myelin were undetected, we showed a correlation between a microglial phagocytic phenotype and a decrease of lipid oxidation during aging. However, despite the observed differences in microglia from GFAP-IL10Tg and GFAP-IL6Tg mice as compared to WT, lipid oxidation was similar in all genotypes. Importantly, we cannot predict

whether the less content of oxidized lipids during aging is the result of the specialized age-related WAM or rather the cause that leads to this microglial shift. In **Figure 5** the main changes observed in WM areas of WT, GFAP-IL10Tg and GFAP-IL6Tg mice during aging are summarized.
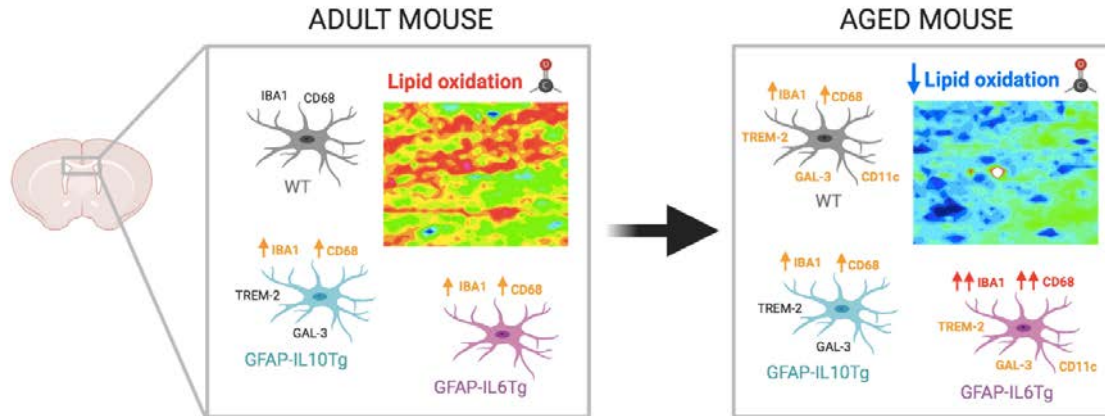
Figure 5. Main changes observed in the corpus callosum of WT, GFAP-IL10Tg and GFAP-IL6Tg mice during aging. Cells represent microglia from WT (grey), GFAP-IL10Tg (blue) and GFAP-IL6Tg (pink) mice in the corpus callosum. Heatmaps represent the content of carbonyl groups (warm colors), as indicative of lipid oxidation, in the corpus callosum. *Created by Biorender.com.*

These findings should be not misunderstood as that IL-10 or IL-6 overproduction does not influence in processes related to myelin damage. In fact, in pathological situations, both IL-10 and IL-6 have been demonstrated to have an important impact in the myelin outcome. For example, our results showed that, after acute demyelination induced by cuprizone, GFAP-IL10Tg mice presented a delay in microglial activation after cuprizone treatment, resulting in a higher myelin conservation than the observed in WT mice (**Supp. Figure 5**). On the other hand, GFAP-IL6Tg mice exhibited an inefficient removal of myelin debris by microglia together with impaired oligodendrocyte differentiation (Petković et al., 2016). IL-10 and IL-6 also exert an important role in animal models of multiple sclerosis. Several studies have shown that IL-10 overexpression confers disease resistance (Rott et al., 1994; Bettelli et al., 1998; Cua et al., 1999; Cua et al., 2001), however, the route of IL-10 delivery can result in different therapeutic outcomes (Croxford et al., 2001; Cua et al., 2001). Interestingly, GFAP-IL6Tg mice develop an atypical experimental autoimmune encephalomyelitis redirected to the cerebellum (Quintana et al., 2009; Giralt et al., 2013). In addition to pathological situations, our group has observed a different postnatal myelination in GFAP-IL10Tg and GFAP-IL6Tg mice as compared to WT. Specifically, transgenic mice presented the same number of Olig2$^+$ cells but higher MBP$^+$ myelin amount than WT mice during primary myelination, suggesting a role of chronic IL-10 and IL-6 overexpression in the maturation of OPCs (unpublished results). Therefore, it is important to mention that the effects of these cytokines in myelin-related processes can be different depending on the type of myelin alteration.

5.6. Hippocampal neurogenesis and memory

Aging is characterized by cognitive impairment and progressive dementia. This feature has been associated with loss of myelinated axons and changes in the neuronal population (Tang et al., 1997; Shobin et al., 2017). Specifically, hippocampal neurogenesis is dramatically affected by aging (Kuhn et al., 1996; Bondolfi et al., 2004; Kuipers et al., 2015) and the subsequent reduction of new neurons in the dentate gyrus is related to learning and memory deficits associated to this life period (Drapeau et al., 2003; Van Praag et al., 2005; Villeda et al., 2011). In our studies we showed that, in addition to aging, chronic overproduction of both IL-10 and IL-6 reduced hippocampal neurogenesis since adulthood (**Article 3 and Supp. Figure 6**). Importantly, the effect of aging was superior to the effect of IL-10 or IL-6 on the reduction of new neurons.

Inflammation is considered detrimental for the generation of new neurons and several studies have reported a negative effect of IL-6 on this process (Vallières et al., 2002; Ekdahl et al., 2003; Monje et al., 2003). Of note, a role for IL-6 in inducing neural stem cells (NSCs) differentiation into astrocytes rather than neurons has been observed (Nakanishi et al., 2007). Oppositely, neurogenesis is increased in situations where IL-6 is upregulated such as after seizures or cerebral ischemia (Parent et al., 1997; Liu et al., 1998; Nakagawa et al., 2000). However, in these pathological situations, IL-6 expression was restricted to a short period together with other brain damage-derived factors that could be counteracting the negative effect that this cytokine may exert in neurogenesis. In concordance with previous studies in young mice (Vallières et al., 2002; Campbell et al., 2014), we reported a decreased hippocampal neurogenesis in adult and aged GFAP-IL6Tg mice with respect to their corresponding WT littermates (**Supp. Figure 6**). This result, together with a reduced LTP in the DG (Bellinger et al., 1995), correlates with a progressive age-related decline in avoidance learning (Heyser et al., 1997). Moreover, our results showed a tendency of spatial memory impairment in aged GFAP-IL6Tg mice using the T-maze test (**Supp. Figure 6**).

On the other hand, some studies have reported a beneficial role of anti-inflammatory cytokines in the promotion of new neurons (Aharoni et al., 2005; Butovsky et al., 2006; Kiyota et al., 2010; Kiyota et al., 2012). However, our results showed that adult GFAP-IL10Tg mice present an important hippocampal neurogenesis reduction (**Article 3**). Similarly, a reduced number of neuroblasts in the subventricular zone was reported by IL-10 administration (Perez-Asensio et al., 2013). In concordance with the impaired neurogenesis detected, we demonstrated age-related hippocampal cognitive deficits in adult mice overexpressing IL-10 as determined by the T-maze and the Morris water maze (**Article 3**). These results were in agreement with the decreased excitability of hippocampal CA1-CA3 synapses and the altered LTP response previously described in GFAP-IL10Tg mice, indicating deficits in synaptic plasticity (Almolda et al., 2015). Thus, we could link chronic IL-10 overexpression with a detrimental effect on the neuronal population in physiology despite its assigned anti-inflammatory and neuroprotective

properties. Moreover, in line with our findings, it has been reported that IL-10 overexpression exacerbates hippocampal-dependent memory impairment (Chakrabarty et al., 2015), whereas IL-10 deficiency partially restores this cognitive deficit (Guillot-Sestier et al., 2015) in mouse models of Alzheimer's disease.

Although the final output of neurogenesis was the same in both transgenic lines, with a ~40% less of neuroblasts in adulthood, the causes leading to this reduced neurogenesis differed between genotypes. While IL-6 overexpression negatively affected the NSCs proliferation, survival, and neuronal differentiation (Vallières et al., 2002), IL-10 overexpression affected the NSCs survival without altering their proliferation (**Article 3**). Although the transmembrane IL-6R has been found in the granular cell layer of the DG (Gadient and Otten, 1995; Vallières and Rivest, 1997), is rarely expressed in NSCs (Islam et al., 2009). However, IL-6/sIL-6R complex has been shown to bind to NSCs and induce their differentiation (Islam et al., 2009). Moreover, defective hippocampal neurogenesis in GFAP-IL6Tg mice is rescued blocking the IL-6 trans-signaling mechanism mediated by sIL-6R (Campbell et al., 2014). Thus, neurogenesis impairment in GFAP-IL6Tg mice is probably produced by a trans-signaling effect of IL-6 on NSCs. On the other hand, our results demonstrated that, although some neurons and astrocytes do, NSCs of the DG did not express IL-10R (**Article 3**). These findings indicate that while IL-6 probably acts directly on NSCs, the influence of IL-10 in neurogenesis must be indirect by changes produced in other cell populations.

5.7. Neuron-microglia interactions

Microglial cells play an important role modulating neurogenesis, which is affected in aging and neurodegeneration (Aarum et al., 2003; Carpentier and Palmer, 2009; Al-Onaizi et al., 2020). Therefore, microglial age-related alterations are proposed to interfere in the neurogenesis decline produced at advanced ages. In this sense, an important factor for neurogenesis regulation is the neuron-microglia communication (Bachstetter et al., 2011; Vukovic et al., 2012; Varnum et al., 2015), which is disrupted during aging (Jurgens and Johnson, 2012). As we mentioned in the previous section, IL-6 effect on neurogenesis is probably given to a direct effect on NSCs, whereas IL-10 effect must be given for changes in other cells that play a role in the process of neurogenesis. Therefore, we focused on the possible microglial involvement in the decreased neurogenesis observed specifically in GFAP-IL10Tg mice (**Article 3**).

By flow cytometry analysis, we studied the expression of some homeostatic molecules related to the communication between neurons and microglia (CD11b$^+$/CD45$^{low/int}$) or macrophages (CD11b$^+$/CD45^{high}) in the hippocampus. Our results demonstrated that the expression of different immunoreceptors during aging was altered specifically in microglial cells, showing an increased CD45, CD200R and SIRPα expression, but a decreased CX3CR1 expression. However, differing with some studies (Jurgens and Johnson, 2012), we did not observe important changes in the

expression of CX3CL1, CD200 or CD47 neuronal ligands by the effect of normal aging. BDNF released by neurons is another "off signal" that has been reported to decrease in the hippocampus during aging (Cortese 2011; Chapman 2012). In contrast, our results showed similar levels of hippocampal BDNF between adult and aged mice, suggesting that age-related hippocampal neurogenesis decrease is independent of this neurotrophic factor.

Interestingly, since adulthood, GFAP-IL10Tg mice showed similar modifications in homeostatic microglial receptors to the observed in aged WT mice together with an increase of CD11b expression, indicating an effect of IL-10 on the microglia-neuron communication. Again, we demonstrated that chronic IL-10 overproduction predicts age-related changes. Since IL-10R was mainly observed in neurons and astrocytes, microglial modifications in GFAP-IL10Tg mice must be given by changes in these cellular types. Presumably, chronic IL-10 overexpression impacts directly on neurons leading to a microglial response in the mentioned homeostatic receptors. Of importance, we showed a reduced CX3CL1 expression in adult GFAP-IL10Tg mice that was accentuated with the age. This IL-10-dependent CX3CL1 decrease could be detected by microglia and lead to the subsequent modifications defined in their homeostatic receptors, especially to the reduction of CX3CR1 expression. The negative effect of altered neuron-microglia communication on neurogenesis has been associated with a pro-inflammatory microglial activation. Specifically, disruption of CX3CR1-CX3CL1 dialogue results in impaired hippocampal neurogenesis by increased microglial production of IL-1β, which directly acts on NSCs (Bachstetter et al., 2011). However, our results demonstrated very low levels of IL-6, IL-1β and TNFα, the main pro-inflammatory cytokines affecting the process of neurogenesis, in GFAP-IL10Tg mice without detectable differences by age. Moreover, we did not observe differences in the BDNF levels by IL-10 overexpression. Of interest, neuronal activity is also involved in microglial responses (Neumann and Wekerle, 1998; Li et al., 2013). Since we know that IL-10 overexpression induces a lower LTP in hippocampal neurons (Almolda et al., 2015), disruption of neuron-microglia dialogue in GFAP-IL10Tg mice could be also due to impairments in LTP.

Altogether, here we showed that hippocampal NSCs survival is impaired by both aging and chronic IL-10 overproduction together with an altered neuron-microglia communication. However, the exact mechanisms by which microglial modifications could affect the promotion of new neurons should be study deeply. Impaired hippocampal neurogenesis by astrocyte-targeted IL-10 overproduction is represented in **Figure 6**.
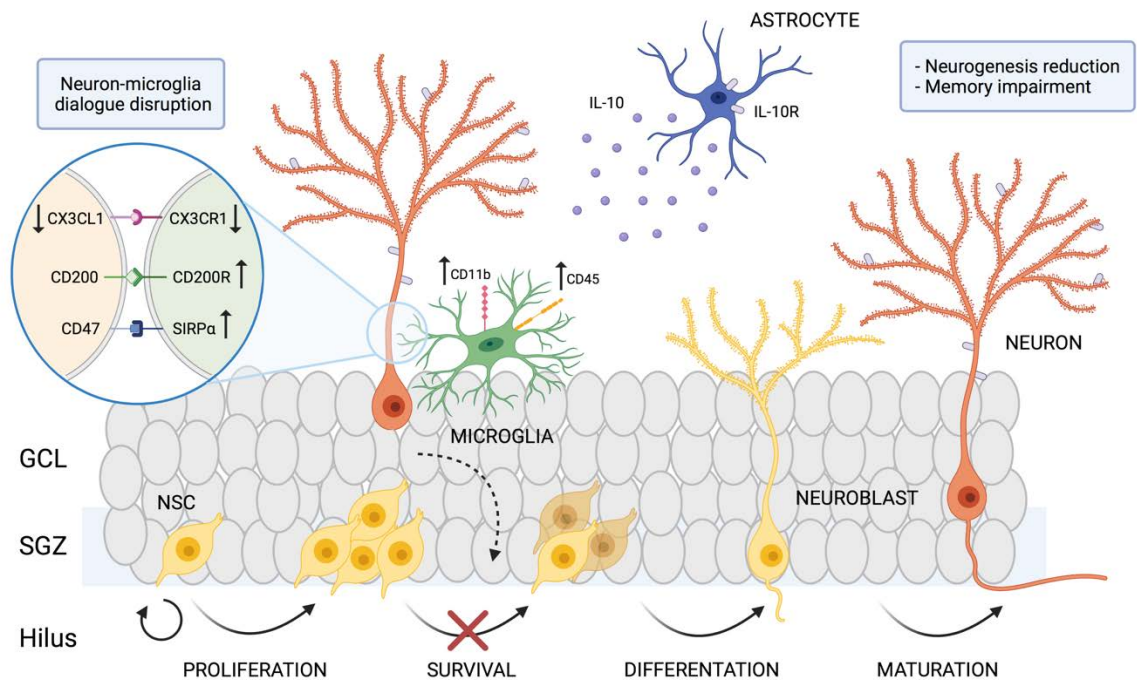
Figure 6. Main changes related to hippocampal neurogenesis in GFAP-IL10Tg mice.
Abbreviations: GCL (granular cell layer), SGZ (subgranular zone), IL-10R (IL-10 receptor), NSC
(neural stem cell). *Created by Biorender.com.*

6. CONCLUSIONS

C ollectively, our work demonstrates that local changes in the CNS microenvironment produced by IL-10 or IL-6 overexpression modify the microglial response to normal aging, especially in relation to their phagocytic function. IL-10 overexpression induces microglial age-related changes at early stages, but it inhibits microglial response to normal aging. IL-6 overexpression results in a higher microglial activation during aging. Furthermore, our data indicate that these cytokine-derived microglial modifications have no apparent effect on the myelin status along life, but they negatively influence the process of hippocampal neurogenesis since adulthood.

Specifically,

- Chronic IL-10 or IL-6 overexpression do not influence animal survival, but IL-6 overexpression induces body weight loss and motor problems at advanced ages.
- Levels of IL-10 and IL-6 are increased in the brain of GFAP-IL10Tg and GFAP-IL6Tg mice, respectively, without modifications upon aging.
- Both chronic IL-10 and IL-6 overexpression induces microglial activation and increase of microglial cell density in adult mice. These changes are maintained in GFAP-IL10Tg mice and enhanced in GFAP-IL6Tg mice upon aging.
- Aging induces a specific TREM-2$^+$/GAL-3$^+$/CD11c$^+$ microglial phagocytic phenotype in WM areas without modifying the functional microglial phagocytic capacity.
- IL-10 overexpression precedes the apparition of age-related phagocytic molecules in adulthood without modifications at advances ages, whereas IL-6 overexpression exacerbates their expression in aging. Both cytokines increase the functional microglial phagocytic capacity during aging.
- Aging promotes a decrease of lipid oxidation in WM areas without modifying the major protein and lipid components of myelin. IL-10 and IL-6 overproduction does not influence in this age-associated lipid oxidation decrease.
- Both IL-10 and IL-6 chronic overexpression decreases hippocampal neurogenesis and induces cognitive deficits since adulthood.
- IL-10 overexpression precedes age-related alterations in molecules associated with neuron-microglia communication that influence neurogenesis.

7. BIBLIOGRAPHY

Aarum J, Sandberg K, Haeberlein SL, Persson MA. Migration and differentiation of neural precursor cells can be directed by microglia. Proc Natl Acad Sci U S A. 2003 Dec 23;100(26):15983-8. doi: 10.1073/pnas.2237050100.

Abutbul S, Shapiro J, Szaingurten-Solodkin I, Levy N, Carmy Y, Baron R, Jung S, Monsonego A. TGF-β signaling through SMAD2/3 induces the quiescent microglial phenotype within the CNS environment. Glia. 2012 Jul;60(7):1160-71. doi: 10.1002/glia.22343.

Aharoni R, Arnon R, Eilam R. Neurogenesis and neuroprotection induced by peripheral immunomodulatory treatment of experimental autoimmune encephalomyelitis. J Neurosci. 2005 Sep 7;25(36):8217-28. doi: 10.1523/JNEUROSCI.1859-05.2005.

Ajami B, Bennett JL, Krieger C, Tetzlaff W, Rossi FM. Local self-renewal can sustain CNS microglia maintenance and function throughout adult life. Nat Neurosci. 2007 Dec;10(12):1538-43. doi: 10.1038/nn2014.

Almolda B, de Labra C, Barrera I, Gruart A, Delgado-Garcia JM, Villacampa N, Vilella A, Hofer MJ, Hidalgo J, Campbell IL, González B, Castellano B. Alterations in microglial phenotype and hippocampal neuronal function in transgenic mice with astrocyte-targeted production of interleukin-10. Brain Behav Immun. 2015 Mar;45:80-97. doi: 10.1016/j.bbi.2014.10.015.

Almolda B, Gonzalez B, Castellano B. Antigen presentation in EAE: role of microglia, macrophages and dendritic cells. Front Biosci (Landmark Ed). 2011 Jan 1;16:1157-71. doi: 10.2741/3781.

Almolda B, Villacampa N, Manders P, Hidalgo J, Campbell IL, González B, Castellano B. Effects of astrocyte-targeted production of interleukin-6 in the mouse on the host response to nerve injury. Glia. 2014 Jul;62(7):1142-61. doi: 10.1002/glia.22668.

Al-Onaizi M, Al-Khalifah A, Qasem D, ElAli A. Role of Microglia in Modulating Adult Neurogenesis in Health and Neurodegeneration. Int J Mol Sci. 2020 Sep 19;21(18):6875. doi: 10.3390/ijms21186875.

Ando S, Kon K, Aino K, Totani Y. Increased levels of lipid peroxides in aged rat brain as revealed by direct assay of peroxide values. Neurosci Lett. 1990 May 31;113(2):199-204. doi: 10.1016/0304-3940(90)90303-q.

Ando S, Tanaka Y, Toyoda Y, Kon K. Turnover of myelin lipids in aging brain. Neurochem Res. 2003 Jan;28(1):5-13. doi: 10.1023/a:1021635826032. PMID: 12587659.

Arimoto T, Choi DY, Lu X, Liu M, Nguyen XV, Zheng N, Stewart CA, Kim HC, Bing G. Interleukin-10 protects against inflammation-mediated degeneration of dopaminergic neurons in substantia nigra. Neurobiol Aging. 2007 Jun;28(6):894-906. doi: 10.1016/j.neurobiolaging.2006.04.011.

Askew K, Li K, Olmos-Alonso A, Garcia-Moreno F, Liang Y, Richardson P, Tipton T, Chapman MA, Riecken K, Beccari S, Sierra A, Molnár Z, Cragg MS, Garaschuk O, Perry VH, Gomez-Nicola D. Coupled Proliferation and Apoptosis Maintain the Rapid Turnover of Microglia in the Adult Brain. Cell Rep. 2017 Jan 10;18(2):391-405. doi: 10.1016/j.celrep.2016.12.041.

Bachstetter AD, Morganti JM, Jernberg J, Schlunk A, Mitchell SH, Brewster KW, Hudson CE, Cole MJ, Harrison JK, Bickford PC, Gemma C. Fractalkine and CX 3 CR1 regulate hippocampal neurogenesis in adult and aged rats. Neurobiol Aging. 2011 Nov;32(11):2030-44. doi: 10.1016/j.neurobiolaging.2009.11.022.

Badimon A, Strasburger HJ, Ayata P, Chen X, Nair A, Ikegami A, Hwang P, Chan AT, Graves SM, Uweru JO, Ledderose C, Kutlu MG, Wheeler MA, Kahan A, Ishikawa M, Wang YC, Loh YE, Jiang JX, Surmeier DJ, Robson SC, Junger WG, Sebra R, Calipari ES, Kenny PJ, Eyo UB, Colonna M, Quintana FJ, Wake H, Gradinaru V, Schaefer A. Negative feedback control of neuronal activity by microglia. Nature. 2020 Oct;586(7829):417-423. doi: 10.1038/s41586-020-2777-8.

Baker MJ, Trevisan J, Bassan P, Bhargava R, Butler HJ, Dorling KM, Fielden PR, Fogarty SW, Fullwood NJ, Heys KA, Hughes C, Lasch P, Martin-Hirsch PL, Obinaju B, Sockalingum GD, Sulé-Suso J, Strong RJ, Walsh MJ, Wood BR, Gardner P, Martin FL. Using Fourier transform IR spectroscopy to analyze biological materials. Nat Protoc. 2014 Aug;9(8):1771-91. doi: 10.1038/nprot.2014.110.

Barnum SR, Jones JL, Müller-Ladner U, Samimi A, Campbell IL. Chronic complement C3 gene expression in the CNS of transgenic mice with astrocyte-targeted interleukin-6 expression. Glia. 1996 Oct;18(2):107-17. doi: 10.1002/(SICI)1098-1136(199610)18:2<107::AID-GLIA3>3.0.CO;2-Y.

Barrientos RM, Higgins EA, Biedenkapp JC, Sprunger DB, Wright-Hardesty KJ, Watkins LR, Rudy JW, Maier SF. Peripheral infection and aging interact to impair hippocampal memory consolidation. Neurobiol Aging. 2006 May;27(5):723-32. doi: 10.1016/j.neurobiolaging.2005.03.010.

Barrientos RM, Kitt MM, Watkins LR, Maier SF. Neuroinflammation in the normal aging hippocampus. Neuroscience. 2015 Nov 19;309:84-99. doi: 10.1016/j.neuroscience.2015.03.007.

Bartzokis G, Cummings JL, Sultzer D, Henderson VW, Nuechterlein KH, Mintz J. White matter structural integrity in healthy aging adults and patients with Alzheimer disease: a magnetic resonance imaging study. Arch Neurol. 2003 Mar;60(3):393-8. doi: 10.1001/archneur.60.3.393.

Battista D, Ferrari CC, Gage FH, Pitossi FJ. Neurogenic niche modulation by activated microglia: transforming growth factor beta increases neurogenesis in the adult dentate gyrus. Eur J Neurosci. 2006 Jan;23(1):83-93. doi: 10.1111/j.1460-9568.2005.04539.x.

Beebe AM, Cua DJ, de Waal Malefyt R. The role of interleukin-10 in autoimmune disease: systemic lupus erythematosus (SLE) and multiple sclerosis (MS). Cytokine Growth Factor Rev. 2002 Aug-Oct;13(4-5):403-12. doi: 10.1016/s1359-6101(02)00025-4.

Bellinger FP, Madamba SG, Campbell IL, Siggins GR. Reduced long-term potentiation in the dentate gyrus of transgenic mice with cerebral overexpression of interleukin-6. Neurosci Lett. 1995 Sep 29;198(2):95-8. doi: 10.1016/0304-3940(95)11976-4.

Beltrán-Castillo S, Eugenín J, von Bernhardi R. Impact of Aging in Microglia-Mediated D-Serine Balance in the CNS. Mediators Inflamm. 2018 Sep 27;2018:7219732. doi: 10.1155/2018/7219732.

Bennett FC, Bennett ML, Yaqoob F, Mulinyawe SB, Grant GA, Hayden Gephart M, Plowey ED, Barres BA. A Combination of Ontogeny and CNS Environment Establishes Microglial Identity. Neuron. 2018 Jun 27;98(6):1170-1183.e8. doi: 10.1016/j.neuron.2018.05.014.

Bennett ML, Bennett FC. The influence of environment and origin on brain resident macrophages and implications for therapy. Nat Neurosci. 2020 Feb;23(2):157-166. doi: 10.1038/s41593-019-0545-6.

Berr C, Balansard B, Arnaud J, Roussel AM, Alpérovitch A. Cognitive decline is associated with systemic oxidative stress: the EVA study. Etude du Vieillissement Artériel. J Am Geriatr Soc. 2000 Oct;48(10):1285-91. doi: 10.1111/j.1532-5415.2000.tb02603.x.

Bettcher BM, Watson CL, Walsh CM, Lobach IV, Neuhaus J, Miller JW, Green R, Patel N, Dutt S, Busovaca E, Rosen HJ, Yaffe K, Miller BL, Kramer JH. Interleukin-6, age, and corpus callosum integrity. PLoS One. 2014 Sep 4;9(9):e106521. doi: 10.1371/journal.pone.0106521.

Bettelli E, Das MP, Howard ED, Weiner HL, Sobel RA, Kuchroo VK. IL-10 is critical in the regulation of autoimmune encephalomyelitis as demonstrated by studies of IL-10- and IL-4-deficient and transgenic mice. J Immunol. 1998 Oct 1;161(7):3299-306.

Biber K, Neumann H, Inoue K, Boddeke HW. Neuronal 'On' and 'Off' signals control microglia. Trends Neurosci. 2007 Nov;30(11):596-602. doi: 10.1016/j.tins.2007.08.007.

Blinzinger K, Kreutzberg G. Displacement of synaptic terminals from regenerating motoneurons by microglial cells. Z Zellforsch Mikrosk Anat. 1968;85(2):145-57. doi: 10.1007/BF00325030.

Bizon JL, Helm KA, Han JS, Chun HJ, Pucilowska J, Lund PK, Gallagher M. Hypothalamic-pituitary-adrenal axis function and corticosterone receptor expression in behaviourally characterized young and aged Long-Evans rats. Eur J Neurosci. 2001 Nov;14(10):1739-51. doi: 10.1046/j.0953-816x.2001.01781.x.

Bluthé RM, Michaud B, Poli V, Dantzer R. Role of IL-6 in cytokine-induced sickness behavior: a study with IL-6 deficient mice. Physiol Behav. 2000 Aug-Sep;70(3-4):367-73. doi: 10.1016/s0031-9384(00)00269-9.

Bohlen CJ, Bennett FC, Tucker AF, Collins HY, Mulinyawe SB, Barres BA. Diverse Requirements for Microglial Survival, Specification, and Function Revealed by Defined-Medium Cultures. Neuron. 2017 May 17;94(4):759-773.e8. doi: 10.1016/j.neuron.2017.04.043.

Björkqvist M, Wild EJ, Thiele J, Silvestroni A, Andre R, Lahiri N, Raibon E, Lee RV, Benn CL, Soulet D, Magnusson A, Woodman B, Landles C, Pouladi MA, Hayden MR, Khalili-Shirazi A, Lowdell MW, Brundin P, Bates GP, Leavitt BR, Möller T, Tabrizi SJ. A novel pathogenic pathway of immune activation detectable before clinical onset in Huntington's disease. J Exp Med. 2008 Aug 4;205(8):1869-77. doi: 10.1084/jem.20080178.

Bolin LM, Strycharska-Orczyk I, Murray R, Langston JW, Di Monte D. Increased vulnerability of dopaminergic neurons in MPTP-lesioned interleukin-6 deficient mice. J Neurochem. 2002 Oct;83(1):167-75. doi: 10.1046/j.1471-4159.2002.01131.x.

Bondolfi L, Ermini F, Long JM, Ingram DK, Jucker M. Impact of age and caloric restriction on neurogenesis in the dentate gyrus of C57BL/6 mice. Neurobiol Aging. 2004 Mar;25(3):333-40. doi: 10.1016/S0197-4580(03)00083-6.

Böttcher C, Schlickeiser S, Sneeboer MAM, Kunkel D, Knop A, Paza E, Fidzinski P, Kraus L, Snijders GJL, Kahn RS, Schulz AR, Mei HE; NBB-Psy, Hol EM, Siegmund B, Glauben R, Spruth EJ, de Witte LD, Priller J. Human microglia regional heterogeneity and phenotypes determined by multiplexed single-cell mass cytometry. Nat Neurosci. 2019 Jan;22(1):78-90. doi: 10.1038/s41593-018-0290-2.

Brewer KL, Bethea JR, Yezierski RP. Neuroprotective effects of interleukin-10 following excitotoxic spinal cord injury. Exp Neurol. 1999 Oct;159(2):484-93. doi: 10.1006/exnr.1999.7173.

Brown GC, Neher JJ. Microglial phagocytosis of live neurons. Nat Rev Neurosci. 2014 Apr;15(4):209-16. doi: 10.1038/nrn3710.

Bruttger J, Karram K, Wörtge S, Regen T, Marini F, Hoppmann N, Klein M, Blank T, Yona S, Wolf Y, Mack M, Pinteaux E, Müller W, Zipp F, Binder H, Bopp T, Prinz M, Jung S, Waisman A. Genetic Cell Ablation Reveals Clusters of Local Self-Renewing Microglia in the Mammalian Central Nervous System. Immunity. 2015 Jul 21;43(1):92-106. doi: 10.1016/j.immuni.2015.06.012.

Butovsky O, Ziv Y, Schwartz A, Landa G, Talpalar AE, Pluchino S, Martino G, Schwartz M. Microglia activated by IL-4 or IFN-gamma differentially induce neurogenesis and oligodendrogenesis from adult stem/progenitor cells. Mol Cell Neurosci. 2006 Jan;31(1):149-60. doi: 10.1016/j.mcn.2005.10.006.

Cacci E, Claasen JH, Kokaia Z. Microglia-derived tumor necrosis factor-alpha exaggerates death of newborn hippocampal progenitor cells in vitro. J Neurosci Res. 2005 Jun 15;80(6):789-97. doi: 10.1002/jnr.20531.

Caligiore D, Pezzulo G, Baldassarre G, Bostan AC, Strick PL, Doya K, Helmich RC, Dirkx M, Houk J, Jörntell H, Lago-Rodriguez A, Galea JM, Miall RC, Popa T, Kishore A, Verschure PF, Zucca R, Herreros I. Consensus Paper: Towards a Systems-Level View of Cerebellar Function: the Interplay Between Cerebellum, Basal Ganglia, and Cortex. Cerebellum. 2017 Feb;16(1):203-229. doi: 10.1007/s12311-016-0763-3.

Campbell IL, Abraham CR, Masliah E, Kemper P, Inglis JD, Oldstone MB, Mucke L. Neurologic disease induced in transgenic mice by cerebral overexpression of interleukin 6. Proc Natl Acad Sci U S A. 1993 Nov 1;90(21):10061-5. doi: 10.1073/pnas.90.21.10061.

Campbell IL, Erta M, Lim SL, Frausto R, May U, Rose-John S, Scheller J, Hidalgo J. Trans-signaling is a dominant mechanism for the pathogenic actions of interleukin-6 in the brain. J Neurosci. 2014 Feb 12;34(7):2503-13. doi: 10.1523/JNEUROSCI.2830-13.2014.

Campuzano O, Castillo-Ruiz MM, Acarin L, Castellano B, Gonzalez B. Increased levels of proinflammatory cytokines in the aged rat brain attenuate injury-induced cytokine response after excitotoxic damage. J Neurosci Res. 2009 Aug 15;87(11):2484-97. doi: 10.1002/jnr.22074.

Cannella B, Gao YL, Brosnan C, Raine CS. IL-10 fails to abrogate experimental autoimmune encephalomyelitis. J Neurosci Res. 1996 Sep 15;45(6):735-46. doi: 10.1002/(SICI)1097-4547(19960915)45:6<735::AID-JNR10>3.0.CO;2-V.

Cannella B, Raine CS. Multiple sclerosis: cytokine receptors on oligodendrocytes predict innate regulation. Ann Neurol. 2004 Jan;55(1):46-57. doi: 10.1002/ana.10764.

Cannon JP, O'Driscoll M, Litman GW. Specific lipid recognition is a general feature of CD300 and TREM molecules. Immunogenetics. 2012 Jan;64(1):39-47. doi: 10.1007/s00251-011-0562-4.

Cardona AE, Pioro EP, Sasse ME, Kostenko V, Cardona SM, Dijkstra IM, Huang D, Kidd G, Dombrowski S, Dutta R, Lee JC, Cook DN, Jung S, Lira SA, Littman DR, Ransohoff RM. Control of microglial neurotoxicity by the fractalkine receptor. Nat Neurosci. 2006 Jul;9(7):917-24. doi: 10.1038/nn1715.

Carpentier PA, Palmer TD. Immune influence on adult neural stem cell regulation and function. Neuron. 2009 Oct 15;64(1):79-92. doi: 10.1016/j.neuron.2009.08.038.

Casano AM, Peri F. Microglia: multitasking specialists of the brain. Dev Cell. 2015 Feb 23;32(4):469-77. doi: 10.1016/j.devcel.2015.01.018.

Castellano B, Bosch-Queralt M, Almolda B, Villacampa N, González B. Purine Signaling and Microglial Wrapping. Adv Exp Med Biol. 2016;949:147-165. doi: 10.1007/978-3-319-40764-7_7.

Chakrabarty P, Jansen-West K, Beccard A, Ceballos-Diaz C, Levites Y, Verbeeck C, Zubair AC, Dickson D, Golde TE, Das P. Massive gliosis induced by interleukin-6 suppresses Abeta deposition in vivo: evidence against inflammation as a driving force for amyloid deposition. FASEB J. 2010 Feb;24(2):548-59. doi: 10.1096/fj.09-141754.

Chakrabarty P, Li A, Ceballos-Diaz C, Eddy JA, Funk CC, Moore B, DiNunno N, Rosario AM, Cruz PE, Verbeeck C, Sacino A, Nix S, Janus C, Price ND, Das P, Golde TE. IL-10 alters immunoproteostasis in APP mice, increasing plaque burden and worsening cognitive behavior. Neuron. 2015 Feb 4;85(3):519-33. doi: 10.1016/j.neuron.2014.11.020.

Chambers JK, Uchida K, Nakayama H. White matter myelin loss in the brains of aged dogs. Exp Gerontol. 2012 Mar;47(3):263-9. doi: 10.1016/j.exger.2011.12.003.

Chan WY, Kohsaka S, Rezaie P. The origin and cell lineage of microglia: new concepts. Brain Res Rev. 2007 Feb;53(2):344-54. doi: 10.1016/j.brainresrev.2006.11.002.

Chapman TR, Barrientos RM, Ahrendsen JT, Hoover JM, Maier SF, Patterson SL. Aging and infection reduce expression of specific brain-derived neurotrophic factor mRNAs in hippocampus. Neurobiol Aging. 2012 Apr;33(4):832.e1-14. doi: 10.1016/j.neurobiolaging.2011.07.015.

Chapman TR, Barrientos RM, Ahrendsen JT, Maier SF, Patterson SL. Synaptic correlates of increased cognitive vulnerability with aging: peripheral immune challenge and aging interact to disrupt theta-burst late-phase long-term potentiation in hippocampal area CA1. J Neurosci. 2010 Jun 2;30(22):7598-603. doi: 10.1523/JNEUROSCI.5172-09.2010.

Chen J, Zhao Y, Liu Y. The role of nucleotides and purinergic signaling in apoptotic cell clearance - implications for chronic inflammatory diseases. Front Immunol. 2014 Dec 23;5:656. doi: 10.3389/fimmu.2014.00656.

Clarke LE, Liddelow SA, Chakraborty C, Münch AE, Heiman M, Barres BA. Normal aging induces A1-like astrocyte reactivity. Proc Natl Acad Sci U S A. 2018 Feb 20;115(8):E1896-E1905. doi: 10.1073/pnas.1800165115.

Clausen A, Doctrow S, Baudry M. Prevention of cognitive deficits and brain oxidative stress with superoxide dismutase/catalase mimetics in aged mice. Neurobiol Aging. 2010 Mar;31(3):425-33. doi: 10.1016/j.neurobiolaging.2008.05.009.

Colton CA. Heterogeneity of microglial activation in the innate immune response in the brain. J Neuroimmune Pharmacol. 2009 Dec;4(4):399-418. doi: 10.1007/s11481-009-9164-4.

Cornejo F, von Bernhardi R. Age-Dependent Changes in the Activation and Regulation of Microglia. Adv Exp Med Biol. 2016;949:205-226. doi: 10.1007/978-3-319-40764-7_10.

Corona AW, Fenn AM, Godbout JP. Cognitive and behavioral consequences of impaired immunoregulation in aging. J Neuroimmune Pharmacol. 2012 Mar;7(1):7-23. doi: 10.1007/s11481-011-9313-4.

Cortese GP, Barrientos RM, Maier SF, Patterson SL. Aging and a peripheral immune challenge interact to reduce mature brain-derived neurotrophic factor and activation of TrkB, PLCgamma1, and ERK in hippocampal synaptoneurosomes. J Neurosci. 2011 Mar 16;31(11):4274-9. doi: 10.1523/JNEUROSCI.5818-10.2011.

Couper KN, Blount DG, Riley EM. IL-10: the master regulator of immunity to infection. J Immunol. 2008 May 1;180(9):5771-7. doi: 10.4049/jimmunol.180.9.5771.

Cox FF, Carney D, Miller AM, Lynch MA. CD200 fusion protein decreases microglial activation in the hippocampus of aged rats. Brain Behav Immun. 2012 Jul;26(5):789-96. doi: 10.1016/j.bbi.2011.10.004.

Cronk JC, Filiano AJ, Louveau A, Marin I, Marsh R, Ji E, Goldman DH, Smirnov I, Geraci N, Acton S, Overall CC, Kipnis J. Peripherally derived macrophages can engraft the brain independent of irradiation and maintain an identity distinct from microglia. J Exp Med. 2018 Jun 4;215(6):1627-1647. doi: 10.1084/jem.20180247.

Croxford JL, Feldmann M, Chernajovsky Y, Baker D. Different therapeutic outcomes in experimental allergic encephalomyelitis dependent upon the mode of delivery of IL-10: a comparison of the effects of protein, adenoviral or retroviral IL-10 delivery into the central nervous system. J Immunol. 2001 Mar 15;166(6):4124-30. doi: 10.4049/jimmunol.166.6.4124.

Cua DJ, Groux H, Hinton DR, Stohlman SA, Coffman RL. Transgenic interleukin 10 prevents induction of experimental autoimmune encephalomyelitis. J Exp Med. 1999 Mar 15;189(6):1005-10. doi: 10.1084/jem.189.6.1005.

Cua DJ, Hutchins B, LaFace DM, Stohlman SA, Coffman RL. Central nervous system expression of IL-10 inhibits autoimmune encephalomyelitis. J Immunol. 2001 Jan 1;166(1):602-8. doi: 10.4049/jimmunol.166.1.602.

Cunningham CL, Martínez-Cerdeño V, Noctor SC. Microglia regulate the number of neural precursor cells in the developing cerebral cortex. J Neurosci. 2013 Mar 6;33(10):4216-33. doi: 10.1523/JNEUROSCI.3441-12.2013.

Cunningham C, Wilcockson DC, Campion S, Lunnon K, Perry VH. Central and systemic endotoxin challenges exacerbate the local inflammatory response and increase neuronal death during chronic neurodegeneration. J Neurosci. 2005 Oct 5;25(40):9275-84. doi: 10.1523/JNEUROSCI.2614-05.2005.

Dace DS, Khan AA, Stark JL, Kelly J, Cross AH, Apte RS. Interleukin-10 overexpression promotes Fas-ligand-dependent chronic macrophage-mediated demyelinating polyneuropathy. PLoS One. 2009 Sep 22;4(9):e7121. doi: 10.1371/journal.pone.0007121.

Damani MR, Zhao L, Fontainhas AM, Amaral J, Fariss RN, Wong WT. Age-related alterations in the dynamic behavior of microglia. Aging Cell. 2011 Apr;10(2):263-76. doi: 10.1111/j.1474-9726.2010.00660.x.

Dantzer R. Cytokine-induced sickness behavior: mechanisms and implications. Ann N Y Acad Sci. 2001 Mar;933:222-34. doi: 10.1111/j.1749-6632.2001.tb05827.x.

Davalos D, Grutzendler J, Yang G, Kim JV, Zuo Y, Jung S, Littman DR, Dustin ML, Gan WB. ATP mediates rapid microglial response to local brain injury in vivo. Nat Neurosci. 2005 Jun;8(6):752-8. doi: 10.1038/nn1472.

Deczkowska A, Keren-Shaul H, Weiner A, Colonna M, Schwartz M, Amit I. Disease-Associated Microglia: A Universal Immune Sensor of Neurodegeneration. Cell. 2018 May 17;173(5):1073-1081. doi: 10.1016/j.cell.2018.05.003.

de Haas AH, Boddeke HW, Biber K. Region-specific expression of immunoregulatory proteins on microglia in the healthy CNS. Glia. 2008 Jun;56(8):888-94. doi: 10.1002/glia.20663. PMID:

de Leeuw FE, de Groot JC, Achten E, Oudkerk M, Ramos LM, Heijboer R, Hofman A, Jolles J, van Gijn J, Breteler MM. Prevalence of cerebral white matter lesions in elderly people: a population based magnetic resonance imaging study. The Rotterdam Scan Study. J Neurol Neurosurg Psychiatry. 2001 Jan;70(1):9-14. doi: 10.1136/jnnp.70.1.9.

del Río-Hortega P. El ''Tercer Elemento'' de los Centros Nerviosos. I. La Microglía en Estado Normal. Bol Soc Esp Biol VIII. 1919a;67–82.

del Río-Hortega P. El "Tercer Elemento de los Centros Nerviosos". II. Intervención de la Microglía en los Procesos Patológicos (Células en Bastoncito y Cuerpos Gránuloadiposos). Bol Soc Esp Biol VIII. 1919b;91–103.

del Río-Hortega P. El ''Tercer Elemento'' de los Centros Nerviosos. III. Naturaleza Probable de la Microglía. Bol Soc Esp Biol VIII. 1919c;108–121.

del Río-Hortega P. El "Tercer Elemento de los Centros Nerviosos". IV. Poder Fagocitario y Movilidad de la Microglía. Bol Soc Esp Biol VIII. 1919d;154–171.

Ding X, Yan Y, Li X, Li K, Ciric B, Yang J, Zhang Y, Wu S, Xu H, Chen W, Lovett-Racke AE, Zhang GX, Rostami A. Silencing IFN-γ binding/signaling in astrocytes versus microglia leads to opposite effects on central nervous system autoimmunity. J Immunol. 2015 May 1;194(9):4251-64. doi: 10.4049/jimmunol.1303321.

Dissing-Olesen L, LeDue JM, Rungta RL, Hefendehl JK, Choi HB, MacVicar BA. Activation of neuronal NMDA receptors triggers transient ATP-mediated microglial process outgrowth. J Neurosci. 2014 Aug 6;34(32):10511-27. doi: 10.1523/JNEUROSCI.0405-14.2014.

Dowlati Y, Herrmann N, Swardfager W, Liu H, Sham L, Reim EK, Lanctôt KL. A meta-analysis of cytokines in major depression. Biol Psychiatry. 2010 Mar 1;67(5):446-57. doi: 10.1016/j.biopsych.2009.09.033.

Drapeau E, Mayo W, Aurousseau C, Le Moal M, Piazza PV, Abrous DN. Spatial memory performances of aged rats in the water maze predict levels of hippocampal neurogenesis. Proc Natl Acad Sci U S A. 2003 Nov 25;100(24):14385-90. doi: 10.1073/pnas.2334169100.

Duarte Azevedo M, Sander S, Tenenbaum L. GDNF, A Neuron-Derived Factor Upregulated in Glial Cells during Disease. J Clin Med. 2020 Feb 7;9(2):456. doi: 10.3390/jcm9020456.

Ekdahl CT, Claasen JH, Bonde S, Kokaia Z, Lindvall O. Inflammation is detrimental for neurogenesis in adult brain. Proc Natl Acad Sci U S A. 2003 Nov 11;100(23):13632-7. doi: 10.1073/pnas.2234031100.

Elmore MRP, Hohsfield LA, Kramár EA, Soreq L, Lee RJ, Pham ST, Najafi AR, Spangenberg EE, Wood MA, West BL, Green KN. Replacement of microglia in the aged brain reverses cognitive, synaptic, and neuronal deficits in mice. Aging Cell. 2018 Dec;17(6):e12832. doi: 10.1111/acel.12832.

Ershler WB, Keller ET. Age-associated increased interleukin-6 gene expression, late-life diseases, and frailty. Annu Rev Med. 2000;51:245-70. doi: 10.1146/annurev.med.51.1.245.

Erta M, Quintana A, Hidalgo J. Interleukin-6, a major cytokine in the central nervous system. Int J Biol Sci. 2012;8(9):1254-66. doi: 10.7150/ijbs.4679.

Eugster HP, Frei K, Kopf M, Lassmann H, Fontana A. IL-6-deficient mice resist myelin oligodendrocyte glycoprotein-induced autoimmune encephalomyelitis. Eur J Immunol. 1998 Jul;28(7):2178-87. doi: 10.1002/(SICI)1521-4141(199807)28:07<2178::AID-IMMU2178>3.0.CO;2-D.

Eyo UB, Peng J, Swiatkowski P, Mukherjee A, Bispo A, Wu LJ. Neuronal hyperactivity recruits microglial processes via neuronal NMDA receptors and microglial P2Y12 receptors after status epilepticus. J Neurosci. 2014 Aug 6;34(32):10528-40. doi: 10.1523/JNEUROSCI.0416-14.2014.

Franceschi C, Bonafè M, Valensin S, Olivieri F, De Luca M, Ottaviani E, De Benedictis G. Inflamm-aging. An evolutionary perspective on immunosenescence. Ann N Y Acad Sci. 2000 Jun;908:244-54. doi: 10.1111/j.1749-6632.2000.tb06651.x.

Frank MG, Barrientos RM, Biedenkapp JC, Rudy JW, Watkins LR, Maier SF. mRNA up-regulation of MHC II and pivotal pro-inflammatory genes in normal brain aging. Neurobiol Aging. 2006 May;27(5):717-22. doi: 10.1016/j.neurobiolaging.2005.03.013.

Frank MG, Barrientos RM, Hein AM, Biedenkapp JC, Watkins LR, Maier SF. IL-1RA blocks E. coli-induced suppression of Arc and long-term memory in aged F344xBN F1 rats. Brain Behav Immun. 2010 Feb;24(2):254-62. doi: 10.1016/j.bbi.2009.10.005.

Fu R, Shen Q, Xu P, Luo JJ, Tang Y. Phagocytosis of microglia in the central nervous system diseases. Mol Neurobiol. 2014 Jun;49(3):1422-34. doi: 10.1007/s12035-013-8620-6.

Gadient RA, Otten U. Expression of interleukin-6 (IL-6) and interleukin-6 receptor (IL-6R) mRNAs in rat brain during postnatal development. Brain Res. 1994 Feb 21;637(1-2):10-4. doi: 10.1016/0006-8993(94)91211-4.

Gadient RA, Otten U. Interleukin-6 and interleukin-6 receptor mRNA expression in rat central nervous system. Ann N Y Acad Sci. 1995 Jul 21;762:403-6. doi: 10.1111/j.1749-6632.1995.tb32348.x.

Gadient RA, Otten UH. Interleukin-6 (IL-6)--a molecule with both beneficial and destructive potentials. Prog Neurobiol. 1997 Aug;52(5):379-90. doi: 10.1016/s0301-0082(97)00021-x.

Garner KM, Amin R, Johnson RW, Scarlett EJ, Burton MD. Microglia priming by interleukin-6 signaling is enhanced in aged mice. J Neuroimmunol. 2018 Nov 15;324:90-99. doi: 10.1016/j.jneuroim.2018.09.002.

Gavilán MP, Revilla E, Pintado C, Castaño A, Vizuete ML, Moreno-González I, Baglietto-Vargas D, Sánchez-Varo R, Vitorica J, Gutiérrez A, Ruano D. Molecular and cellular characterization of the age-related neuroinflammatory processes occurring in normal rat hippocampus: potential relation with the loss of somatostatin GABAergic neurons. J Neurochem. 2007 Nov;103(3):984-96. doi: 10.1111/j.1471-4159.2007.04787.x.

Geinisman Y, de Toledo-Morrell L, Morrell F. Loss of perforated synapses in the dentate gyrus: morphological substrate of memory deficit in aged rats. Proc Natl Acad Sci U S A. 1986 May;83(9):3027-31. doi: 10.1073/pnas.83.9.3027.

Gijbels K, Brocke S, Abrams JS, Steinman L. Administration of neutralizing antibodies to interleukin-6 (IL-6) reduces experimental autoimmune encephalomyelitis and is associated with elevated levels of IL-6 bioactivity in central nervous system and circulation. Mol Med. 1995 Nov;1(7):795-805.

Ginhoux F, Greter M, Leboeuf M, Nandi S, See P, Gokhan S, Mehler MF, Conway SJ, Ng LG, Stanley ER, Samokhvalov IM, Merad M. Fate mapping analysis reveals that adult microglia derive from primitive macrophages. Science. 2010 Nov 5;330(6005):841-5. doi: 10.1126/science.1194637.

Giralt M, Ramos R, Quintana A, Ferrer B, Erta M, Castro-Freire M, Comes G, Sanz E, Unzeta M, Pifarré P, García A, Campbell IL, Hidalgo J. Induction of atypical EAE mediated by transgenic production of IL-6 in astrocytes in the absence of systemic IL-6. Glia. 2013 Apr;61(4):587-600. doi: 10.1002/glia.22457.

Godbout JP, Chen J, Abraham J, Richwine AF, Berg BM, Kelley KW, Johnson RW. Exaggerated neuroinflammation and sickness behavior in aged mice following activation of the peripheral innate immune system. FASEB J. 2005 Aug;19(10):1329-31. doi: 10.1096/fj.05-3776fje.

Godbout JP, Johnson RW. Interleukin-6 in the aging brain. J Neuroimmunol. 2004 Feb;147(1-2):141-4. doi: 10.1016/j.jneuroim.2003.10.031.

Gomez Perdiguero E, Klapproth K, Schulz C, Busch K, Azzoni E, Crozet L, Garner H, Trouillet C, de Bruijn MF, Geissmann F, Rodewald HR. Tissue-resident macrophages originate from yolk-sac-derived erythro-myeloid progenitors. Nature. 2015 Feb 26;518(7540):547-51. doi: 10.1038/nature13989.

Gosselin D, Link VM, Romanoski CE, Fonseca GJ, Eichenfield DZ, Spann NJ, Stender JD, Chun HB, Garner H, Geissmann F, Glass CK. Environment drives selection and function of enhancers controlling tissue-specific macrophage identities. Cell. 2014 Dec 4;159(6):1327-40. doi: 10.1016/j.cell.2014.11.023.

Gosselin D, Skola D, Coufal NG, Holtman IR, Schlachetzki JCM, Sajti E, Jaeger BN, O'Connor C, Fitzpatrick C, Pasillas MP, Pena M, Adair A, Gonda DD, Levy ML, Ransohoff RM, Gage FH, Glass CK. An environment-dependent transcriptional network specifies human microglia identity. Science. 2017 Jun 23;356(6344):eaal3222. doi: 10.1126/science.aal3222.

Grabert K, Michoel T, Karavolos MH, Clohisey S, Baillie JK, Stevens MP, Freeman TC, Summers KM, McColl BW. Microglial brain region-dependent diversity and selective regional sensitivities to aging. Nat Neurosci. 2016 Mar;19(3):504-16. doi: 10.1038/nn.4222.

Guillot-Sestier MV, Doty KR, Gate D, Rodriguez J Jr, Leung BP, Rezai-Zadeh K, Town T. Il10 deficiency rebalances innate immunity to mitigate Alzheimer-like pathology. Neuron. 2015 Feb 4;85(3):534-48. doi: 10.1016/j.neuron.2014.12.068.

Gupta A, Hasan M, Chander R, Kapoor NK. Age-related elevation of lipid peroxidation products: diminution of superoxide dismutase activity in the central nervous system of rats. Gerontology. 1991;37(6):305-9. doi: 10.1159/000213277.

Guttmann CR, Jolesz FA, Kikinis R, Killiany RJ, Moss MB, Sandor T, Albert MS. White matter changes with normal aging. Neurology. 1998 Apr;50(4):972-8. doi: 10.1212/wnl.50.4.972.

Gyengesi E, Rangel A, Ullah F, Liang H, Niedermayer G, Asgarov R, Venigalla M, Gunawardena D, Karl T, Münch G. Chronic Microglial Activation in the GFAP-IL6 Mouse Contributes to Age-Dependent Cerebellar Volume Loss and Impairment in Motor Function. Front Neurosci. 2019 Apr 3;13:303. doi: 10.3389/fnins.2019.00303.

Halliwell B. Reactive oxygen species and the central nervous system. J Neurochem. 1992 Nov;59(5):1609-23. doi: 10.1111/j.1471-4159.1992.tb10990.x. Erratum in: J Neurochem. 2012 Mar;120(5):850.

Hammond TR, Dufort C, Dissing-Olesen L, Giera S, Young A, Wysoker A, Walker AJ, Gergits F, Segel M, Nemesh J, Marsh SE, Saunders A, Macosko E, Ginhoux F, Chen J, Franklin RJM, Piao X, McCarroll SA, Stevens B. Single-Cell RNA Sequencing of Microglia throughout the Mouse Lifespan and in the Injured Brain Reveals Complex Cell-State Changes. Immunity. 2019 Jan 15;50(1):253-271.e6. doi: 10.1016/j.immuni.2018.11.004.

Hanisch UK, Kettenmann H. Microglia: active sensor and versatile effector cells in the normal and pathologic brain. Nat Neurosci. 2007 Nov;10(11):1387-94. doi: 10.1038/nn1997.

Harman D. Aging: a theory based on free radical and radiation chemistry. J Gerontol. 1956 Jul;11(3):298-300. doi: 10.1093/geronj/11.3.298.

Hart AD, Wyttenbach A, Perry VH, Teeling JL. Age related changes in microglial phenotype vary between CNS regions: grey versus white matter differences. Brain Behav Immun. 2012 Jul;26(5):754-65. doi: 10.1016/j.bbi.2011.11.006.

Hashimoto D, Chow A, Noizat C, Teo P, Beasley MB, Leboeuf M, Becker CD, See P, Price J, Lucas D, Greter M, Mortha A, Boyer SW, Forsberg EC, Tanaka M, van Rooijen N, García-Sastre A, Stanley ER, Ginhoux F, Frenette PS, Merad M. Tissue-resident macrophages self-maintain locally throughout adult life with minimal contribution from circulating monocytes. Immunity. 2013 Apr 18;38(4):792-804. doi: 10.1016/j.immuni.2013.04.004.

Henry CJ, Huang Y, Wynne AM, Godbout JP. Peripheral lipopolysaccharide (LPS) challenge promotes microglial hyperactivity in aged mice that is associated with exaggerated induction of both pro-inflammatory IL-1beta and anti-inflammatory IL-10 cytokines. Brain Behav Immun. 2009 Mar;23(3):309-17. doi: 10.1016/j.bbi.2008.09.002.

Hernández J, Molinero A, Campbell IL, Hidalgo J. Transgenic expression of interleukin 6 in the central nervous system regulates brain metallothionein-I and -III expression in mice. Brain Res Mol Brain Res. 1997 Aug;48(1):125-31. doi: 10.1016/s0169-328x(97)00087-9.

Heyser CJ, Masliah E, Samimi A, Campbell IL, Gold LH. Progressive decline in avoidance learning paralleled by inflammatory neurodegeneration in transgenic mice expressing interleukin 6 in the brain. Proc Natl Acad Sci U S A. 1997 Feb 18;94(4):1500-5. doi: 10.1073/pnas.94.4.1500.

Hickman SE, Allison EK, El Khoury J. Microglial dysfunction and defective beta-amyloid clearance pathways in aging Alzheimer's disease mice. J Neurosci. 2008 Aug 13;28(33):8354-60. doi: 10.1523/JNEUROSCI.0616-08.2008.

Hickman SE, Kingery ND, Ohsumi TK, Borowsky ML, Wang LC, Means TK, El Khoury J. The microglial sensome revealed by direct RNA sequencing. Nat Neurosci. 2013 Dec;16(12):1896-905. doi: 10.1038/nn.3554.

Hinman JD, Abraham CR. What's behind the decline? The role of white matter in brain aging. Neurochem Res. 2007 Dec;32(12):2023-31. doi: 10.1007/s11064-007-9341-x.

Hoeffel G, Chen J, Lavin Y, Low D, Almeida FF, See P, Beaudin AE, Lum J, Low I, Forsberg EC, Poidinger M, Zolezzi F, Larbi A, Ng LG, Chan JK, Greter M, Becher B, Samokhvalov IM, Merad M, Ginhoux F. C-Myb(+) erythro-myeloid progenitor-derived fetal monocytes give rise to adult tissue-resident macrophages. Immunity. 2015 Apr 21;42(4):665-78. doi: 10.1016/j.immuni.2015.03.011.

Hong S, Beja-Glasser VF, Nfonoyim BM, Frouin A, Li S, Ramakrishnan S, Merry KM, Shi Q, Rosenthal A, Barres BA, Lemere CA, Selkoe DJ, Stevens B. Complement and microglia mediate early synapse loss in Alzheimer mouse models. Science. 2016 May 6;352(6286):712-716. doi: 10.1126/science.aad8373.

Hoyos HC, Rinaldi M, Mendez-Huergo SP, Marder M, Rabinovich GA, Pasquini JM, Pasquini LA. Galectin-3 controls the response of microglial cells to limit cuprizone-induced demyelination. Neurobiol Dis. 2014 Feb;62:441-55. doi: 10.1016/j.nbd.2013.10.023.

Hsieh CL, Koike M, Spusta SC, Niemi EC, Yenari M, Nakamura MC, Seaman WE. A role for TREM2 ligands in the phagocytosis of apoptotic neuronal cells by microglia. J Neurochem. 2009 May;109(4):1144-56. doi: 10.1111/j.1471-4159.2009.06042.x.

Hu X, Liou AK, Leak RK, Xu M, An C, Suenaga J, Shi Y, Gao Y, Zheng P, Chen J. Neurobiology of microglial action in CNS injuries: receptor-mediated signaling mechanisms and functional roles. Prog Neurobiol. 2014 Aug-Sep;119-120:60-84. doi: 10.1016/j.pneurobio.2014.06.002.

Hüll M, Strauss S, Berger M, Volk B, Bauer J. The participation of interleukin-6, a stress-inducible cytokine, in the pathogenesis of Alzheimer's disease. Behav Brain Res. 1996 Jun;78(1):37-41. doi: 10.1016/0166-4328(95)00213-8.

Hunter CA, Jones SA. IL-6 as a keystone cytokine in health and disease. Nat Immunol. 2015 May;16(5):448-57. doi: 10.1038/ni.3153. Erratum in: Nat Immunol. 2017 Oct 18;18(11):1271.

Hutchins AP, Diez D, Miranda-Saavedra D. The IL-10/STAT3-mediated anti-inflammatory response: recent developments and future challenges. Brief Funct Genomics. 2013 Nov;12(6):489-98. doi: 10.1093/bfgp/elt028.

Hwang IK, Lee CH, Li H, Yoo KY, Choi JH, Kim DW, Kim DW, Suh HW, Won MH. Comparison of ionized calcium-binding adapter molecule 1 immunoreactivity of the hippocampal dentate gyrus and CA1 region in adult and aged dogs. Neurochem Res. 2008 Jul;33(7):1309-15. doi: 10.1007/s11064-007-9584-6.

Ichinohe N, Mori F, Shoumura K. A di-synaptic projection from the lateral cerebellar nucleus to the laterodorsal part of the striatum via the central lateral nucleus of the thalamus in the rat. Brain Res. 2000 Oct 13;880(1-2):191-7. doi: 10.1016/s0006-8993(00)02744-x.

Islam O, Gong X, Rose-John S, Heese K. Interleukin-6 and neural stem cells: more than gliogenesis. Mol Biol Cell. 2009 Jan;20(1):188-99. doi: 10.1091/mbc.e08-05-0463.

Ji K, Akgul G, Wollmuth LP, Tsirka SE. Microglia actively regulate the number of functional synapses. PLoS One. 2013;8(2):e56293. doi: 10.1371/journal.pone.0056293.

Jurgens HA, Johnson RW. Dysregulated neuronal-microglial cross-talk during aging, stress and inflammation. Exp Neurol. 2012 Jan;233(1):40-8. doi: 10.1016/j.expneurol.2010.11.014.

Kaplin AI, Deshpande DM, Scott E, Krishnan C, Carmen JS, Shats I, Martinez T, Drummond J, Dike S, Pletnikov M, Keswani SC, Moran TH, Pardo CA, Calabresi PA, Kerr DA. IL-6 induces regionally selective spinal cord injury in patients with the neuroinflammatory disorder transverse myelitis. J Clin Invest. 2005 Oct;115(10):2731-41. doi: 10.1172/JCI25141.

Kasckow J, Xiao C, Herman JP. Glial glucocorticoid receptors in aged Fisher 344 (F344) and F344/Brown Norway rats. Exp Gerontol. 2009 May;44(5):335-43. doi: 10.1016/j.exger.2009.02.003.

Katusic ZS, Austin SA. Endothelial nitric oxide: protector of a healthy mind. Eur Heart J. 2014 Apr;35(14):888-94. doi: 10.1093/eurheartj/eht544.

Keren-Shaul H, Spinrad A, Weiner A, Matcovitch-Natan O, Dvir-Szternfeld R, Ulland TK, David E, Baruch K, Lara-Astaiso D, Toth B, Itzkovitz S, Colonna M, Schwartz M, Amit I. A Unique Microglia Type Associated with Restricting Development of Alzheimer's Disease. Cell. 2017 Jun 15;169(7):1276-1290.e17. doi: 10.1016/j.cell.2017.05.018.

Kishimoto T, Akira S, Narazaki M, Taga T. Interleukin-6 family of cytokines and gp130. Blood. 1995 Aug 15;86(4):1243-54.

Kiyota T, Ingraham KL, Swan RJ, Jacobsen MT, Andrews SJ, Ikezu T. AAV serotype 2/1-mediated gene delivery of anti-inflammatory interleukin-10 enhances neurogenesis and cognitive function in APP+PS1 mice. Gene Ther. 2012 Jul;19(7):724-33. doi: 10.1038/gt.2011.126.

Kiyota T, Okuyama S, Swan RJ, Jacobsen MT, Gendelman HE, Ikezu T. CNS expression of anti-inflammatory cytokine interleukin-4 attenuates Alzheimer's disease-like pathogenesis in APP+PS1 bigenic mice. FASEB J. 2010 Aug;24(8):3093-102. doi: 10.1096/fj.10-155317.

Klempin F, Kempermann G. Adult hippocampal neurogenesis and aging. Eur Arch Psychiatry Clin Neurosci. 2007 Aug;257(5):271-80. doi: 10.1007/s00406-007-0731-5.

Koenigsknecht-Talboo J, Landreth GE. Microglial phagocytosis induced by fibrillar beta-amyloid and IgGs are differentially regulated by proinflammatory cytokines. J Neurosci. 2005 Sep 7;25(36):8240-9. doi: 10.1523/JNEUROSCI.1808-05.2005.

Kohama SG, Goss JR, Finch CE, McNeill TH. Increases of glial fibrillary acidic protein in the aging female mouse brain. Neurobiol Aging. 1995 Jan-Feb;16(1):59-67. doi: 10.1016/0197-4580(95)80008-f.

Knoblach SM, Faden AI. Interleukin-10 improves outcome and alters proinflammatory cytokine expression after experimental traumatic brain injury. Exp Neurol. 1998 Sep;153(1):143-51. doi: 10.1006/exnr.1998.6877.

Krasemann S, Madore C, Cialic R, Baufeld C, Calcagno N, El Fatimy R, Beckers L, O'Loughlin E, Xu Y, Fanek Z, Greco DJ, Smith ST, Tweet G, Humulock Z, Zrzavy T, Conde-Sanroman P, Gacias M, Weng Z, Chen H, Tjon E, Mazaheri F, Hartmann K, Madi A, Ulrich JD, Glatzel M, Worthmann A, Heeren J, Budnik B, Lemere C, Ikezu T, Heppner FL, Litvak V, Holtzman DM, Lassmann H, Weiner HL, Ochando J, Haass C, Butovsky O. The TREM2-APOE Pathway Drives the Transcriptional Phenotype of Dysfunctional Microglia in Neurodegenerative Diseases. Immunity. 2017 Sep 19;47(3):566-581.e9. doi: 10.1016/j.immuni.2017.08.008.

Kreisel T, Wolf B, Keshet E, Licht T. Unique role for dentate gyrus microglia in neuroblast survival and in VEGF-induced activation. Glia. 2019 Apr;67(4):594-618. doi: 10.1002/glia.23505.

Kuhn HG, Dickinson-Anson H, Gage FH. Neurogenesis in the dentate gyrus of the adult rat: age-related decrease of neuronal progenitor proliferation. J Neurosci. 1996 Mar 15;16(6):2027-33. doi: 10.1523/JNEUROSCI.16-06-02027.1996.

Kuipers SD, Schroeder JE, Trentani A. Changes in hippocampal neurogenesis throughout early development. Neurobiol Aging. 2015 Jan;36(1):365-79. doi: 10.1016/j.neurobiolaging.2014.07.033.

Lavin Y, Winter D, Blecher-Gonen R, David E, Keren-Shaul H, Merad M, Jung S, Amit I. Tissue-resident macrophage enhancer landscapes are shaped by the local microenvironment. Cell. 2014 Dec 4;159(6):1312-26. doi: 10.1016/j.cell.2014.11.018.

Lawson LJ, Perry VH, Dri P, Gordon S. Heterogeneity in the distribution and morphology of microglia in the normal adult mouse brain. Neuroscience. 1990;39(1):151-70. doi: 10.1016/0306-4522(90)90229-w.

Lawson LJ, Perry VH, Gordon S. Turnover of resident microglia in the normal adult mouse brain. Neuroscience. 1992;48(2):405-15. doi: 10.1016/0306-4522(92)90500-2.

Ledeboer A, Brevé JJ, Wierinckx A, van der Jagt S, Bristow AF, Leysen JE, Tilders FJ, Van Dam AM. Expression and regulation of interleukin-10 and interleukin-10 receptor in rat astroglial and microglial cells. Eur J Neurosci. 2002 Oct;16(7):1175-85. doi: 10.1046/j.1460-9568.2002.02200.x.

Lee M, Schwab C, McGeer PL. Astrocytes are GABAergic cells that modulate microglial activity. Glia. 2011 Jan;59(1):152-65. doi: 10.1002/glia.21087.

Lee CK, Weindruch R, Prolla TA. Gene-expression profile of the ageing brain in mice. Nat Genet. 2000 Jul;25(3):294-7. doi: 10.1038/77046.

Letiembre M, Hao W, Liu Y, Walter S, Mihaljevic I, Rivest S, Hartmann T, Fassbender K. Innate immune receptor expression in normal brain aging. Neuroscience. 2007 Apr 25;146(1):248-54. doi: 10.1016/j.neuroscience.2007.01.004.

Leutner S, Eckert A, Müller WE. ROS generation, lipid peroxidation and antioxidant enzyme activities in the aging brain. J Neural Transm (Vienna). 2001;108(8-9):955-67. doi: 10.1007/s007020170015.

Li Q, Cheng Z, Zhou L, Darmanis S, Neff NF, Okamoto J, Gulati G, Bennett ML, Sun LO, Clarke LE, Marschallinger J, Yu G, Quake SR, Wyss-Coray T, Barres BA. Developmental Heterogeneity of Microglia and Brain Myeloid Cells Revealed by Deep Single-Cell RNA Sequencing. Neuron. 2019 Jan 16;101(2):207-223.e10. doi: 10.1016/j.neuron.2018.12.006.

Li Y, Du XF, Du JL. Resting microglia respond to and regulate neuronal activity in vivo. Commun Integr Biol. 2013 Jul 1;6(4):e24493. doi: 10.4161/cib.24493.

Lichtenwalner RJ, Forbes ME, Bennett SA, Lynch CD, Sonntag WE, Riddle DR. Intracerebroventricular infusion of insulin-like growth factor-I ameliorates the age-related decline in hippocampal neurogenesis. Neuroscience. 2001;107(4):603-13. doi: 10.1016/s0306-4522(01)00378-5.

Lim SH, Park E, You B, Jung Y, Park AR, Park SG, Lee JR. Neuronal synapse formation induced by microglia and interleukin 10. PLoS One. 2013 Nov 22;8(11):e81218. doi: 10.1371/journal.pone.0081218.

Linnartz B, Neumann H. Microglial activatory (immunoreceptor tyrosine-based activation motif)- and inhibitory (immunoreceptor tyrosine-based inhibition motif)-signaling receptors for recognition of the neuronal glycocalyx. Glia. 2013 Jan;61(1):37-46. doi: 10.1002/glia.22359.

Liu J, Solway K, Messing RO, Sharp FR. Increased neurogenesis in the dentate gyrus after transient global ischemia in gerbils. J Neurosci. 1998 Oct 1;18(19):7768-78. doi: 10.1523/JNEUROSCI.18-19-07768.1998.

López-Otín C, Blasco MA, Partridge L, Serrano M, Kroemer G. The hallmarks of aging. Cell. 2013 Jun 6;153(6):1194-217. doi: 10.1016/j.cell.2013.05.039.

Lucin KM, Wyss-Coray T. Immune activation in brain aging and neurodegeneration: too much or too little? Neuron. 2009 Oct 15;64(1):110-22. doi: 10.1016/j.neuron.2009.08.039.

Lund H, Pieber M, Parsa R, Han J, Grommisch D, Ewing E, Kular L, Needhamsen M, Espinosa A, Nilsson E, Överby AK, Butovsky O, Jagodic M, Zhang XM, Harris RA. Competitive repopulation of an empty microglial niche yields functionally distinct subsets of microglia-like cells. Nat Commun. 2018 Nov 19;9(1):4845. doi: 10.1038/s41467-018-07295-7.

Lynch MA. Age-related impairment in long-term potentiation in hippocampus: a role for the cytokine, interleukin-1 beta? Prog Neurobiol. 1998 Dec;56(5):571-89. doi: 10.1016/s0301-0082(98)00054-9. PMID: 9775404.

Lyons A, Downer EJ, Crotty S, Nolan YM, Mills KH, Lynch MA. CD200 ligand receptor interaction modulates microglial activation in vivo and in vitro: a role for IL-4. J Neurosci. 2007 Aug 1;27(31):8309-13. doi: 10.1523/JNEUROSCI.1781-07.2007.

Lyons A, Lynch AM, Downer EJ, Hanley R, O'Sullivan JB, Smith A, Lynch MA. Fractalkine-induced activation of the phosphatidylinositol-3 kinase pathway attenuates microglial activation in vivo and in vitro. J Neurochem. 2009 Sep;110(5):1547-56. doi: 10.1111/j.1471-4159.2009.06253.x.

Maes M, Scharpé S, Meltzer HY, Bosmans E, Suy E, Calabrese J, Cosyns P. Relationships between interleukin-6 activity, acute phase proteins, and function of the hypothalamic-pituitary-adrenal axis in severe depression. Psychiatry Res. 1993 Oct;49(1):11-27. doi: 10.1016/0165-1781(93)90027-e.

Maher FO, Martin DS, Lynch MA. Increased IL-1beta in cortex of aged rats is accompanied by downregulation of ERK and PI-3 kinase. Neurobiol Aging. 2004 Jul;25(6):795-806. doi: 10.1016/j.neurobiolaging.2003.08.007.

Maher FO, Nolan Y, Lynch MA. Downregulation of IL-4-induced signalling in hippocampus contributes to deficits in LTP in the aged rat. Neurobiol Aging. 2005 May;26(5):717-28. doi: 10.1016/j.neurobiolaging.2004.07.002.

Manich G, Gómez-López AR, Almolda B, Villacampa N, Recasens M, Shrivastava K, González B, Castellano B. Differential Roles of TREM2+ Microglia in Anterograde and Retrograde Axonal Injury Models. Front Cell Neurosci. 2020 Nov 20;14:567404. doi: 10.3389/fncel.2020.567404.

Manich G, Recasens M, Valente T, Almolda B, González B, Castellano B. Role of the CD200-CD200R Axis During Homeostasis and Neuroinflammation. Neuroscience. 2019 May 1;405:118-136. doi: 10.1016/j.neuroscience.2018.10.030.

Masuda T, Sankowski R, Staszewski O, Böttcher C, Amann L, Sagar, Scheiwe C, Nessler S, Kunz P, van Loo G, Coenen VA, Reinacher PC, Michel A, Sure U, Gold R, Grün D, Priller J, Stadelmann C, Prinz M. Spatial and temporal heterogeneity of mouse and human microglia at single-cell resolution. Nature. 2019 Feb;566(7744):388-392. doi: 10.1038/s41586-019-0924-x. Erratum in: Nature. 2019 Apr;568(7751):E4.

Mattson MP, Magnus T. Ageing and neuronal vulnerability. Nat Rev Neurosci. 2006 Apr;7(4):278-94. doi: 10.1038/nrn1886.

Mizoguchi K, Ikeda R, Shoji H, Tanaka Y, Maruyama W, Tabira T. Aging attenuates glucocorticoid negative feedback in rat brain. Neuroscience. 2009 Mar 3;159(1):259-70. doi: 10.1016/j.neuroscience.2008.12.020.

Monje ML, Toda H, Palmer TD. Inflammatory blockade restores adult hippocampal neurogenesis. Science. 2003 Dec 5;302(5651):1760-5. doi: 10.1126/science.1088417.

Moore KW, de Waal Malefyt R, Coffman RL, O'Garra A. Interleukin-10 and the interleukin-10 receptor. Annu Rev Immunol. 2001;19:683-765. doi: 10.1146/annurev.immunol.19.1.683.

Mosher KI, Wyss-Coray T. Microglial dysfunction in brain aging and Alzheimer's disease. Biochem Pharmacol. 2014 Apr 15;88(4):594-604. doi: 10.1016/j.bcp.2014.01.008.

Mott RT, Ait-Ghezala G, Town T, Mori T, Vendrame M, Zeng J, Ehrhart J, Mullan M, Tan J. Neuronal expression of CD22: novel mechanism for inhibiting microglial proinflammatory cytokine production. Glia. 2004 May;46(4):369-79. doi: 10.1002/glia.20009.

Mrak RE, Griffin WS. Glia and their cytokines in progression of neurodegeneration. Neurobiol Aging. 2005 Mar;26(3):349-54. doi: 10.1016/j.neurobiolaging.2004.05.010.

Müller T, Blum-Degen D, Przuntek H, Kuhn W. Interleukin-6 levels in cerebrospinal fluid inversely correlate to severity of Parkinson's disease. Acta Neurol Scand. 1998 Aug;98(2):142-4. doi: 10.1111/j.1600-0404.1998.tb01736.x.

Nakagawa E, Aimi Y, Yasuhara O, Tooyama I, Shimada M, McGeer PL, Kimura H. Enhancement of progenitor cell division in the dentate gyrus triggered by initial limbic seizures in rat models of epilepsy. Epilepsia. 2000 Jan;41(1):10-8. doi: 10.1111/j.1528-1157.2000.tb01498.x.

Nakanishi M, Niidome T, Matsuda S, Akaike A, Kihara T, Sugimoto H. Microglia-derived interleukin-6 and leukaemia inhibitory factor promote astrocytic differentiation of neural stem/progenitor cells. Eur J Neurosci. 2007 Feb;25(3):649-58. doi: 10.1111/j.1460-9568.2007.05309.x.

Neher JJ, Cunningham C. Priming Microglia for Innate Immune Memory in the Brain. Trends Immunol. 2019 Apr;40(4):358-374. doi: 10.1016/j.it.2019.02.001.

Neumann H, Kotter MR, Franklin RJ. Debris clearance by microglia: an essential link between degeneration and regeneration. Brain. 2009 Feb;132(Pt 2):288-95. doi: 10.1093/brain/awn109.

Neumann H, Wekerle H. Neuronal control of the immune response in the central nervous system: linking brain immunity to neurodegeneration. J Neuropathol Exp Neurol. 1998 Jan;57(1):1-9. doi: 10.1097/00005072-199801000-00001.

Nichols NR, Day JR, Laping NJ, Johnson SA, Finch CE. GFAP mRNA increases with age in rat and human brain. Neurobiol Aging. 1993 Sep-Oct;14(5):421-9. doi: 10.1016/0197-4580(93)90100-p.

Njie EG, Boelen E, Stassen FR, Steinbusch HW, Borchelt DR, Streit WJ. Ex vivo cultures of microglia from young and aged rodent brain reveal age-related changes in microglial function. Neurobiol Aging. 2012 Jan;33(1):195.e1-12. doi: 10.1016/j.neurobiolaging.2010.05.008.

Nimmerjahn A, Kirchhoff F, Helmchen F. Resting microglial cells are highly dynamic surveillants of brain parenchyma in vivo. Science. 2005 May 27;308(5726):1314-8. doi: 10.1126/science.1110647.

Niraula A, Sheridan JF, Godbout JP. Microglia Priming with Aging and Stress. Neuropsychopharmacology. 2017 Jan;42(1):318-333. doi: 10.1038/npp.2016.185.

Nolan Y, Maher FO, Martin DS, Clarke RM, Brady MT, Bolton AE, Mills KH, Lynch MA. Role of interleukin-4 in regulation of age-related inflammatory changes in the hippocampus. J Biol Chem. 2005 Mar 11;280(10):9354-62. doi: 10.1074/jbc.M412170200.

Norden DM, Fenn AM, Dugan A, Godbout JP. TGFβ produced by IL-10 redirected astrocytes attenuates microglial activation. Glia. 2014 Jun;62(6):881-95. doi: 10.1002/glia.22647.

Norden DM, Godbout JP. Review: microglia of the aged brain: primed to be activated and resistant to regulation. Neuropathol Appl Neurobiol. 2013 Feb;39(1):19-34. doi: 10.1111/j.1365-2990.2012.01306.x.

Norden DM, Trojanowski PJ, Walker FR, Godbout JP. Insensitivity of astrocytes to interleukin 10 signaling following peripheral immune challenge results in prolonged microglial activation in the aged brain. Neurobiol Aging. 2016 Aug;44:22-41. doi: 10.1016/j.neurobiolaging.2016.04.014.

Nugent AA, Lin K, van Lengerich B, Lianoglou S, Przybyla L, Davis SS, Llapashtica C, Wang J, Kim DJ, Xia D, Lucas A, Baskaran S, Haddick PCG, Lenser M, Earr TK, Shi J, Dugas JC, Andreone BJ, Logan T, Solanoy HO, Chen H, Srivastava A, Poda SB, Sanchez PE, Watts RJ, Sandmann T, Astarita G, Lewcock JW, Monroe KM, Di Paolo G. TREM2 Regulates Microglial Cholesterol Metabolism upon Chronic Phagocytic Challenge. Neuron. 2020 Mar 4;105(5):837-854.e9. doi: 10.1016/j.neuron.2019.12.007.

Olah M, Biber K, Vinet J, Boddeke HW. Microglia phenotype diversity. CNS Neurol Disord Drug Targets. 2011 Feb;10(1):108-18. doi: 10.2174/187152711794488575.

Olejniczak M, Urbanek MO, Krzyzosiak WJ. The role of the immune system in triplet repeat expansion diseases. Mediators Inflamm. 2015;2015:873860. doi: 10.1155/2015/873860.

Palm NW, Medzhitov R. Pattern recognition receptors and control of adaptive immunity. Immunol Rev. 2009 Jan;227(1):221-33. doi: 10.1111/j.1600-065X.2008.00731.x.

Paloneva J, Manninen T, Christman G, Hovanes K, Mandelin J, Adolfsson R, Bianchin M, Bird T, Miranda R, Salmaggi A, Tranebjaerg L, Konttinen Y, Peltonen L. Mutations in two genes encoding different subunits of a receptor signaling complex result in an identical disease phenotype. Am J Hum Genet. 2002 Sep;71(3):656-62. doi: 10.1086/342259.

Pannese E. Morphological changes in nerve cells during normal aging. Brain Struct Funct. 2011 Jun;216(2):85-9. doi: 10.1007/s00429-011-0308-y.

Paolicelli RC, Bolasco G, Pagani F, Maggi L, Scianni M, Panzanelli P, Giustetto M, Ferreira TA, Guiducci E, Dumas L, Ragozzino D, Gross CT. Synaptic pruning by microglia is necessary for normal brain development. Science. 2011 Sep 9;333(6048):1456-8. doi: 10.1126/science.1202529.

Parent JM, Yu TW, Leibowitz RT, Geschwind DH, Sloviter RS, Lowenstein DH. Dentate granule cell neurogenesis is increased by seizures and contributes to aberrant network reorganization in the adult rat hippocampus. J Neurosci. 1997 May 15;17(10):3727-38. doi: 10.1523/JNEUROSCI.17-10-03727.1997.

Park KW, Lee HG, Jin BK, Lee YB. Interleukin-10 endogenously expressed in microglia prevents lipopolysaccharide-induced neurodegeneration in the rat cerebral cortex in vivo. Exp Mol Med. 2007 Dec 31;39(6):812-9. doi: 10.1038/emm.2007.88.

Parkhurst CN, Yang G, Ninan I, Savas JN, Yates JR 3rd, Lafaille JJ, Hempstead BL, Littman DR, Gan WB. Microglia promote learning-dependent synapse formation through brain-derived neurotrophic factor. Cell. 2013 Dec 19;155(7):1596-609. doi: 10.1016/j.cell.2013.11.030.

Pasquini LA, Millet V, Hoyos HC, Giannoni JP, Croci DO, Marder M, Liu FT, Rabinovich GA, Pasquini JM. Galectin-3 drives oligodendrocyte differentiation to control myelin integrity and function. Cell Death Differ. 2011 Nov;18(11):1746-56. doi: 10.1038/cdd.2011.40.

Perez-Asensio FJ, Perpiñá U, Planas AM, Pozas E. Interleukin-10 regulates progenitor differentiation and modulates neurogenesis in adult brain. J Cell Sci. 2013 Sep 15;126(Pt 18):4208-19. doi: 10.1242/jcs.127803.

Perry VH. A revised view of the central nervous system microenvironment and major histocompatibility complex class II antigen presentation. J Neuroimmunol. 1998 Oct 1;90(2):113-21. doi: 10.1016/s0165-5728(98)00145-3.

Perry VH, Matyszak MK, Fearn S. Altered antigen expression of microglia in the aged rodent CNS. Glia. 1993 Jan;7(1):60-7. doi: 10.1002/glia.440070111.

Petković F, Campbell IL, Gonzalez B, Castellano B. Astrocyte-targeted production of interleukin-6 reduces astroglial and microglial activation in the cuprizone demyelination model: Implications for myelin clearance and oligodendrocyte maturation. Glia. 2016 Dec;64(12):2104-2119. doi: 10.1002/glia.23043. Epub 2016 Aug 18. PMID: 27535761.

Piccio L, Buonsanti C, Mariani M, Cella M, Gilfillan S, Cross AH, Colonna M, Panina-Bordignon P. Blockade of TREM-2 exacerbates experimental autoimmune encephalomyelitis. Eur J Immunol. 2007 May;37(5):1290-301. doi: 10.1002/eji.200636837.

Pluvinage JV, Haney MS, Smith BAH, Sun J, Iram T, Bonanno L, Li L, Lee DP, Morgens DW, Yang AC, Shuken SR, Gate D, Scott M, Khatri P, Luo J, Bertozzi CR, Bassik MC, Wyss-Coray T. CD22 blockade restores homeostatic microglial phagocytosis in ageing brains. Nature. 2019 Apr;568(7751):187-192. doi: 10.1038/s41586-019-1088-4.

Pocock JM, Kettenmann H. Neurotransmitter receptors on microglia. Trends Neurosci. 2007 Oct;30(10):527-35. doi: 10.1016/j.tins.2007.07.007.

Poliani PL, Wang Y, Fontana E, Robinette ML, Yamanishi Y, Gilfillan S, Colonna M. TREM2 sustains microglial expansion during aging and response to demyelination. J Clin Invest. 2015 May;125(5):2161-70. doi: 10.1172/JCI77983.

Potvin S, Stip E, Sepehry AA, Gendron A, Bah R, Kouassi E. Inflammatory cytokine alterations in schizophrenia: a systematic quantitative review. Biol Psychiatry. 2008 Apr 15;63(8):801-8. doi: 10.1016/j.biopsych.2007.09.024.

Quintana A, Müller M, Frausto RF, Ramos R, Getts DR, Sanz E, Hofer MJ, Krauthausen M, King NJ, Hidalgo J, Campbell IL. Site-specific production of IL-6 in the central nervous system retargets and enhances the inflammatory response in experimental autoimmune encephalomyelitis. J Immunol. 2009 Aug 1;183(3):2079-88. doi: 10.4049/jimmunol.0900242.

Radak Z, Zhao Z, Goto S, Koltai E. Age-associated neurodegeneration and oxidative damage to lipids, proteins and DNA. Mol Aspects Med. 2011 Aug;32(4-6):305-15. doi: 10.1016/j.mam.2011.10.010.

Raj D, Yin Z, Breur M, Doorduin J, Holtman IR, Olah M, Mantingh-Otter IJ, Van Dam D, De Deyn PP, den Dunnen W, Eggen BJL, Amor S, Boddeke E. Increased White Matter Inflammation in Aging- and Alzheimer's Disease Brain. Front Mol Neurosci. 2017 Jun 30;10:206. doi: 10.3389/fnmol.2017.00206.

Ramesh G, MacLean AG, Philipp MT. Cytokines and chemokines at the crossroads of neuroinflammation, neurodegeneration, and neuropathic pain. Mediators Inflamm. 2013;2013:480739. doi: 10.1155/2013/480739.

Rao MS, Hattiangady B, Shetty AK. The window and mechanisms of major age-related decline in the production of new neurons within the dentate gyrus of the hippocampus. Aging Cell. 2006 Dec;5(6):545-58. doi: 10.1111/j.1474-9726.2006.00243.x.

Raposo M, Bettencourt C, Ramos A, Kazachkova N, Vasconcelos J, Kay T, Bruges-Armas J, Lima M. Promoter Variation and Expression Levels of Inflammatory Genes IL1A, IL1B, IL6 and TNF in Blood of Spinocerebellar Ataxia Type 3 (SCA3) Patients. Neuromolecular Med. 2017 Mar;19(1):41-45. doi: 10.1007/s12017-016-8416-8.

Raz N, Lindenberger U, Rodrigue KM, Kennedy KM, Head D, Williamson A, Dahle C, Gerstorf D, Acker JD. Regional brain changes in aging healthy adults: general trends, individual differences and modifiers. Cereb Cortex. 2005 Nov;15(11):1676-89. doi: 10.1093/cercor/bhi044.

Recasens M, Almolda B, Pérez-Clausell J, Campbell IL, González B, Castellano B. Chronic exposure to IL-6 induces a desensitized phenotype of the microglia. J Neuroinflammation. 2021 Jan 22;18(1):31. doi: 10.1186/s12974-020-02063-1.

Recasens M, Shrivastava K, Almolda B, González B, Castellano B. Astrocyte-targeted IL-10 production decreases proliferation and induces a downregulation of activated microglia/macrophages after PPT. Glia. 2019 Apr;67(4):741-758. doi: 10.1002/glia.23573.

Reichert F, Rotshenker S. Galectin-3/MAC-2 in experimental allergic encephalomyelitis. Exp Neurol. 1999 Dec;160(2):508-14. doi: 10.1006/exnr.1999.7229.

Remington LT, Babcock AA, Zehntner SP, Owens T. Microglial recruitment, activation, and proliferation in response to primary demyelination. Am J Pathol. 2007 May;170(5):1713-24. doi: 10.2353/ajpath.2007.060783.

Réu P, Khosravi A, Bernard S, Mold JE, Salehpour M, Alkass K, Perl S, Tisdale J, Possnert G, Druid H, Frisén J. The Lifespan and Turnover of Microglia in the Human Brain. Cell Rep. 2017 Jul 25;20(4):779-784. doi: 10.1016/j.celrep.2017.07.004.

Reyes TM, Fabry Z, Coe CL. Brain endothelial cell production of a neuroprotective cytokine, interleukin-6, in response to noxious stimuli. Brain Res. 1999 Dec 18;851(1-2):215-20. doi: 10.1016/s0006-8993(99)02189-7.

Richwine AF, Godbout JP, Berg BM, Chen J, Escobar J, Millard DK, Johnson RW. Improved psychomotor performance in aged mice fed diet high in antioxidants is associated with reduced ex vivo brain interleukin-6 production. Brain Behav Immun. 2005 Nov;19(6):512-20. doi: 10.1016/j.bbi.2004.12.005.

Ritzel RM, Patel AR, Pan S, Crapser J, Hammond M, Jellison E, McCullough LD. Age- and location-related changes in microglial function. Neurobiol Aging. 2015 Jun;36(6):2153-63. doi: 10.1016/j.neurobiolaging.2015.02.016.

Rocha SM, Cristovão AC, Campos FL, Fonseca CP, Baltazar G. Astrocyte-derived GDNF is a potent inhibitor of microglial activation. Neurobiol Dis. 2012 Sep;47(3):407-15. doi: 10.1016/j.nbd.2012.04.014.

Rodrigues Siqueira I, Fochesatto C, da Silva Torres IL, Dalmaz C, Alexandre Netto C. Aging affects oxidative state in hippocampus, hypothalamus and adrenal glands of Wistar rats. Life Sci. 2005 Dec 5;78(3):271-8. doi: 10.1016/j.lfs.2005.04.044.

Rose-John S, Neurath MF. IL-6 trans-signaling: the heat is on. Immunity. 2004 Jan;20(1):2-4. doi: 10.1016/s1074-7613(04)00003-2.

Rotshenker S, Reichert F, Gitik M, Haklai R, Elad-Sfadia G, Kloog Y. Galectin-3/MAC-2, Ras and PI3K activate complement receptor-3 and scavenger receptor-AI/II mediated myelin phagocytosis in microglia. Glia. 2008 Nov 15;56(15):1607-13. doi: 10.1002/glia.20713.

Rott O, Fleischer B, Cash E. Interleukin-10 prevents experimental allergic encephalomyelitis in rats. Eur J Immunol. 1994 Jun;24(6):1434-40. doi: 10.1002/eji.1830240629.

Safaiyan S, Besson-Girard S, Kaya T, Cantuti-Castelvetri L, Liu L, Ji H, Schifferer M, Gouna G, Usifo F, Kannaiyan N, Fitzner D, Xiang X, Rossner MJ, Brendel M, Gokce O, Simons M. White matter aging drives microglial diversity. Neuron. 2021 Apr 7;109(7):1100-1117.e10. doi: 10.1016/j.neuron.2021.01.027.

Safaiyan S, Kannaiyan N, Snaidero N, Brioschi S, Biber K, Yona S, Edinger AL, Jung S, Rossner MJ, Simons M. Age-related myelin degradation burdens the clearance function of microglia during aging. Nat Neurosci. 2016 Aug;19(8):995-8. doi: 10.1038/nn.4325.

Salat DH, Buckner RL, Snyder AZ, Greve DN, Desikan RS, Busa E, Morris JC, Dale AM, Fischl B. Thinning of the cerebral cortex in aging. Cereb Cortex. 2004 Jul;14(7):721-30. doi: 10.1093/cercor/bhh032.

Salminen A, Kaarniranta K, Kauppinen A. Inflammaging: disturbed interplay between autophagy and inflammasomes. Aging (Albany NY). 2012 Mar;4(3):166-75. doi: 10.18632/aging.100444.

Samoilova EB, Horton JL, Hilliard B, Liu TS, Chen Y. IL-6-deficient mice are resistant to experimental autoimmune encephalomyelitis: roles of IL-6 in the activation and differentiation of autoreactive T cells. J Immunol. 1998 Dec 15;161(12):6480-6.

Sawada M, Suzumura A, Hosoya H, Marunouchi T, Nagatsu T. Interleukin-10 inhibits both production of cytokines and expression of cytokine receptors in microglia. J Neurochem. 1999 Apr;72(4):1466-71. doi: 10.1046/j.1471-4159.1999.721466.x.

Saxton RA, Tsutsumi N, Su LL, Abhiraman GC, Mohan K, Henneberg LT, Aduri NG, Gati C, Garcia KC. Structure-based decoupling of the pro- and anti-inflammatory functions of interleukin-10. Science. 2021 Mar 19;371(6535):eabc8433. doi: 10.1126/science.abc8433.

Sloane JA, Hollander W, Moss MB, Rosene DL, Abraham CR. Increased microglial activation and protein nitration in white matter of the aging monkey. Neurobiol Aging. 1999 Jul-Aug;20(4):395-405. doi: 10.1016/s0197-4580(99)00066-4.

Schafer DP, Lehrman EK, Kautzman AG, Koyama R, Mardinly AR, Yamasaki R, Ransohoff RM, Greenberg ME, Barres BA, Stevens B. Microglia sculpt postnatal neural circuits in an activity and complement-dependent manner. Neuron. 2012 May 24;74(4):691-705. doi: 10.1016/j.neuron.2012.03.026.

Schafer DP, Lehrman EK, Stevens B. The "quad-partite" synapse: microglia-synapse interactions in the developing and mature CNS. Glia. 2013 Jan;61(1):24-36. doi: 10.1002/glia.22389.

Scharfman H, Goodman J, Macleod A, Phani S, Antonelli C, Croll S. Increased neurogenesis and the ectopic granule cells after intrahippocampal BDNF infusion in adult rats. Exp Neurol. 2005 Apr;192(2):348-56. doi: 10.1016/j.expneurol.2004.11.016.

Schilling T, Nitsch R, Heinemann U, Haas D, Eder C. Astrocyte-released cytokines induce ramification and outward K+ channel expression in microglia via distinct signalling pathways. Eur J Neurosci. 2001 Aug;14(3):463-73. doi: 10.1046/j.0953-816x.2001.01661.x.

Schöbitz B, de Kloet ER, Sutanto W, Holsboer F. Cellular localization of interleukin 6 mRNA and interleukin 6 receptor mRNA in rat brain. Eur J Neurosci. 1993 Nov 1;5(11):1426-35. doi: 10.1111/j.1460-9568.1993.tb00210.x.

Schöbitz B, Pezeshki G, Pohl T, Hemmann U, Heinrich PC, Holsboer F, Reul JM. Soluble interleukin-6 (IL-6) receptor augments central effects of IL-6 in vivo. FASEB J. 1995 May;9(8):659-64. doi: 10.1096/fasebj.9.8.7768358.

Schwenkgrub J, Joniec-Maciejak I, Sznejder-Pachołek A, Wawer A, Ciesielska A, Bankiewicz K, Członkowska A, Członkowski A. Effect of human interleukin-10 on the expression of nitric oxide synthases in the MPTP-based model of Parkinson's disease. Pharmacol Rep. 2013;65(1):44-9. doi: 10.1016/s1734-1140(13)70962-9.

Sei Y, Vitković L, Yokoyama MM. Cytokines in the central nervous system: regulatory roles in neuronal function, cell death and repair. Neuroimmunomodulation. 1995 May-Jun;2(3):121-33. doi: 10.1159/000096881.

Shanaki M. Astrocyte-targeted production of IL-10 reduces the neuroinflammatory response and the neurodegeneration after TBI. [PhD dissertation]. Barcelona: Universitat Autònoma de Barcelona; 2020

Sheffield LG, Berman NE. Microglial expression of MHC class II increases in normal aging of nonhuman primates. Neurobiol Aging. 1998 Jan-Feb;19(1):47-55. doi: 10.1016/s0197-4580(97)00168-1.

Shemer A, Grozovski J, Tay TL, Tao J, Volaski A, Süß P, Ardura-Fabregat A, Gross-Vered M, Kim JS, David E, Chappell-Maor L, Thielecke L, Glass CK, Cornils K, Prinz M, Jung S. Engrafted parenchymal brain macrophages differ from microglia in transcriptome, chromatin landscape and response to challenge. Nat Commun. 2018 Dec 6;9(1):5206. doi: 10.1038/s41467-018-07548-5.

Shi Q, Chowdhury S, Ma R, Le KX, Hong S, Caldarone BJ, Stevens B, Lemere CA. Complement C3 deficiency protects against neurodegeneration in aged plaque-rich APP/PS1 mice. Sci Transl Med. 2017 May 31;9(392):eaaf6295. doi: 10.1126/scitranslmed.aaf6295.

Shi Q, Colodner KJ, Matousek SB, Merry K, Hong S, Kenison JE, Frost JL, Le KX, Li S, Dodart JC, Caldarone BJ, Stevens B, Lemere CA. Complement C3-Deficient Mice Fail to Display Age-Related Hippocampal Decline. J Neurosci. 2015 Sep 23;35(38):13029-42. doi: 10.1523/JNEUROSCI.1698-15.2015.

Shobin E, Bowley MP, Estrada LI, Heyworth NC, Orczykowski ME, Eldridge SA, Calderazzo SM, Mortazavi F, Moore TL, Rosene DL. Microglia activation and phagocytosis: relationship with aging and cognitive impairment in the rhesus monkey. Geroscience. 2017 Apr;39(2):199-220. doi: 10.1007/s11357-017-9965-y.

Sierra A, de Castro F, Del Río-Hortega J, Rafael Iglesias-Rozas J, Garrosa M, Kettenmann H. The "Big-Bang" for modern glial biology: Translation and comments on Pío del Río-Hortega 1919 series of papers on microglia. Glia. 2016 Nov;64(11):1801-40. doi: 10.1002/glia.23046.

Sierra A, Encinas JM, Deudero JJ, Chancey JH, Enikolopov G, Overstreet-Wadiche LS, Tsirka SE, Maletic-Savatic M. Microglia shape adult hippocampal neurogenesis through apoptosis-coupled phagocytosis. Cell Stem Cell. 2010 Oct 8;7(4):483-95. doi: 10.1016/j.stem.2010.08.014.

Sierra A, Gottfried-Blackmore AC, McEwen BS, Bulloch K. Microglia derived from aging mice exhibit an altered inflammatory profile. Glia. 2007 Mar;55(4):412-24. doi: 10.1002/glia.20468.

Sierra A, Paolicelli RC, Kettenmann H. Cien Años de Microglía: Milestones in a Century of Microglial Research. Trends Neurosci. 2019 Nov;42(11):778-792. doi: 10.1016/j.tins.2019.09.004.

Smith ME. Phagocytosis of myelin in demyelinative disease: a review. Neurochem Res. 1999 Feb;24(2):261-8. doi: 10.1023/a:1022566121967.

Smith SE, Li J, Garbett K, Mirnics K, Patterson PH. Maternal immune activation alters fetal brain development through interleukin-6. J Neurosci. 2007 Oct 3;27(40):10695-702. doi: 10.1523/JNEUROSCI.2178-07.2007.

Streit WJ. Microglia and neuroprotection: implications for Alzheimer's disease. Brain Res Brain Res Rev. 2005 Apr;48(2):234-9. doi: 10.1016/j.brainresrev.2004.12.013.

Streit WJ, Hurley SD, McGraw TS, Semple-Rowland SL. Comparative evaluation of cytokine profiles and reactive gliosis supports a critical role for interleukin-6 in neuron-glia signaling during regeneration. J Neurosci Res. 2000 Jul 1;61(1):10-20. doi: 10.1002/1097-4547(20000701)61:1<10::AID-JNR2>3.0.CO;2-E.

Streit WJ, Sammons NW, Kuhns AJ, Sparks DL. Dystrophic microglia in the aging human brain. Glia. 2004 Jan 15;45(2):208-12. doi: 10.1002/glia.10319.

Strle K, Zhou JH, Broussard SR, Venters HD, Johnson RW, Freund GG, Dantzer R, Kelley KW. IL-10 promotes survival of microglia without activating Akt. J Neuroimmunol. 2002 Jan;122(1-2):9-19. doi: 10.1016/s0165-5728(01)00444-1.

Strong R, Miller RA, Astle CM, Floyd RA, Flurkey K, Hensley KL, Javors MA, Leeuwenburgh C, Nelson JF, Ongini E, Nadon NL, Warner HR, Harrison DE. Nordihydroguaiaretic acid and aspirin increase lifespan of genetically heterogeneous male mice. Aging Cell. 2008 Oct;7(5):641-50. doi: 10.1111/j.1474-9726.2008.00414.x.

Takahashi K, Rochford CD, Neumann H. Clearance of apoptotic neurons without inflammation by microglial triggering receptor expressed on myeloid cells-2. J Exp Med. 2005 Feb 21;201(4):647-57. doi: 10.1084/jem.20041611.

Tan YL, Yuan Y, Tian L. Microglial regional heterogeneity and its role in the brain. Mol Psychiatry. 2020 Feb;25(2):351-367. doi: 10.1038/s41380-019-0609-8.

Tang Y, Nyengaard JR, Pakkenberg B, Gundersen HJ. Age-induced white matter changes in the human brain: a stereological investigation. Neurobiol Aging. 1997 Nov-Dec;18(6):609-15. doi: 10.1016/s0197-4580(97)00155-3.

Terao A, Apte-Deshpande A, Dousman L, Morairty S, Eynon BP, Kilduff TS, Freund YR. Immune response gene expression increases in the aging murine hippocampus. J Neuroimmunol. 2002 Nov;132(1-2):99-112. doi: 10.1016/s0165-5728(02)00317-x.

Tian L, Cai Q, Wei H. Alterations of antioxidant enzymes and oxidative damage to macromolecules in different organs of rats during aging. Free Radic Biol Med. 1998 Jun;24(9):1477-84. doi: 10.1016/s0891-5849(98)00025-2.

Trapp BD, Wujek JR, Criste GA, Jalabi W, Yin X, Kidd GJ, Stohlman S, Ransohoff R. Evidence for synaptic stripping by cortical microglia. Glia. 2007 Mar;55(4):360-8. doi: 10.1002/glia.20462.

Tremblay MÈ, Lowery RL, Majewska AK. Microglial interactions with synapses are modulated by visual experience. PLoS Biol. 2010 Nov 2;8(11):e1000527. doi: 10.1371/journal.pbio.1000527.

Tremblay MÈ, Zettel ML, Ison JR, Allen PD, Majewska AK. Effects of aging and sensory loss on glial cells in mouse visual and auditory cortices. Glia. 2012 Apr;60(4):541-58. doi: 10.1002/glia.22287.

Tripathi RB, Jackiewicz M, McKenzie IA, Kougioumtzidou E, Grist M, Richardson WD. Remarkable Stability of Myelinating Oligodendrocytes in Mice. Cell Rep. 2017 Oct 10;21(2):316-323. doi: 10.1016/j.celrep.2017.09.050.

Uzawa A, Mori M, Arai K, Sato Y, Hayakawa S, Masuda S, Taniguchi J, Kuwabara S. Cytokine and chemokine profiles in neuromyelitis optica: significance of interleukin-6. Mult Scler. 2010 Dec;16(12):1443-52. doi: 10.1177/1352458510379247.

Vallières L, Campbell IL, Gage FH, Sawchenko PE. Reduced hippocampal neurogenesis in adult transgenic mice with chronic astrocytic production of interleukin-6. J Neurosci. 2002 Jan 15;22(2):486-92. doi: 10.1523/JNEUROSCI.22-02-00486.2002.

Vallières L, Rivest S. Regulation of the genes encoding interleukin-6, its receptor, and gp130 in the rat brain in response to the immune activator lipopolysaccharide and the proinflammatory cytokine interleukin-1beta. J Neurochem. 1997 Oct;69(4):1668-83. doi: 10.1046/j.1471-4159.1997.69041668.x.

van Praag H, Shubert T, Zhao C, Gage FH. Exercise enhances learning and hippocampal neurogenesis in aged mice. J Neurosci. 2005 Sep 21;25(38):8680-5. doi: 10.1523/JNEUROSCI.1731-05.2005.

Varnum MM, Kiyota T, Ingraham KL, Ikezu S, Ikezu T. The anti-inflammatory glycoprotein, CD200, restores neurogenesis and enhances amyloid phagocytosis in a mouse model of Alzheimer's disease. Neurobiol Aging. 2015 Nov;36(11):2995-3007. doi: 10.1016/j.neurobiolaging.2015.07.027.

Vaughan DW, Peters A. Neuroglial cells in the cerebral cortex of rats from young adulthood to old age: an electron microscope study. J Neurocytol. 1974 Oct;3(4):405-29. doi: 10.1007/BF01098730.

Villacampa N, Almolda B, Vilella A, Campbell IL, González B, Castellano B. Astrocyte-targeted production of IL-10 induces changes in microglial reactivity and reduces motor neuron death after facial nerve axotomy. Glia. 2015 Jul;63(7):1166-84. doi: 10.1002/glia.22807.

Villeda SA, Luo J, Mosher KI, Zou B, Britschgi M, Bieri G, Stan TM, Fainberg N, Ding Z, Eggel A, Lucin KM, Czirr E, Park JS, Couillard-Després S, Aigner L, Li G, Peskind ER, Kaye JA, Quinn JF, Galasko DR, Xie XS, Rando TA, Wyss-Coray T. The ageing systemic milieu negatively regulates neurogenesis and cognitive function. Nature. 2011 Aug 31;477(7362):90-4. doi: 10.1038/nature10357.

Vitkovic L, Bockaert J, Jacque C. "Inflammatory" cytokines: neuromodulators in normal brain? J Neurochem. 2000 Feb;74(2):457-71. doi: 10.1046/j.1471-4159.2000.740457.x.

von Bernhardi R, Eugenín-von Bernhardi L, Eugenín J. Microglial cell dysregulation in brain aging and neurodegeneration. Front Aging Neurosci. 2015 Jul 20;7:124. doi: 10.3389/fnagi.2015.00124.

Vukovic J, Colditz MJ, Blackmore DG, Ruitenberg MJ, Bartlett PF. Microglia modulate hippocampal neural precursor activity in response to exercise and aging. J Neurosci. 2012 May 9;32(19):6435-43. doi: 10.1523/JNEUROSCI.5925-11.2012.

Wake H, Moorhouse AJ, Jinno S, Kohsaka S, Nabekura J. Resting microglia directly monitor the functional state of synapses in vivo and determine the fate of ischemic terminals. J Neurosci. 2009 Apr 1;29(13):3974-80. doi: 10.1523/JNEUROSCI.4363-08.2009.

Wang Y, Cella M, Mallinson K, Ulrich JD, Young KL, Robinette ML, Gilfillan S, Krishnan GM, Sudhakar S, Zinselmeyer BH, Holtzman DM, Cirrito JR, Colonna M. TREM2 lipid sensing sustains the microglial response in an Alzheimer's disease model. Cell. 2015 Mar 12;160(6):1061-71. doi: 10.1016/j.cell.2015.01.049.

Wei J, Xu H, Davies JL, Hemmings GP. Increase of plasma IL-6 concentration with age in healthy subjects. Life Sci. 1992;51(25):1953-6. doi: 10.1016/0024-3205(92)90112-3.

Weinhard L, di Bartolomei G, Bolasco G, Machado P, Schieber NL, Neniskyte U, Exiga M, Vadisiute A, Raggioli A, Schertel A, Schwab Y, Gross CT. Microglia remodel synapses by presynaptic trogocytosis and spine head filopodia induction. Nat Commun. 2018 Mar 26;9(1):1228. doi: 10.1038/s41467-018-03566-5.

Wertz MH, Pineda SS, Lee H, Kulicke R, Kellis M, Heiman M. Interleukin-6 deficiency exacerbates Huntington's disease model phenotypes. Mol Neurodegener. 2020 May 24;15(1):29. doi: 10.1186/s13024-020-00379-3.

Wlodarczyk A, Holtman IR, Krueger M, Yogev N, Bruttger J, Khorooshi R, Benmamar-Badel A, de Boer-Bergsma JJ, Martin NA, Karram K, Kramer I, Boddeke EW, Waisman A, Eggen BJ, Owens T. A novel microglial subset plays a key role in myelinogenesis in developing brain. EMBO J. 2017 Nov 15;36(22):3292-3308. doi: 10.15252/embj.201696056.

Wlodarczyk A, Løbner M, Cédile O, Owens T. Comparison of microglia and infiltrating CD11c+ cells as antigen presenting cells for T cell proliferation and cytokine response. J Neuroinflammation. 2014 Mar 25;11:57. doi: 10.1186/1742-2094-11-57.

Wong AM, Patel NV, Patel NK, Wei M, Morgan TE, de Beer MC, de Villiers WJ, Finch CE. Macrosialin increases during normal brain aging are attenuated by caloric restriction. Neurosci Lett. 2005 Dec 23;390(2):76-80. doi: 10.1016/j.neulet.2005.07.058.

Wu Y, Dissing-Olesen L, MacVicar BA, Stevens B. Microglia: Dynamic Mediators of Synapse Development and Plasticity. Trends Immunol. 2015 Oct;36(10):605-613. doi: 10.1016/j.it.2015.08.008.

Wu SY, Pan BS, Tsai SF, Chiang YT, Huang BM, Mo FE, Kuo YM. BDNF reverses aging-related microglial activation. J Neuroinflammation. 2020 Jul 14;17(1):210. doi: 10.1186/s12974-020-01887-1.

Wu Y, Zhang AQ, Yew DT. Age related changes of various markers of astrocytes in senescence-accelerated mice hippocampus. Neurochem Int. 2005 Jun;46(7):565-74. doi: 10.1016/j.neuint.2005.01.002.

Wynne AM, Henry CJ, Huang Y, Cleland A, Godbout JP. Protracted downregulation of CX3CR1 on microglia of aged mice after lipopolysaccharide challenge. Brain Behav Immun. 2010 Oct;24(7):1190-201. doi: 10.1016/j.bbi.2010.05.011.

Xie Z, Morgan TE, Rozovsky I, Finch CE. Aging and glial responses to lipopolysaccharide in vitro: greater induction of IL-1 and IL-6, but smaller induction of neurotoxicity. Exp Neurol. 2003 Jul;182(1):135-41. doi: 10.1016/s0014-4886(03)00057-8.

Ye SM, Johnson RW. Increased interleukin-6 expression by microglia from brain of aged mice. J Neuroimmunol. 1999 Jan 1;93(1-2):139-48. doi: 10.1016/s0165-5728(98)00217-3.

Ye SM, Johnson RW. An age-related decline in interleukin-10 may contribute to the increased expression of interleukin-6 in brain of aged mice. Neuroimmunomodulation. 2001;9(4):183-92. doi: 10.1159/000049025.

Zhang H, Li F, Yang Y, Chen J, Hu X. SIRP/CD47 signaling in neurological disorders. Brain Res. 2015 Oct 14;1623:74-80. doi: 10.1016/j.brainres.2015.03.012.

Zhou Z, Peng X, Insolera R, Fink DJ, Mata M. Interleukin-10 provides direct trophic support to neurons. J Neurochem. 2009 Sep;110(5):1617-27. doi: 10.1111/j.1471-4159.2009.06263.x.

Zhu Y, Carvey PM, Ling Z. Age-related changes in glutathione and glutathione-related enzymes in rat brain. Brain Res. 2006 May 23;1090(1):35-44. doi: 10.1016/j.brainres.2006.03.063.

8. ANNEXES

I. SCIENTIFIC PUBLICATIONS

Article 1:
Sanchez-Molina, P., Kreuzer, M., Benseny-Cases, N., Valente, T., Almolda, B., González, B., Castellano, B., Perálvarez-Marín, A. (2020). From mouse to human: Comparative analysis between grey and white matter by synchrotron-Fourier transformed infrared microspectroscopy. *Biomolecules*, *10*(8), E1099. https://doi.org/10.3390/biom10081099

Article 2:
Sanchez-Molina, P., Almolda, B., Benseny-Cases, N., González, B., Perálvarez-Marín, A., Castellano, B. (2021). Specific microglial phagocytic phenotype and decrease of lipid oxidation in white matter areas during aging: implications of different microenvironments. *Neurobiology of Aging, 105,* 280-295. https://doi.org/10.1016/j.neurobiolaging.2021.03.015

Article 3:
Sanchez-Molina, P., Almolda, B., Giménez-Llort, L., González, B., Castellano, B. (2021). Chronic IL-10 overproduction anticipates the age-related disruption of microglia-neuron dialogue resulting in impaired hippocampal neurogenesis and spatial memory. *Under review in Brain, Behavior, and Immunity.*

II. SUPPLEMENTARY FIGURES

III. PARTICIPATION IN SCIENTIFIC MEETINGS

Communication

From Mouse to Human: Comparative Analysis between Grey and White Matter by Synchrotron-Fourier Transformed Infrared Microspectroscopy

Paula Sanchez-Molina [1,2], **Martin Kreuzer [3]**, **Núria Benseny-Cases [3]**, **Tony Valente [1,2]**, **Beatriz Almolda [1,2]**, **Berta González [1,2]**, **Bernardo Castellano [1,2]** and **Alex Perálvarez-Marín [1,4,*]**

[1] Institute of Neurosciences, Universitat Autònoma de Barcelona, 08193 Bellaterra, Barcelona, Spain; paula.sanchez@uab.cat (P.S.-M.); tony.valente@uab.cat (T.V.); beatriz.almolda@uab.cat (B.A.); berta.gonzalez@uab.cat (B.G.); bernardo.castellano@uab.cat (B.C.)

[2] Department of Cell Biology, Physiology and Immunology, Universitat Autònoma de Barcelona, 08193 Bellaterra, Barcelona, Spain

[3] ALBA Synchrotron Light Source, Carrer de la Llum 2-26, 08290 Cerdanyola del Vallès, Barcelona, Catalonia, Spain; mkreuzer@cells.es (M.K.); nbenseny@cells.es (N.B.-C.)

[4] Biophysics Unit, Department of Biochemistry and Molecular Biology, Universitat Autònoma de Barcelona, 08193 Bellaterra, Barcelona, Catalonia, Spain

[*] Correspondence: alex.peralvarez@uab.cat; Tel.: +34-93-581-4504

Abstract: Fourier Transform Infrared microspectroscopy (µFTIR) is a very useful method to analyze the biochemical properties of biological samples in situ. Many diseases affecting the central nervous system (CNS) have been studied using this method, to elucidate alterations in lipid oxidation or protein aggregation, among others. In this work, we describe in detail the characteristics between grey matter (GM) and white matter (WM) areas of the human brain by µFTIR, and we compare them with the mouse brain (strain C57BL/6), the most used animal model in neurological disorders. Our results show a clear different infrared profile between brain areas in the lipid region of both species. After applying a second derivative in the data, we established a 1.5 threshold value for the lipid/protein ratio to discriminate between GM and WM areas in non-pathological conditions. Furthermore, we demonstrated intrinsic differences of lipids and proteins by cerebral area. Lipids from GM present higher C=CH, C=O and CH$_3$ functional groups compared to WM in humans and mice. Regarding proteins, GM present lower Amide II amounts and higher intramolecular β-sheet structure amounts with respect to WM in both species. However, the presence of intermolecular β-sheet structures, which is related to β-aggregation, was only observed in the GM of some human individuals. The present study defines the relevant biochemical properties of non-pathological human and mouse brains by µFTIR as a benchmark for future studies involving CNS pathological samples.

Keywords: infrared spectroscopy; grey matter; white matter; lipid oxidation; protein structure; central nervous system

---

1. Introduction

Fourier Transform Infrared microspectroscopy (µFTIR) is an in situ method that offers the possibility of analyzing in detail the biochemical properties of fixed and non-fixed cells and tissues with no needed of staining, homogenization or further manipulations that can alter the nature of the samples. Lipid peroxidation, de/phosphorylation and protein conformations are some of the

measurements that the infrared spectrum can provide with a high spatial resolution and sensitivity at the microscopic level [1–3].

The intrinsic chemical characteristics of a biological sample is essential information to understand pathophysiological processes. Among others, numerous studies have benefited from this method to elucidate biochemical and molecular features of different pathologies that affect the central nervous system (CNS). The brain is composed of two main areas clearly differentiated: grey matter (GM) and white matter (WM). GM is characterized by the presence of neuronal bodies, whereas WM is characterized by the absence of neuronal bodies and a high presence of myelinated axons. Depending on the disease, the affected brain area may be different and, therefore, biomedical studies are usually focused in one specific anatomical region. μFTIR analyses have been performed in different cerebral areas affected by neurodegenerative disorders, such as Alzheimer's [4–7], Parkinson's [8] and Huntington's [9] diseases, to detect protein aggregation and lipid peroxidation. Infrared radiation it is also very useful to evaluate demyelinating diseases, such as multiple sclerosis, quantifying the amount and the status of lipids in WM areas. A decrease in the lipid content, together with a high lipid oxidation, is a characteristic feature observed by μFTIR in demyelinated areas [10–12]. In addition, some authors have studied by infrared spectroscopy the effect of CNS related pathologies on GM and WM, at the same time finding different alterations by area [9,11,13–15]. However, to properly understand the molecular mechanism of pathologies, the characterization of non-pathological tissues needs to be established first. Furthermore, it is important to highlight that most of the studies performed in the CNS are carried out in rodents and, in consequence, it is crucial to determine the differences and the similarities between humans and rodents with the aim of evaluating the reproducibility and applicability of this method, comparing animal models to human.

In the present study, we characterize the protein and lipid composition and their infrared spectral properties in GM and WM areas by μFTIR. Moreover, this work compares the regional-related properties observed by this method in the human brain with those of the mouse, which is the most widely used experimental model in the neuroscience field.

2. Materials and Methods

2.1. Human Samples

Postmortem human brain tissue was obtained from the Neurological Tissue Bank at the Biobanc-Hospital Clínic-IDIBAPS (Barcelona, Spain). The whole procedure was performed in accordance with the Helsinki Declaration, the Convention of the Council of Europe on Human Rights and Biomedicine and approved by the Ethical Committee of the Autonomous University of Barcelona and the Ethical Committee of Clinical Research-Hospital Clinic de Barcelona (A1-OF15016, 05/20/2015). Frontal cortex samples from individuals ($n = 7$) with no clinical neurological manifestations were used in this study (five women and two men; 78 ± 7.3 years old; 15.2 ± 6.6 h of postmortem delay).

2.2. Animal Samples

C57BL/6 mice ($n = 5$) were used in the present study (four females and one male). In order to mimic the experimental conditions between species, the age of the mice was 20–22 months old. Animals were maintained in conventional plastic cages with food and water ad libitum, in a 12 h light/dark cycle, at 22 ± 2 °C and 50–60% humidity. All experimental animal work was conducted according to Spanish regulations (Ley 32/2007, Real Decreto 1201/2005, Ley 9/2003 and Real Decreto 178/2004) in agreement with European Union directives (86/609/CEE, 91/628/CEE) and was approved by the Ethical Committee of the Autonomous University of Barcelona.

2.3. Sample Preparation

Human brains were frozen at the Neurological Tissue Bank and stored at −80 °C until use. For this study, cerebral frontal cortex samples containing grey matter (GM) and white matter (WM)

areas were used. Mice were euthanized under an anesthesia solution of xylazine (30 mg/kg) and ketamine (120 mg/kg) and intracardially perfused for 10 min with 4% paraformaldehyde in 0.1 M phosphate buffer (pH 7.4). The brains were immediately post-fixed in the same solution for 4 h at 4 °C, cryoprotected with 30% sucrose solution in 0.1 M phosphate buffer for 48 h at 4 °C, frozen in ice-cold 2-methylbutane (320404, Sigma-Aldrich, St. Louis, MO, USA) and stored at −80 °C until use. The areas of study in mice were the cerebral cortex and the corpus callosum (bregma between 0.86 mm and −1.22 mm coordinates) as representative areas of GM and WM, respectively. Prior to μFTIR analysis, frozen sections from human and mouse brains containing the areas of interest were cut 8 μm thick on a cryostat (CM3050S Leica) and mounted onto polished calcium fluoride (CaF_2) optical windows (CAFP20-1, Crystran, UK). To minimize water contribution, sections on CaF_2 slides were air-dried at room temperature and stored in a vacuum protected from light until use.

2.4. μFTIR Data Acquisition

Fourier Transform Infrared microspectroscopy (μFTIR) based on synchrotron radiation was carried out at the MIRAS beamline of ALBA synchrotron light source (Catalonia, Spain) [16]. A Hyperion 3000 microscope equipped with a 36× magnification objective and coupled to a Vertex 70 spectrometer (Bruker, Billerica, MA, USA) was used. The spectra collection was performed in transmission mode at 4 cm^{-1} spectral resolution, 10 μm × 10 μm aperture dimensions and 128 scans. All spectra were obtained by means of Opus 7.5 software (Bruker, Billerica, MA, USA). The measuring range was 4000–600 cm^{-1} wavenumbers, and zero filling was performed with fast Fourier transform (FFT), so that we obtained one point every 2 cm^{-1} in the final spectra. Background spectra were collected from a clean area of each CaF_2 window every 10 min. A mercury cadmium telluride (MCT) detector was used, and both the microscope and spectrometer were continuously purged with a flow of dried air. For each studied area, approximately 100 spectra with a step size of 50 μm × 50 μm for human samples and 30 μm × 30 μm for mouse samples were acquired. In order to represent regional differences with high spatial resolution in the tissue, maps of 200 spectra with a step size of 6 μm × 6 μm were performed in one representative sample of each species containing GM and WM areas.

2.5. μFTIR Spectra Analysis

Principal Component Analysis (PCA) was done using the open source software package Orange (Bioinformatics Laboratory of the University of Ljubljana, Version 3.23, Ljubljana, Slovenia) with the spectroscopy add-on (Version 0.4.9) [17]. The analysis was focused on the lipid region (3050–2800 cm^{-1}) and the protein region (1800–1500 cm^{-1}) of the spectra. The PCA were performed after the second derivatives were calculated and unit vector normalizations were performed on each spectrum for each region. The second derivatives were calculated with a polynomial order of 2 and a window size of 5 points for the lipid region and 17 points for the protein region. For a statistical and detailed study of lipid and protein composition, Unscrambler X software (CAMO Software, Oslo, Norway) was used. In this software, second derivation using the Savitsky–Golay algorithm with an eleven-point smoothing filter and a polynomial order of 3 was applied on the spectra to eliminate the baseline contribution and enhance narrow bands. After that, we measured the absorptions at the following wavenumbers related to functional groups of biochemical interest: ~2921 cm^{-1} (CH_2 asymmetric stretching vibrations), ~2962 cm^{-1} (CH_3 asymmetric stretching vibrations), ~3012 cm^{-1} (C=CH, unsaturated olefinic group), ~1743 cm^{-1} (C=O, carbonyl group), ~1656 cm^{-1} (α-helix protein structure), ~1637 cm^{-1} (intramolecular β-sheet protein structure), ~1625 cm^{-1} (intermolecular β-sheet protein structure) and ~1548 cm^{-1} (Amide II). The absorbances at the mentioned wavenumbers, 2 cm^{-1} before and at 2 cm^{-1} after, were obtained and averaged to represent the peaks of interest. CH_2 and CH_3, especially CH_2, are functional groups mostly present in lipids, while α-helix and β-sheet structures belong to the Amide I functional group band present in proteins. To account for variations in the tissue thickness, CH_3, C=CH and C=O peaks were normalized by the CH_2 band (as an approximation of the

total lipid content), whereas Amide II and β-sheet peaks were normalized by the total protein content (Amide I or α-helix bands).

2.6. Statistical Analysis

Statistical analysis and graphical representation were performed using the Graph Pad Prism$^{®}$ software. To determine differences between GM and WM, Student's *t*-test was carried out on human and mouse data. For statistically significance, we considered *p*-value < 0.05. All data are expressed as mean values ± standard error of the mean (SEM).

3. Results

In this section, we present the mean spectra in the range 3500–1250 cm^{-1} wavenumbers and the PCA of the lipid and protein regions of GM and WM samples belonging to humans and mice. Moreover, statistical analyses were applied for the study of CH_3 (d^2A_{2962}/d^2A_{2921}), C=CH (d^2A_{3012}/d^2A_{2921}) and C=O (d^2A_{1743}/d^2A_{2921}) compositions with respect to the lipid content, and Amide II ($d^2A_{1548}/d^2A_{1656+1637}$), intramolecular β-sheet structure (d^2A_{1637}/d^2A_{1656}) and intermolecular β-sheet structure ($d^2A_{1625}/d^2A_{1656+1637}$) with respect to the protein content, comparing their infrared absorptions between GM and WM in human and murine brain samples.

3.1. Different Chemical Profile of the Brain Tissue

In order to visualize the infrared profile of GM and WM areas, all spectra from each cerebral region were averaged in both species. µFTIR data show a clear different spectrum profile for each brain area characterized by higher CH_2 (~2920 cm^{-1} and ~2850 cm^{-1}) and CH_3 (~2960 cm^{-1}) peaks in WM with respect to the GM area; however, Amide I (~1650 cm^{-1}) and Amide II (~1550 cm^{-1}) peaks are very similar in both areas, as shown in Figure 1A,B. CH_2 and CH_3 groups are mainly related to lipids, which are very abundant in myelin, while Amide I and II groups are related to proteins. Our results demonstrate that lipid/protein (CH_2/Amide I) amount is statistically higher in WM compared with GM, as shown in Figure 2A,B. This different chemical composition is also observed by high resolution imaging tissue maps, where GM and WM from the same sample were captured, as shown in Figure 2C,D. All the mentioned observations are present in humans and mice.

3.2. Principal Component Analysis of Brain Areas and Species

Principal Component Analysis (PCA) was applied to calculate Euclidean distances between each spectral dataset and to cluster the spectral properties of the four sample groups (WM and GM for humans and mice). The PCA scores plots directly unravel differences and similarities among the spectra, while the PCA loadings detail the spectral differences between the clusters. The analysis is shown in Figure 3—left panels show the comparison of the C-H bond region (3050–2800 cm^{-1}). This region is mainly dominated by the infrared absorption of lipids in the system. Figure 3A shows the score plot and Figure 3B shows the corresponding PC1 (59%) and PC2 (17%) loadings. The score plot distribution shows that PC1 clearly differentiates human and mouse data, while PC2 differentiates between GM and WM. PC1 loading indicates that slight shifts characterize the differences between human and mouse samples, while PC2 indicates that differences between 3012 cm^{-1} (C=CH bond), 2921 cm^{-1} (CH_2 group) and 2962 cm^{-1} (CH_3 group) intensities differentiate between WM and GM. For a better illustration of differences, the average spectra of the second derivative of each group are plotted in Figure 3C. Right panels in Figure 3 show the PCA corresponding to the 1800–1500 cm^{-1} region where carbonyl groups and the Amide I and II absorb. The score plot in Figure 3D shows that, as in the C–H bond region, PC1 (54%) discriminates between humans and mice and PC2 (17%) between GM and WM. The loadings in Figure 3E indicate the wavelengths that allow for distinguishing between groups. The strongest contribution arises at 1625 cm^{-1} for PC1 and at 1637 cm^{-1} for PC2, indicating more intermolecular β-sheet structures for human samples, especially in GM, and more intramolecular β-sheet structures in human and mouse GM samples. Moreover, the contribution at

1685 cm^{-1} of PC1 suggests differences in the antiparallel β-sheet structures for humans and mice. As also observed in the representation of the average spectra of the second derivative of each group, as shown in Figure 3F, small changes in protein secondary structure discriminate between human and mouse spectra. Differently, changes in the intensity of the carbonyl band with a maximum at 1741 cm^{-1} discriminate between WM and GM.
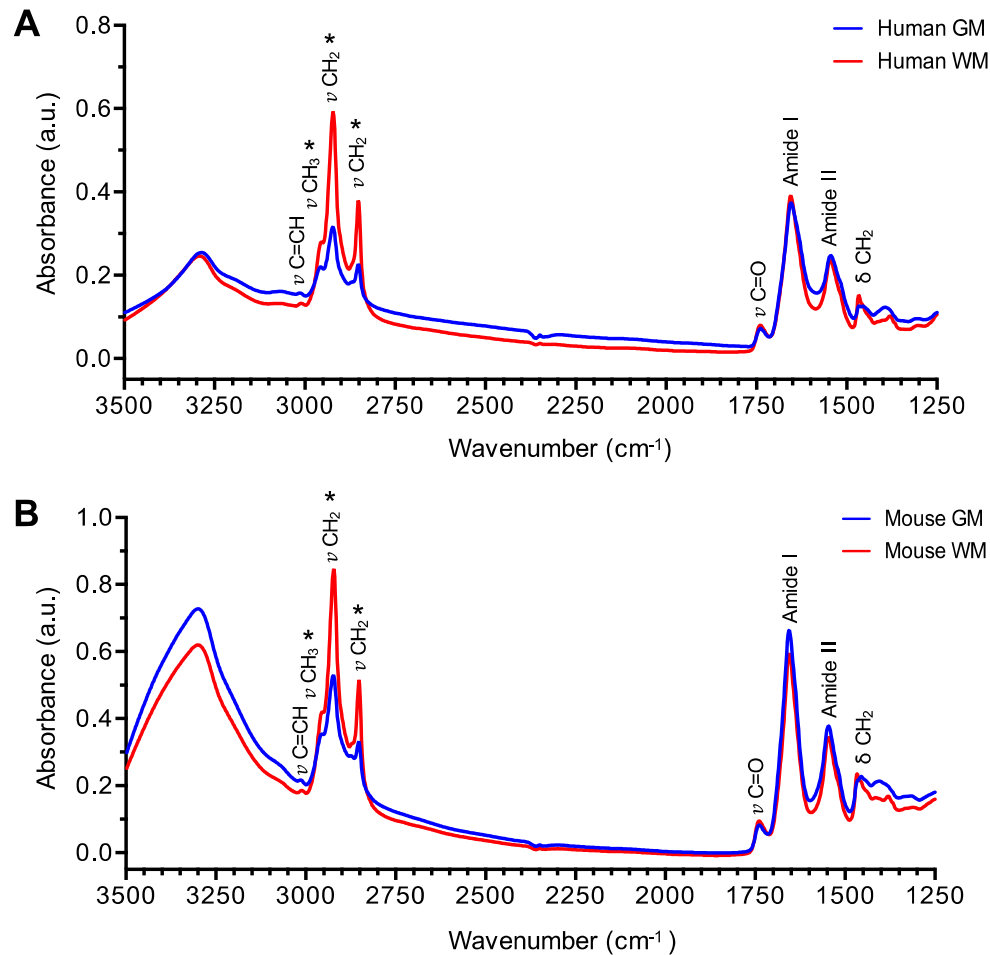
Figure 1. μFTIR profile of grey matter (GM) and white matter (WM). Spectra of GM (blue line) and WM (red line) areas were collected and average for human (**A**) and mouse (**B**) brain samples. Note the increased absorptions of CH_2 and CH_3 peaks (*) in WM with respect to GM. a.u.—arbitrary units.
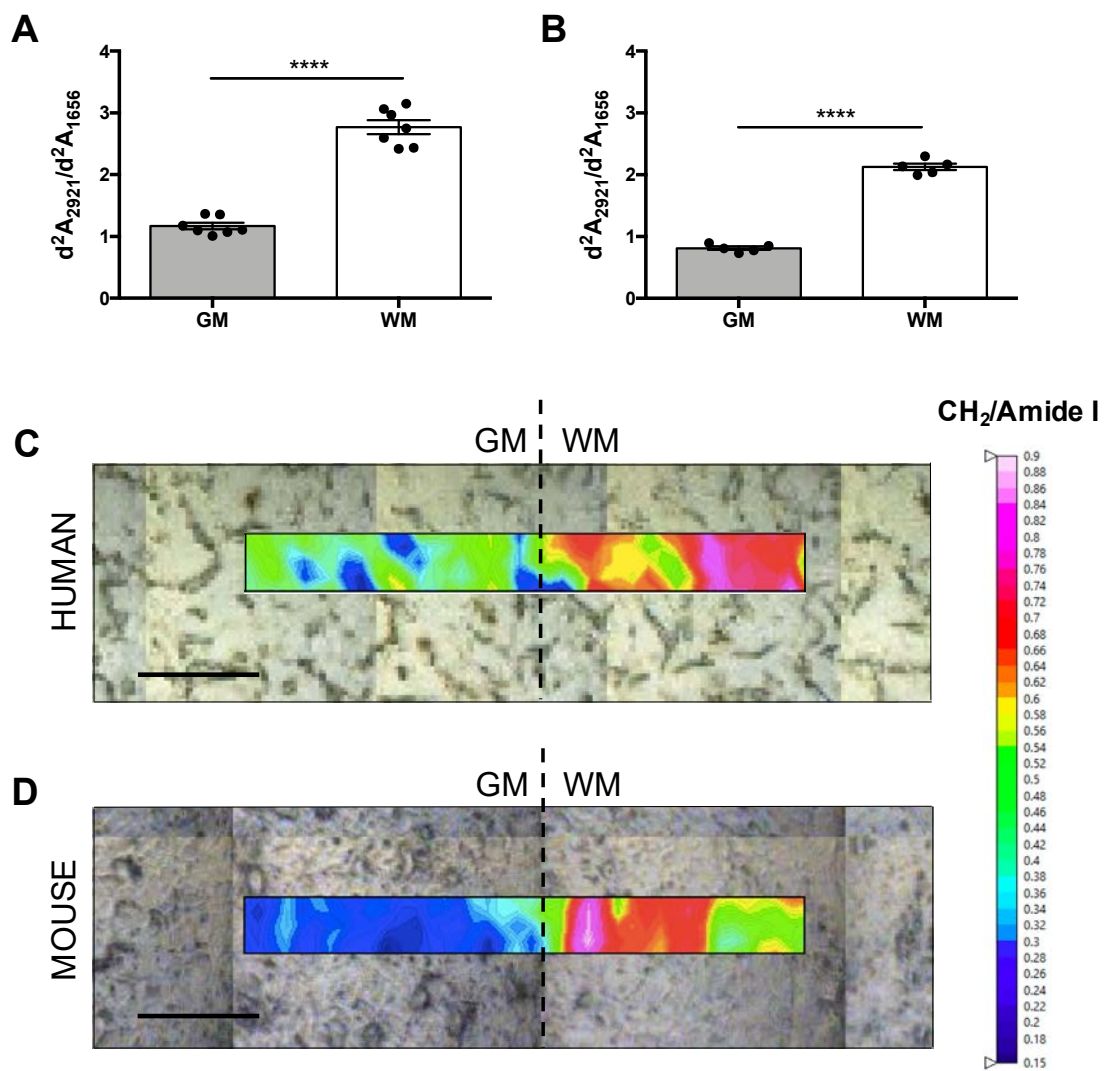
Figure 2. Lipid/Protein composition by µFTIR in grey matter (GM) and white matter (WM). Quantification of CH_2/Amide I absorbance after second derivative (d^2A_{2921}/d^2A_{1656}) in humans (**A**) and mice (**B**) confirms higher lipid amount in WM with respect to GM. Each dot in the graphs correspond to the mean of approximately 100 infrared measurements from a subject. Representative in situ heat maps from human (**C**) and murine (**D**) cerebral tissue showing CH_2/Amide I ratio. Dashed lines in the tissue images represent the limit between GM and WM. **** *p*-value < 0.0001. Scale bar = 50 µm.

LIPID REGION　　　　　　　　　　**PROTEIN REGION**
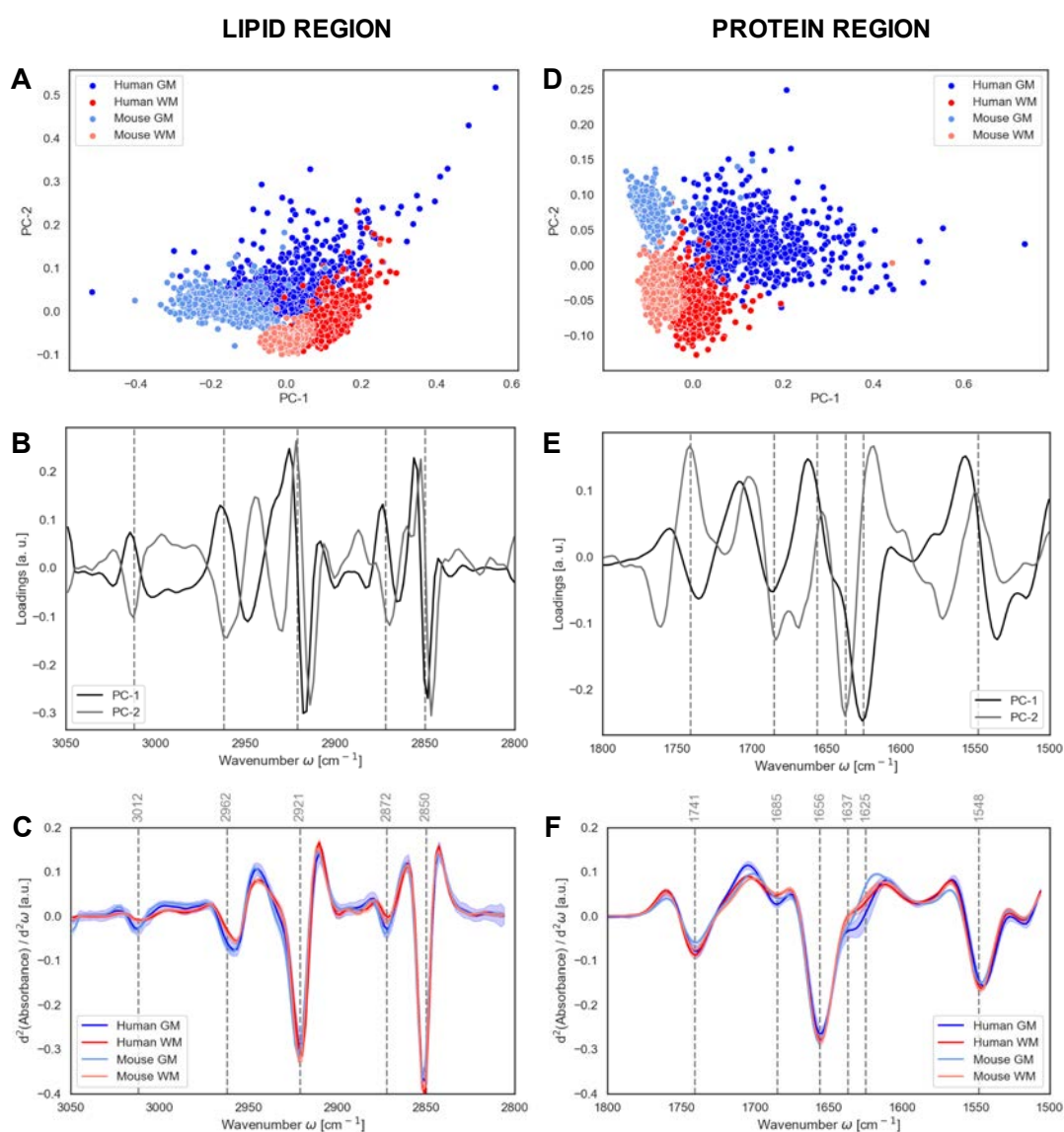
Figure 3. Principal Component Analysis (PCA) of grey matter (GM) and white matter (WM). PCA of the normalized second derivatives of the lipid region (3050–2800 cm^{-1}) and protein region (1800–1500 cm^{-1}), showing the scores plots (**A,D**), the resulting loadings for PC-1 and PC-2 (**B,E**) and the average spectra (**C,F**) of the two regions, respectively. Spectra shadowing in C and F indicates standard deviation. a.u.—arbitrary units.

3.3. Protein and Lipid Properties Differ by Cerebral Region

To thoroughly analyze the typical properties of lipids and proteins in brain areas, ratios for different infrared wavenumber absorptions after the second derivative were performed. For lipids, we quantified carbonyl (C=O), unsaturated olefinic (C=CH) and methyl (CH_3) group absorbances with respect to the total lipidic amount in the sample, normalizing by the CH_2 absorbance. Our results show that lipids in the GM area of humans and mice contain more carbonyl (d^2A_{1743}/d^2A_{2921}), olefinic (d^2A_{3012}/d^2A_{2921}) and methyl (d^2A_{2962}/d^2A_{2921}) groups with respect to the WM area, as shown in Figure 4A–C. Regarding proteins, we quantified Amide II, intramolecular β-sheet and intramolecular β-sheet absorbances with respect to the total protein amount normalizing by the Amide I absorbance. Compared to GM, our data show that proteins of WM present more absorption in the Amide II groups ($d^2A_{1548}/d^2A_{1656+1637}$), that account for the N–H and C–H absorption, and less intramolecular β-sheet structures (d^2A_{1637}/d^2A_{1656}) in humans and mice, as shown in Figure 4D,E. Interestingly, intermolecular

β-sheet structures ($d^2A_{1625}/d^2A_{1656+1637}$) seem not to be present in mice, whereas in humans we can observe their presence in the GM area belonging to four of the seven subjects studied, as shown in Figure 4F. Attending to the mean values of the samples, this work also provides evidence of higher heterogeneity, especially in the C–H region, in GM than in WM, as shown in Figure 4.
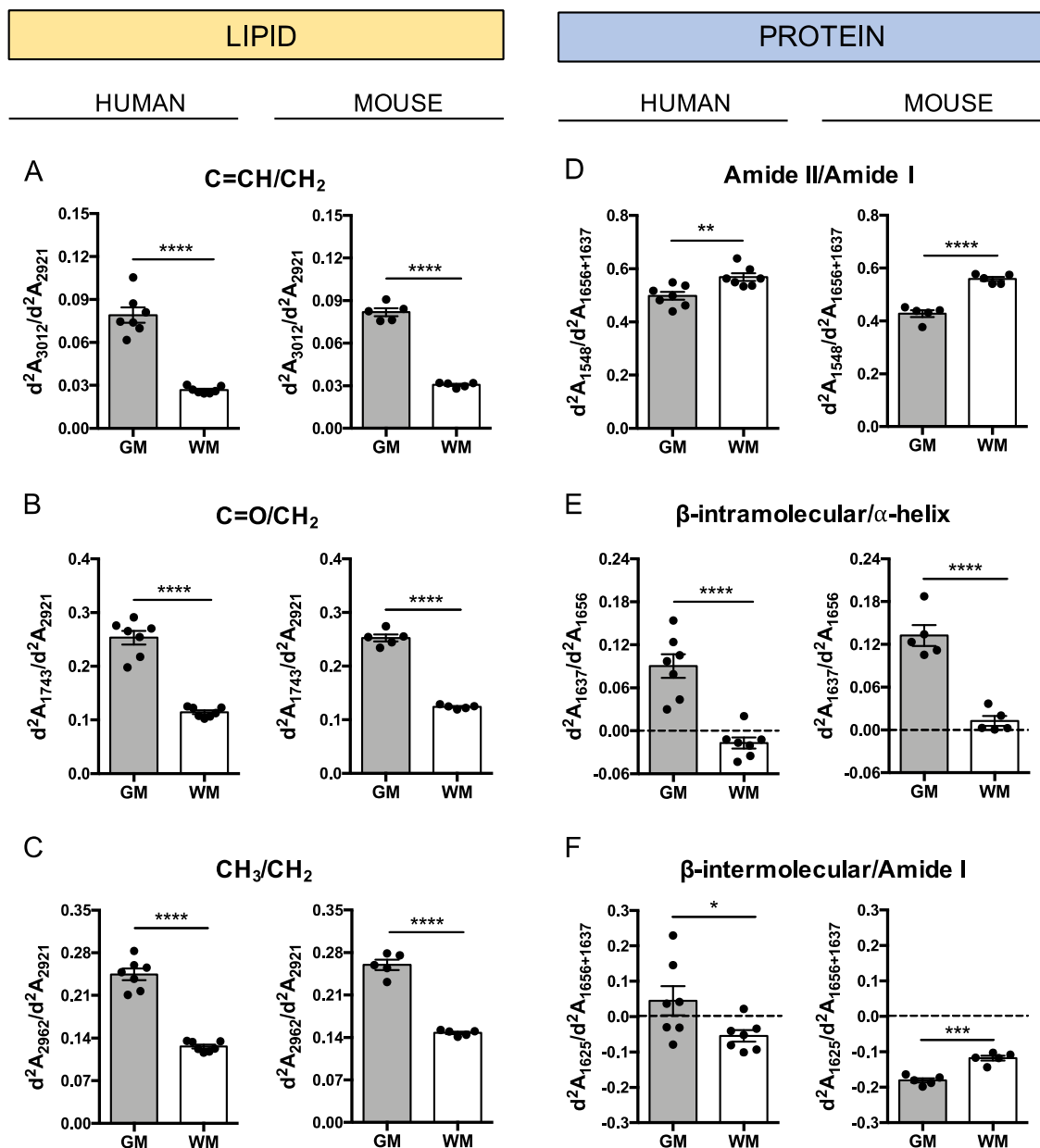
Figure 4. Chemical properties of lipids and proteins in grey matter (GM) and white matter (WM). Graphs represents absorbance second derivative (d^2A) ratios of functional groups related to lipids (**A**–**C**) and proteins (**D**–**F**) in human and murine brain samples. Each dot in the graphs correspond to the mean of approximately 100 infrared measurements from a subject. * *p*-value < 0.05; ** *p*-value < 0.01; *** *p*-value < 0.001; **** *p*-value < 0.0001.

4. Discussion

The present work shows that synchrotron-based µFTIR is a very sensitive and reproducible method for biochemical analyses of GM and WM areas of both human and mouse brain tissues. Furthermore, the molecular features reported by µFTIR based on synchrotron light can be simultaneously compared with histological features observed in the same examined sample.

Depending on the tissue sample processing (e.g., paraffin embedding, freezing, chemical fixation, etc.) and the data analysis (e.g., spectral correction, normalization, derivation, etc.), the infrared values obtained may vary. Although Mazur and collaborators showed no significant differences in the infrared output of unfixed versus formalin-fixed cells [18,19], Hackett and collaborators demonstrated some slight differences in the infrared spectrum of the cryo-fixed tissue before and after formalin fixation [20]. However, our data in both cryo-fixed and paraformaldehyde-fixed tissue show a specific composition between brain areas already reported in rats [9,15,21] and humans [11], regardless of histological sample processing. A special note of caution is due for the analysis of specific wavenumbers, such as phosphate and sugars, depending on the chemistry of sample processing (phosphate buffer, sugar-based cryoprotectants, etc.). Because of differential sample processing between human and murine samples in this study, we did not analyze the phosphate region to avoid the substantial contribution of the buffer in murine samples compared to human samples.

Our infrared spectra confirm the different biochemical compositions between brain areas characterized by a higher amount of lipid content in WM compared to GM, showing a significantly higher lipid/protein (CH_2/Amide I) ratio in WM with respect to GM. We can considerer the lipid/protein ratio to distinguish between brain areas by the μFTIR method, considering that second derivative absorption values < 1.5 correspond with measures in GM, whereas values > 1.5 correspond with measures in WM. Despite the different sample processing used between species, this discrimination can be perfectly applied to human and mouse samples. Thus, this lipid/protein 1.5 threshold value is an interesting GM versus WM discrimination factor, that may allow unsupervised μFTIR large data acquisition in human or murine whole brain samples. As a potential diagnostic method, values greater than 1.5 in GM or values lower than 1.5 in WM could be indicative of lipid and/or protein alterations in the brains of mice and humans. A similar lipid/protein threshold value (1.05) between GM and WM was established by Bonda and collaborators in rat brain cryo-fixed samples [9], supporting the use of the μFTIR method to discriminate between brain regions in humans, mice and rats. However, our data in cryo-fixed human samples show values that are slightly different to those reported in the study of Bonda et al. [9], but very similar to those of paraformaldehyde-fixed murine samples, which may, albeit unlikely, mean that mouse is more similar to human than rat as an animal model. A more likely explanation is that differential sample processing (fixation procedure) and data processing (water subtraction, calculation of area, derivation, etc.) can account for variability between studies.

In addition, we are able to clearly visualize WM and GM in the tissue by high resolution infrared maps based on lipid/protein ratio with no need of other histological or biochemical procedures. Among the many biological differences between GM and WM, one of the most significant is that GM is predominantly composed of rich-protein neuronal somas and WM by myelinated neuronal axons [22]. Since WM is mainly constituted by multilamellar myelin sheaths and the lipid composition of myelin is ~70% dry weight [23], the higher content of lipid in WM can be attributed to this multilamellar structure surrounding the axons. In addition to neurons and myelin, we have to considerer that both GM and WM are composed by glial cells [24,25]. Cellular density and intrinsic features of glial cells differ in each brain area and, therefore, they probably also participate in the specific tissue chemical composition described in this study.

The PCA allows us to identify spectral differences and similarities between the four sample groups. On the one hand, we observed that humans and mice share common spectral features ($3012\ cm^{-1}$ and $2962\ cm^{-1}$), while the distinction can be made between GM and WM. On the other hand, strong differences for the PC1 of the protein region ($1741\ cm^{-1}$ and $1625\ cm^{-1}$) were found between humans and mice.

Our results show that lipid characteristics vary between GM and WM in humans and mice. In both species, CH_3/CH_2, C=CH/CH_2 and C=O/CH_2 ratios were higher in GM compared to WM. Since lipids are composed mostly by long CH_2 chains and to a lesser extent by methyl groups, CH_2 groups are used to measure the lipid content of a sample, while CH_3 groups could be useful to determine the lipid chain length. Cholesterol and cerebrosides are the most abundant lipids in myelin, constituting

approximately 27% and 19%, respectively, of the lipids in human WM [21,26]. Whereas cholesterol is also highly present in GM, high concentration of cerebroside is specific for WM but not for GM. As an example, galactocerebrosides, the main cerebrosides present in the WM, are composed of two chains of numerous CH_2 groups and only two CH_3 groups at the end of the chains, arguing for a differential observation depending on lipid tail length in the ratio CH_3/CH_2. However, as it is shown in Benseny-Cases et al. [27], proteins have a similar number of CH_2 and CH_3 groups in their lateral chains, whereas lipids have significantly more CH_2 than CH_3 in their hydrophobic tail. Thus, changes in the lipid/protein ratio also implies changes in the C–H region (3000–2000 cm^{-1}). Absorptions of olefinic C=CH functional group at 3012 cm^{-1} and C=O functional group at 1743 cm^{-1} were used to evaluate lipid unsaturation and lipid carbonyl content, respectively. C=CH and C=O bands examined by μFTIR are absent in cholesterol, galactocerebroside, sphingomyelin and sulfatide lipids, which are characteristic of WM, and present in some phospholipids [28]. Thus, our results show higher C=CH/CH_2 and C=O/CH_2 ratios in GM with respect to WM and are in agreement with these data. However, Krafft et al. showed a C=CH peak in galactocerebroside, sphingomyelin and sulfatide lipids by Raman spectroscopy [29]. On the other hand, it is known that free radicals mainly react with carbon double bond sites present in unsaturated lipids, resulting in carbonyl compound formation and lipid chain fragmentation [30–33]. Therefore, the high expression of C=O groups is related to the stable end-products of lipid peroxidation and, in consequence, the analyses of lipid oxidation status, measuring C=O/CH_2 content by μFTIR, have been performed in different studies [15,27,34]. Taking these data into account, our observations suggest that the lipids in GM could be more oxidized than in WM. Since carbon double bonds are the main target of free radicals, lipid oxidation should result in less olefinic content, however, we found a higher C=CH/CH_2 ratio in GM than WM. Some authors have attributed this high C=CH absorption to the accumulation of lipid peroxidation end-products, which contain numerous double bonds [4,35,36]. Altogether, the lower lipid content associated with the higher olefinic and carbonyl content in GM, could be interpreted as a higher oxidative status of GM with respect to WM. Brain tissue, especially WM, is very vulnerable to oxidative stress due to the presence of a rich lipid content, high oxidative metabolic activity and low antioxidant mechanisms [37]. However, in non-pathological samples, we observed more markers related to oxidation in GM than WM. The possible accumulation of oxidized lipids in GM could be due to the greater vulnerability to oxidative stress that neurons present [38].

Regarding protein composition, we also found differences between GM and WM areas. Analyzing the ratio Amide II/Amide I, we observed higher Amide II absorption (1548 cm^{-1}) in human and mouse WM with respect to GM. Mathematical methods, such as deconvolution or the second derivation of the Amide I band, allow us to detect α-helix at ~1656 cm^{-1} and intramolecular β-sheet at ~1637 cm^{-1} protein secondary conformations by μFTIR [1,39,40]. Our Amide I analysis reveals that WM is composed by fewer intramolecular β-sheet structures (d^2A_{1637}/d^2A_{1656}) compared with GM. These results were observed in both human and mouse brains. In addition to the principal β-sheet structure at ~1637 cm^{-1}, more β-components have been detected in the infrared spectra after resolution enhancement. The presence of a band at ~1625 cm^{-1} represents an unusual intermolecular β-sheet structure [41] that has been observed in β-amyloid plaques [4,42–44], α-synuclein [45] and prion proteins [46]. In consequence, this band is used as a marker of protein β-aggregation in several pathologies [5,6,9,45–47]. Infrared absorption intensity of the ratio $d^2A_{1625}/d^2A_{1656+1637}$ after second derivative shows negative values in human WM and in both mouse brain areas. This low vibrational intensity at 1625 cm^{-1} could be due to no expression of aggregated proteins in these areas. Interestingly, some humans show positive values at this wavelength in GM. Considering studied samples belong to aged humans, the apparition of this peak could be due to the age-dependent onset of protein aggregation [48–50]. Murine samples also belong to aged mice and there is no expression of this band. This finding may indicate that in mice there is no production of β-aggregation in non-pathological conditions, while humans are susceptible to produce it in GM. Furthermore, a weak band at ~1685 cm^{-1}, which is assigned to antiparallel β-sheet structures [41,51], was also observed in the GM of humans.

The antiparallel β-sheet structure has been described as a signature of β-amyloid oligomers being absent in fibrils [42,52]. Thereby, infrared absorptions at both 1685 cm^{-1} and 1625 cm^{-1} in the GM of some individuals could suggest the presence of oligomeric β-amyloid aggregates. This assumption is consistent with the fact that only genetically modified mice are capable to accumulate β-amyloid [53], and on the contrary, has been reported that healthy elder humans can present β-amyloid plaques in GM areas [48–50]. Furthermore, the β-aggregation, observed specifically in the GM of some individuals, is in agreement with the weaker mechanisms that present neurons to avoid protein aggregation with respect to other cells types of the CNS [54,55]. Nevertheless, β-aggregation in healthy aged individuals and in pathophysiology, both in human and murine samples, raises an issue that requires further research.

In summary, this work demonstrates by μFTIR: (i) a specific lipid/protein composition of GM and WM areas; (ii) a different presence of lipid and protein functional groups by cerebral area; (iii) that the regional differences observed in the human brain are fairly reproduced in mice, with the exception of β-aggregation content. These similarities between species in non-pathological conditions make the mouse a good experimental animal model. μFTIR comparative biology studies, but also comparative sample and data processing studies [18–20] are essential to assess and understand differences and similarities between species, especially for disease-related animal models. Specifically, the study of lipid-related disorders in mice could be very reliable in humans due to the high reproducibility observed in the lipid characteristics of GM and WM; however, the study of protein-related pathologies in mouse models requires a proper assessment sample and data processing variables.

5. Conclusions

The understanding of the brain biochemical properties in non-pathological conditions shown in this work will help us to study the molecular dynamics in different pathologies affecting GM, WM or both. Interestingly, this study provides evidence of mice (strain C57BL/6) as good animal models to reproduce human properties of the brain. Thus, μFTIR is a powerful tool to progress in the knowledge of CNS physiology and pathology performed in mice, by which data can be extrapolated to humans.

References

1. Kong, J.; Yu, S. Fourier transform infrared spectroscopic analysis of protein secondary structures. *Acta Biochim. Biophys. Sin. (Shanghai)* **2007**, *39*, 549–559. [CrossRef] [PubMed]
2. Lamba, O.P.; Lal, S.; Yappert, M.C.; Lou, M.F.; Borchman, D. Spectroscopic detection of lipid peroxidation products and structural changes in a sphingomyelin model system. *Biochim. Biophys. Acta* **1991**, *1081*, 181–187. [CrossRef]
3. Sarver, R.W., Jr.; Krueger, W.C. Protein secondary structure from Fourier transform infrared spectroscopy: A data base analysis. *Anal. Biochem.* **1991**, *194*, 89–100. [CrossRef]
4. Benseny-Cases, N.; Klementieva, O.; Cotte, M.; Ferrer, I.; Cladera, J. Microspectroscopy (muFTIR) reveals co-localization of lipid oxidation and amyloid plaques in human Alzheimer disease brains. *Anal. Chem.* **2014**, *86*, 12047–12054. [CrossRef] [PubMed]

5.   Benseny-Cases, N.; Alvarez-Marimon, E.; Aso, E.; Carmona, M.; Klementieva, O.; Appelhans, D.; Ferrer, I.; Cladera, J. In situ structural characterization of early amyloid aggregates in Alzheimer's disease transgenic mice and Octodon degus. *Sci. Rep.* **2020**, *10*, 5888. [CrossRef]

6.   Klementieva, O.; Willen, K.; Martinsson, I.; Israelsson, B.; Engdahl, A.; Cladera, J.; Uvdal, P.; Gouras, G.K. Pre-plaque conformational changes in Alzheimer's disease-linked Abeta and APP. *Nat. Commun.* **2017**, *8*, 14726. [CrossRef] [PubMed]

7.   Liao, C.R.; Rak, M.; Lund, J.; Unger, M.; Platt, E.; Albensi, B.C.; Hirschmugl, C.J.; Gough, K.M. Synchrotron FTIR reveals lipid around and within amyloid plaques in transgenic mice and Alzheimer's disease brain. *Analyst* **2013**, *138*, 3991–3997. [CrossRef]

8.   Szczerbowska-Boruchowska, M.; Dumas, P.; Kastyak, M.Z.; Chwiej, J.; Lankosz, M.; Adamek, D.; Krygowska-Wajs, A. Biomolecular investigation of human substantia nigra in Parkinson's disease by synchrotron radiation Fourier transform infrared microspectroscopy. *Arch. Biochem. Biophys.* **2007**, *459*, 241–248. [CrossRef]

9.   Bonda, M.; Perrin, V.; Vileno, B.; Runne, H.; Kretlow, A.; Forro, L.; Luthi-Carter, R.; Miller, L.M.; Jeney, S. Synchrotron infrared microspectroscopy detecting the evolution of Huntington's disease neuropathology and suggesting unique correlates of dysfunction in white versus gray brain matter. *Anal. Chem.* **2011**, *83*, 7712–7720. [CrossRef]

10.   Heraud, P.; Caine, S.; Campanale, N.; Karnezis, T.; McNaughton, D.; Wood, B.R.; Tobin, M.J.; Bernard, C.C. Early detection of the chemical changes occurring during the induction and prevention of autoimmune-mediated demyelination detected by FT-IR imaging. *Neuroimage* **2010**, *49*, 1180–1189. [CrossRef]

11.   Choo, L.P.; Jackson, M.; Halliday, W.C.; Mantsch, H.H. Infrared spectroscopic characterisation of multiple sclerosis plaques in the human central nervous system. *Biochim. Biophys. Acta* **1993**, *1182*, 333–337. [CrossRef]

12.   LeVine, S.M.; Wetzel, D.L. Chemical analysis of multiple sclerosis lesions by FT-IR microspectroscopy. *Free Radic. Biol. Med.* **1998**, *25*, 33–41. [CrossRef]

13.   Ali, M.H.M.; Rakib, F.; Abdelalim, E.M.; Limbeck, A.; Mall, R.; Ullah, E.; Mesaeli, N.; McNaughton, D.; Ahmed, T.; Al-Saad, K. Fourier-Transform Infrared Imaging Spectroscopy and Laser Ablation -ICPMS New Vistas for Biochemical Analyses of Ischemic Stroke in Rat Brain. *Front. Neurosci.* **2018**, *12*, 647. [CrossRef] [PubMed]

14.   Leskovjan, A.C.; Kretlow, A.; Miller, L.M. Fourier transform infrared imaging showing reduced unsaturated lipid content in the hippocampus of a mouse model of Alzheimer's disease. *Anal. Chem.* **2010**, *82*, 2711–2716. [CrossRef] [PubMed]

15.   Cakmak, G.; Miller, L.M.; Zorlu, F.; Severcan, F. Amifostine, a radioprotectant agent, protects rat brain tissue lipids against ionizing radiation induced damage: An FTIR microspectroscopic imaging study. *Arch. Biochem. Biophys.* **2012**, *520*, 67–73. [CrossRef]

16.   Yousef, I.; Ribó, L.; Crisol, A.; Šics, I.; Ellis, G.; Ducic, T.; Kreuzer, M.; Benseny-Cases, N.; Quispe, M.; Dumas, P.; et al. MIRAS: The Infrared Synchrotron Radiation Beamline at ALBA. *Synchrotron Radiat. News* **2017**, *30*, 4–6. [CrossRef]

17.   Demšar, J.; Curk, T.; Erjavec, A.; Gorup, Č.; Hočevar, T.; Milutinovič, M.; Možina, M.; Polajnar, M.; Toplak, M.; Starič, A.; et al. Orange: Data mining toolbox in python. *J. Mach. Learn. Res.* **2013**, *14*, 2349–2353.

18.   Mazur, A.I.; Marcsisin, E.J.; Bird, B.; Miljković, M.; Diem, M. Evaluating different fixation protocols for spectral cytopathology, part 1. *Anal. Chem.* **2012**, *84*, 1259–1266. [CrossRef]

19.   Mazur, A.I.; Marcsisin, E.J.; Bird, B.; Miljković, M.; Diem, M. Evaluating different fixation protocols for spectral cytopathology, part 2: Cultured cells. *Anal. Chem.* **2012**, *84*, 8265–8271. [CrossRef]

20.   Hackett, M.J.; McQuillan, J.A.; El-Assaad, F.; Aitken, J.B.; Levina, A.; Cohen, D.D.; Siegele, R.; Carter, E.A.; Grau, G.E.; Hunt, N.H.; et al. Chemical alterations to murine brain tissue induced by formalin fixation: Implications for biospestroscopic imaging and mapping studies of disease pathogenesis. *Analyst* **2011**, *136*, 2941–2952. [CrossRef]

21.   Levine, S.M.; Wetzel, D.L.B. Analysis of Brain Tissue by FT-IR Microspectroscopy. *Appl. Spectrosc. Rev.* **1993**, *28*, 385–412. [CrossRef]

22.   Purves, D.A.; Augustine, G.J.; Fitzpatrick, D.; Hall, W.C.; LaMantia, A.S.; McNamara, J.O.; White, L.E. *Neuroscience*, 3th ed.; Sinauer Associates: Sunderland, MA, USA, 2004.

23. Norton, W.T.; Poduslo, S.E. Myelination in rat brain: Changes in myelin composition during brain maturation. *J. Neurochem.* **1973**, *21*, 759–773. [CrossRef] [PubMed]

24. von Bartheld, C.S.; Bahney, J.; Herculano-Houzel, S. The search for true numbers of neurons and glial cells in the human brain: A review of 150 years of cell counting. *J. Comp. Neurol.* **2016**, *524*, 3865–3895. [CrossRef] [PubMed]

25. Herculano-Houzel, S. The glia/neuron ratio: How it varies uniformly across brain structures and species and what that means for brain physiology and evolution. *Glia* **2014**, *62*, 1377–1391. [CrossRef] [PubMed]

26. Olsson, N.U.; Harding, A.J.; Harper, C.; Salem, N., Jr. High-performance liquid chromatography method with light-scattering detection for measurements of lipid class composition: Analysis of brains from alcoholics. *J. Chromatogr. B Biomed. Appl.* **1996**, *681*, 213–218. [CrossRef]

27. Benseny-Cases, N.; Alvarez-Marimon, E.; Castillo-Michel, H.; Cotte, M.; Falcon, C.; Cladera, J. Synchrotron-Based Fourier Transform Infrared Microspectroscopy (muFTIR) Study on the Effect of Alzheimer's Abeta Amorphous and Fibrillar Aggregates on PC12 Cells. *Anal. Chem.* **2018**, *90*, 2772–2779. [CrossRef]

28. Dreissig, I.; Machill, S.; Salzer, R.; Krafft, C. Quantification of brain lipids by FTIR spectroscopy and partial least squares regression. *Spectrochim. Acta A Mol. Biomo.l Spectrosc.* **2009**, *71*, 2069–2075. [CrossRef]

29. Krafft, C.; Neudert, L.; Simat, T.; Salzer, R. Near infrared Raman spectra of human brain lipids. *Spectrochim. Acta A Mol. Biomol. Spectrosc.* **2005**, *61*, 1529–1535. [CrossRef]

30. Rice-Evans, C.A. Formation of free radicals and mechanisms of action in normal biochemical processes and pathological states. In *Free Radical Damage and its Control*; Rice-Evans, C.A., Burdon, R.H., Eds.; Elsevier Science: Amsterdam, The Netherlands, 1994; Volume 28, pp. 131–153.

31. de Zwart, L.L.; Meerman, J.H.; Commandeur, J.N.; Vermeulen, N.P. Biomarkers of free radical damage applications in experimental animals and in humans. *Free Radic. Biol. Med.* **1999**, *26*, 202–226. [CrossRef]

32. Niki, E.; Yoshida, Y.; Saito, Y.; Noguchi, N. Lipid peroxidation: Mechanisms, inhibition, and biological effects. *Biochem. Biophys. Res. Commun.* **2005**, *338*, 668–676. [CrossRef]

33. Yin, H.; Xu, L.; Porter, N.A. Free radical lipid peroxidation: Mechanisms and analysis. *Chem. Rev.* **2011**, *111*, 5944–5972. [CrossRef] [PubMed]

34. Rakib, F.; Ali, C.M.; Yousuf, M.; Afifi, M.; Bhatt, P.R.; Ullah, E.; Al-Saad, K.; Ali, M.H.M. Investigation of Biochemical Alterations in Ischemic Stroke Using Fourier Transform Infrared Imaging Spectroscopy—A Preliminary Study. *Brain Sci.* **2019**, *9*, 293. [CrossRef] [PubMed]

35. Severcan, F.; Gorgulu, G.; Gorgulu, S.T.; Guray, T. Rapid monitoring of diabetes-induced lipid peroxidation by Fourier transform infrared spectroscopy: Evidence from rat liver microsomal membranes. *Anal. Biochem.* **2005**, *339*, 36–40. [CrossRef] [PubMed]

36. Liu, K.B.; Bose, R.; Mantsch, H.H. Infrared spectroscopic study of diabetic platelets. *Vib. Spectrosc.* **2002**, *28*, 131–136. [CrossRef]

37. Halliwell, B. Reactive oxygen species and the central nervous system. *J. Neurochem.* **1992**, *59*, 1609–1623. [CrossRef] [PubMed]

38. Lassmann, H.; van Horssen, J. Oxidative stress and its impact on neurons and glia in multiple sclerosis lesions. *Biochim. Biophys. Acta* **2016**, *1862*, 506–510. [CrossRef]

39. Byler, D.M.; Susi, H. Examination of the secondary structure of proteins by deconvolved FTIR spectra. *Biopolymers* **1986**, *25*, 469–487. [CrossRef]

40. Dong, A.; Huang, P.; Caughey, W.S. Protein secondary structures in water from second-derivative amide I infrared spectra. *Biochemistry* **1990**, *29*, 3303–3308. [CrossRef]

41. Arrondo, J.L.; Young, N.M.; Mantsch, H.H. The solution structure of concanavalin A probed by FT-IR spectroscopy. *Biochim. Biophys. Acta* **1988**, *952*, 261–268. [CrossRef]

42. Peralvarez-Marin, A.; Barth, A.; Graslund, A. Time-resolved infrared spectroscopy of pH-induced aggregation of the Alzheimer Abeta(1-28) peptide. *J. Mol. Biol.* **2008**, *379*, 589–596. [CrossRef]

43. Benseny-Cases, N.; Cocera, M.; Cladera, J. Conversion of non-fibrillar beta-sheet oligomers into amyloid fibrils in Alzheimer's disease amyloid peptide aggregation. *Biochem. Biophys. Res. Commun.* **2007**, *361*, 916–921. [CrossRef] [PubMed]

44. Rak, M.; Del Bigio, M.R.; Mai, S.; Westaway, D.; Gough, K. Dense-core and diffuse Abeta plaques in TgCRND8 mice studied with synchrotron FTIR microspectroscopy. *Biopolymers* **2007**, *87*, 207–217. [CrossRef] [PubMed]

45. Conway, K.A.; Harper, J.D.; Lansbury, P.T., Jr. Fibrils formed in vitro from alpha-synuclein and two mutant forms linked to Parkinson's disease are typical amyloid. *Biochemistry* **2000**, *39*, 2552–2563. [CrossRef] [PubMed]

46. Kretlow, A.; Wang, Q.; Beekes, M.; Naumann, D.; Miller, L.M. Changes in protein structure and distribution observed at pre-clinical stages of scrapie pathogenesis. *Biochim. Biophys. Acta* **2008**, *1782*, 559–565. [CrossRef] [PubMed]

47. Miller, L.M.; Bourassa, M.W.; Smith, R.J. FTIR spectroscopic imaging of protein aggregation in living cells. *Biochim. Biophys. Acta* **2013**, *1828*, 2339–2346. [CrossRef]

48. Price, J.L.; Morris, J.C. Tangles and plaques in nondemented aging and "preclinical" Alzheimer's disease. *Ann. Neurol.* **1999**, *45*, 358–368. [CrossRef]

49. Rodrigue, K.M.; Kennedy, K.M.; Devous, M.D., Sr.; Rieck, J.R.; Hebrank, A.C.; Diaz-Arrastia, R.; Mathews, D.; Park, D.C. beta-Amyloid burden in healthy aging: Regional distribution and cognitive consequences. *Neurology* **2012**, *78*, 387–395. [CrossRef]

50. Spies, P.E.; Verbeek, M.M.; van Groen, T.; Claassen, J.A. Reviewing reasons for the decreased CSF Abeta42 concentration in Alzheimer disease. *Front. Biosci.* **2012**, *17*, 2024–2034. [CrossRef]

51. Kubelka, J.; Keiderling, T.A. Differentation of Beta-Sheet Forming Structures: Ab Initio-Based Simulations of IR Absorption nd Vibrational CD for Model Peptide and Protein Beta-Sheets. *J. Am. Chem. Soc.* **2001**, *123*, 12048–12058. [CrossRef]

52. Cerf, E.; Sarroukh, R.; Tamamizu-Kato, S.; Breydo, L.; Derclaye, S.; Dufrene, Y.F.; Narayanaswami, V.; Goormaghtigh, E.; Ruysschaert, J.M.; Raussens, V. Antiparallel beta-sheet: A signature structure of the oligomeric amyloid beta-peptide. *Biochem. J.* **2009**, *421*, 415–423. [CrossRef]

53. Elder, G.A.; Gama Sosa, M.A.; De Gasperi, R. Transgenic mouse models of Alzheimer's disease. *Mt. Sinai. J. Med.* **2010**, *77*, 69–81. [CrossRef] [PubMed]

54. Kundra, R.; Dobson, C.M.; Vendruscolo, M. A Cell- and Tissue-Specific Weakness of the Protein Homeostasis System Underlies Brain Vulnerability to Protein Aggregation. *iScience* **2020**, *23*, 100934. [CrossRef] [PubMed]

55. Fu, H.; Possenti, A.; Freer, R.; Nakano, Y.; Hernandez Villegas, N.C.; Tang, M.; Cauhy, P.V.M.; Lassus, B.A.; Chen, S.; Fowler, S.L.; et al. A tau homeostasis signature is linked with the cellular and regional vulnerability of excitatory neurons to tau pathology. *Nat. Neurosci.* **2019**, *22*, 47–56. [CrossRef] [PubMed]

Specific microglial phagocytic phenotype and decrease of lipid oxidation in white matter areas during aging: implications of different microenvironments

Paula Sanchez-Molina[a,b], Beatriz Almolda[a,b], Núria Benseny-Cases[c], Berta González[a,b], Alex Perálvarez-Marín[a,d], Bernardo Castellano[a,b]

[a]Institute of Neurosciences. Universitat Autònoma de Barcelona, 08193 Bellaterra, Barcelona, Spain.
[b]Department of Cell Biology, Physiology and Immunology. Universitat Autònoma de Barcelona, 08193 Bellaterra, Barcelona, Spain.
[c]ALBA Synchrotron Light Source, Carrer de la Llum 2-26, 08290 Cerdanyola del Vallès, Catalonia, Spain.
[d]Biophysics Unit, Department of Biochemistry and Molecular Biology. Universitat Autònoma de Barcelona, 08193 Bellaterra, Catalonia, Spain.

Corresponding author:
Beatriz Almolda
Unitat d'Histologia, Torre M5.
Facultat de Medicina
Universitat Autònoma de Barcelona
08193 Bellaterra, Barcelona, Spain
Tel: +34935811826
Fax: +34935812392
e-mail: beatriz.almolda@uab.cat

ABSTRACT

Physiological aging is characterised by an imbalance of pro-inflammatory and anti-inflammatory mediators leading to neuroinflammation. Microglial cells, which are highly regulated by the local microenvironment, undergo specific changes depending upon the brain area during aging. The aim of this study is to evaluate the influence of age over microglial cells along different brain areas and microenvironments. For this purpose, transgenic mice with overproduction of either the anti-inflammatory IL-10 cytokine or the pro-inflammatory IL-6 cytokine were used. Our results show that, during aging, microglial cells located in white matter (WM) areas maintain their phagocytic capacity but present a specific phagocytic phenotype with receptors involved in myelin recognition, arguing for aging-derived myelin damage. Whereas IL-10 overproduction anticipates the age-related microglial phagocytic phenotype, maintaining it over time, IL-6 overproduction exacerbates this phenotype in aging. These modifications were linked with a higher efficiency of myelin engulfment by microglia in aged transgenic animals. Moreover, we show, in a novel way, lower lipid oxidation during aging in WM areas, regardless of the genotype. The novelty of the insights presented in this study open a window to deeply investigate myelin lipid oxidation and the role of microglial cells in its regulation during physiological aging.

Key words: aging, neuroinflammation, phagocytosis, microglia, myelin, lipid oxidation, cytokines

1. INTRODUCTION

Aging is a physiological process characterised by high molecular oxidative stress, mainly in the form of reactive oxygen species (ROS) (Harman, 1956). In the central nervous system (CNS) specifically, aging is associated with an imbalance between ROS-induced inflammation and anti-inflammatory agents. Brain homeostasis alteration usually leads to different types of dementia, and it is one of the greatest risk factors for developing neurodegenerative processes, such as Alzheimer's or Parkinson's diseases (Griffin, 2006; Mrak and Griffin, 2005; Radak et al., 2011; von Bernhardi, 2007).

Microglial cells, as the main intrinsic CNS immune cells, play a relevant role in the regulation of neuroinflammatory processes. Microglial cells present different characteristics depending on i) the inflammatory and/or aging scenario (Butovsky and Weiner, 2018; Cornejo and von Bernhardi, 2016; Holtman et al., 2015), and ii) the cerebral region (de Haas et al., 2008; Olah et al., 2011; Tan et al., 2020). A distinct morphology, a more activated phenotype and alterations in their phagocytic capacity are the principal features reported in aged microglia (Perry et al., 1993; Ritzel et al., 2015; Streit et al., 2004; Streit et al., 2014), which can differ between brain areas (Hart et al., 2012; Raj et al., 2017).

Especially during aging, the microglial phagocytic function is critical to eliminate extracellular debris, protein aggregates, apoptotic cells, and neurotoxic compounds produced as a consequence of the characteristic pro-inflammatory microenvironment at this life stage. However, how the microglial phagocytic function is affected by aging is a poorly understood issue. At the molecular level, aged microglia increases the production of oxidative radicals, nitric oxide and pro-inflammatory cytokines such as IL-6, IL-1β and TNFα (Godbout and Johnson, 2004; Sierra et al., 2007; Ye and Johnson, 1999), while it decreases the levels of IL-10 (Frank et al., 2006; Ye and Johnson, 2001) and IL-4 (Maher et al., 2005) anti-inflammatory cytokines. Aging-derived changes in microglia could be summarised in a dysfunctional phenotype where the microglial neuroprotective functions are lost (Mosher and Wyss-Coray, 2014; Streit, 2006; Streit et al., 2004; Streit et al., 2009) and inflammatory activation is exacerbated, leading to neuron excitotoxicity, neuronal damage, and finally neurodegeneration (Beltrán-Castillo et al., 2018; Norden and Godbout, 2013; von Bernhardi et al., 2015).

The differences between adult and aged microglia, as well as, regional differences, show the importance of the surrounding microenvironment on these cells. Thus, the aim of the present study is to evaluate the influence that the local microenvironment exerts on microglial cells along different areas of the aged brain.

For this purpose, adult and aged mice from two different transgenic lines with chronic CNS-restricted overproduction of either the anti-inflammatory IL-10 cytokine (Almolda et al., 2015) or the pro-inflammatory IL-6 cytokine (Campbell et al., 1993) were used. In these animals, different brain areas of grey matter (GM) and white matter (WM) were analysed.

2. MATERIAL AND METHODS

2.1. Animals and experimental groups

Two transgenic mice lines, on the C57BL/6 background, with astrocyte-targeted production of either IL-10 (GFAP-IL10Tg) (Almolda et al., 2015) or IL-6 (GFAP-IL6Tg) (Campbell et al., 1993) and their corresponding wild-type (WT) littermates were used in the present study. For each genotype, animals of both sexes were randomly distributed into two experimental groups according to age: one group of adult mice (4-5 months old; n = 46) and one group of aged mice (18-22 months old; n = 32). During the study, animals were maintained in conventional plastic cages with food and water *ad libitum,* in a 12 h light/dark cycle and at 22 ^{o}C ± 2 ^{o}C and 50%-60% humidity. All experimental animal work was conducted according to Spanish regulations (Ley 32/2007, Real Decreto 1201/2005, Ley 9/2003 and Real Decreto 178/2004) in agreement with European Union directives (86/609/CEE, 91/628/CEE) and was approved by the Ethical Committee of the Autonomous University of Barcelona.

2.2. Tissue processing for histological analysis

Animals were euthanised under an anaesthesia solution of xylazine (30 mg/kg) and ketamine (120 mg/kg) and intracardially perfused for 10 min with 4% paraformaldehyde in 0.1 M phosphate buffer (pH 7.4). The brains were quickly removed, post-fixed for 4 h at 4 ^{o}C in the same fixative, cryoprotected with 30% sucrose solution in 0.1 M phosphate buffer for 48 h at 4 ^{o}C and, finally, frozen in ice-cold 2-methylbutane (320404, Sigma-Aldrich) and stored at -80 ^{o}C. Series of coronal parallel sections of the brain from bregma 0.86 mm to bregma -2.46 mm coordinates were obtained using a cryostat (CM3050S Leica). 10-µm-thick brain sections were mounted in gelatinized slides and stored at -20 ^{o}C until use. 30-µm-thick free-floating sections were stored at -20 ^{o}C in a 0.01 M anti-freeze solution containing 20% sucrose, 30% ethylene glycol and 1% polyvinylpyrrolidone (PVP) until use (adapted from de Olmos et al., 1978).

2.3. Single immunohistochemistry

To study the effects that IL-10 and IL-6 overproduction exert in an age-dependent manner through the brain, we performed immunohistochemistry in coronal brain sections (30-µm-thick) containing representative areas of grey matter (cerebral cortex and hippocampus) and white matter (corpus callosum and fimbria). For the visualisation of microglial morphology, distribution and general activation, sections were immunostained with antibodies against IBA1 and MHC-II. Microglial cell density was determined by PU.1 immunostaining (Walton et al., 2000). To characterise the microglial phagocytic phenotype, macrosalin (CD68), a triggering receptor expressed on myeloid cells 2 (TREM-2), Galectin-3 (GAL-3) and CD11c markers were used. Finally, MBP and APP immunostainings were used for studying myelin and axonal damage, respectively. In all cases, frozen free-floating sections were washed in Tris-buffered saline (TBS; 0.05 M, pH 7.4) to eliminate the anti-freeze solution and incubated for 10 min with 2% H_2O_2 and 70% methanol in distilled H_2O to inhibit endogenous peroxidase. In the case of PU.1, previous to the endogenous peroxidase blocking step, an antigen retrieval treatment to a major exposure of PU.1 nuclear antigen was used, incubating the sections with sodium citrate buffer (pH 8.5) for 40 min at 80 $^{\circ}$C and 20 min at room temperature (RT). After washes with TBS containing 1% Triton X-100 (0.05 M, pH 7.4), sections were incubated for 1 h at RT in a blocking buffer (BB) containing 10% foetal bovine serum (FBS) and 0.3% bovine serum albumin (BSA) in TBS + 1% Triton X-100. For the TREM-2 marker, sections were blocked with TBS containing 0.5% Triton X-100 and 0.2% gelatin (48723, Fluka). After the blocking step, sections were incubated with the corresponding primary antibodies (**Table 1**) diluted in their corresponding BB, overnight at 4 $^{\circ}$C and 1 h at RT, except for the TREM-2 antibody, which was incubated 48 h at RT. Sections incubated in BB lacking the primary antibody were used as negative control, whereas spleen sections were used as positive control. After washes with TBS containing 1% or 0.5% Triton, sections were incubated for 1 h at RT with their corresponding biotinylated secondary antibodies (**Table 2**) diluted in their respective blocking solutions. Then, sections were washed and incubated for 1 h at RT with horseradish peroxidase (HRP)-conjugated streptavidin (1:500; SA-5004, Vector Laboratories). After washes with TBS and Tris-buffered (TB; 0.05 M, pH 7.4), the product of the reaction was visualised by incubating the sections for 3 min in a 3,3-diaminobenzidine (DAB) Substrate Kit (SK-4100, Vector Laboratories) following the manufacturer's instructions. Afterwards, sections were washed in TB, mounted onto gelatinised slides and air dried at RT. To provide cytological details, some slides were counter-stained with 0.1% toluidine blue diluted in Walpole's buffer (0.05 M, pH 4.5). Finally, sections were dehydrated in graded

alcohols, washed in N-butyl alcohol in the case of toluidine staining, immersed in xylene and cover-slipped with DPX mounting media.

2.4. Double immunofluorescence

Double immunolabelling showing IBA1 and CD68 markers was performed to determine CD68 expression in microglial cells. Frozen free-floating brain sections were washed in TBS (0.05 M, pH 7.4) and TBS containing 1% Triton X-100 (0.05 M, pH 7.4) to eliminate the anti-freeze solution. After incubation for 1 h at RT in a BB containing 10% FBS and 3% BSA in TBS + 1% Triton X-100, sections were incubated with IBA1 primary antibody (**Table 1**) diluted in the BB overnight at 4 °C and 1 h at RT. After washes with TBS containing 1% Triton, sections were incubated for 1 h at RT with an anti-rabbit Alexa-Fluor-488 conjugated secondary antibody (**Table 2**) diluted in BB. Following another blocking incubation for 1 h at RT, sections were incubated with CD68 primary antibody (**Table 1**) followed by anti-rat Alexa-Fluor-555 conjugated secondary antibody (**Table 2**) using the time and temperatures described for IBA1. Following washes with TBS containing 1% Triton and TBS, sections were incubated with 4,9,6-diamidino-2-phenylindole (DAPI) (1:10000; D9542, Sigma-Aldrich) in TB for 5 min at RT to stain the cell nuclei. Finally, sections were washed with TB, mounted on slides and cover-slipped with Fluoromount (0100-01, SouthernBiotech) mounting medium. Representative photos of the cerebral cortex and the corpus callosum were captured using a Zeiss LSM700 confocal microscope.

2.5. Luxol Fast Blue staining

In addition to MBP, Luxol Fast Blue (LFB) staining was used to visualise myelin. 10-μm-thick frozen brain sections mounted on slides were dehydrated in 50%, 70% and 95% ethanol and incubated in LFB solution (0.1% Luxol Fast Blue MBS and 0.05% Glacial Acetic Acid 10% in ethanol 95%) for 2 h at 60 °C. After washes in 95% ethanol and distilled water, dips in 0.05% lithium carbonate solution followed by 70% ethanol were performed. Finally, sections were dehydrated with 95% and 100% ethanol, washed in xylene and covered with DPX mounting media.

2.6. Densitometric analysis

To analyse IBA1 and CD68 expression, photographs at 20x magnification were taken in the cerebral cortex, hippocampus, corpus callosum and fimbria from at least two different brain sections of each animal. A minimum of 12 photographs of the cerebral cortex, 12 photographs of the hippocampus, 8 photographs of the corpus callosum and 8 photographs of the fimbria were captured for each animal. To analyse TREM-2 and

GAL-3 expression, photographs at 10x magnification were taken in the corpus callosum and fimbria. For these areas, a minimum of 6 photographs from at least two different brain sections was captured per animal. To quantify MBP and LFB expression, photographs at 20x magnification were taken in the medial corpus callosum from at least five brain sections per animal. All photographs were obtained with a DXM 1200F Nikon digital camera mounted on a brightfield Nikon Eclipse 80i microscope and using the ACT-1 2.20 software (Nikon Corporation). By means of the AnalySIS® software (Soft Imaging System, Germany), both the percentage of area occupied by the immunolabelling and the immunostaining intensity (mean grey value mean) were measured for each photograph. For all of the markers mentioned, 3-5 animals of each experimental group were analyzed.

2.7. Microglial cell density quantification

To quantify microglial cell density, photographs at 10x magnification in the cerebral cortex, hippocampus, corpus callosum and fimbria from at least two different brain sections stained for PU.1 marker (Walton et al., 2000) were captured for each animal with the same device and software described above. A minimum of 8 photographs of the cerebral cortex, 8 photographs of the hippocampus, 6 photographs of the corpus callosum and 6 photographs of the fimbria were taken per animal. The number of PU.1+ cells in the region of interest was obtained using the "Image-based Tool for Counting Nuclei" (ITCN) plug-in from NIH ImageJ® software (Wayne Rasband, National Institutes of Health; USA). Data were averaged and converted to cells/mm^2. Quantification of CD11c+ cells was carried out manually at 20x magnification in at least six brain sections of the cerebral cortex, hippocampus, corpus callosum and fimbria per animal. For both analyses, 3-5 animals of each experimental group were quantified.

2.8. Myelin isolation and fluorescent labelling

Brain-derived myelin was isolated from WT mice following the protocol described by Rolfe et al. (2017). Briefly, six animals were dislocated and brains were quickly removed, cut into pieces and homogenised in a cold 0.32 M sucrose solution prepared in 0.1 M Tris-HCl buffer. Next, 9 mL of the homogenised brain solution was added to the top of 15 mL of 0.83 M sucrose solution prepared in 0.1 M Tris-HCl buffer and centrifuged at 100,000 g for 45 min at 4 °C. After that, myelin was collected from the interface of the two sucrose densities, homogenised with 0.1 M Tris-HCl buffer and centrifuged twice at 100,000 g for 45 min at 4 °C. Followed by a centrifugation at 16,000 g for 10 min at 4 °C in 0.1 M Phosphate-Buffered Saline (PBS), the resulting pellet of myelin was weighed and reconstituted in 0.1 M PBS to a final concentration of

100 mg/mL. To be able to detect internalised myelin in cellular phagolysosomes, 277.5 µg of purified myelin was incubated with 25 µL of pHrodo™ Green STP Ester (P35369, Thermo Fisher) in a total volume of 250 µL of 0.1 M PBS (pH 8) for 45 min at RT. After spinning at 4,000 g for 10 min at 4 °C, pHrodo-conjugated myelin was resuspended in 950 µL of 0.1 M PBS (pH 7.2) to obtain a final concentration of 0.3 µg/µL.

2.9 Myelin phagocytosis assay

To measure phagocytic capacity of microglial cells belonging to the white matter, we quantified the ingestion of pHrodo-conjugated myelin by microglial cells isolated from the corpus callosum using the flow cytometry procedure, as in Gómez-López et al. (2021). Briefly, under an intraperitoneal anaesthetic solution of xylazine (30 mg/kg) and ketamine (120 mg/kg), mice were perfused intracardially with cold 0.1 M PBS (pH 7.4) for 1 min and corpus callosum were quickly dissected. After dissociation of the tissue with a 160 µm nylon mesh, the resulting cell suspension was passed through a 70 µm cell strainer and incubated in a digestion solution composed of deoxyribonuclease I (D5025, Sigma-Aldrich) and collagenase IV (17104019, Thermo Fisher) in Hank's Balanced Salt Solution (HBSS; 14025050, Thermo Fisher) for 30 min at 37 °C. To distinguish between different cellular phases, cell suspensions were centrifuged in a density gradient of Percoll® (GE17-0891-02, Sigma-Aldrich) for 20 min at 600 g. While the upper layer corresponding to myelin was removed, the intermediate phase containing cells was collected, centrifuged and incubated with 3 µg of pHrodo-conjugated myelin in 250 µL of Dulbecco's Modified Eagle Medium/Nutrient Mixture F-12 (DMEM/F-12; 31330038, Thermo Fisher) with 10% FBS for 4 h at 37 ºC. Cell suspensions without pHrodo-conjugated myelin incubation were used as negative control. After washes of 0.1 M PBS with 2% FBS for 5 min at 310 g, Fc receptors on microglial cells were blocked by incubating them with CD16/32 primary antibody (1:250; 553142, BD Biosciences) for 20 min at 4 °C. Subsequently, each cellular suspension was divided in two and incubated with either CD45-PerCP (1:400; 557235, BD Biosciences) and CD11b-APC-Cy7 (1:400; 557657, BD Biosciences) primary antibodies or their respective isotype controls (1:400; BD Biosciences) for 30 min at 4 °C in a conical 96-well plate. Finally, cell suspensions were washed and centrifuged in 0.1 M PBS with 2% FBS for 4 min at 1,700 rpm. A BD FACSCanto™ flow cytometer with the BD FACSDiva™ software was used to acquire and read the samples. Data analysis was performed by means of FlowJo™ software.

2.10. Tissue processing for SR-µFTIR analysis

For synchrotron radiation-Fourier transform infrared microspectroscopy (SR-µFTIR) analysis, animals were euthanised under an anaesthesia solution of xylazine (30 mg/kg) and ketamine (120 mg/kg) and intracardially perfused for 10 min with 4% paraformaldehyde in 0.1 M phosphate buffer (pH 7.4). The brains were quickly removed, post-fixed for 4 h at 4 °C in the same fixative and cryoprotected with 30% sucrose solution in 0.1 M phosphate buffer for 48 h at 4 °C. Finally, brains were frozen in ice-cold 2-methylbutane (320404, Sigma-Aldrich) and stored at -80 °C until use. Series of coronal parallel sections (9-µm-thick) between bregma 0.86 mm and bregma -1.22 mm coordinates were cut on a cryostat (CM3050S Leica) and mounted onto polished calcium fluoride (CaF_2) optical windows (CAFP20-1, Crystran; UK). To minimise water contribution, brain sections on CaF_2 windows were air-dried at RT and stored in a vacuum chamber protected from light until use.

2.11. SR-µFTIR data acquisition

SR-µFTIR was performed at the MIRAS beamline at ALBA Synchrotron (Catalonia, Spain) (Yousef et al., 2017). A Hyperion 3000 microscope equipped with a 36x magnification objective coupled to a Vertex 70 spectrometer (Bruker, Billerica; MA, USA) and a mercury cadmium telluride (MCT) detector were used. Both the microscope and spectrometer were continuously purged with a flow of dried air. Spectra were collected in transmission mode at 4 cm^{-1} resolution, 10 µm x 10 µm aperture dimensions and 64 scans and obtained by means of Opus 7.5 software (Bruker, Billerica; MA, USA). The measuring range was 600-4000 cm^{-1} wavenumber. Zero filling was performed with fast Fourier transform (FFT); therefore, one point every 2 cm^{-1} was obtained in the final spectra. Background spectra were collected from a clean area of each CaF_2 window every 10 min. For each animal, a minimum of 120 spectra with a step size of 30 µm x 30 µm was acquired in the cerebral cortex and corpus callosum areas of two different coronal brain sections (**Figure 7A,B**). A total of 4-5 animals per group were used for this experimental procedure. Furthermore, a tissue infrared-map of 900 spectra with a step size of 6 µm x 6 µm was performed in one representative animal of each experimental group.

2.12. SR-µFTIR spectra analysis

The spectra obtained from the tissue samples were firstly visualised in Opus 7.5 software (Bruker, Billerica; MA, USA) and those exhibiting a low signal-to-noise ratio were eliminated. For data processing, The Unscrambler X software (CAMO Software; Oslo, Norway) was used. Second derivative of the spectra was calculated using a Savitsky-Golay algorithm with an eleven-point smoothing filter and a polynomial order

of 3 to eliminate the baseline contribution and enhance narrow bands. The spectroscopic infrared peaks at different wavenumbers are well established to correspond with biomolecules and functional organic groups (**Figure 7C**). In this study we focused the analysis on the determination of the amount of lipid, with respect to the total amount of protein in the tissue using the ratios for CH_2/Amide I (d^2A_{2921}/d^2A_{1656} and d^2A_{1467}/d^2A_{1656}). Also, the lipid oxidation was determined by calculating the increase of the carbonyl group (C=O) using the d^2A_{1743}/d^2A_{2921} ratio and the increase of the unsaturated olefinic group (C=CH) calculating the d^2A_{3012}/d^2A_{2921} ratio, as in Benseny-Cases et al. (2018), Lamba et al. (1991) and LeVine and Wetzel (1998).

2.13. Tissue processing for biochemical analysis

Mice were euthanised under an intraperitoneal anaesthetic solution of xylazine (30 mg/kg) and ketamine (120 mg/kg) and perfused intracardially with cold 0.1 M PBS at pH 7.4 for 1 min. The cerebral cortex and corpus callosum were quickly dissected, frozen in liquid nitrogen and stored at -80 °C. Tissue was homogenised using a polytron homogenizer in a lysis buffer containing 25 mM HEPES at pH 7.4 (H3375, Sigma-Aldrich), 0.2% IGEPAL (I-3021, Sigma-Aldrich), 5 mM $MgCl_2$ (A376433, Merck), 1.3 mM EDTA at pH 8 (20302, VWR), 1 mM EGTA at pH 8 (E4378, Sigma-Aldrich), 1 mM PMSF (P7626, Sigma-Aldrich), protease inhibitor cocktail (1:100; P8343, Sigma-Aldrich) and phosphatase inhibitor cocktail (1:100; P0044, Sigma-Aldrich) in deionized water. After 2 h at 4 °C, tissue lysates were centrifuged at 13,000 rpm for 5 min at 4 °C. Then, the supernatants were collected and stored aliquoted at -80 °C until use.

2.14. Luminex bead-based multiplex assay

Total protein concentration of the cerebral cortex and the corpus callosum lysates were determined with a commercial Pierce BCA Protein Assay Kit (23225, Thermo Scientific) according to the manufacturer's instructions. To quantify IL-10, IL-6, IL-1β and TNFα cytokine levels, Luminex® Multiple Analyte Profiling (xMAP®) technology was performed according to the MILLIPLEX® $_{MAP}$ Kit (MHSTCMAG-70K, Merck) manufacturer's protocol. Briefly, 25 µL of each sample (total protein concentration of 3 µg/µL), standards and controls were added to their corresponding wells in a 96-well plate. Additionally, 25 µL of Assay Buffer were added to the samples' wells, whereas 25 µL of lysis buffer (See "2.13. Tissue processing for biochemical analysis" section) were added to standard and control wells. In all wells, 25 µL of magnetic beads were added and incubated on a plate-shaker (700 rpm) overnight at 4 °C. After removing wells' contents with a handheld magnet and three washes with Wash Buffer, 25 µL of Detection Antibodies were added into each well and incubated with agitation for 1 h at

RT. Next, 25 µL of Streptavidin-Phycoerythrin was also added to each well and incubated with agitation for 30 min at RT. Finally, the wells were washed three times with Wash Buffer, and 150 µL of Drive Fluid were added. Followed by a 5 min shaking, a Luminex MAGPIX® instrument with xPONENT® 4.2 software was used to read and analyse the plate.

2.15. Statistical analysis

Statistical analysis and graphical representation were performed using the Graph Pad Prism® software. In this study, we were interested in determining i) differences between transgenic and WT animals of the same age and ii) differences between aged and adult animals of the same genotype; for this reason, Student's t-test was used. Statistical significance was considered with $p < 0.05$ for all of the tests performed. All experimental results are expressed as mean values ± standard error of the mean (SEM).

3. RESULTS

3.1. Microglial activation and cell density

To characterise microglial morphology, activation and cell density, IBA1, MHC-II and PU.1 immunolabelling from different brain areas of grey matter (cerebral cortex and hippocampus) and white matter (corpus callosum and fimbria) **(Figures 1 and 2; Suppl. Figures 1 and 2)** was analysed.

During aging, a regional-dependent microglial activation was observed by an increase of IBA1 expression together with morphological changes. Whereas microglia from the cerebral cortex undergoes slight changes, microglia from hippocampus, corpus callosum and fimbria become highly activated, presenting a significant increase of IBA1 levels **(Figure 1R; Suppl. Figure 1D,R)**. In these cerebral regions, aged microglial cells exhibited a larger soma and thicker processes, as compared to adult microglia. To study microglial cell density, microglial nuclei were quantified with the myeloid transcription factor PU.1 (Walton et al., 2000). In parallel to the greater activation observed, microglial cell density was also increased during aging with differences between the studied areas. Thus, while microglial cell density was not modified in the cerebral cortex, cell density was increased in the hippocampus, corpus callosum and fimbria of aged mice **(Figure 2; Suppl. Figure 2)**. This increase was more pronounced in the white matter areas, which presented about twice the cell density in aging than in adulthood. Moreover, we show the presence of a high

microglial cell density **(Figure 2E; Suppl. Figure 2E)** and IBA1 immunolabelling **(Figure 1R; Suppl. Figure 1R)** in specific locations belonging to white matter areas during aging. However, despite the described microglial activation upon aging, no expression of MHC-II in microglial cells was observed (data not shown).
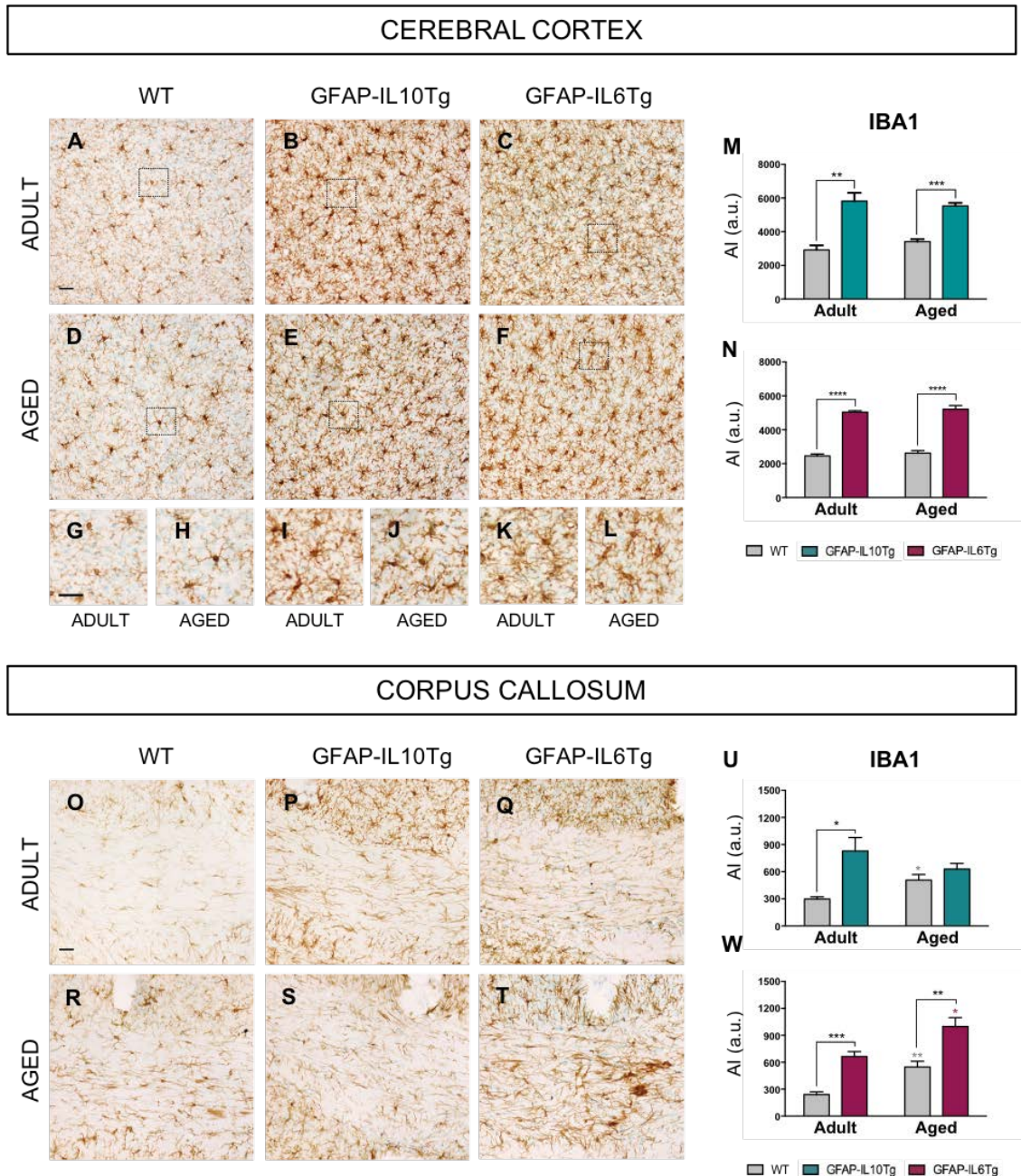
Figure 1. Microglial activation and morphology represented by IBA1 immunohistochemistry in the cerebral cortex and the corpus callosum. Representative images of IBA1 immunohistochemistry in the cerebral cortex (A-L) and the corpus callosum (O-T) of WT, GFAP-IL10Tg and GFAP-IL6Tg mice. Insets in A-F images show the microglial morphology at high magnification in the cerebral cortex (G-L). Graphs show the quantification of the immunostained area multiply by the immunostaining intensity of IBA1 in the cerebral cortex (M,N) and the corpus callosum (U,W) of GFAP-IL10Tg (M,U) and GFAP-IL6Tg (N,W) mice with respect to their corresponding WT littermates. Grey and magenta asterisks are referred to significant differences by age between WT and GFAP-IL6Tg mice, respectively. Data are represented as the mean $\pm$ SEM. $*p < 0.05$, $**p < 0.01$, $***p < 0.001$, $****p < 0.0001$. AI (Area x Intensity); a.u. (arbitrary units). Scale bar = 30 μm.

| CEREBRAL CORTEX | CORPUS CALLOSUM |
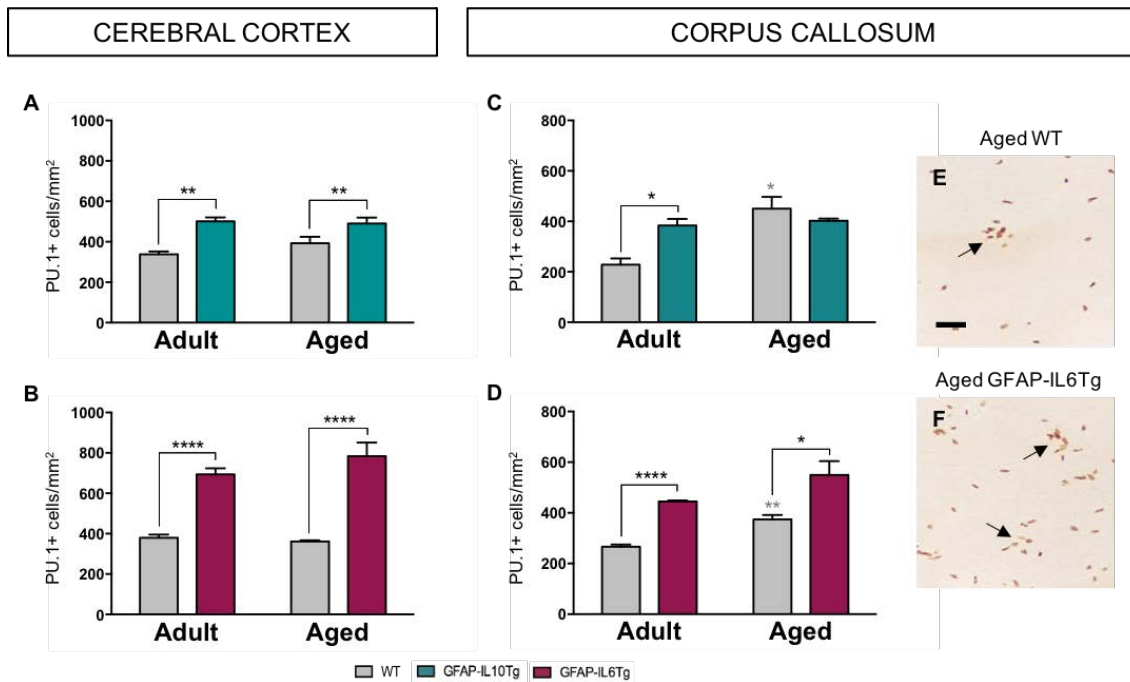
Figure 2. Microglial cell density represented by PU.1 immunohistochemistry in the cerebral cortex and the corpus callosum. Graphs show the quantification of PU.1 cell density in the cerebral cortex (A,B) and the corpus callosum (C,D) of GFAP-IL10Tg (A,C) and GFAP-IL6Tg (B,D) mice with respect to their corresponding WT littermates. Grey asterisks are referred to significant differences by age between WT mice. Data are represented as the mean $\pm$ SEM. $*p < 0.05$, $**p < 0.01$, $****p < 0.0001$. Representative photographs showing accumulations of microglial cells (arrows) observed in the corpus callosum of aged WT (E) and aged GFAP-IL6Tg (F) mice. Scale bar = 30 μm

Additionally, our results show that modifications in the brain microenvironment affect the age-related microglial activation. Both IL-10 and IL-6 transgenic overproduction induces an increase of IBA1 expression **(Figure 1B,C,P,Q; Suppl. Figure 1B,C,P,Q)** and microglial cell density **(Figure 2; Suppl. Figure 2)** in all areas studied during adulthood. In GFAP-IL10Tg mice, this induction remains unaltered along time, resulting in a higher activation and cell density than in WT mice in the grey matter areas during aging **(Figures 1M and 2A; Suppl. Figures 1M and 2A)**, but being similar to WT in the white matter areas **(Figures 1U and 2C; Suppl. Figure 1U)**. In this way, we show that microglial activation observed in adult GFAP-IL10Tg mice is similar to that observed during aging in the white matter areas of WT mice. On the other hand, IBA1 expression in GFAP-IL6Tg was exacerbated along time in the hippocampus, corpus callosum and fimbria **(Figure 1W; Suppl. Figure 1N,W)**. Thus, these animals presented a greater microglial activation than WT during aging in all of the areas studied. Likewise, more microglial cell density was detected by IL-6 overproduction **(Figure 2B,D; Suppl. Figure 2B,D)**. Concomitant with this activation, a high microglial cell density **(Figure 2F; Suppl. Figure 2F)** and IBA1 immunolabelling **(Figure 1T; Suppl. Figure 1T)** in specific locations of the white matter areas were remarkably visualised in aged GFAP-IL6Tg mice. Another feature affected by the IL-10 and IL-6

13

transgenic overproduction was the microglial morphology. In all areas studied, microglia from both transgenic animals showed a larger soma and thicker processes than WT microglia since adulthood **(Figure 1; Suppl. Figure 1)**. Remarkably, microglial cells from the hippocampal CA1 region of these animals, at both ages, presented a distinctive elongated morphology following the same direction as the dendrites of the pyramidal neurons of this area **(Suppl. Figure 1I-L)**.

3.2. Microglial phagocytic phenotype

Detection of macrosalin (CD68) was used to determine lysosomal phagocytic activity in grey matter (cerebral cortex and hippocampus) and white matter (corpus callosum and fimbria) areas **(Figure 3; Suppl. Figure 3)**.

In contrast to the slight CD68 immunolabelling observed in adult mice, an intense staining of CD68 restricted to the microglial cell soma was detected during aging in the cerebral cortex and the hippocampus of WT mice **(Figure 3D,L-N; Suppl. Figure 3D)**. In the corpus callosum and the fimbria, CD68 expression was also considerably increased in aged animals; however, its cellular distribution was more heterogeneous, including microglial soma and processes **(Figure 3AD,AL-AN; Suppl. Figure 3L)**.

As we observed with IBA1 and PU.1 markers, both IL-10 and IL-6 transgenic overproduction induces an increase of CD68 expression in adulthood for all areas studied, but in aging, the expression of this molecule is differently affected depending on the cytokine. While GFAP-IL10Tg animals presented similar levels of CD68 at both ages **(Figure 3G,AG; Suppl. Figure 3G,O)**, GFAP-IL6Tg animals showed an age-dependent CD68 increase reaching higher levels than those observed in aged WT mice **(Figure 3H,AH; Suppl. Figure 3H,P)**. The distribution of CD68 in the grey matter of aged transgenic animals was also different to that observed in WT, being localised not only in the perinuclear region, but also in microglial ramifications.

In addition to analysing the lysosomal phagocytic activity, triggering receptor expressed on myeloid cells 2 (TREM-2), Galectin-3 (GAL-3), and CD11c markers were used to determine the expression of phagocytic receptors on microglial cells **(Figure 4; Suppl. Figure 4)**.

During aging, we show an upregulation of TREM-2, GAL-3 and CD11c expression specifically in the white matter areas of WT mice. While the expression of TREM-2 in the cerebral cortex and the hippocampus was weakly visualised and localised perinuclearly at both ages (data not shown), a significant increase of the TREM-2 immunolabelling in the microglial cell soma and processes was observed in the corpus callosum and the fimbria of aged mice **(Figure 4A,D; Suppl. Figure 4A,D)**.

In parallel, the expression of GAL-3 and CD11c molecules was absent in the grey matter areas regardless of age, but *de novo* expression of both markers was observed in the white matter areas of WT mice upon aging **(Figure 4I,L; Suppl. Figure 4I,L)**.
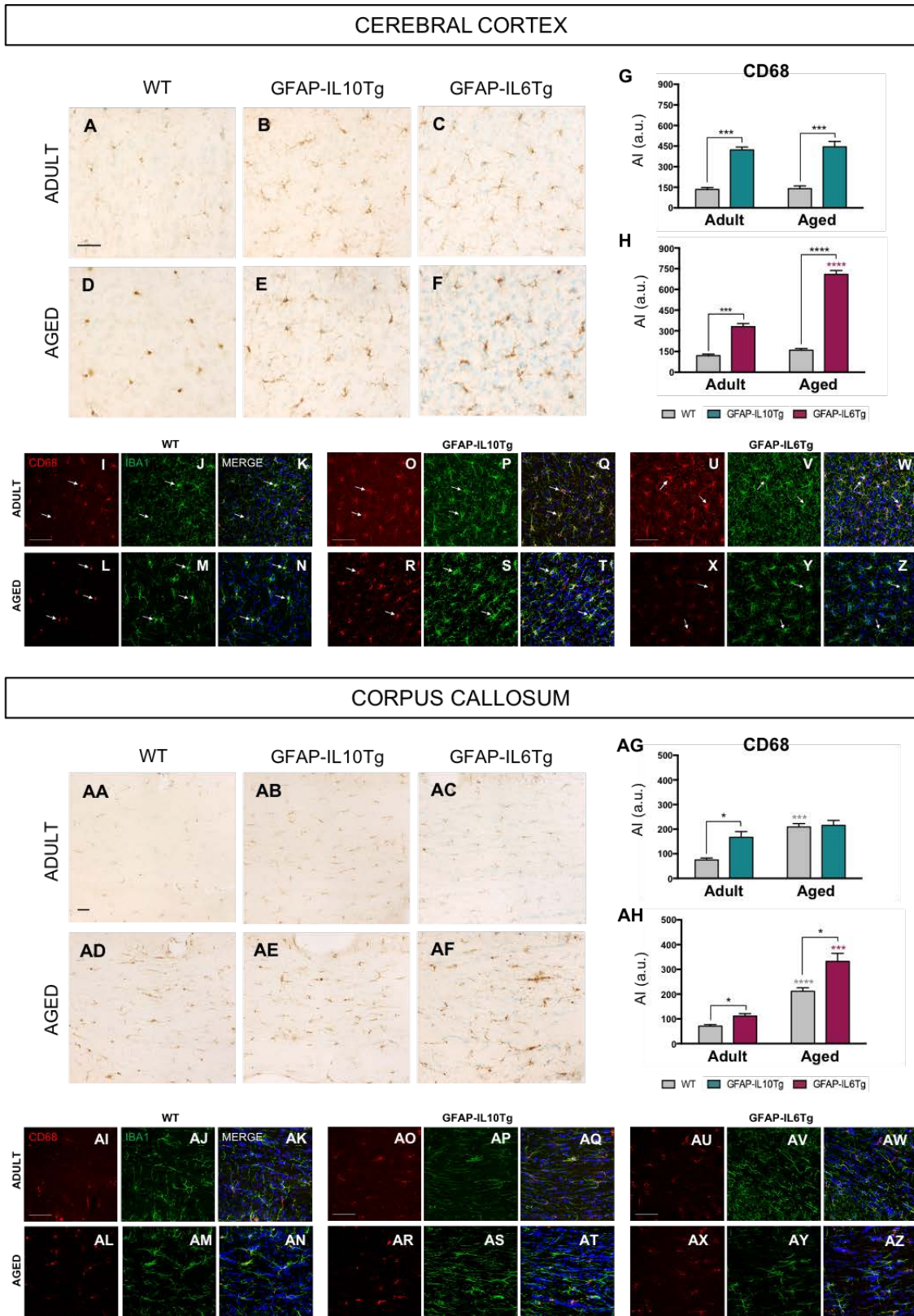
Figure 3. Microglial phagocytic capacity represented by CD68 immunostainings in the cerebral cortex and the corpus callosum. Representative images of CD68 immunohistochemistry in the cerebral cortex (A-F) and the corpus callosum (AA-AF) of WT, GFAP-IL10Tg and GFAP-IL6Tg mice. Graphs show the quantification of the immunostained area multiply by the immunostaining intensity of CD68 in the cerebral cortex (G,H) and the corpus callosum (AG,AH) of GFAP-IL10Tg (G,AG) and GFAP-IL6Tg (H,AH) mice with respect to their corresponding WT littermates. Note the restricted perinuclear distribution of CD68 in the cerebral cortex of aged WT animals (D,L) in contrast with the distribution along the microglial ramifications of GFAP-IL10Tg (E,R) and GFAP-IL6Tg (F,X) mice. Representative images of CD68 and IBA1 double-immunofluorescence in the cerebral cortex (I-Z) and the corpus callosum (AI-AZ) of WT, GFAP-IL10Tg and GFAP-IL6Tg mice. Yellow color indicates co-localization. Grey and magenta asterisks are referred to significant differences by age between WT and GFAP-IL6Tg mice respectively. Data are represented as the mean ± SEM. *$p < 0.05$, ***$p < 0.001$, ****$p < 0.0001$. AI (Area x Intensity); a.u. (arbitrary units). Scale bar (A,AA) = 30 μm. Scale bar (I,O,U,AI,AO,AU) = 50 μm
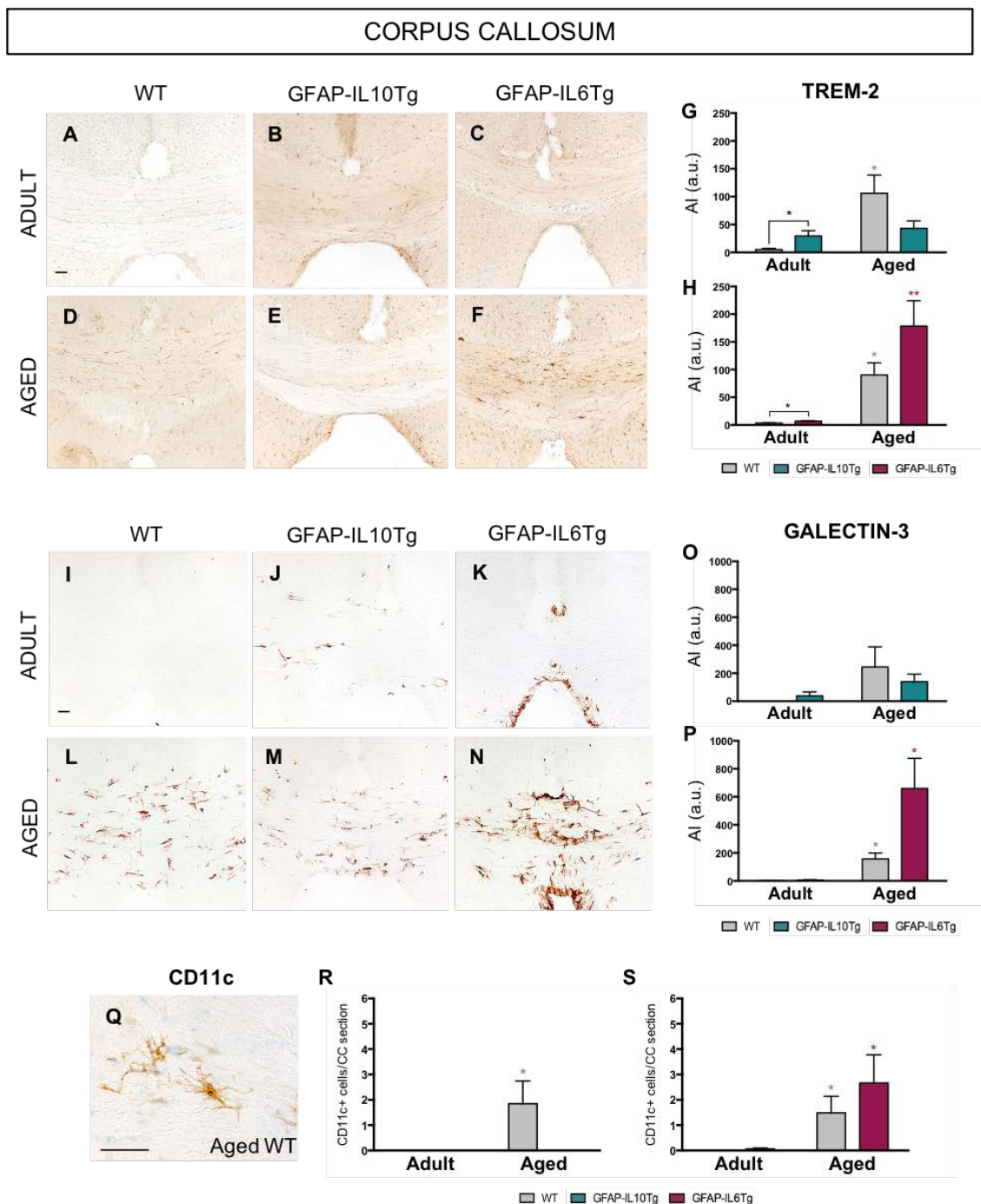
Figure 4. Microglial phagocytic phenotype represented by TREM-2, Galectin-3 and CD11c immunohistochemistries in the corpus callosum. Representative images of TREM-2 (A-F) and Galectin-3 (I-N) immunohistochemistries in the corpus callosum of WT, GFAP-IL10Tg and GFAP-IL6Tg mice. Graphs show the quantification of the immunostained area multiply by the immunostaining intensity of TREM-2 (G,H) and Galectin-3 (O,P) in the corpus callosum of GFAP-IL10Tg (G,O) and GFAP-IL6Tg (H, P) mice with respect to their corresponding WT littermates. The number of CD11c positive cells (Q) per section was quantified in the corpus callosum of GFAP-IL10Tg (R) and GFAP-IL6Tg (S) mice with respect to their corresponding WT littermates. Grey and magenta asterisks are referred to significant differences by age between WT and GFAP-IL6Tg mice, respectively. Data are represented as the mean $\pm$ SEM. *$p <$ 0.05, **$p <$ 0.01. AI (Area x Intensity); a.u. (arbitrary units); CC (corpus callosum). Scale bar = 50 μm.

Specific changes in the expression of TREM-2, GAL-3 and CD11c are shown in transgenic animals with overproduction of IL-10 or IL-6. In GFAP-IL10Tg mice, TREM-2 and GAL-3 were observed in the corpus callosum **(Figure 4B,G,J,O)** and the fimbria **(Suppl. Figure 4B,G,J,O)** since adulthood, with only modifications along time in the case of GAL-3 in the fimbria. However, the earlier-mentioned age-related CD11c expression was absent in this transgenic line **(Figure 4R; Suppl. Figure 4R)**. On the other hand, GFAP-IL6Tg mice showed an upregulation of TREM-2, GAL-3 and CD11c expression during aging, reaching levels similar to those observed in aged WT mice **(Figure 4H,P,S)**. Especially in the aged fimbria, the levels of TREM-2 and GAL-3 were higher in animals with IL-6 overproduction, comparing them with WT mice **(Suppl. Figure 4H,P)**.

3.3. Functional phagocytosis of microglial cells

To elucidate whether the observed increase of phagocytic markers on microglial cells belonging to the white matter areas correlate with a functional increase of phagocytosis, a myelin phagocytosis assay by flow cytometry in the corpus callosum was performed **(Figure 5)**.

After isolating live CD45$^+$/CD11b$^+$ cells **(Figure 5A,B)**, we show that around 35% of them phagocytose pHrodo-conjugated myelin, however, no differences in this percentage were observed between ages or genotypes **(Figure 5D)**. In this assay, we also measured the intrinsic microglial phagocytic capacity by quantifying the cellular mean fluorescence intensity (MFI) emitted in the FITC channel. In physiological conditions, our results show that microglial cells maintain the same phagocytic capacity during aging **(Figure 5E)**. Nevertheless, we demonstrated that microenvironmental alterations by both IL-10 and IL-6 modify the efficiency of myelin engulfment by microglial cells. Thus, overexpression of IL-6 induces an increase of the microglial phagocytic capacity since adulthood, while overexpression of IL-10 upregulates the cellular ingestion of myelin exclusively in aging **(Figure 5E)**.
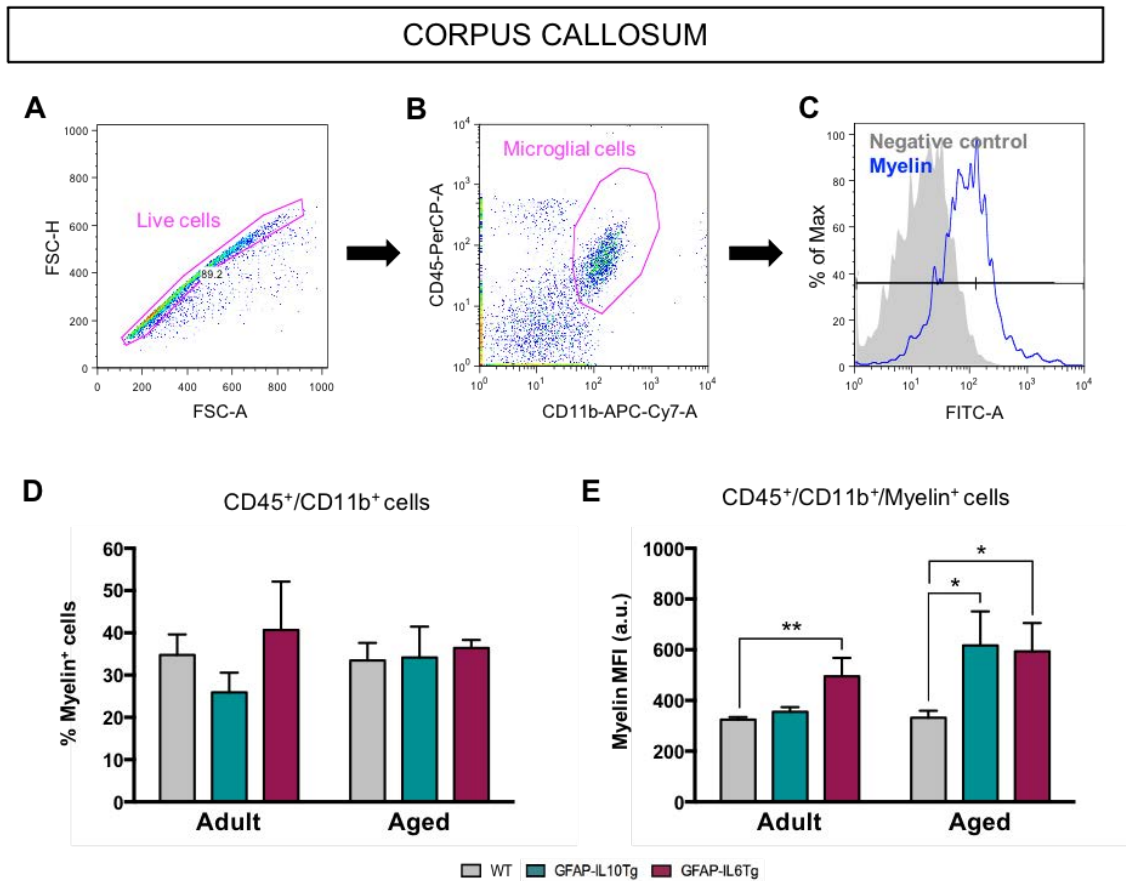
Figure 5. Functional myelin phagocytosis by microglial cells from the corpus callosum. Flow cytometry analysis showing gating strategy of live cells (A) and microglial population by CD45 and CD11b fluorescent staining (B). The selected region in panel B corresponds to the cell population used in this study. Fluorescence histogram showing myelin negative control versus pHrodo-conjugated myelin (C) was used to distinguish between phagocytic and non-phagocytic microglial cells. Graphs show the percentage of CD45$^+$/CD11b$^+$ cells phagocyting myelin (D) and their individual myelin phagocytic capacity (E). Data are represented as the mean $\pm$ SEM. *$p < 0.05$, **$p < 0.01$. MFI (Mean Fluorescence Intensity); a.u. (arbitrary units).

3.4. Demyelination and axonal damage

Taking into account that major differences in the microglial phenotype were observed in the WM areas, possible structural myelin alterations in aging or induced by the overproduction of IL-6 and IL-10 were assessed by analysing the expression of myelin basic protein (MBP) and the main lipid content by Luxol fast blue (LFB). Our results show no differences in the MBP or LFB staining between ages or genotypes **(Figure 6)**.

Furthermore, amyloid precursor protein (APP) positive bulbs were analysed to evaluate possible axonal damage. APP accumulation was mostly absent in all of the groups studied. In particular, some APP+ bulbs were observed in the axons of aged GFAP-IL6Tg mice (data not shown).
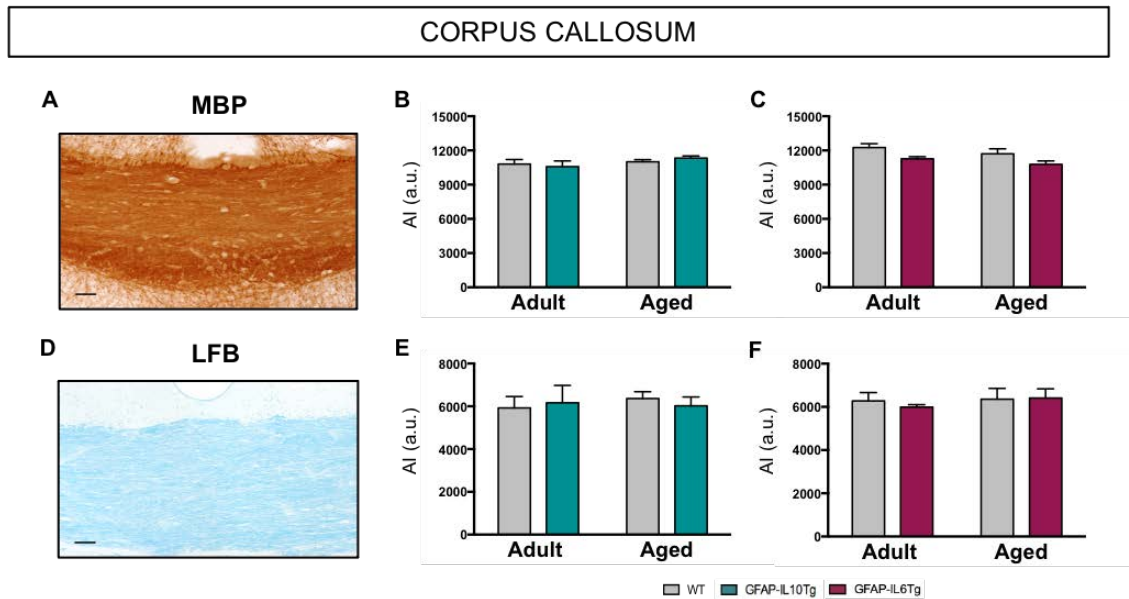
Figure 6. Myelin density represented by MBP immunohistochemistry and LFB staining in the corpus callosum. Representative images of MBP immunohistochemistry (A) and LFB staining (D) in the corpus callosum. Quantification of the stained area multiply by the staining intensity of MBP (B,C) and LFB (E,F) in the corpus callosum is represented in the graphs. Data are represented as the mean ± SEM. AI (Area x Intensity); a.u. (arbitrary units). Scale bar = 30 μm.

3.5. Tissue lipid/protein content and lipid oxidation

Since oxidative stress is one of the main aging hallmarks, and the lipid content of myelin is very high, we evaluated the lipid/protein ratio and the presence of lipid oxidation by synchrotron radiation-Fourier transformed infrared microspectroscopy (SR-μFTIR) in the cerebral cortex and the corpus callosum as representative areas of GM and WM, respectively **(Figure 7)**.

The representative infrared spectra acquired in the cerebral cortex and the corpus callosum confirm the regional biochemical differences between GM and WM areas, previously reported by our group (Sanchez-Molina et al., 2020). High absorptions in the infrared bands corresponding to lipid acyl chains (CH_2) and methyl groups (CH_3), were found on WM, when compared to GM, regardless of age or genotype **(Figure 7C)**. However, no major differences in the lipid/protein ratio (d^2A_{2921}/d^2A_{1656} and d^2A_{1467}/d^2A_{1656}) were observed in the cerebral cortex **(Figure 7D-K)** or the corpus callosum **(Figure 7T-AA)** by the effect of the age or the genotype.

Regarding lipid oxidation, the infrared absorbance was measured at 1743 cm^{-1} to detect carbonyl groups (C=O) and at 3012 cm^{-1} to detect olefinic groups (C=CH). To normalise for the total amount of lipid present in the tissue, C=O and C=CH absorptions were represented, with respect to the CH_2 absorption at 2921 cm^{-1}. For these ratios, differences between animals were specifically detected in the corpus callosum. In this area, a reduction of carbonyl groups (d^2A_{1743}/d^2A_{2921}) was found during aging regardless of the genotype **(Figure 7AB-AH)**.
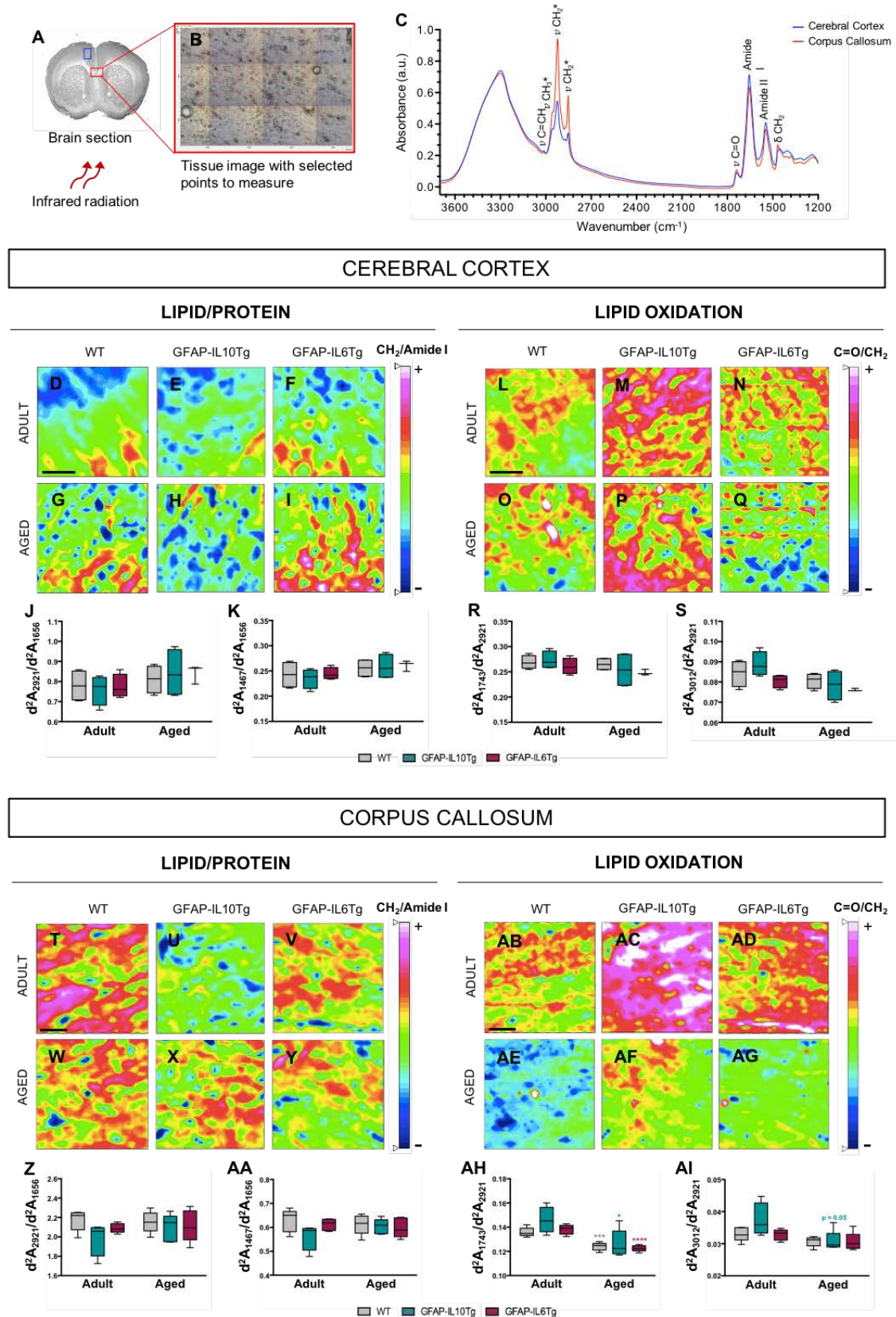
Figure 7. Lipid/Protein ratio and lipid oxidation represented by synchrotron-based μFTIR analysis in the cerebral cortex and the corpus callosum. Representative image of the different points in the cerebral cortex (blue square) and the corpus callosum (red square) tissue sections measured by infrared spectroscopy in WT, GFAP-IL10Tg and GFAP-IL6Tg mice (A,B). Representative average infrared spectra from cerebral cortex (blue line) and corpus callosum (red line) indicating the assignments of the main absorptions peaks to chemical functional groups is represented in (C). Asterisks indicate higher

absorptions of CH_3 and CH_2 in the corpus callosum compared to the cerebral cortex. Tissue heat-maps represent lipid/protein (CH_2/Amide I) content (D-I,T-Y) and lipid oxidation ($C=O/CH_2$) status (L-Q,AB-AG) in the cerebral cortex and the corpus callosum. Graphs show the infrared absorptions after the second derivative of vCH_2/Amide I (J,Z), δCH_2/Amide I (K,AA), $vC=O/vCH_2$ (R,AH) and $vC=CH/vCH_2$ (S,AI) ratios. Grey, cyan and magenta asterisks are referred to significant differences by age between WT, GFAP-IL10Tg and GFAP-IL6Tg mice, respectively. Data are represented as the mean $\pm$ SEM. *$p < 0.05$, ***$p < 0.001$. a.u. (arbitrary units); d^2A (second derivative absorbance). Scale bar = 50 μm.

3.6. Determination of cytokine levels

Finally, IL-10, IL-6, IL-1β and TNFα cytokine levels were measured by Luminex® assay in the cerebral cortex and the corpus callosum as representative areas of GM and WM, respectively **(Figure 8)**.
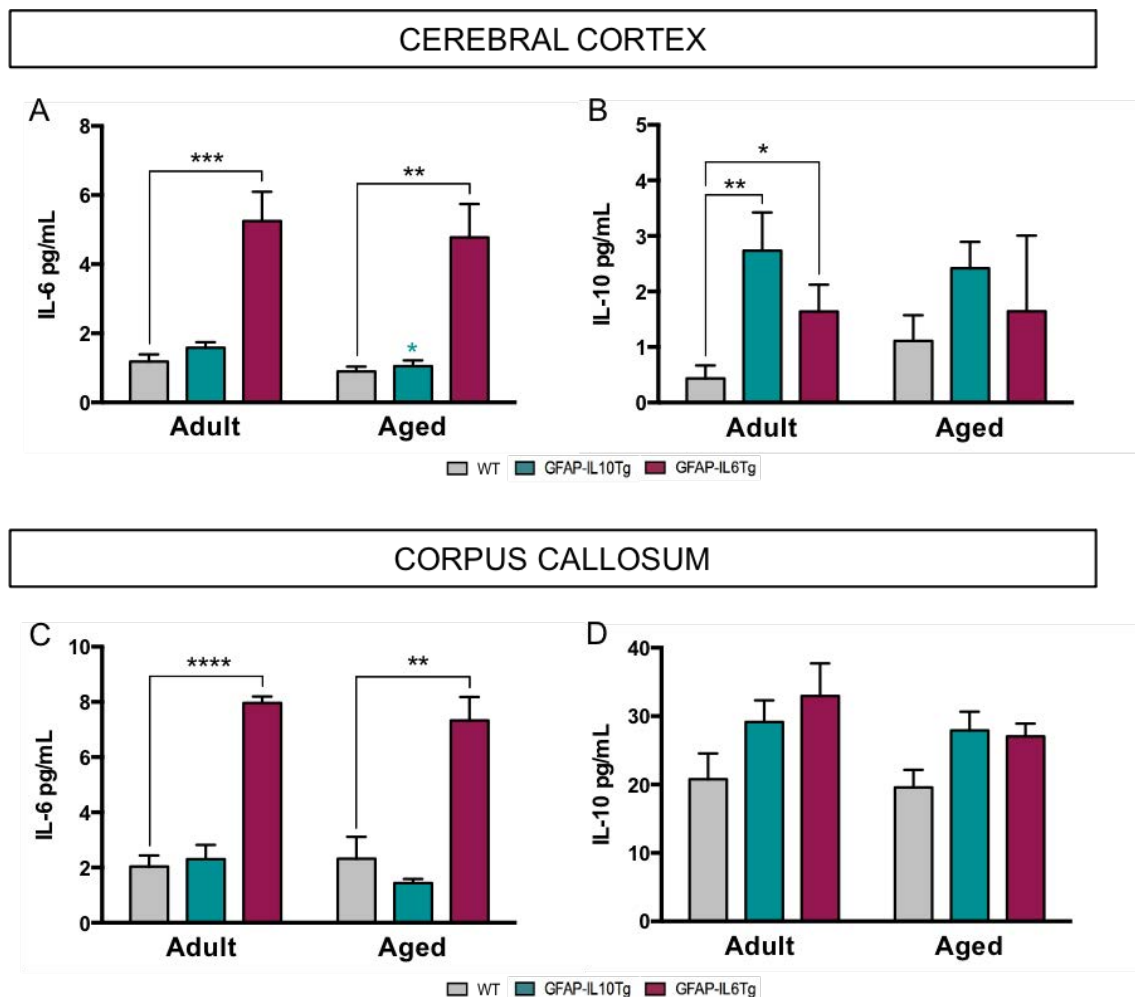
Figure 8. IL-10 and IL-6 levels represented by Luminex analysis in the cerebral cortex and the corpus callosum. Quantification of IL-6 (A,C) and IL-10 (B,D) levels in the cerebral cortex (A,B) and the corpus callosum (C,D) of WT, GFAP-IL10Tg and GFAP-IL6Tg mice. Cyan asterisk is referred to significant differences by age between GFAP-IL10Tg mice. Data are represented as the mean $\pm$ SEM. *$p < 0.05$, **$p < 0.01$, ***$p < 0.001$, ****$p < 0.0001$.

Our results showed no differences in the levels of IL-10 and IL-6 cytokines due to the effect of normal aging, nevertheless, we observed significant variations because of the effect of IL-10 and IL-6 cytokine transgenic overproduction. GFAP-IL10Tg mice

presented higher levels of IL-10 than WT mice during adulthood without variations along time in the cerebral cortex **(Figure 8B)**. However, no modifications in the levels of IL-10 were found in the corpus callosum of this transgenic line at any age **(Figure 8D)**. Additionally, a decrease of IL-6 levels was observed in GFAP-IL10Tg mice with aging **(Figure 8A)**. In GFAP-IL6Tg animals, levels of IL-6 were higher than in WT at both ages in the two studied areas **(Figure 8A,C)**. Moreover, in the cerebral cortex of these transgenic animals, IL-10 expression was also increased specifically in adulthood **(Figure 8B)**. The values obtained for IL-1β and TNFα cytokines were lower than were the minimum detectable concentration calculated by MILLIPLEX® Analyst 5.1 software in all of the animals, making it impossible to obtain reliable results.

4. DISCUSSION

This work provides evidence of differences in microglial activation and phenotype between brain areas and ages, together with biochemical changes at the tissue level. Our data show that during aging, microglia from the WM areas acquire a specific phenotype specialised in the recognition and phagocytosis of altered myelin. This phenotype is characterised by the expression of CD68, TREM-2, GAL-3 and CD11c molecules. However, in the WM, the percentage of phagocytic microglial cells and their intrinsic phagocytic capacity is unaltered with aging. Moreover, this study highlights the importance of the local microenvironment in the fate of microglial cells and their efficiency of myelin phagocytosis along time, but without influencing in the lipid oxidation associated to aging.

During physiological aging, we corroborated a pronounced microglial activation and cell density in WM areas, whereas microglia in GM areas remained similar to those found in adulthood (Hart et al., 2012; Sheffield and Berman, 1998; Sloane et al., 1999). Transgenic overproduction of IL-10 and IL-6 induces an exacerbation of microglial activation in GM areas, whereas in WM only GFAP-IL6Tg mice showed higher levels of reactivity than WT, indicating that microenvironmental effects are different between WM and GM. Modifications of microglial activation in both transgenic animals have already been reported during adulthood in our previous works (Almolda et al., 2014; Almolda et al., 2015; Recasens et al., 2019) and also corroborated by this study, which also focuses on the effect of transgenic IL-10 and IL-6 overproduction during aging. The effect observed in adult mice was only exacerbated by age in the case of GFAP-IL6Tg animals, and specifically in WM, indicating again that this is the most affected area by both age and genotype.

In agreement with previous studies (Perry et al., 1993; Wong et al., 2005), microglia in WT mice presented a higher phagocytic phenotype during aging, characterised by enhanced expression of the lysosomal marker CD68, among others. Whereas GFAP-IL10Tg and GFAP-IL6Tg mice presented greater CD68 expression than WT in the GM areas, expression of CD68 in the WM areas was exacerbated only in GFAP-IL6Tg mice during aging. Similar to aging, CD68 is increased in several diseases (Petkovic et al., 2016; Raj et al., 2017), but also in a physiological situation, such as the early postnatal brain, where phagocytosis of apoptotic cells, myelin and synapses is required (Hammond et al., 2019).

Interestingly, microglia from WM areas presented a specific phagocytic phenotype characterised by an increase of CD68+ lysosomes and a *de novo* expression of TREM-2, GAL-3 and CD11c molecules in aging, as already observed for mice and humans (Hart et al., 2012; Raj et al., 2017). In pathological situations, a different microglial phenotype in WM areas, with respect to GM, has also been observed (Lee et al., 2019).

TREM-2 is an immunoglobulin superfamily membrane receptor expressed in myeloid cells. Current studies, trying to unveil TREM-2 ligands, have shown that TREM-2 has a specific affinity for anionic lipid recognition (Cannon et al., 2012; Wang et al., 2015), such as damage-associated lipids interacting with fibrillar β-amyloid (Wang et al., 2015). Our results show TREM-2 expression in aged animals is mainly restricted to WM areas, arguing for microglia as sensors of myelinated axons, oligodendrocytes and/or astrocytes in these areas. Furthermore, TREM-2 deficiency leads to demyelination processes, such as Nasu-Hakola disease (Paloneva et al., 2000; Paloneva et al., 2002) or impairments in microglial clearance of myelin debris after cuprizone-demyelination and experimental autoimmune encephalomyelitis (EAE) (Poliani et al., 2015; Piccio et al., 2007). These data indicate that TREM-2 recognises myelin-associated lipids pointing to TREM-2+ microglial cells of WM areas as specialised microglia detecting myelin-damage during aging. In addition to lipid recognition, a very recent work has demonstrated TREM-2 as a key regulator of cholesterol metabolism derived from myelin phagocytosis (Nugent et al., 2020).

Similar to TREM-2, both GAL-3 and CD11c have been reported to be upregulated in demyelination situations like EAE (Reichert and Rotshenker, 1999; Wlodarczyk et al., 2014), optic nerve degeneration (Reichert and Rotshenker, 1996) and cuprizone-demyelination (Remington et al., 2007). Specifically, GAL-3 has been shown to mediate microglial phagocytosis of myelin (Rotshenker et al., 2008). In addition to myelin phagocytosis, a role of GAL-3 and CD11c in oligodendrocyte survival and differentiation has been described (Hoyos et al., 2014; Pasquini et al., 2011;

Wlodarczyk et al., 2017). Thus, animals with a deficiency of GAL-3 present basal hypomyelination and myelin structure abnormalities (Pasquini et al., 2011), as well as an inability to promote remyelination after demyelination by cuprizone (Hoyos et al., 2014).

Moreover, CD68, TREM-2, GAL-3 and CD11c have also been related to damage-associated microglia (DAM) in neurodegeneration and aging (Keren-Shaul et al., 2017; Krasemann et al., 2017), together with upregulation of other genes implicated in apoptotic cells and myelin debris phagocytosis and lipid metabolism (Deczkowska et al., 2018; Keren-Shaul et al., 2017). Curiously, proliferating-associated microglia (PAM) cells also express the markers observed in the WM areas of aged animals, such as CD68, TREM-2, GAL-3 and CD11c. PAM cells are present in WM areas during postnatal development, and they are specialised in the clearance of apoptotic oligodendrocytes and myelin debris that takes place in the primary myelination (Li et al., 2019; Wlodarczyk et al., 2017), suggesting that this specific phenotype might also be required for the detection of altered myelin during aging.

Considering all of these data, the age-related phagocytic microglial phenotype observed in WM areas argues for myelin deterioration during physiological aging and, therefore, the need of a specialised phagocytic microglia for the recognition of damaged products. Accordingly, a study in mice shows an increase of myelin fragments inside of aged microglia (Safaiyan et al., 2016). In this line, several magnetic resonance imaging studies in humans have shown a decline in the volume of WM areas in elderly brains (Bartzokis et al., 2003; Guttmann et al., 1998; Hinman and Abraham, 2007) and a reduction of myelin density by histological analysis in aged dogs (Chambers et al., 2012). Nonetheless, to the best of our knowledge, there is no evidence of demyelination by physiological aging in rodents, and we were not able to find differences in either the total lipid amount or in the major protein component of myelin.

Another explanation of the observed microglial phagocytic phenotype in WM areas during aging could be the high heterogeneity that microglial cells present in the different brain areas. Thus, microglia from WM areas could undergo specific phagocytic changes during aging, in comparison to GM areas. In contrast to studies reporting a deficient phagocytosis in aged microglia (Pluvinage et al., 2019; Ritzel et al., 2015), we demonstrate herein that microglia isolated from the WM of aged mice present the same phagocytic activity that microglia from adult mice when exposed to myelin debris. This result reinforces the idea that, during aging, the microglial shift to a more phagocytic phenotype in the WM areas is given to the detection of myelin damage in the tissue instead of intrinsic cellular factors.

In order to go deeper into the biochemical tissue state during aging and considering that DAM signature is associated to lipid metabolism genes, WM and GM areas along time were analysed by SR-μFTIR. Our results show a lower lipid oxidation in the WM area of aged animals without variations in the total lipid amount, with respect to protein. In addition to the specific lipid properties previously described between brain areas in mice and humans by SR-μFTIR analysis (Sanchez-Molina et al., 2020), with these data we also show a regional vulnerability of the brain-lipid alterations by the effect of age in mice. To our knowledge, this is the first study reporting a decrease of lipid oxidation during physiological aging, which is in contrast to many studies that have reported an increase (Ando et al., 1990; Clausen et al., 2010; Leutner et al., 2001) or absence of changes (Cini and Moretti, 1995). Considering that oxidant species can affect proteins or DNA without affecting lipids (Halliwell, 1987), an important aspect to take into account is the analysis methodology. Most of the previous studies reporting an increase in lipid oxidation were biochemical assays in brain homogenates, with limitations to i) disregarding contributions of other macromolecules other than lipids, and ii) the difficulty to discriminate between specific brain regions, such as WM and GM areas, which, as we show, are significantly different regarding lipid oxidation.

Our results, together with studies reporting high oligodendrocyte stability along the lifespan (Tripathi et al., 2017) and the possibility of changes in myelin lipid composition without modifications in the total lipid amount (Norton and Poduslo, 1973), reinforce the idea that age affects myelin quality rather than myelin quantity. Alterations in lipid composition usually have an impact on the structure and permeability of membranes; specifically, lipid oxidation is considered as a precursor of neurological disorders (Shichiri, 2014). In this work, we show changes in the carbonyl content of lipids from WM during aging, however, the final cellular result of this modification is difficult to predict. Indeed, we cannot elucidate whether the observed lower lipid oxidation is a negative consequence of the process of aging or a beneficial mechanism response to combat this process. Based on the observed phagocytic microglial phenotype, it is likely that while microglial cells recognise and remove altered lipids, a lipid renovation takes place reaching lipid levels similar to those of adulthood. This would be consistent with studies that show a higher lipid turnover of myelin in the aged brain (Ando et al., 2003), but this premise requires further investigation.

In this study, the influence of pro- and anti-inflammatory cytokines chronic production on microglial cells was also evaluated. Interestingly, we observed that IL-6 and IL-10 exert similar effects on microglial phenotype since adulthood, such as an increase of microglial cell density, activation and CD68 expression. This result is unexpected if we consider the opposite effects attributed to these cytokines in many

pathological situations. As a specific example, previous results from our research group demonstrated that after retrograde axonal injury, GFAP-IL6Tg mice presented an increase in motor neuron cell death (Almolda et al., 2014) whereas in GFAP-IL10Tg mice, neuronal death decreased (Villacampa et al., 2015). On the contrary, here we show microglial regulation in a physiological situation; therefore, we are not able to know whether the similar activation observed in adult GFAP-IL10Tg and GFAP-IL6Tg animals could mean a similar microglial function in age-related pathologies. In this way, we report an increase of microglial density and IBA1 and CD68 expression in the hippocampus of both transgenic mouse models under basal conditions, however, after the perforant pathway transection, the hippocampal microglial response and lesion outcome is different according to IL-10 or IL-6 overproduction (Recasens et al., 2019; Recasens et al., 2021). Another important aspect to take into account related to the changes produced in the microenvironment by transgenic cytokines is homeostatic compensation. In this line, our results show that overexpression of the pro-inflammatory IL-6 cytokine leads to an upregulation of IL-10 production in adulthood. Curiously, the overexpression of the anti-inflammatory IL-10 does not result in any compensation by a pro-inflammatory cytokine, assuming that chronic IL-6 overproduction must be counterbalanced for the promotion of life, whereas it is not necessary when it comes to IL-10. Thus, the resulting microenvironmental signals in both transgenic lines could be similar for microglial cells in the absence of harmful stimuli.

As an interesting datum, adult microglia from WM areas of GFAP-IL10Tg, but not those of GFAP-IL6Tg mice, already express TREM-2 and GAL-3 receptors. The early appearance of these myelin-related receptors, which were also observed in aged WT mice, could be explained by the reported IL-10-induced myelin phagocytosis stimulation (Smith, 1999). Nevertheless, isolated microglia from the corpus callosum of adult GFAP-IL10Tg mice present the same phagocytic capacity that microglia from adult WT mice. On the other hand, although the intrinsic microglial phagocytic capacity was increased, the expression of CD68, TREM-2 and GAL-3 markers was barely modified upon aging in transgenic mice. Accordingly, previous results from our group show a maintenance of microglial activation after perforant pathway transection (Recasens et al., 2019) and traumatic brain injury (Shanaki, 2020) in GFAP-IL10Tg mice. Taken together, these observations lead to hypothesise that IL-10 overproduction induces an increased microglial activation in physiological conditions, but, however, it avoids normal microglial responses under inflammatory conditions, such as aging. The onset of phagocytic receptors in the WM of GFAP-IL10Tg mice during adulthood could also be explained by premature tissue deterioration in these

transgenic animals and, therefore, a need to eliminate myelin debris at these early stages. Supporting this hypothesis, we found a tendency to higher lipid oxidation in the WM area of adult GFAP-IL10Tg mice, as compared to adult WT mice, by SR-µFTIR analysis together with a tendency for lower lipid content.

In contrast to GFAP-IL10Tg animals, mice with IL-6 overproduction presented higher microglial density, activation, and expression of CD68, TREM-2, and GAL-3 molecules in WM areas, as compared to WT mice during aging, especially in the fimbria. These data could indicate that the tissue in aged GFAP-IL6Tg animals is more damaged by the effect of a high pro-inflammatory microenvironment, and therefore, highest microglial activation is induced. This would be in agreement with a work that associates higher IL-6 levels with lower WM integrity in older individuals (Bettcher et al., 2014). Additionally, in myelin disorders, such as transverse myelitis (Kaplin et al., 2005) or neuromyelitis optica (Uzawa et al., 2010), elevated IL-6 levels have been directly associated with the pathogenesis. However, histological and biochemical analysis by SR-µFTIR demonstrated that WM composition of GFAP-IL6Tg mice was similar to WT mice along time, indicating that this environment does not exacerbate the myelin damage. Another possibility of the exacerbated microglial activation shown in aged GFAP-IL6Tg mice could be due to the presence of primed microglia induced by the influence of IL-6 overexpression. This hypothesis would be in concordance with the observed higher phagocytic capacity after myelin debris exposure that GFAP-IL6Tg mice present, with respect to WT since adulthood. Microglial priming has been reported in the aged brain, pointing to IL-6 as a key contributor of this process (Garner et al., 2018; Godbout et al., 2005; Norden and Godbout, 2013). Thus, age-related myelin deterioration may be similar in WT and GFAP-IL6Tg mice, but microglial cells from transgenic mice are primed since adulthood, exacerbating the microglial phagocytic response during aging, as compared to WT animals.

To summarise, this study shows that microglial cells acquire a specific phagocytic phenotype involved in myelin recognition solely in WM areas during aging, suggesting age-related myelin damage. The specific phagocytic function of microglia in these areas may trigger lipid renovation of oxidised products at advanced ages, arguing for the lower lipid oxidation in WM areas of aged animals, although the microglial phagocytic capacity remained unaltered during aging. Moreover, this work shows that overproduction of IL-10 accelerates the specific microglial activation observed in the WM areas of aged WT mice, which is sustained throughout aging. On the other hand, overproduction of IL-6 enhances microglial activation and phagocytic capacity in adult and aged mice, with a special upregulation of phagocytic markers in WM areas during aging, although lipid properties are similar to those of WT animals

throughout aging. Despite the fact that both transgenic animals present a different microglial phagocytic phenotype in WM areas, their functional phagocytosis is equally increased during aging. Interestingly, in these opposite inflammatory scenarios, lipid properties are equally altered as in normal aging, arguing for age as a greater lipid regulator than are cytokines.

Conflicts of interest

The authors declare no conflict of interest.

Author contributions

Paula Sanchez-Molina: Conceptualisation, Methodology, Data curation, Formal analysis, Investigation, Writing - original draft, Writing - review and editing. **Beatriz Almolda:** Conceptualisation, Investigation, Supervision, Writing - review and editing. **Núria Benseny-Cases:** Conceptualisation, Methodology, Data curation, Investigation. **Berta González:** Conceptualisation, Investigation, Writing - review and editing. **Alex Perálvarez-Marín:** Conceptualisation, Investigation, Writing - review and editing, Funding acquisition. **Bernardo Castellano:** Conceptualisation, Investigation, Writing - review and editing, Funding acquisition.

Acknowledgments

REFERENCES

Almolda B, de Labra C, Barrera I, Gruart A, Delgado-Garcia JM, Villacampa N, Vilella A, Hofer MJ, Hidalgo J, Campbell IL, González B, Castellano B. Alterations in microglial phenotype and hippocampal neuronal function in transgenic mice with astrocyte-targeted production of interleukin-10. Brain Behav Immun. 2015;45:80-97. doi: 10.1016/j.bbi.2014.10.015.

Almolda B, Villacampa N, Manders P, Hidalgo J, Campbell IL, González B, Castellano B. Effects of astrocyte-targeted production of interleukin-6 in the mouse on the host response to nerve injury. Glia. 2014;62(7):1142-61. doi: 10.1002/glia.22668.

Ando S, Kon K, Aino K, Totani Y. Increased levels of lipid peroxides in aged rat brain as revealed by direct assay of peroxide values. Neurosci Lett. 1990;113(2):199-204. doi: 10.1016/0304-3940(90)90303-q.

Ando S, Tanaka Y, Toyoda Y, Kon K. Turnover of myelin lipids in aging brain. Neurochem Res. 2003;28(1):5-13. doi: 10.1023/a:1021635826032.

Bartzokis G, Cummings JL, Sultzer D, Henderson VW, Nuechterlein KH, Mintz J. White matter structural integrity in healthy aging adults and patients with Alzheimer disease: a magnetic resonance imaging study. Arch Neurol. 2003;60(3):393-8. doi: 10.1001/archneur.60.3.393.

Beltrán-Castillo S, Eugenín J, von Bernhardi R. Impact of Aging in Microglia-Mediated D-Serine Balance in the CNS. Mediators Inflamm. 2018;2018:7219732. doi: 10.1155/2018/7219732.

Benseny-Cases N, Álvarez-Marimon E, Castillo-Michel H, Cotte M, Falcon C, Cladera J. Synchrotron-Based Fourier Transform Infrared Microspectroscopy (μFTIR) Study on the Effect of Alzheimer's Aβ Amorphous and Fibrillar Aggregates on PC12 Cells. Anal Chem. 2018;90(4):2772-2779. doi: 10.1021/acs.analchem.7b04818.

Bettcher BM, Watson CL, Walsh CM, Lobach IV, Neuhaus J, Miller JW, Green R, Patel N, Dutt S, Busovaca E, Rosen HJ, Yaffe K, Miller BL, Kramer JH. Interleukin-6, age, and corpus callosum integrity. PLoS One. 2014;9(9):e106521. doi: 10.1371/journal.pone.0106521.

Butovsky O, Weiner HL. Microglial signatures and their role in health and disease. Nat Rev Neurosci. 2018;19(10):622-635. doi: 10.1038/s41583-018-0057-5.

Campbell IL, Abraham CR, Masliah E, Kemper P, Inglis JD, Oldstone MB, Mucke L. Neurologic disease induced in transgenic mice by cerebral overexpression of interleukin 6. Proc Natl Acad Sci U S A. 1993;90(21):10061-5. doi: 10.1073/pnas.90.21.10061.

Cannon JP, O'Driscoll M, Litman GW. Specific lipid recognition is a general feature of CD300 and TREM molecules. Immunogenetics. 2012;64(1):39-47. doi: 10.1007/s00251-011-0562-4.

Chambers JK, Uchida K, Nakayama H. White matter myelin loss in the brains of aged dogs. Exp Gerontol. 2012;47(3):263-9. doi: 10.1016/j.exger.2011.12.003.

Cini M, Moretti A. Studies on lipid peroxidation and protein oxidation in the aging brain. Neurobiol Aging. 1995;16(1):53-7. doi: 10.1016/0197-4580(95)80007-e.

Clausen A, Doctrow S, Baudry M. Prevention of cognitive deficits and brain oxidative stress with superoxide dismutase/catalase mimetics in aged mice. Neurobiol Aging. 2010;31(3):425-33. doi: 10.1016/j.neurobiolaging.2008.05.009.

Cornejo F, von Bernhardi R. Age-Dependent Changes in the Activation and Regulation of Microglia. Adv Exp Med Biol. 2016;949:205-226. doi: 10.1007/978-3-319-40764-7_10.

Deczkowska A, Amit I, Schwartz M. Microglial immune checkpoint mechanisms. Nat Neurosci. 2018;21(6):779-786. doi: 10.1038/s41593-018-0145-x.

de Haas AH, Boddeke HW, Biber K. Region-specific expression of immunoregulatory proteins on microglia in the healthy CNS. Glia. 2008;56(8):888-94. doi: 10.1002/glia.20663.

de Olmos J, Hardy H, Heimer L. The afferent connections of the main and the accessory olfactory bulb formations in the rat: an experimental HRP-study. J Comp Neurol. 1978;181(2):213-44. doi: 10.1002/cne.901810202.

Frank MG, Barrientos RM, Biedenkapp JC, Rudy JW, Watkins LR, Maier SF. mRNA up-regulation of MHC II and pivotal pro-inflammatory genes in normal brain aging. Neurobiol Aging. 2006;27(5):717-22. doi: 10.1016/j.neurobiolaging.2005.03.013.

Garner KM, Amin R, Johnson RW, Scarlett EJ, Burton MD. Microglia priming by interleukin-6 signaling is enhanced in aged mice. J Neuroimmunol. 2018;324:90-99. doi: 10.1016/j.jneuroim.2018.09.002.

Godbout JP, Chen J, Abraham J, Richwine AF, Berg BM, Kelley KW, Johnson RW. Exaggerated neuroinflammation and sickness behavior in aged mice following activation of the peripheral innate immune system. FASEB J. 2005;19(10):1329-31. doi: 10.1096/fj.05-3776fje.

Godbout JP, Johnson RW. Interleukin-6 in the aging brain. J Neuroimmunol. 2004;147(1-2):141-4. doi: 10.1016/j.jneuroim.2003.10.031.

Gómez-López AR, Manich G, Recasens M, Almolda B, González B, Castellano B. Evaluation of myelin phagocytosis by microglia/macrophages in the nervous tissue using flow cytometry. Curr Protoc. 2021;1(3):e73. doi: 10.1002/cpz1.73.

Griffin WS. Inflammation and neurodegenerative diseases. Am J Clin Nutr. 2006;83(2):470S-474S. doi: 10.1093/ajcn/83.2.470S.

Guttmann CR, Jolesz FA, Kikinis R, Killiany RJ, Moss MB, Sandor T, Albert MS. White matter changes with normal aging. Neurology. 1998;50(4):972-8. doi: 10.1212/wnl.50.4.972.

Halliwell B. Oxidants and human disease: some new concepts. FASEB J. 1987;1(5):358-64.

Hammond TR, Dufort C, Dissing-Olesen L, Giera S, Young A, Wysoker A, Walker AJ, Gergits F, Segel M, Nemesh J, Marsh SE, Saunders A, Macosko E, Ginhoux F, Chen J, Franklin RJM, Piao X, McCarroll SA, Stevens B. Single-Cell RNA Sequencing of Microglia throughout the Mouse Lifespan and in the Injured Brain Reveals Complex Cell-State Changes. Immunity. 2019;50(1):253-271.e6. doi: 10.1016/j.immuni.2018.11.004.

HARMAN D. Aging: a theory based on free radical and radiation chemistry. J Gerontol. 1956;11(3):298-300. doi: 10.1093/geronj/11.3.298.

Hart AD, Wyttenbach A, Perry VH, Teeling JL. Age related changes in microglial phenotype vary between CNS regions: grey versus white matter differences. Brain Behav Immun. 2012;26(5):754-65. doi: 10.1016/j.bbi.2011.11.006.

Hinman JD, Abraham CR. What's behind the decline? The role of white matter in brain aging. Neurochem Res. 2007;32(12):2023-31. doi: 10.1007/s11064-007-9341-x.

Holtman IR, Raj DD, Miller JA, Schaafsma W, Yin Z, Brouwer N, Wes PD, Möller T, Orre M, Kamphuis W, Hol EM, Boddeke EW, Eggen BJ. Induction of a common microglia gene expression signature by aging and neurodegenerative conditions: a co-expression meta-analysis. Acta Neuropathol Commun. 2015;3:31. doi: 10.1186/s40478-015-0203-5.

Hoyos HC, Rinaldi M, Mendez-Huergo SP, Marder M, Rabinovich GA, Pasquini JM, Pasquini LA. Galectin-3 controls the response of microglial cells to limit cuprizone-induced demyelination. Neurobiol Dis. 2014;62:441-55. doi: 10.1016/j.nbd.2013.10.023.

Kaplin AI, Deshpande DM, Scott E, Krishnan C, Carmen JS, Shats I, Martinez T, Drummond J, Dike S, Pletnikov M, Keswani SC, Moran TH, Pardo CA, Calabresi PA, Kerr DA. IL-6 induces regionally selective spinal cord injury in patients with the neuroinflammatory disorder transverse myelitis. J Clin Invest. 2005;115(10):2731-41. doi: 10.1172/JCI25141.

Keren-Shaul H, Spinrad A, Weiner A, Matcovitch-Natan O, Dvir-Szternfeld R, Ulland TK, David E, Baruch K, Lara-Astaiso D, Toth B, Itzkovitz S, Colonna M, Schwartz M, Amit I. A Unique Microglia Type Associated with Restricting Development of Alzheimer's Disease. Cell. 2017;169(7):1276-1290.e17. doi: 10.1016/j.cell.2017.05.018.

Krasemann S, Madore C, Cialic R, Baufeld C, Calcagno N, El Fatimy R, Beckers L, O'Loughlin E, Xu Y, Fanek Z, Greco DJ, Smith ST, Tweet G, Humulock Z, Zrzavy T, Conde-Sanroman P, Gacias M, Weng Z, Chen H, Tjon E, Mazaheri F, Hartmann K, Madi A, Ulrich JD, Glatzel M, Worthmann A, Heeren J, Budnik B, Lemere C, Ikezu T, Heppner FL, Litvak V, Holtzman DM, Lassmann H, Weiner HL, Ochando J, Haass C, Butovsky O. The TREM2-APOE Pathway Drives the Transcriptional Phenotype of Dysfunctional Microglia in Neurodegenerative Diseases. Immunity. 2017;47(3):566-581.e9. doi: 10.1016/j.immuni.2017.08.008.

Lamba OP, Lal S, Yappert MC, Lou MF, Borchman D. Spectroscopic detection of lipid peroxidation products and structural changes in a sphingomyelin model system. Biochim Biophys Acta. 1991;1081(2):181-7. doi: 10.1016/0005-2760(91)90024-c.

Lee J, Hamanaka G, Lo EH, Arai K. Heterogeneity of microglia and their differential roles in white matter pathology. CNS Neurosci Ther. 2019;25(12):1290-1298. doi: 10.1111/cns.13266.

Leutner S, Eckert A, Müller WE. ROS generation, lipid peroxidation and antioxidant enzyme activities in the aging brain. J Neural Transm (Vienna). 2001;108(8-9):955-67. doi: 10.1007/s007020170015.

LeVine SM, Wetzel DL. Chemical analysis of multiple sclerosis lesions by FT-IR microspectroscopy. Free Radic Biol Med. 1998;25(1):33-41. doi: 10.1016/s0891-5849(98)00019-7.

Li Q, Cheng Z, Zhou L, Darmanis S, Neff NF, Okamoto J, Gulati G, Bennett ML, Sun LO, Clarke LE, Marschallinger J, Yu G, Quake SR, Wyss-Coray T, Barres BA. Developmental Heterogeneity of Microglia and Brain Myeloid Cells Revealed by Deep Single-Cell RNA Sequencing. Neuron. 2019;101(2):207-223.e10. doi: 10.1016/j.neuron.2018.12.006.

Maher FO, Nolan Y, Lynch MA. Downregulation of IL-4-induced signalling in hippocampus contributes to deficits in LTP in the aged rat. Neurobiol Aging. 2005;26(5):717-28. doi: 10.1016/j.neurobiolaging.2004.07.002.

Mosher KI, Wyss-Coray T. Microglial dysfunction in brain aging and Alzheimer's disease. Biochem Pharmacol. 2014;88(4):594-604. doi: 10.1016/j.bcp.2014.01.008.

Mrak RE, Griffin WS. Glia and their cytokines in progression of neurodegeneration. Neurobiol Aging. 2005;26(3):349-54. doi: 10.1016/j.neurobiolaging.2004.05.010.

Norden DM, Godbout JP. Review: microglia of the aged brain: primed to be activated and resistant to regulation. Neuropathol Appl Neurobiol. 2013;39(1):19-34. doi: 10.1111/j.1365-2990.2012.01306.x.

Norton WT, Poduslo SE. Myelination in rat brain: changes in myelin composition during brain maturation. J Neurochem. 1973;21(4):759-73. doi: 10.1111/j.1471-4159.1973.tb07520.x.

Nugent AA, Lin K, van Lengerich B, Lianoglou S, Przybyla L, Davis SS, Llapashtica C, Wang J, Kim DJ, Xia D, Lucas A, Baskaran S, Haddick PCG, Lenser M, Earr TK, Shi J, Dugas JC, Andreone BJ, Logan T, Solanoy HO, Chen H, Srivastava A, Poda SB, Sanchez PE, Watts RJ, Sandmann T, Astarita G, Lewcock JW, Monroe KM, Di Paolo G. TREM2 Regulates Microglial Cholesterol Metabolism upon Chronic Phagocytic Challenge. Neuron. 2020;105(5):837-854.e9. doi: 10.1016/j.neuron.2019.12.007.

Olah M, Biber K, Vinet J, Boddeke HW. Microglia phenotype diversity. CNS Neurol Disord Drug Targets. 2011;10(1):108-18. doi: 10.2174/187152711794488575.

Paloneva J, Kestilä M, Wu J, Salminen A, Böhling T, Ruotsalainen V, Hakola P, Bakker AB, Phillips JH, Pekkarinen P, Lanier LL, Timonen T, Peltonen L. Loss-of-function mutations in TYROBP (DAP12) result in a presenile dementia with bone cysts. Nat Genet. 2000;25(3):357-61. doi: 10.1038/77153.

Paloneva J, Manninen T, Christman G, Hovanes K, Mandelin J, Adolfsson R, Bianchin M, Bird T, Miranda R, Salmaggi A, Tranebjaerg L, Konttinen Y, Peltonen L. Mutations in two genes encoding different subunits of a receptor signaling complex result in an identical disease phenotype. Am J Hum Genet. 2002;71(3):656-62. doi: 10.1086/342259.

Pasquini LA, Millet V, Hoyos HC, Giannoni JP, Croci DO, Marder M, Liu FT, Rabinovich GA, Pasquini JM. Galectin-3 drives oligodendrocyte differentiation to control myelin integrity and function. Cell Death Differ. 2011;18(11):1746-56. doi: 10.1038/cdd.2011.40.

Perry VH, Matyszak MK, Fearn S. Altered antigen expression of microglia in the aged rodent CNS. Glia. 1993;7(1):60-7. doi: 10.1002/glia.440070111.

Petković F, Campbell IL, Gonzalez B, Castellano B. Astrocyte-targeted production of interleukin-6 reduces astroglial and microglial activation in the cuprizone demyelination model: Implications for myelin clearance and oligodendrocyte maturation. Glia. 2016;64(12):2104-2119. doi: 10.1002/glia.23043.

Piccio L, Buonsanti C, Mariani M, Cella M, Gilfillan S, Cross AH, Colonna M, Panina-Bordignon P. Blockade of TREM-2 exacerbates experimental autoimmune encephalomyelitis. Eur J Immunol. 2007;37(5):1290-301. doi: 10.1002/eji.200636837.

Pluvinage JV, Haney MS, Smith BAH, Sun J, Iram T, Bonanno L, Li L, Lee DP, Morgens DW, Yang AC, Shuken SR, Gate D, Scott M, Khatri P, Luo J, Bertozzi CR, Bassik MC, Wyss-Coray T. CD22 blockade restores homeostatic microglial phagocytosis in ageing brains. Nature. 2019;568(7751):187-192. doi: 10.1038/s41586-019-1088-4.

Poliani PL, Wang Y, Fontana E, Robinette ML, Yamanishi Y, Gilfillan S, Colonna M. TREM2 sustains microglial expansion during aging and response to demyelination. J Clin Invest. 2015;125(5):2161-70. doi: 10.1172/JCI77983.

Radak Z, Zhao Z, Goto S, Koltai E. Age-associated neurodegeneration and oxidative damage to lipids, proteins and DNA. Mol Aspects Med. 2011;32(4-6):305-15. doi: 10.1016/j.mam.2011.10.010.

Raj D, Yin Z, Breur M, Doorduin J, Holtman IR, Olah M, Mantingh-Otter IJ, Van Dam D, De Deyn PP, den Dunnen W, Eggen BJL, Amor S, Boddeke E. Increased White Matter Inflammation in Aging- and Alzheimer's Disease Brain. Front Mol Neurosci. 2017;10:206. doi: 10.3389/fnmol.2017.00206.

Recasens M, Almolda B, Pérez-Clausell J, Campbell IL, González B, Castellano B. Chronic exposure to IL-6 induces a desensitized phenotype of the microglia. J Neuroinflammation. 2021;18(1):31. doi: 10.1186/s12974-020-02063-1.

Recasens M, Shrivastava K, Almolda B, González B, Castellano B. Astrocyte-targeted IL-10 production decreases proliferation and induces a downregulation of activated microglia/macrophages after PPT. Glia. 2019;67(4):741-758. doi: 10.1002/glia.23573.

Reichert F, Rotshenker S. Deficient activation of microglia during optic nerve degeneration. J Neuroimmunol. 1996;70(2):153-61. doi: 10.1016/s0165-5728(96)00112-9.

Reichert F, Rotshenker S. Galectin-3/MAC-2 in experimental allergic encephalomyelitis. Exp Neurol. 1999;160(2):508-14. doi: 10.1006/exnr.1999.7229.

Remington LT, Babcock AA, Zehntner SP, Owens T. Microglial recruitment, activation, and proliferation in response to primary demyelination. Am J Pathol. 2007;170(5):1713-24. doi: 10.2353/ajpath.2007.060783.

Ritzel RM, Patel AR, Pan S, Crapser J, Hammond M, Jellison E, McCullough LD. Age- and location-related changes in microglial function. Neurobiol Aging. 2015;36(6):2153-63. doi: 10.1016/j.neurobiolaging.2015.02.016.

Rolfe AJ, Bosco DB, Broussard EN, Ren Y. In Vitro Phagocytosis of Myelin Debris by Bone Marrow-Derived Macrophages. J Vis Exp. 2017;30(130):56322. doi: 10.3791/56322.

Rotshenker S, Reichert F, Gitik M, Haklai R, Elad-Sfadia G, Kloog Y. Galectin-3/MAC-2, Ras and PI3K activate complement receptor-3 and scavenger receptor-AI/II mediated myelin phagocytosis in microglia. Glia. 2008;56(15):1607-13. doi: 10.1002/glia.20713.

Safaiyan S, Kannaiyan N, Snaidero N, Brioschi S, Biber K, Yona S, Edinger AL, Jung S, Rossner MJ, Simons M. Age-related myelin degradation burdens the clearance function of microglia during aging. Nat Neurosci. 2016;19(8):995-8. doi: 10.1038/nn.4325.

Sanchez-Molina P, Kreuzer M, Benseny-Cases N, Valente T, Almolda B, González B, Castellano B, Perálvarez-Marín A. From Mouse to Human: Comparative Analysis between Grey and White Matter by Synchrotron-Fourier Transformed Infrared Microspectroscopy. Biomolecules. 2020;10(8):1099. doi: 10.3390/biom10081099.

Shanaki M. Astrocyte-targeted production of IL-10 reduces the neuroinflammatory response and the neurodegeneration after TBI. [PhD dissertation]. Barcelona: Universitat Autònoma de Barcelona; 2020

Sheffield LG, Berman NE. Microglial expression of MHC class II increases in normal aging of nonhuman primates. Neurobiol Aging. 1998;19(1):47-55. doi: 10.1016/s0197-4580(97)00168-1.

Shichiri M. The role of lipid peroxidation in neurological disorders. J Clin Biochem Nutr. 2014;54(3):151-60. doi: 10.3164/jcbn.14-10.

Sierra A, Gottfried-Blackmore AC, McEwen BS, Bulloch K. Microglia derived from aging mice exhibit an altered inflammatory profile. Glia. 2007;55(4):412-24. doi: 10.1002/glia.20468.

Sloane JA, Hollander W, Moss MB, Rosene DL, Abraham CR. Increased microglial activation and protein nitration in white matter of the aging monkey. Neurobiol Aging. 1999;20(4):395-405. doi: 10.1016/s0197-4580(99)00066-4.

Smith ME. Phagocytosis of myelin in demyelinative disease: a review. Neurochem Res. 1999;24(2):261-8. doi: 10.1023/a:1022566121967.

Streit WJ. Microglial senescence: does the brain's immune system have an expiration date? Trends Neurosci. 2006;29(9):506-10. doi: 10.1016/j.tins.2006.07.001.

Streit WJ, Braak H, Xue QS, Bechmann I. Dystrophic (senescent) rather than activated microglial cells are associated with tau pathology and likely precede neurodegeneration in Alzheimer's disease. Acta Neuropathol. 2009;118(4):475-85. doi: 10.1007/s00401-009-0556-6.

Streit WJ, Sammons NW, Kuhns AJ, Sparks DL. Dystrophic microglia in the aging human brain. Glia. 2004;45(2):208-12. doi: 10.1002/glia.10319.

Streit WJ, Xue QS, Tischer J, Bechmann I. Microglial pathology. Acta Neuropathol Commun. 2014;2:142. doi: 10.1186/s40478-014-0142-6.

Tan YL, Yuan Y, Tian L. Microglial regional heterogeneity and its role in the brain. Mol Psychiatry. 2020;25(2):351-367. doi: 10.1038/s41380-019-0609-8.

Tripathi RB, Jackiewicz M, McKenzie IA, Kougioumtzidou E, Grist M, Richardson WD. Remarkable Stability of Myelinating Oligodendrocytes in Mice. Cell Rep. 2017;21(2):316-323. doi: 10.1016/j.celrep.2017.09.050.

Uzawa A, Mori M, Arai K, Sato Y, Hayakawa S, Masuda S, Taniguchi J, Kuwabara S. Cytokine and chemokine profiles in neuromyelitis optica: significance of interleukin-6. Mult Scler. 2010;16(12):1443-52. doi: 10.1177/1352458510379247.

Villacampa N, Almolda B, Vilella A, Campbell IL, González B, Castellano B. Astrocyte-targeted production of IL-10 induces changes in microglial reactivity and reduces motor neuron death after facial nerve axotomy. Glia. 2015;63(7):1166-84. doi: 10.1002/glia.22807.

von Bernhardi R. Glial cell dysregulation: a new perspective on Alzheimer disease. Neurotox Res. 2007;12(4):215-32. doi: 10.1007/BF03033906.

von Bernhardi R, Eugenín-von Bernhardi L, Eugenín J. Microglial cell dysregulation in brain aging and neurodegeneration. Front Aging Neurosci. 2015;7:124. doi: 10.3389/fnagi.2015.00124.

Walton MR, Gibbons H, MacGibbon GA, Sirimanne E, Saura J, Gluckman PD, Dragunow M. PU.1 expression in microglia. J Neuroimmunol. 2000;104(2):109-15. doi: 10.1016/s0165-5728(99)00262-3.

Wang Y, Cella M, Mallinson K, Ulrich JD, Young KL, Robinette ML, Gilfillan S, Krishnan GM, Sudhakar S, Zinselmeyer BH, Holtzman DM, Cirrito JR, Colonna M. TREM2 lipid sensing sustains the microglial response in an Alzheimer's disease model. Cell. 2015;160(6):1061-71. doi: 10.1016/j.cell.2015.01.049.

Wlodarczyk A, Holtman IR, Krueger M, Yogev N, Bruttger J, Khoroshi R, Benmamar-Badel A, de Boer-Bergsma JJ, Martin NA, Karram K, Kramer I, Boddeke EW, Waisman A, Eggen BJ, Owens T. A novel microglial subset plays a key role in myelinogenesis in developing brain. EMBO J. 2017;36(22):3292-3308. doi: 10.15252/embj.201696056.

Wlodarczyk A, Løbner M, Cédile O, Owens T. Comparison of microglia and infiltrating CD11c⁺ cells as antigen presenting cells for T cell proliferation and cytokine response. J Neuroinflammation. 2014;11:57. doi: 10.1186/1742-2094-11-57.

Wong AM, Patel NV, Patel NK, Wei M, Morgan TE, de Beer MC, de Villiers WJ, Finch CE. Macrosialin increases during normal brain aging are attenuated by caloric restriction. Neurosci Lett. 2005;390(2):76-80. doi: 10.1016/j.neulet.2005.07.058.

Ye SM, Johnson RW. Increased interleukin-6 expression by microglia from brain of aged mice. J Neuroimmunol. 1999;93(1-2):139-48. doi: 10.1016/s0165-5728(98)00217-3.

Ye SM, Johnson RW. An age-related decline in interleukin-10 may contribute to the increased expression of interleukin-6 in brain of aged mice. Neuroimmunomodulation. 2001;9(4):183-92. doi: 10.1159/000049025.

Yousef I, Ribó L, Criso, A, Šics I, Ellis G, Ducic T, Kreuzer M, Benseny-Cases N, Quispe M, Dumas P, Lefrançois S, Moreno T, García G, Ferrer S, Nicolas J, Aranda MAG. MIRAS: The infrared synchrotron radiation beamline at ALBA. Synchrotron Radiat. News. 2017;30(4):4-6. doi: 10.1080/08940886.2017.1338410

TABLES

Table 1. List of primary antibodies used for immunohistochemistry and immunofluorescence.

Target	Host	Dilution	Cat. Number	Manufacturer
IBA1	Rabbit	1:3000	019-19741	Wako
PU.1	Rabbit	1:400	2258S	Cell Signaling
MHC-II	Rat hybridoma	1:25	TIB-120	ATCC
CD68	Rat	1:1000	MCA1957	Bio-Rad
TREM-2	Sheep	1:400	AF1729	R&D Systems
Galectin-3	Rat	1:500	125401	BioLegend
CD11c	Hamster	1:500	74935	Genetex
APP	Rabbit	1:2000	A8717	Sigma-Aldrich
MBP	Rat	1:1000	Ab7349	Abcam

Table 2. List of secondary antibodies used for immunohistochemistry and immunofluorescence.

	Host	Dilution	Cat. Number	Manufacturer
Anti-Rabbit Biotinylated	Goat	1:500	BA-1000	Vector Laboratories
Anti-Rat Biotinylated	Rabbit	1:500	BA-4001	Vector Laboratories
Anti-Sheep Biotinylated	Rabbit	1:500	BA-6000	Vector Laboratories
Anti-Hamster Biotinylated	Goat	1:500	BA-9100	Vector Laboratories
Anti-Rabbit Alexa-Fluor-488	Donkey	1:500	A-21206	Invitrogen
Anti-Rat Alexa-Fluor-555	Goat	1:500	A-21434	Invitrogen

SUPPLEMENTARY FIGURES
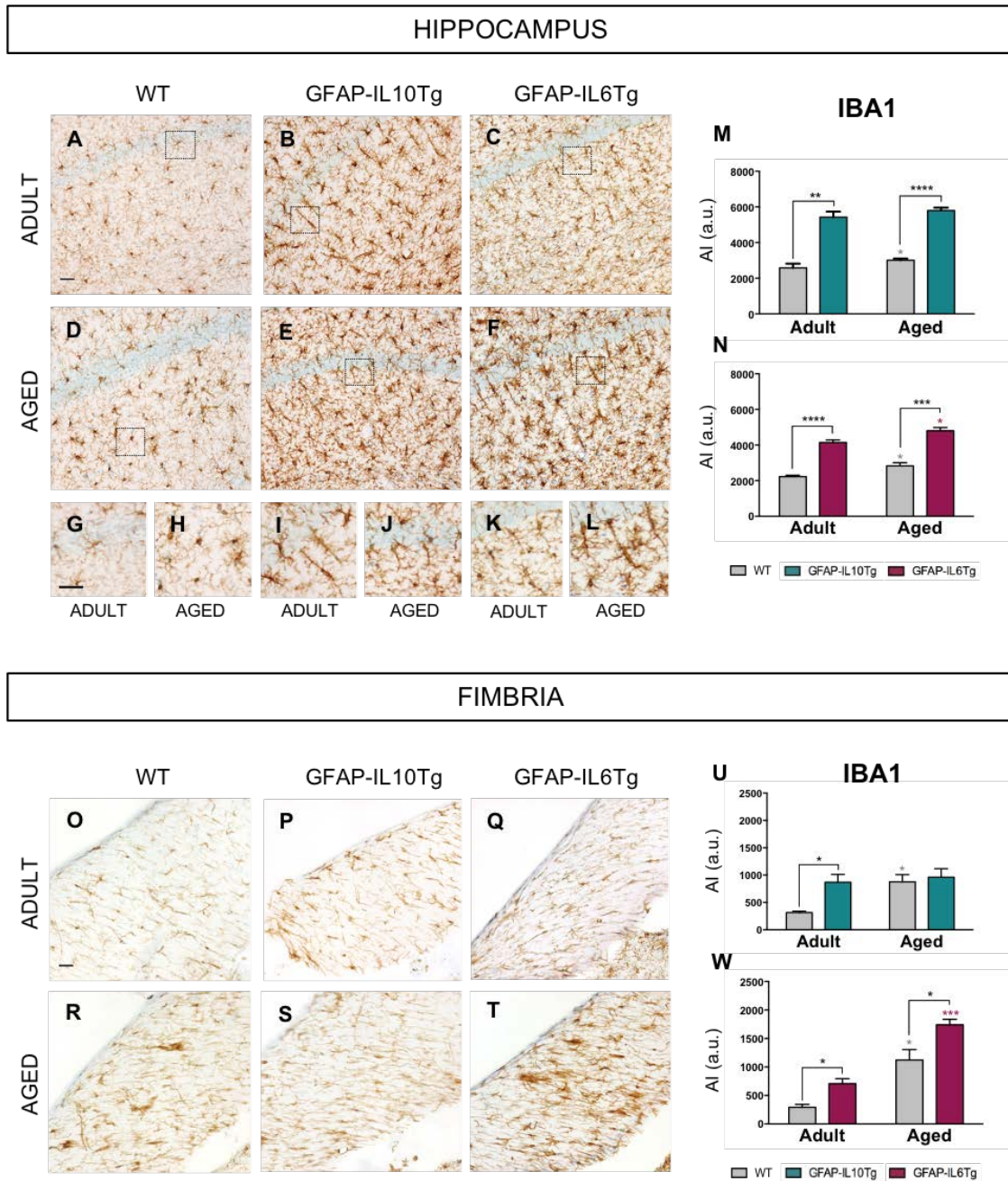
Suppl. Figure 1. Microglial activation and morphology represented by IBA1 immunohistochemistry in the hippocampus and the fimbria. Representative images of IBA1 immunohistochemistry in the hippocampus (A-L) and the fimbria (O-T) of WT, GFAP-IL10Tg and GFAP-IL6Tg mice. Insets in A-F images show the microglial morphology in the CA1 hippocampal area at high magnification (G-L). Note the elongated morphology characteristic of both transgenic mice (I-L). Graphs show the quantification of the IBA1 immunostained area multiply by the IBA1 immunostaining intensity in the hippocampus (M,N) and the fimbria (U,W) of GFAP-IL10Tg (M,U) and GFAP-IL6Tg (N,W) mice with respect to their corresponding WT littermates. Grey and magenta asterisks are referred to significant differences by age between WT and GFAP-IL6Tg mice, respectively. Data are represented as the mean ± SEM. *$p < 0.05$, **$p < 0.01$, ***$p < 0.001$, ****$p < 0.0001$. AI (Area x Intensity); a.u. (arbitrary units). Scale bar = 30 μm.
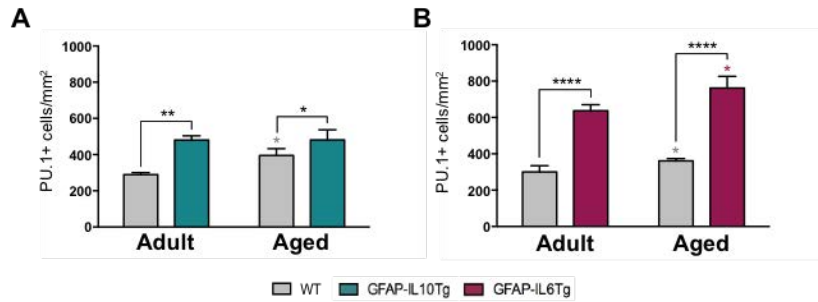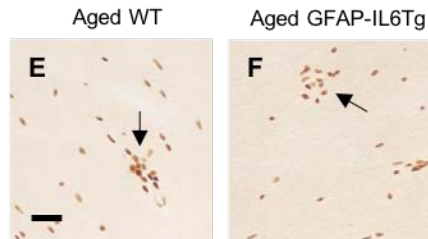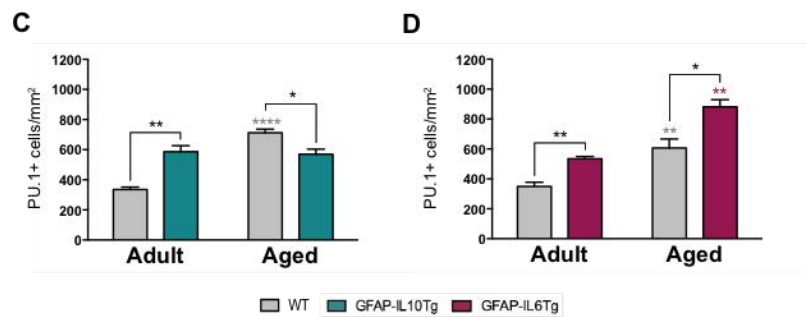
Suppl. Figure 2. Microglial cell density represented by PU.1 immunohistochemistry in the hippocampus and the fimbria. Graphs showing the quantification of PU.1 cell density in the hippocampus (A,B) and the fimbria (C,D) of GFAP-IL10Tg (A,C) and GFAP-IL6Tg mice (B,D) mice with respect to their corresponding WT littermates. Grey asterisks are referred to significant differences by age between WT mice. Data are represented as the mean $\pm$ SEM. $*p < 0.05$, $**p < 0.01$, $****p < 0.0001$. Representative photographs showing accumulations of microglial cells (arrows) observed in the fimbria of aged WT (E) and aged GFAP-IL6Tg (F) mice. Scale bar = 30 μm.
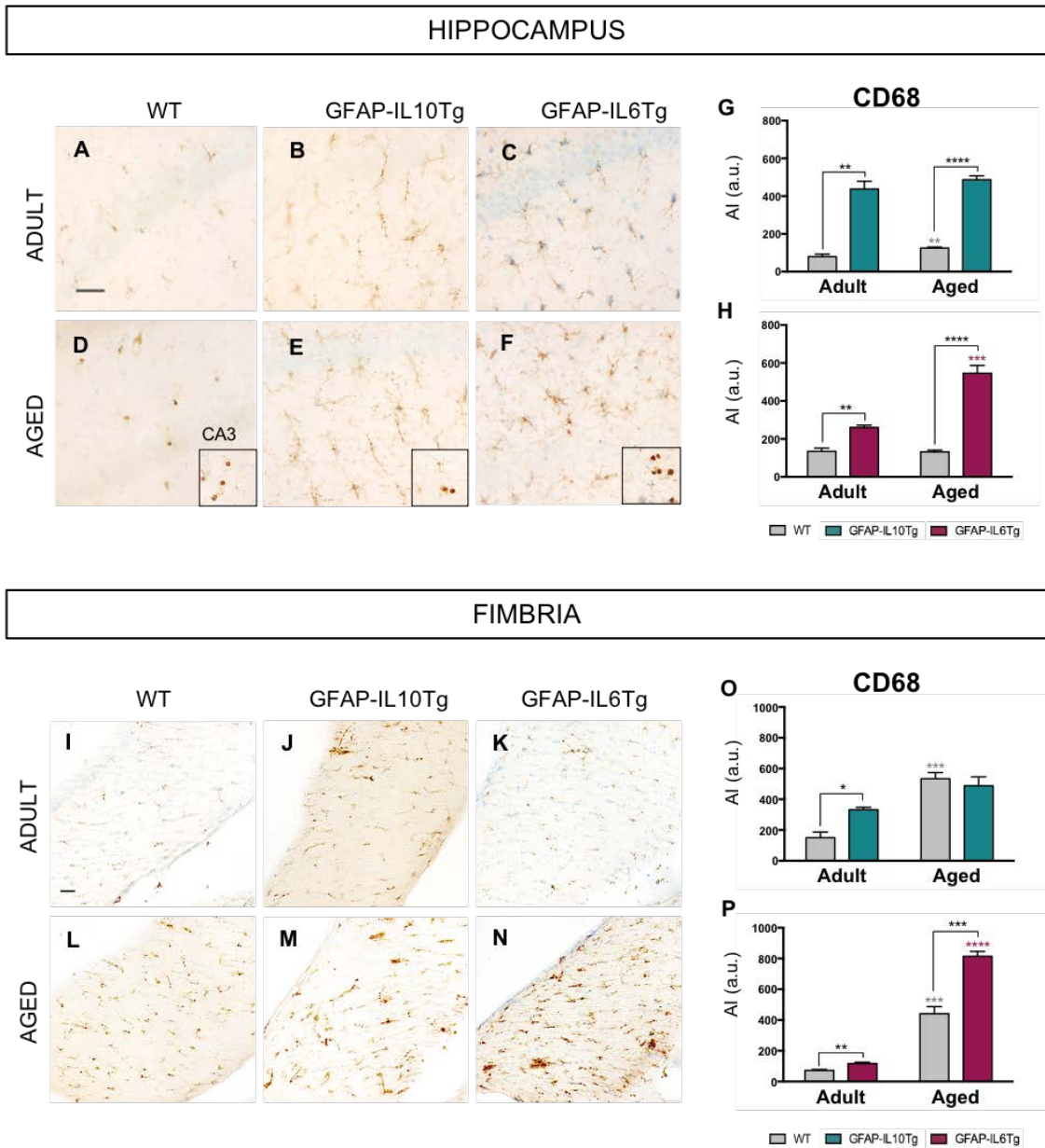
Suppl. Figure 3. Microglial phagocytic capacity represented by CD68 immunohistochemistry in the hippocampus and the fimbria. Representative images of CD68 immunohistochemistry in the hippocampus (A-F) and the fimbria (I-N) of WT, GFAP-IL10Tg and GFAP-IL6Tg mice. Insets in D-F images show characteristic CD68 accumulations found in the CA3 hippocampal region. Graphs show the quantification of the CD68 immunostained area multiply by the CD68 immunostaining intensity in the hippocampus (G,H) and the fimbria (O,P) of GFAP-IL10Tg (G,O) and GFAP-IL6Tg (H,P) mice with respect to their corresponding WT littermates. Grey and magenta asterisks are referred to significant differences by age between WT and GFAP-IL6Tg mice, respectively. Data are represented as the mean ± SEM. *$p <$ 0.05, **$p <$ 0.01, ***$p <$ 0.001, ****$p <$ 0.0001. AI (Area x Intensity); a.u. (arbitrary units). Scale bar = 30 μm.
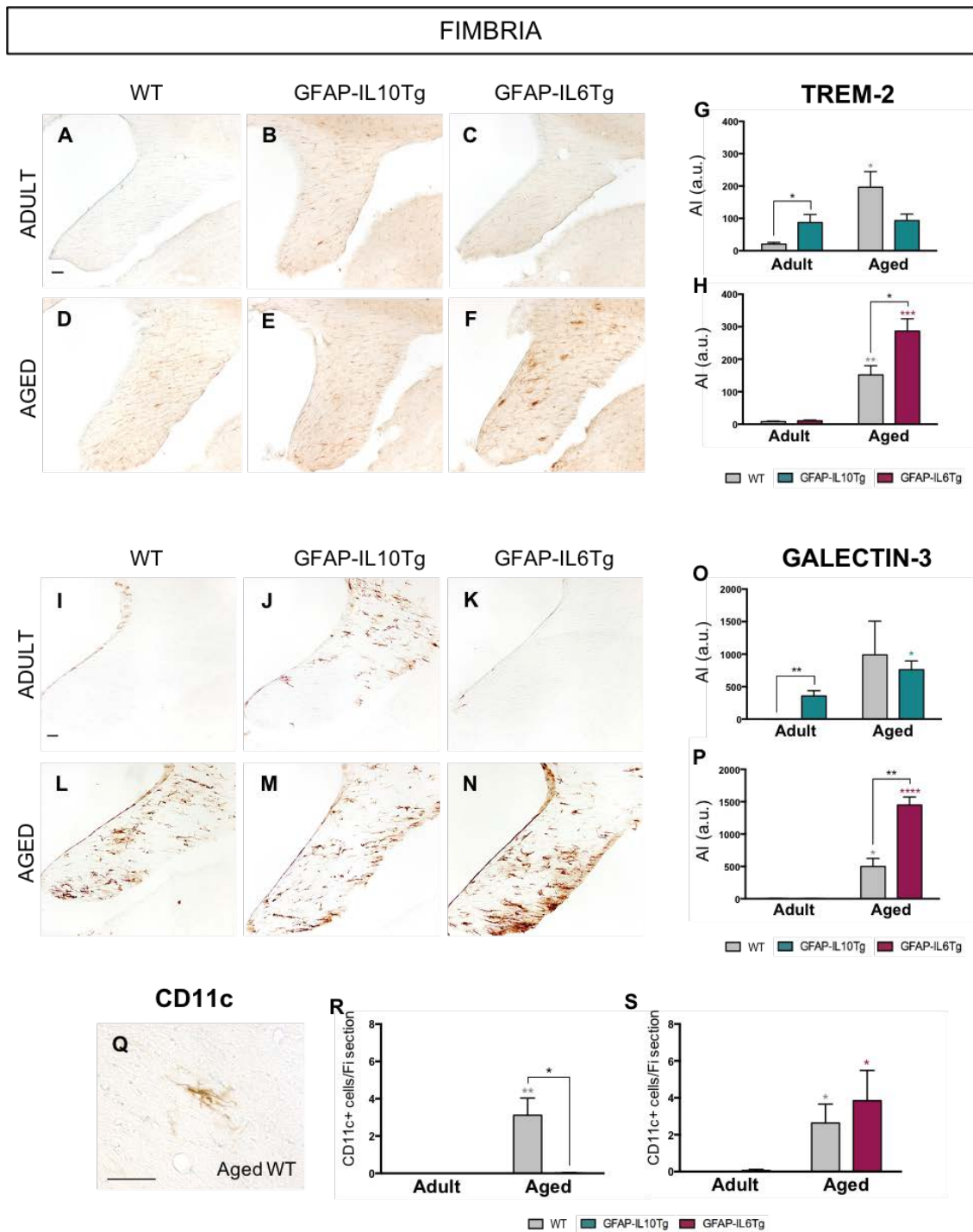
Suppl. Figure 4. Microglial phagocytic phenotype represented by TREM-2, Galectin-3 and CD11c immunohistochemistries in the fimbria. Representative images of TREM-2 (A-F) and Galectin-3 (I-N) immunohistochemistries in the fimbria of WT, GFAP-IL10Tg and GFAP-IL6Tg mice. Graphs show the quantification of the immunostained area multiply by the immunostaining intensity of TREM-2 (G,H) and Galectin-3 (O,P) in the fimbria of GFAP-IL10Tg (G,O) and GFAP-IL6Tg (H,P) mice with respect to their corresponding WT littermates. The number of CD11c positive cells (Q) per section was quantified in the fimbria of GFAP-IL10Tg (R) and GFAP-IL6Tg (S) mice with respect to their corresponding WT littermates. Grey, cyan and magenta asterisks are referred to significant differences by age between WT, GFAP-IL10Tg and GFAP-IL6Tg mice, respectively. Data are represented as the mean ± SEM. *$p < 0.05$, **$p < 0.01$, ***$p < 0.001$, ****$p < 0.0001$. AI (Area x Intensity); a.u. (arbitrary units); Fi (fimbria). Scale bar = 50 μm.

Chronic IL-10 overproduction anticipates the age-related disruption of microglia-neuron dialogue resulting in impaired hippocampal neurogenesis and spatial memory

Paula Sanchez-Molina[a,b*], Beatriz Almolda[a,b*], Lydia Giménez-Llort[a,c], Berta González[a,b], Bernardo Castellano[a,b]

[a]Institute of Neurosciences. Universitat Autònoma de Barcelona, 08193 Bellaterra, Barcelona, Spain.
[b]Department of Cell Biology, Physiology and Immunology. Universitat Autònoma de Barcelona, 08193 Bellaterra, Barcelona, Spain.
[c]Department of Psychiatry and Forensic Medicine. Universitat Autònoma de Barcelona, 08193 Bellaterra, Barcelona, Spain.

Corresponding author:
Paula Sanchez-Molina
Unitat d'Histologia, Facultat de Medicina
Universitat Autònoma de Barcelona
08193 Bellaterra, Barcelona, Spain
Tel: +34935811826
e-mail address: paula.sanchez@uab.cat

*These authors contributed equally to this work.

ABSTRACT

The subgranular zone of the dentate gyrus is an adult neurogenic niche where new neurons are continuously generated. A dramatic hippocampal neurogenesis decline occurs with increasing age, contributing to cognitive deficits. The process of neurogenesis is intimately regulated by the microenvironment, being inflammation considered a strong negative factor for this process. Thus, we hypothesize that the reduction of new neurons in the aged brain could be attributed to the age-related microenvironmental changes towards a pro-inflammatory status. In this work, we evaluated whether an anti-inflammatory microenvironment could counteract the negative effect of age on promoting new hippocampal neurons. Surprisingly, our results show that transgenic animals chronically overexpressing IL-10 by astrocytes, present a decreased hippocampal neurogenesis since adulthood resulting from an impairment in the survival of neural newborn cells without differences in cell proliferation. In parallel, hippocampal-dependent spatial learning and memory processes were affected by IL-10 overproduction as assessed by the Morris water maze test. Microglial cells, which are key players in the neurogenesis process, presented a different phenotype in transgenic animals characterized by high activation together with alterations in receptors involved in neuronal communication, such as CD200R, SIRPα and CX3CR1. Interestingly, the changes described in adult transgenic animals were similar to those observed by the effect of normal aging. Thus, our data suggest that chronic IL-10 overproduction mimics the physiological age-related disruption of microglia-neuron dialogue resulting in an anticipated hippocampal neurogenesis decrease and spatial memory impairment.

Key words: Neurogenesis, IL-10, Aging, Microglia, Memory, CX3CR1, CD200R, SIRPα, Hippocampus

1. INTRODUCTION

Neurogenesis is the process of new cells formation from neural stem/progenitor cells (NSCs), which have the ability to proliferate and differentiate into astrocytes, oligodendrocytes, or neurons (Akkermann et al., 2017; Bond et al., 2020; Hirabayashi and Gotoh, 2005; Mira and Morante, 2020; Taupin and Gage, 2002). After the nervous system development in the embryonic stage, neurogenesis remains physiologically active in specific cerebral regions of mammals (Altman and Das, 1965; Eriksson et al., 1998; Kaplan and Hinds, 1977). Specifically, two neurogenic niches have been described in the adult mammal brain: the subventricular zone (SVZ) of the lateral ventricles and the subgranular zone (SGZ) of the hippocampal dentate gyrus (Imayoshi et al., 2009; Ming and Song, 2005).

The newborn neurons formed in the SGZ during adulthood, migrate through the granular cell layer of the dentate gyrus and are integrated into the existing neuronal circuits participating in the hippocampal-dependent memory (Saxe et al., 2006; Snyder et al., 2005; Stanfield and Trice, 1988). During aging, a dramatic decrease of NSCs proliferation, leading to reduced neurogenesis, is specifically observed in the dentate gyrus (Bondolfi et al., 2004; Kuhn et al., 1996; Kuipers et al., 2015) concomitant with age-related cognitive deficits (Drapeau et al., 2003; Van Praag et al., 2005; Villeda et al., 2011).

The systemic and the local microenvironment is one of the main factors that regulate adult neurogenesis (Borsini et al., 2015; Carpentier and Palmer, 2009; Palmer et al., 2000; Villeda et al., 2011). In the aged hippocampus, the microenvironment is altered towards a pro-inflammatory and oxidized status (Cornejo and von Bernhardi, 2016; Lucin and Wyss-Coray, 2009; Ojo et al., 2015). Numerous studies demonstrate that inflammation is detrimental to the process of neurogenesis (Carpentier and Palmer, 2009; Ekdahl et al., 2003; Monje et al., 2003). Thus, induction of pro-inflammatory molecules, such as IL-6 (Monje et al., 2003; Vallières et al., 2002), IL-1β (Goshen et al., 2008; Koo and Duman, 2008; Ryan et al., 2013), TNF-α (Cacci et al., 2005; Sheng et al., 2005) and nitric oxide (Packer et al., 2003), has an inhibitory effect on the generation of new hippocampal neurons. Contrary to pro-inflammatory signaling, fewer it is known about the influence of anti-inflammatory molecules on neurogenesis. However, some studies have demonstrated that growth factors (Battista et al., 2006; Lichtenwalner et al., 2001; Scharfman et al., 2005; Wagner et al., 1999; Zigova et al., 1998) and anti-inflammatory cytokines (Aharoni et al., 2005; Butovsky et al., 2006; Kiyota et al., 2010; Kiyota et al., 2012) promote neurogenesis.

In this context, microglial cells play an important role in regulating neuroinflammation and, therefore, neurogenesis. Accordingly, it has been demonstrated that a pro-inflammatory microglial activation impacts negatively on the hippocampal neurogenesis by the secretion of pro-inflammatory cytokines (Cacci et al., 2005; Carpentier and Palmer, 2009; Monje et al., 2003; Nakanishi et al., 2007). In agreement, Ekdahl and collaborators showed a significant negative correlation between the number of LPS-activated microglia and the number of newborn neurons in the hippocampal neurogenic niche (Ekdahl et al., 2003). The importance of microglia-neuron communication in both neurogenesis and aging must also be highlighted. In this sense, alterations in the "do-not-eat-me" signaling, which maintains microglial cells in a homeostatic state, impact the generation of new neurons (Bachstetter et al., 2011; Varnum et al., 2015; Vukovic et al., 2012). In addition to microglial cells, other immune cells, such as lymphocytes, can modulate neurogenesis crossing blood vessels located in the neurogenic niche (Aharoni et al., 2005; Wolf et al., 2009).

Because most of the studies exploring the influence of the neurogenic microenvironment have been performed *in vitro* or by acute administration of specific molecules, it is of special interest to study the effect of a local and chronic microenvironment under physiological conditions *in vivo*. Specifically, the anti-inflammatory IL-10 cytokine has been described to influence neurogenesis differently *in vivo* depending on the administration route and the neurogenic niche. Thus, hippocampal IL-10 gene delivery by adeno-associated virus enhances neurogenesis and cognitive function in an Alzheimer's disease mouse model (Kiyota et al., 2012), whereas intraventricular IL-10 administration reduces neurogenesis of the SVZ (Perez-Asensio et al., 2013). Of special interest are previous results from our research group describing neuronal and microglial modifications in the hippocampus of adult and aged mice with astrocyte-targeted overproduction of IL-10 (Almolda et al., 2015; Sanchez-Molina et al., 2021). Considering the direct association between higher inflammation and lower neurogenesis in aging, the present study aimed to evaluate the impact that an anti-inflammatory microenvironment produced by chronic astrocyte-targeted IL-10 overproduction exerts on the aged hippocampal neurogenesis under physiological conditions.

2. MATERIAL AND METHODS

2.1. Animals

Transgenic mice with astrocyte-targeted overproduction of IL-10 (GFAP-IL10Tg) and their corresponding wild-type (WT) littermates were used in this study. GFAP-IL10Tg

mice generation on the C57BL/6 background was described previously (Almolda et al., 2015). Genotype determination was performed by polymerase chain reaction (PCR) analysis of DNA obtained from mice tail biopsies. Animals of both sexes were distributed in two experimental groups according to the age: adult (4-6 months old) and aged (18-24 months old) mice. Animals were maintained in standard cages with food and water *ad libitum*, in a 12 h light/dark cycle (lights on at 8 a.m.), 22 ± 2 °C and 50-60% humidity. All experimental animal work was conducted according to Spanish regulations (Ley 32/2007, Real Decreto 1201/2005, Ley 9/2003 and Real Decreto 178/2004) in agreement with EU Directive (2010/63/UE) on this subject. The study complies with the ARRIVE guidelines developed by the NC3Rs and aims to reduce the number of animals used.

2.2. Behavioral assessment

A set of four behavioral tests was performed in adult (4-5 months old) and aged (18-19 months old) mice of both genotypes (*n* = 7-12 by experimental group) to characterize the anxious profile, locomotion and cognitive function of the animals. Physical status and animal survival were also evaluated.

Corner test: Neophobia in a new standard home-cage was measured as the number of visited corners and rearings during 30 seconds.

Open field test: Animals were placed in the center of a white apparatus (48 × 33 × 25 cm) and observed for 5 min. Vertical activity was manually quantified, counting the rearing latency and the number of rearings for each minute of the test. Horizontal activity, including total distance traveled, total time in movement, and the time in the apparatus center/periphery, was analyzed using the ANY-maze behavioral tracking system. Latency, number, and duration of grooming episodes, defecations, and urine were also recorded to measure emotionality.

T-maze: Working memory was measured using a T-shaped black maze (short arms of 30 cm). Animals were placed at the beginning of the vertical arm facing the wall and observed for 3 minutes. The time of reaching the three-arms intersection (nose criteria) and the number of errors (exploration of an already explored arm) were manually recorded.

Morris water maze: Hippocampal-dependent spatial short- and long-term learning and memory were analyzed during 5 consecutive days using three paradigms consisting of cue- and place-learning tasks and a probe trial for short-term memory **(Figure 4A-C)**. The test was carried out in a circular pool (120 cm diameter, 60 cm height) with opaque white water at 25 °C and surrounded by black curtains. On the first day, a cue-learning task with a flag in a visible platform (7 cm diameter) was performed

(4 trials of 1 min maximum, 60 min intertrial time), and escape latencies to reach the platform were recorded. The following four days, reversal place-learning tasks measuring the escape latencies were performed (4 trials of 1 min maximum, 60 min intertrial time) with the platform hidden 1 cm below the water surface and external cues in the black walls. In both paradigms, the animals were introduced into the pool by a different cardinal point per trial. Mice that failed to find the platform within the 60 seconds were manually guided and placed on it for 10 seconds -such as for the successful animals- before taking them out of the pool. On the fifth day, two hours after the last place-learning trial, the platform was removed and a probe was performed recording the mice trajectory in the pool for 1 min. The time the mouse spent swimming in the quadrant where the platform was previously located was used as indicator of memory. The ANY-maze behavioral tracking system was used to record and analyze this test.

2.3. BrdU administration

5-Bromo-2'-deoxyuridine (BrdU), a synthetic thymidine analog, was used to study neural stem cell proliferation because it is incorporated into DNA during S-phase cell cycle. One 100 mg/kg dose of BrdU (B5002, Sigma-Aldrich) diluted in NaCl (pH 7.4) was intraperitoneally injected during five consecutive days in adult (5 months old) and aged (19 months old) mice of both genotypes. A set of animals (n = 3-5) were euthanized one day after the last BrdU administration to evaluate cell proliferation, whereas another set of animals (n = 4-8) were euthanized two weeks after the last BrdU administration to evaluate cell survival **(Figure 1F)**.

2.4. Tissue processing for histological analysis

Under an intraperitoneal anesthetic solution of xylazine (30 mg/kg) and ketamine (120 mg/kg), mice were intracardially perfused for 10 min with 4% paraformaldehyde in 0.1 M phosphate buffer (pH 7.4). The brains were quickly removed, post-fixed for 4 h at 4 °C in the same fixative solution, cryoprotected with 30% sucrose in 0.1 M phosphate buffer for 48 h at 4 °C, frozen in ice-cold 2-methylbutane (320404, Sigma-Aldrich) and stored at -80 °C. Parallel coronal sections (30-μm-thick) of the telencephalon containing the hippocampus were obtained using a CM 3050S Leica cryostat and were stored at -20 °C in an anti-freeze solution containing 20% sucrose, 30% ethylene glycol and 1% polyvinylpyrrolidone until use.

2.5. Single immunohistochemistry

For the visualization of neuroblasts and proliferating cells, brain sections were immunostained with antibodies against doublecortin (DCX) and BrdU, respectively, in adult (4-5 months old) and aged (19-20 months old) mice of both genotypes. Frozen free-floating sections were washed in Tris-buffered saline (TBS; 0.05 M, pH 7.4) to eliminate the anti-freeze solution and incubated for 10 min with 2% H_2O_2 and 70% methanol in distilled H_2O to inhibit endogenous peroxidase. For BrdU immunostaining, DNA denaturation incubating the sections in 0.082 N HCl at 4 °C for 10 min followed by another incubation in 0.82 N HCl at 37 °C for 30 min was performed, then sections were neutralized with 0.1 M sodium borate (pH 8.5). After washes with TBS containing 1% Triton X-100 (TBS-T; 0.05 M, pH 7.4), all sections were incubated for 1 h at room temperature (RT) in a blocking buffer (BB) containing 10% fetal bovine serum (FBS) in TBS-T. Afterwards, sections were incubated overnight at 4 °C plus 1 h at RT with anti-DCX (1:1000; ab77450, Abcam) or anti-BrdU (1:100; ab6326, Abcam) primary antibodies diluted in BB. Neonatal brain sections were used as positive control for DCX, whereas the corresponding small intestine sections of animals treated with BrdU were used as positive control for BrdU. Sections incubated in BB lacking the primary antibody were used as negative control. After washes with TBS-T, sections were incubated for 1 h at RT with biotinylated anti-rabbit (1:500; BA-1000, Vector Laboratories) and anti-rat (1:500; BA-4001, Vector Laboratories) secondary antibodies diluted in BB for DCX and BrdU immunostaining, respectively. Then, sections were washed with TBS-T and incubated for 1 h at RT with horseradish peroxidase (HRP)-conjugated streptavidin (1:500; SA-5004, Vector Laboratories). After washes with TBS and Tris-buffered (TB; 0.05 M, pH 7.4), the immunolabeling was visualized incubating the sections for 3 min with a DAB Substrate Kit (SK-4100, Vector Laboratories) following the manufacturer's instructions. Nickel was additionally added in the revealed of BrdU. Afterwards, sections were washed in TB, mounted onto gelatinized slides and air dried at RT. To provide cytological details of DCX immunostaining, sections were counter-stained with 0.1% toluidine blue diluted in Walpole's buffer (0.05 M, pH 4.5). Finally, sections were dehydrated in graded alcohols, washed in N-butyl alcohol in the case of toluidine staining, immersed in xylene and coverslipped with DPX mounting medium.

2.6 Double immunofluorescence

To evaluate whether proliferating cells express IL-10 receptor (IL-10R), double immunolabeling against BrdU and IL-10R markers was performed in animals sacrificed

one day after the last BrdU administration. A double immunofluorescence against IL-10R and GFAP was also performed. Frozen free-floating brain sections were washed in TBS and DNA denaturation was performed as is explained in the above section for BrdU immunostaining. After washes with TBS-T, brain sections were incubated for 1 h at RT in a BB containing 10% FBS in TBS-T followed by anti-BrdU primary antibody (1:100; ab6326, Abcam) or anti-GFAP primary antibody (1:6000; G3893, Sigma-Aldrich) diluted in the BB, overnight at 4 °C and 1 h at RT. After washes with TBS-T, sections were incubated for 1 h at RT with an anti-rat AlexaFluor-488 conjugated secondary antibody (1:1000; A-11006, Thermo Fisher) or an anti-mouse AlexaFluor-488 conjugated secondary antibody (1:1000; A-11029, Thermo Fisher) diluted in BB. Following another blocking incubation for 1 h at RT, sections were incubated with anti-IL-10RA primary antibody (1:100; ab225820, Abcam) diluted in the BB for 48 h at 4 °C and 1 h at RT. Then, incubations for 1 h at RT with biotinylated anti-rabbit secondary antibody (1:500; BA-1000, Vector Laboratories) followed by incubation with AlexaFluor-555 conjugated streptavidin (1:1000; S32355, Thermo Fisher) were performed. After washes with TBS-T and TBS, sections were incubated with 4,9,6-diamidino-2-phenylindole (DAPI) (1:10000; D9542, Sigma-Aldrich) in TB for 5 min at RT to stain the cell nuclei. Finally, sections were washed with TB, mounted on slides and coverslipped with Fluoromount (0100-01, SouthernBiotech) mounting medium. Representative photos in the dentate gyrus were captured at 63x magnification using a Zeiss LSM700 confocal microscope.

2.7. Cell quantification

Photographs were captured with a DXM 1200F Nikon digital camera mounted on a brightfield Nikon Eclipse 80i microscope using the software ACT-1 2.20 (Nikon Corporation). A minimum of 4 animals of each age group was analyzed using the sections immunostained for DCX and BrdU. For each animal, at least 6 dentate gyrus (DG) areas from the hippocampus were used to count manually the number of DCX$^+$ cells in each DG section using the 40x magnification. BrdU$^+$ cells from at least 12 hippocampal sections, were quantified manually in the DG and the hilus region at 40x magnification.

2.8. Blood collection

Under an anesthetic solution of xylazine (30 mg/kg) and ketamine (120 mg/kg), mouse blood was intracardially extracted from the right ventricle and centrifugated at 9,300 x g for 5 min at 4 °C. After that, serum was collected and stored at -80 °C until use.

2.9. Tissue processing for biochemical analysis

Under an intraperitoneal anesthetic solution of xylazine (30 mg/kg) and ketamine (120 mg/kg), mice were intracardially perfused with cold 0.1 M Phosphate-Buffered Saline (PBS) at pH 7.4 for 1 min. Hippocampus was quickly dissected, frozen in liquid nitrogen and stored at -80 °C. Tissue was homogenized using a polytron homogenizer in a lysis buffer containing 25 mM HEPES at pH 7.4 (H3375, Sigma-Aldrich), 0.2% IGEPAL (I-3021, Sigma-Aldrich), 5 mM $MgCl_2$ (A376433, Merck), 1.3 mM EDTA at pH 8 (20302, VWR), 1 mM EGTA at pH 8 (E4378, Sigma-Aldrich), 1 mM PMSF (P7626, Sigma-Aldrich), protease inhibitor cocktail (1:100; P8343, Sigma-Aldrich) and phosphatase inhibitor cocktail (1:100; P0044, Sigma-Aldrich) in deionized water. After 2 h at 4 °C, tissue lysates were centrifuged at 15,600 x g for 5 min at 4 °C. Then, the supernatants were collected and stored aliquoted at -80 °C until use. In all the study, the hippocampus of each animal was analyzed separately.

2.10. Luminex bead-based multiplex assay

Total protein concentration of each hippocampal lysate was determined with a commercial Pierce BCA Protein Assay Kit (23225, Thermo Scientific) according to the manufacturer's instructions. To quantify specific proteins, Luminex® Multiple Analyte Profiling (xMAP®) technology was used. In adult (6 months old) and aged (21 months old) animals of both genotypes, IL-10, IL-6, IL-1β and TNF-α cytokines levels were measured by MILLIPLEX® MAP Kit (MCYTOMAG-70K, Merck) in hippocampal (n = 6-9 by experimental group) and serum (n = 4-5 by experimental group) samples. In the same animals, hippocampal levels of brain-derived neurotrophic factor (BDNF) and fractalkine (CX3CL1) were measured by MILLIPLEX® MAP Kit (MMYOMAG-74K, Merck). Both Luminex multiplex assays were performed according to the manufacturer's protocol. Briefly, 25 µL of each sample (total protein concentration of 3 µg/µL), standards or controls were added to their corresponding wells in a 96-well plate. Besides, 25 µL of Assay Buffer were added to samples wells, whereas 25 µL of lysis buffer (see "2.9. Tissue processing for biochemical analysis" section) were added to standard and control wells. In all the wells, 25 µL of magnetic beads conjugated with the antibodies of interest were added and incubated on a plate-shaker overnight at 4 °C. After removing wells content with a handheld magnet and two washes with Wash Buffer, 25 µL of Detection Antibodies were added into each well and incubated with agitation for 1 h at RT. Next, 25 µL of Streptavidin-Phycoerythrin was also added to each well and incubated with agitation for 30 min at RT. Finally, the wells were washed twice with Wash Buffer and 150 µL of Drive Fluid were added, followed by a 5 min

shaking. Luminex MAGPIX® instrument with xPONENT® 4.2 software was used to read and analyze the plate.

2.11. Flow cytometry

Characterization of microglial and neuronal populations was performed by flow cytometry. Under an intraperitoneal anesthetic solution of xylazine (30 mg/kg) and ketamine (120 mg/kg), adult (5-6 months old) and aged (23-24 months old) animals of both genotypes (n = 7-8 by experimental group) were intracardially perfused with cold 0.1 M PBS at pH 7.4 for 1 min. Hippocampi were quickly dissected and dissociated with a 160 µm nylon mesh in Hank's Balanced Salt Solution (HBSS) with 10% FBS and passed into a centrifuge tube through a 70 µm cell strainer. The splenocytes cell suspension obtained from one animal was used as positive control throughout the procedure. After three centrifugations for 10 min at 310 x g (24 °C) retaining the pellet, the homogenized tissue was digested in a solution composed of 1.25% deoxyribonuclease I (D5025, Sigma-Aldrich) and 0.5% collagenase IV (17104019, Thermo Fisher) in HBSS for 30 min at 37 °C. Cellular suspensions were centrifuged for 10 min at 310 x g (24 °C), then a density gradient was generated by using 1.122 g/mL and 1.088 g/mL of Percoll® (GE17-0891-02, Sigma-Aldrich) and centrifuging for 20 min at 600 x g (24 °C) without brake. The upper phase corresponding to myelin was removed, and the intermediate phase containing cells was collected. Cellular suspensions were centrifugated for 5 min at 860 x g, and 200 µL of each sample diluted in PBS with 2% FBS were seeded in a 96-wells conical bottom plate. Each sample was divided into five wells attending to the following treatments: microglial primary antibodies combination, neuronal primary antibodies combination, microglial isotypes control combination, neuronal isotypes control combination and unstained samples. After a centrifugation for 4 min at 515 x g (4 °C), FcγIII (CD16) and FcγII (CD32) receptors expressed on cells were blocked adding 50 µL of CD16/32 antibody (1:250; 553142, BD Biosciences) diluted in PBS with 2% FBS to all the wells for 20 min at 4 °C. After adding 150 µL of PBS with 2% FBS and centrifuging for 4 min at 515 x g (4 °C), surface markers of microglial cells and neurons were immunolabeled by incubating for 30 min at 4 °C in 50 µL of CD45-PerCP (1:400; 557235, BD Bioscience), CD11b-APC-Cy7 (1:400; 557657, BD Bioscience), CX3CR1-PE (1:400; FAB5825P, RD Systems), CD200R-AlexaFluor-647 (1:50; 566345, BD Bioscience), SIRPα-FITC (1:50; 144005, BioLegend), CD200-PE (1:400; 123807, BioLegend) and CD47-APC-Cy7 (1:50; 127525, BioLegend) antibodies diluted in PBS with 2% FBS. Samples in parallel wells were incubated with their corresponding conjugated-isotype control combinations (1:400; BD Biosciences). To immunolabel the intracellular marker NeuN, wells containing neuronal combinations of primary antibodies

and isotype controls were treated with 200 µL of a Fixation/Permeabilization solution (00-5123-43 and 00-5223-56, eBioscience) for 40 min at 4 °C. After centrifugations with a 1X permeabilization buffer (00-8333-56, eBioscience) for 4 min at 515 x g (4 °C), 50 µL of biotinylated-NeuN antibody (1:400; MAB377B, Millipore) diluted in the permeabilization buffer were added to the corresponding wells and incubated for 30 min at 4 °C. Afterwards, wells to study the neuronal combinations were incubated with Streptavidin-Cy5 (1:400; PA45001, Sigma-Aldrich) diluted in the permeabilization buffer for 20 min at 4 °C. After centrifugations, all samples were resuspended in 150 µL of PBS with 2% FBS and transferred from plate wells to cytometry tubes. Finally, 50 µL of CytoCount™ (S2366, Dako) fluorescent beads were added to the samples. Cell suspensions were acquired and read using a BD FACSCanto™ flow cytometer with the BD FACSDiva™ software. Analysis of the data was performed using the FlowJo™ software.

2.12. Statistical analysis

Statistics and graphical representation were performed using the GraphPad Prism® software. To determine differences between the different groups of animals, unpaired Student's t-test or two-way ANOVA were used. p-value < 0.05 was considered statistically significant. All experimental results are expressed as mean ± SEM.

3. RESULTS

3.1. Decreased hippocampal neurogenesis

To study net neurogenesis, the number of doublecortin (DCX) positive cells, a specific marker of neuroblasts and immature neurons, was quantified in the granular cellular layer (GCL) of the dentate gyrus. In all experimental groups, DCX$^+$ cell bodies were found in the subgranular zone (SGZ) or the inner GCL **(Figure 1A-D)**. DCX$^+$ cells displayed the typical morphology of neuroblasts, extending dendrites from the GCL through to the molecular cell layer **(Figure 1A-D)**. Our results showed a dramatic decrease of DCX$^+$ cells number with aging regardless of genotype **(Figure 1E)**. Moreover, GFAP-IL10Tg mice presented lower number of DCX$^+$ cells with respect to WT mice at both ages **(Figure 1E)**.

WT   GFAP-IL10Tg

A   DCX   B

ADULT

C   D

AGED

E

F   BrdU injections   Sacrifice   Sacrifice

Days 1   2   3   4   5   6   19
          Proliferation   *Survival*

G   Proliferation   H   Survival

I   WT   J   GFAP-IL10Tg   K   DAPI IL-10R BrdU

GCL   GCL   WT

SGZ   SGZ

Hilus   Hilus   L

                                         GFAP-IL10Tg

BrdU
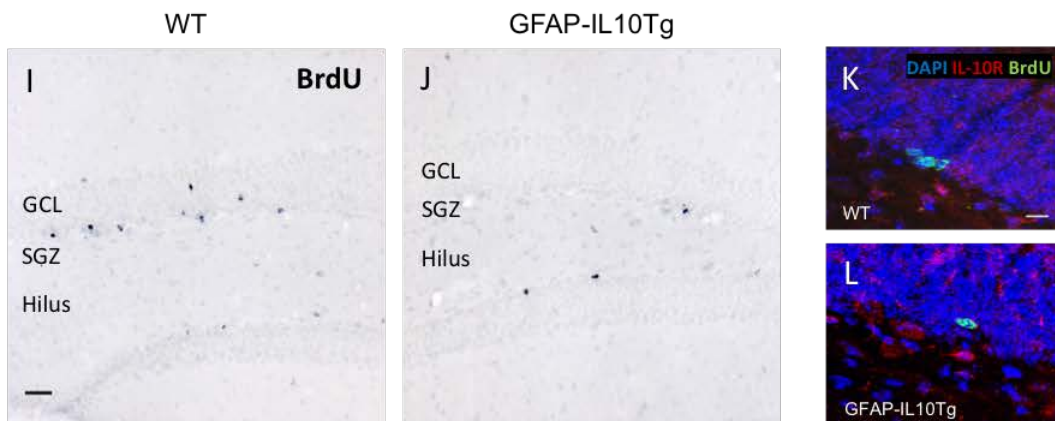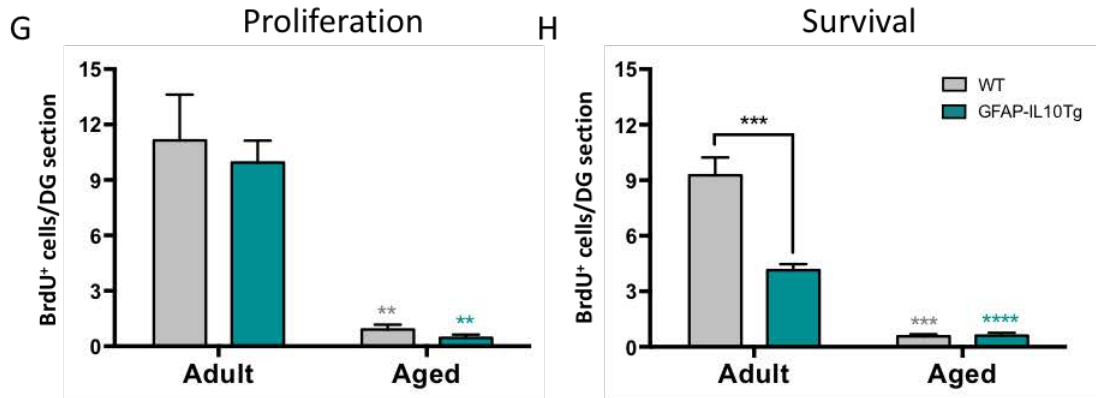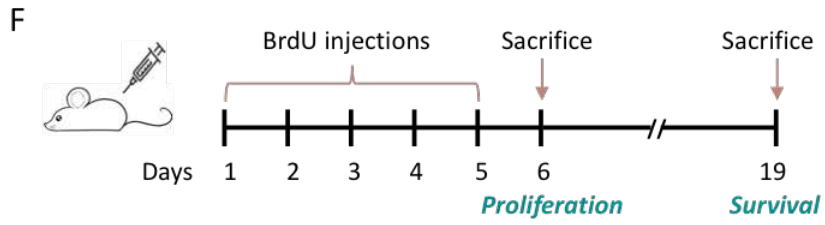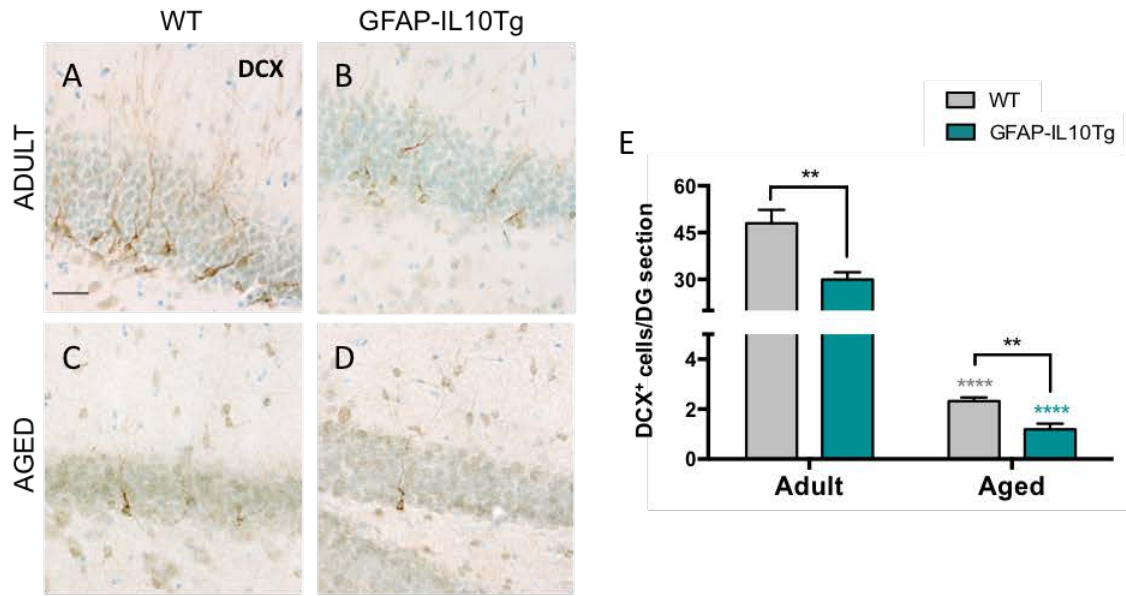
Figure 1. Hippocampal neurogenesis is decreased in GFAP-IL10Tg mice by low survival of neural proliferating cells. Representative images showing doublecortin (DCX) immunostaining in the granular cell layer of WT (A, C) and GFAP-IL10Tg (B, D) mice during adulthood (A, B) and aging (C, D). Quantification of DCX$^+$ cells per dentate gyrus (DG) section is represented in the graph (E). Temporal scheme of intraperitoneal BrdU administration (5 consecutive days) and time points of mice sacrifice (day 6 and 19) is shown in the panel (F). Graphs showing the number of proliferating BrdU$^+$ cells (G) and surviving BrdU$^+$ cells (H) per dentate gyrus section. Representative images showing BrdU immunostaining in the dentate gyrus after two weeks of the last BrdU administration (survival time) in adult WT (I) and GFAP-IL10Tg (J) mice. Representative images showing BrdU and IL-10 receptor (IL-10R) double immunostaining in the dentate gyrus after one day of the last BrdU administration in adult WT (K) and GFAP-IL10Tg (L) mice. Grey and cyan asterisks are referred to significant differences by age between WT or GFAP-IL10Tg mice, respectively. **$p < 0.01$, ***$p < 0.001$, ****$p < 0.0001$. Data are represented as the mean $\pm$ SEM. DCX: doublecortin, BrdU: 5-Bromo-2'-deoxyuridine, DG: dentate gyrus, GCL: granular cell layer, SGZ: subgranular zone, IL-10R: IL-10 receptor. Scale bar = 30 μm (A, I) and 100 μm (K).

To determine whether the reduced neurogenesis observed in transgenic animals with respect to WT was due to a lower proliferation rate of NSCs, we visualized BrdU-labeled mitotic cells located in the SGZ one day after five consecutive days of BrdU administration. In the adult SGZ of the hippocampus, BrdU$^+$ cells were visualized in clusters indicating recent mitotic divisions. In both genotypes, an important reduction in the number of proliferating BrdU$^+$ cells was observed during aging **(Figure 1G).** However, no differences in the number of BrdU$^+$ cells were found between WT and GFAP-IL10Tg mice at any age in the proliferation period **(Figure 1G)**. The hippocampal hilus is another proliferating, but non neurogenic (Bondolfi et al., 2004), region of the adult CNS. In this area, a lower number of proliferating cells compared to the SGZ was observed. Like in the SGZ, BrdU$^+$ cells number in the hilus decrease with aging (although in a less pronounced way) and no differences were detected between genotypes (data not shown).

Before NSCs differentiation, some NSCs undergo apoptosis in a period taking approximately 15 days after their proliferation (Encinas et al., 2011; Sierra et al., 2010). Therefore, the next step we addressed was to analyze putative differences between WT and GFAP-IL10Tg animals in terms of NSCs survival. Thus, following 5 days of consecutive BrdU injections, the number of surviving BrdU$^+$ cells was quantified two weeks after the last administration. At this time point, a slight reduction in the number of BrdU$^+$ cells comparing with the number of BrdU$^+$ cells quantified one day after the last BrdU administration was observed in adult WT mice **(Figure 1G,H)**. This reduction was significantly higher in adult GFAP-IL10Tg mice compared to WT mice, showing that animals overexpressing IL-10 present a lower NSC survival rate in adulthood with respect to WT animals **(Figure H-J)**. In aging, these differences were attenuated by the general low number of proliferating NSCs **(Figure 1H)**.

To determine whether IL-10 could be directly affecting NSCs survival, we evaluated IL-10 receptor (IL-10R) expression in proliferating NSCs before their differentiation by a double immunofluorescence against BrdU and IL-10R. Our results

demonstrated no expression of IL-10R in BrdU⁺ cells of the SGZ **(Figure 1K,L)**. IL-10R expression was mainly observed in neuronal dendrites and astrocytes of the hippocampal CA area, and in some neuronal bodies located in the hippocampal hilus (data not shown). No variations in the expression pattern of IL-10R by age or genotype were observed.

3.2. Unaltered animal survival and physical status

No differences in survival between WT and GFAP-IL10Tg mice up to 24 months of age were observed. All animals reached the age of sacrifice without evidences of motor problems or physical deterioration. Body weight was increased in WT and GFAP-IL10Tg mice upon aging without differences between genotypes (data not shown).

3.3. Neophobia and spatial memory impairment

Prior to cognition measurement, locomotion and anxiety of mice were evaluated by the corner test and the open field test. As compared to adult WT mice, a lower number of visited corners was observed by the effect of both age and genotype in the corner test for neophobia **(Figure 2A**). This neophobia was also shown in aged GFAP-IL10Tg mice in the open field test as a delayed rearing latency than age-matched WT mice **(Figure 2B)**. However, the total vertical and horizontal locomotor activity recorded during the 5 min of the test was similar between all animal groups studied when considering rearings, distance traveled and time spent in the center of the open field, indicating no differences in total locomotion or anxiety-like behavior by age or genotype **(Figure 2C-F)**. Changes in emotionality were also found as indicated by a longer grooming latency in aged transgenic mice than WT mice counterparts **(Figure 2G),** though the number and the total duration of grooming did not reach statistical significance **(Figure 2H,I)**. In this test, no urine and a very low number of defecations were recorded in all the studied groups.
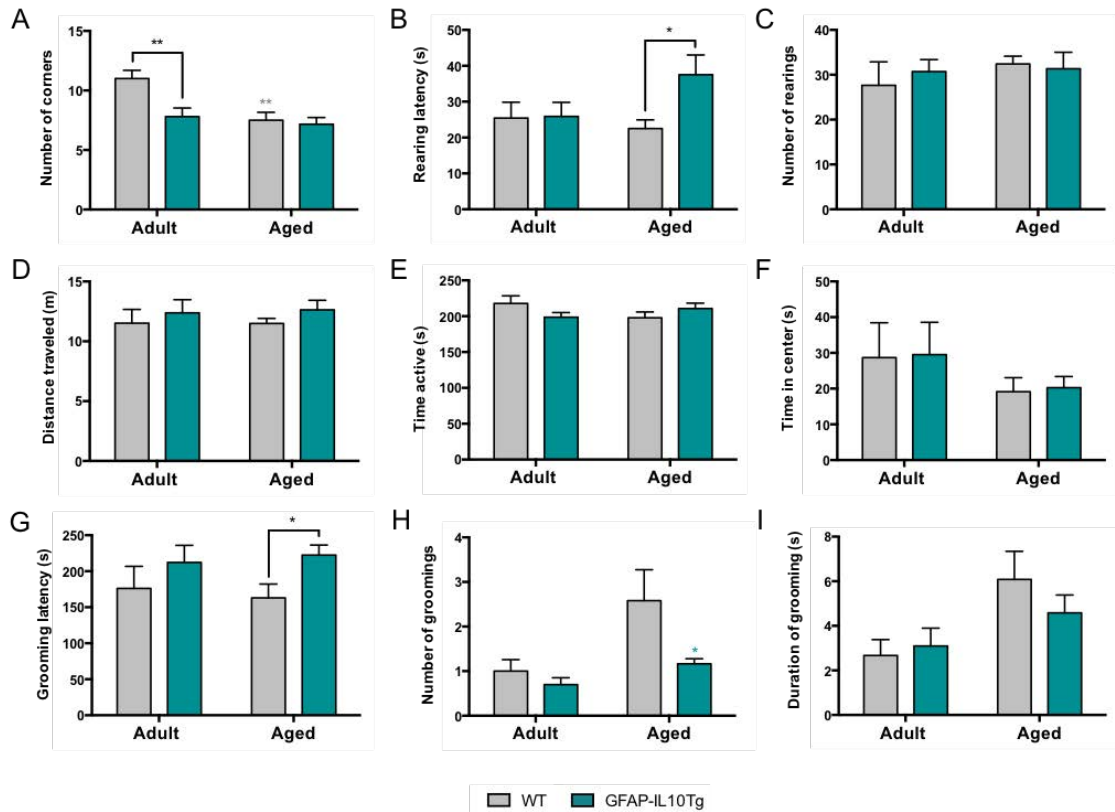
Figure 2. GFAP-IL10Tg mice present increased neophobia, but normal total locomotion. Graph showing the number of visited corners in the corner test as measure of neophobia (A). In the open field test, vertical activity as measured by the rearing latency (B) and the number of total rearings (C). Horizontal activity is graphically represented by the distance traveled (D), the time active (E) and the time in the center of the apparatus (F). Quantification of grooming latency (G), total number of groomings (H) and total duration of grooming episodes (I) in the open field test. Grey and cyan asterisks are referred to significant differences by age between WT or GFAP-IL10Tg mice, respectively. *$p < 0.05$, **$p < 0.01$. Data are represented as the mean ± SEM.

Since neurogenesis of the dentate gyrus is involved in hippocampal-dependent memory, two spatial learning and memory tests, the T-maze and the Morris water maze, were used to evaluate possible cognitive deficits in working, short- and long-term learning and memory.

Working memory was assessed using the spontaneous alternation in the T-maze, where the number of arms-exploratory errors was quantified. In this memory task, the overall incidence of GFAP-IL10Tg mice doing more than one single error (50%, 5/10 in adulthood, 6/12 in aging) was higher compared to WT mice (18.75%, 1/6 in adulthood, 2/10 in aging), indicating working memory affectation **(Figure 3A)**. The latency to the arms intersection, which is related to coping with stress, showed a trend to be delayed with aging and IL-10 overexpression albeit did not reach statistical significance **(Figure 3B)**.
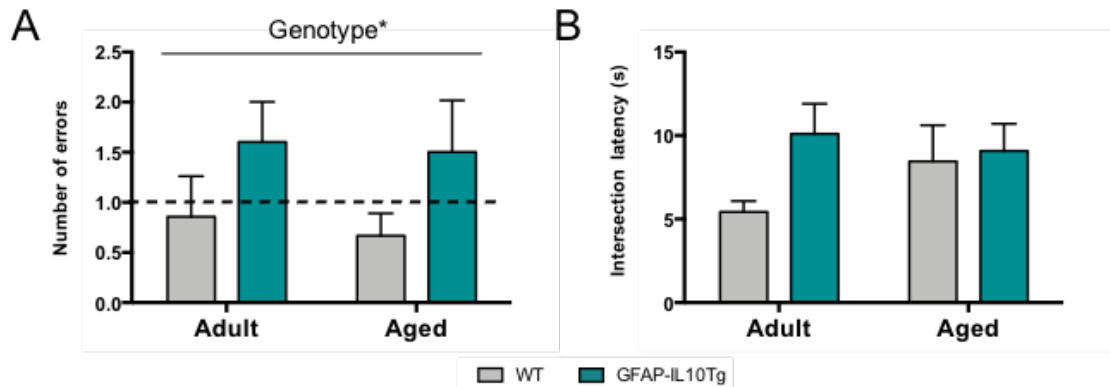
Figure 3. Working memory deficits in GFAP-IL10Tg mice assessed by the T-maze. Graphs showing the number of errors that mice made by exploring the same arm again in the maze, indicating significant differences in the overall incidence of more than one single error between genotypes (A), and the latency to cross the intersection between vertical and horizontal arms (B) in WT and GFAP-IL10Tg mice. Data are represented as the mean ± SEM.

For spatial short- and long-term learning and memory, three paradigms were used in the Morris water maze. On the first day, aged GFAP-IL10Tg mice showed poor cognitive capacity requesting more time to reach the visible cued platform than the aged WT group **(Figure 4D)**. In the reversal place-learning task for spatial learning and memory, day (Two-way ANOVA, $p < 0.001$) and group (Two-way ANOVA, $p < 0.0001$) effects were found **(Figure 4E)**. Here, the aged transgenic mice showed the worst performance in the task, unveiling long-term learning and memory deficits **(Figure 4E)**. Two hours after the last trial, the platform was removed and spatial memory was evaluated measuring the time that animals spent in the quadrant where the platform was previously located **(Figure 4G,H)**. Our results demonstrated that spatial memory was impaired with aging and that this deficit was already observed in GFAP-IL10Tg mice since adulthood **(Figure 4F)**. In summary, these paradigms showed that animals with IL-10 overexpression presented hippocampal cognitive deficits in long-term learning acquisition and memory processes at old age, but short-term memory impairment was subjacent earlier.
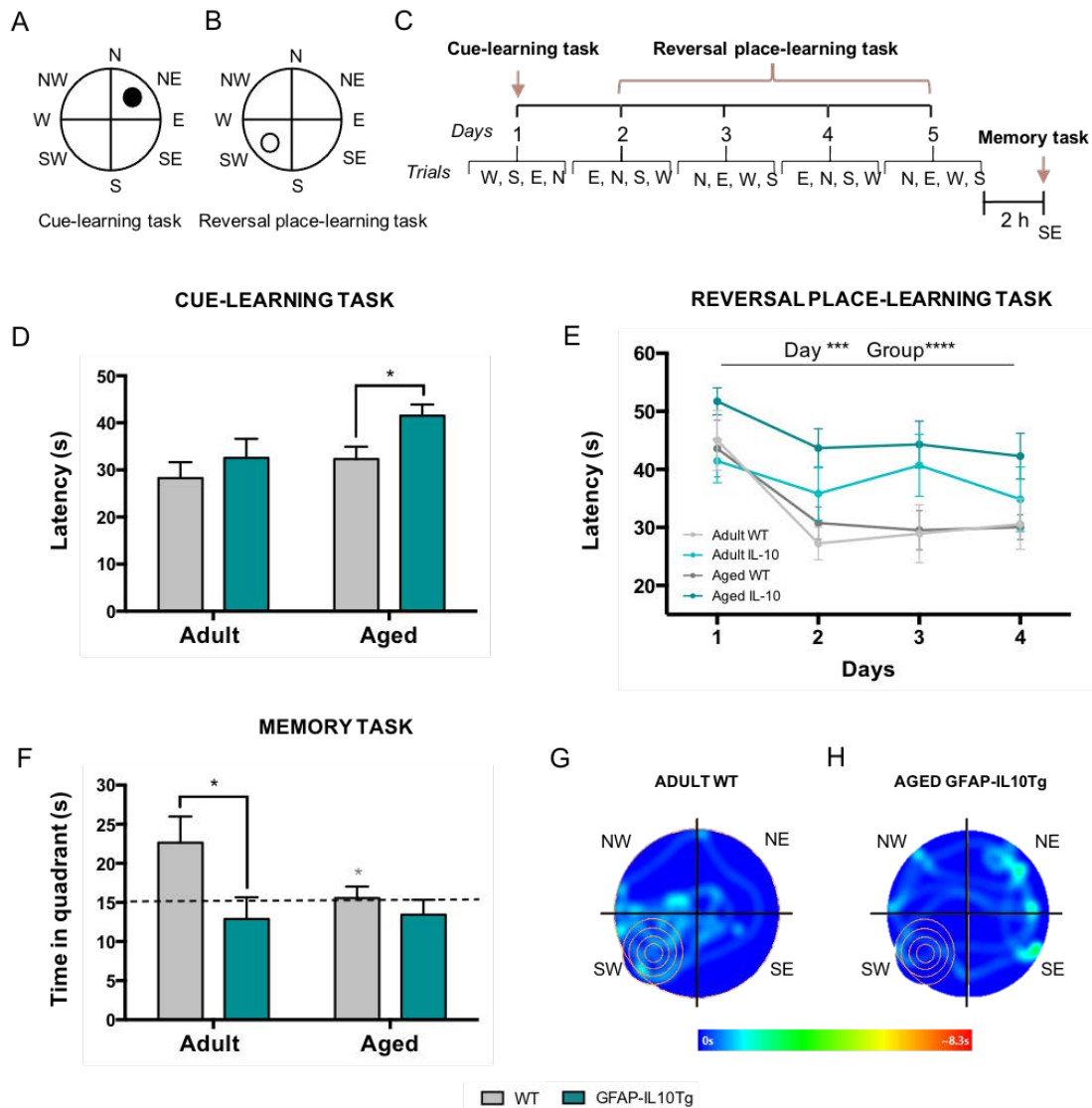
Figure 4. Short- and long-term spatial learning and memory impairment in GFAP-IL10Tg mice assessed by the Morris water maze. Swimming pool representation showing a visible platform (black circle) in the cue-learning task (A) and a hidden platform (white circle) in the place-learning task (B) of the Morris water maze. Temporal scheme for the 3 paradigms for learning and memory performed in the Morris water maze (C). Graphs show the latency to reach the visible platform on the first day of test (D) and the hidden platform on the next consecutive four days of test (E). After platform removal, the time spent in the quadrant where the platform was is represented in the graph (F). Panels (G, H) show representative swimming pool heat-maps indicating mouse path in the memory task. Grey asterisk is referred to significant differences by age between WT mice. *$p < 0.05$, ***$p < 0.001$, ****$p < 0.0001$. Data are represented as the mean $\pm$ SEM. N: north, NE: northeast, E: east, SE: southeast, S: south, SW: southwest, W: west, NW: northwest.

3.4. Increased hippocampal and serological IL-10 levels

To address whether the observed neurological and behavioral alterations in transgenic animals correlated with IL-10 overproduction, IL-10 levels in the hippocampus and the serum of animals were measured by Luminex assay. Our data demonstrated that GFAP-IL10Tg mice presented higher levels of IL-10 respect to WT

mice in both hippocampal and serum samples, but no effect of IL-10 expression by the age was observed for any genotype **(Figure 5A,C)**.

Because growth factors are involved in the process of neurogenesis, hippocampal BDNF levels were measured. Although high BDNF expression was detected in all the studied groups, no differences by age or genotype were observed **(Figure 5B)**. The levels of pro-inflammatory IL-6, IL-1β and TNF-α cytokines were also measured in the hippocampus and the serum, as possible negative regulators of neurogenesis. Very low or undetected levels of these cytokines, without differences between the studied experimental groups, were detected in the hippocampus (data not shown). Only a tendency to IL-6 increase in the serum of aged animals was observed regardless the genotype **(Figure 5D)**.
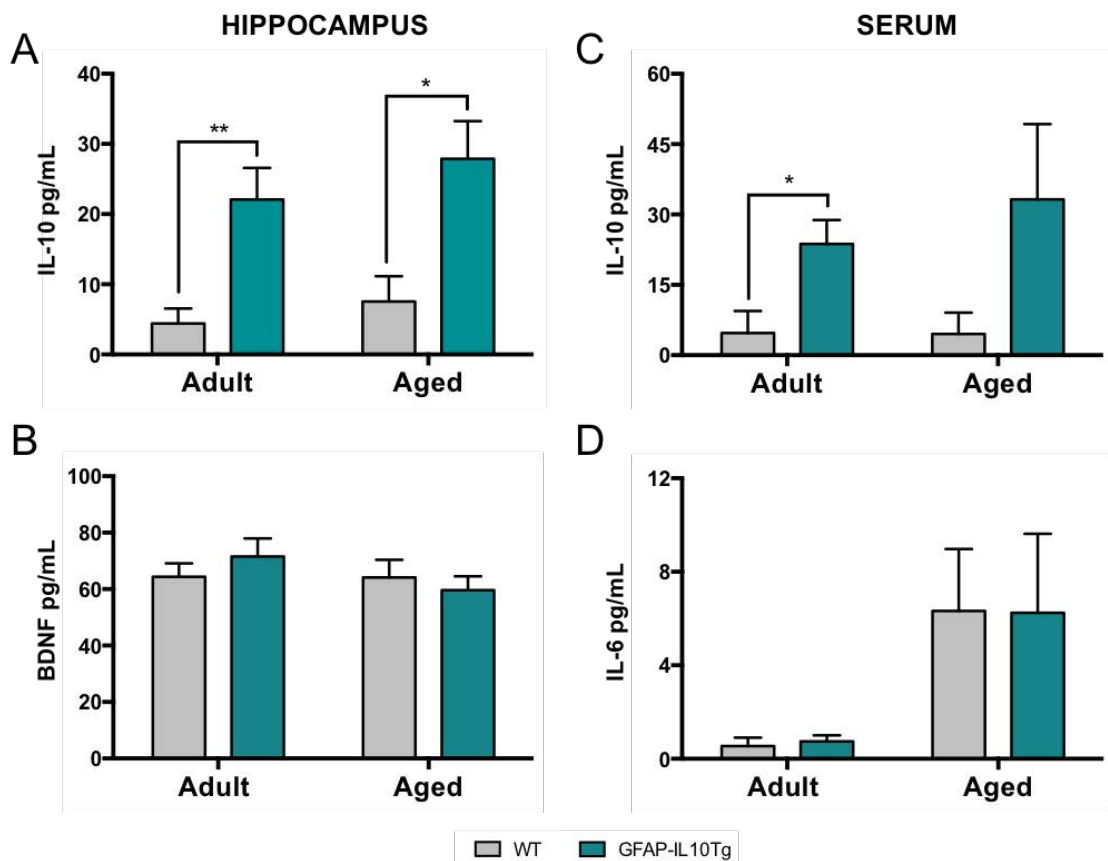
Figure 5. Increased levels of IL-10 in the hippocampus and the serum of GFAP-IL10Tg mice. Graphs showing quantitative IL-10 (A) and BDNF (B) protein expression in the hippocampus and IL-10 (C) and IL-6 (D) protein expression in the serum of WT and GFAP-IL10Tg mice by Luminex assay. *$p < 0.05$, **$p < 0.01$. Data are represented as the mean ± SEM. BDNF: brain-derived neurotrophic factor.

3.5. Different hippocampal immune cells profile

Immune cells, especially lymphocytes, macrophages and microglia, play a role in the process of neurogenesis. By flow cytometry we distinguished three leucocyte

populations: non-myeloid cells (CD11b$^-$/CD45$^+$), high-activated myeloid cells (CD11b$^+$/CD45^{high}) and low/intermediate-activated myeloid cells (CD11b$^+$/CD45$^{low/int}$).
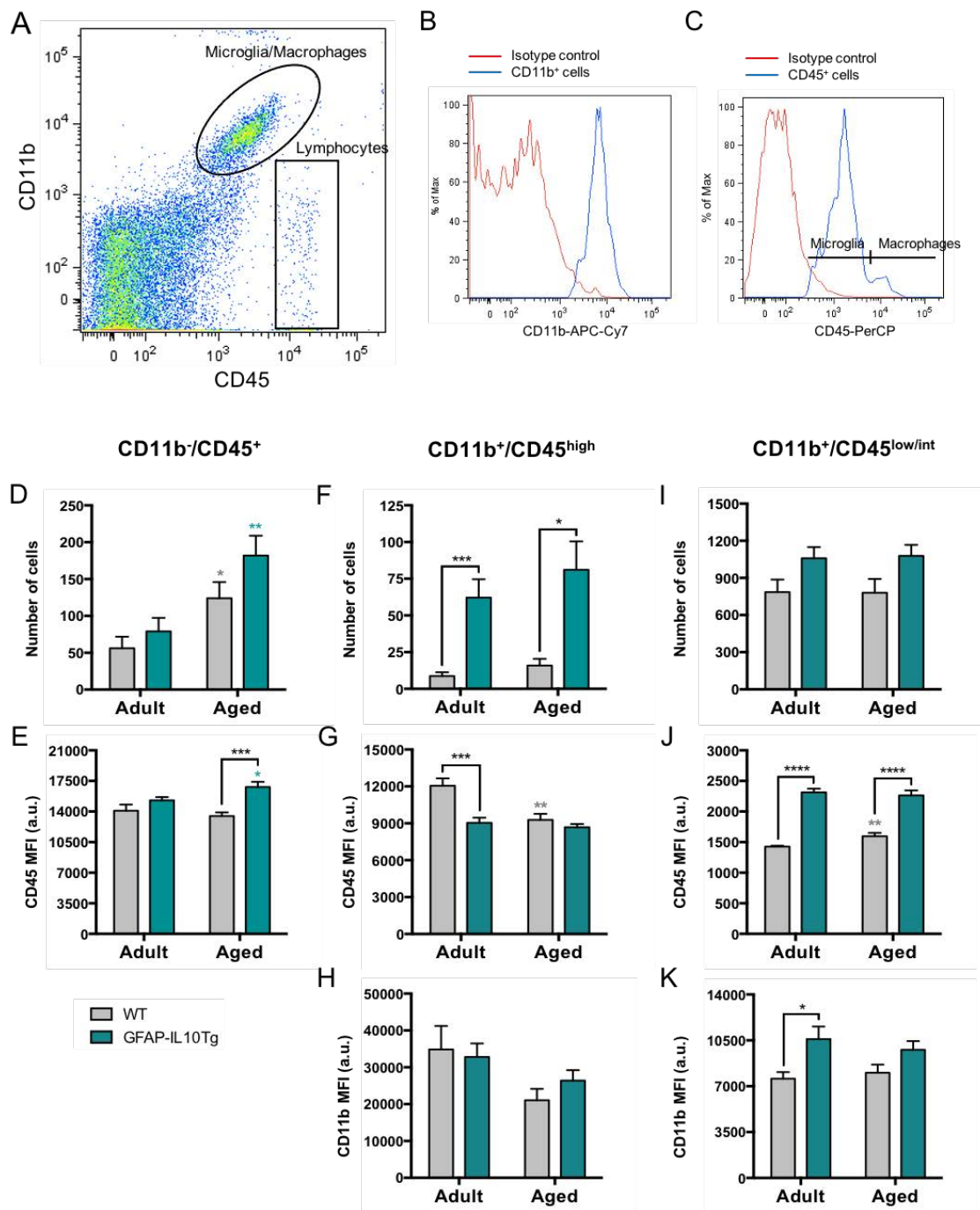

Figure 6. Elevated number of CD11b$^+$/CD45^{high} cells and high activation of CD11b$^+$/CD45$^{low/int}$ cells in GFAP-IL10Tg mice. Gate strategy showing the selection region of myeloid and non-myeloid cell populations by CD11b and CD45 expression is represented in panel (A). Histograms representing isotype control and positive staining of CD11b-APC-Cy7 (B) and CD45-PerCP (C) isotypes/antibodies. Histogram (C) showing the separation between CD11b$^+$/CD45$^{low/int}$ (microglia) and CD11b$^+$/CD45^{high} (macrophages) populations by CD45-PerCP fluorescence intensity. Graphs showing the number of CD11b$^-$/CD45$^+$ (D), CD11b$^+$/CD45^{high} (F) and CD11b$^+$/CD45$^{low/int}$ (I) cells in the hippocampus of WT and GFAP-IL10Tg mice. CD45 (E, G, J) and CD11b (H, K) cell expression is represented by the mean fluorescent intensity in CD11b$^-$/CD45$^+$ (E), CD11b$^+$/CD45^{high} (G, H) and CD11b$^+$/CD45$^{low/int}$ (J, K) cells. Grey and cyan asterisks are referred to significant differences by age between WT or GFAP-IL10Tg mice, respectively. *$p < 0.05$,

Non-myeloid cells number was increased by the age in both genotypes, but no differences between WT and GFAP-IL10Tg mice were observed **(Figure 6D)**. However, the expression of CD45 in these cells was higher in GFAP-IL10Tg respect to WT mice during aging **(Figure 6E)**. On the other hand, no effect by the age was observed in the number of myeloid cells, although transgenic animals presented more CD11b$^+$/CD45$^+$ cells than WT at both ages **(Figure 6F,I)**. Our results showed that CD45 expression on CD11b$^+$/CD45^{high} cells decreased in WT with aging, whereas GFAP-IL10Tg mice already present similar CD45 levels to those observed in aged WT mice since adulthood **(Figure 6G)**. Oppositely, CD45 expression on CD11b$^+$/CD45$^{low/int}$ cells was increased by both aging and IL-10 overexpression **(Figure 6J)**. However, the effect of IL-10 overproduction on CD45 expression was more pronounced than the effect produced by normal aging **(Figure 6J)**. Regarding CD11b expression, a higher level was found in the CD11b$^+$/CD45$^{low/int}$ cells from adult GFAP-IL10Tg with respect to WT animals **(Figure 6K)**, while no differences by age or genotype were observed in CD11b$^+$/CD45^{high} cells **(Figure 6H)**.

3.6. Altered microglia-neuron communication

Considering that microglia/macrophages (CD11b$^+$/CD45$^+$) cell number, as well as CD45 and CD11b expression, were different between WT and GFAP-IL10Tg mice since adulthood when neurogenesis impairment was already observed in transgenic mice, we studied myeloid receptors that are involved in neuronal communication as possible modulators of the generation of newborn neurons. CD200R, SIRPα and CX3CR1 expression were analyzed separately in CD11b$^+$/CD45^{high} and CD11b$^+$/CD45$^{low/int}$ cells. No differences of CD200R, SIRPα or CX3CR1 expression by the effect of the age or the genotype were observed in CD11b$^+$/CD45^{high} cells **(Figure 7G-I)**. However, in CD11b$^+$/CD45$^{low/int}$ cells, both age and genotype modified the expression of these receptors. Our results showed that CD200R and SIRPα levels increased with normal aging and under IL-10 transgenic overproduction **(Figure 7J,K)**. Thus, CD200R and SIRPα expression in GFAP-IL10Tg mice along the lifespan was similar to the observed in aged WT mice **(Figure 7J,K)**. On the contrary, CX3CR1 expression decreased in aged and transgenic animals **(Figure 7L)**. In this case, the reduction of CX3CR1 caused by IL-10 overproduction was higher than the produced by normal aging **(Figure 7L)**.
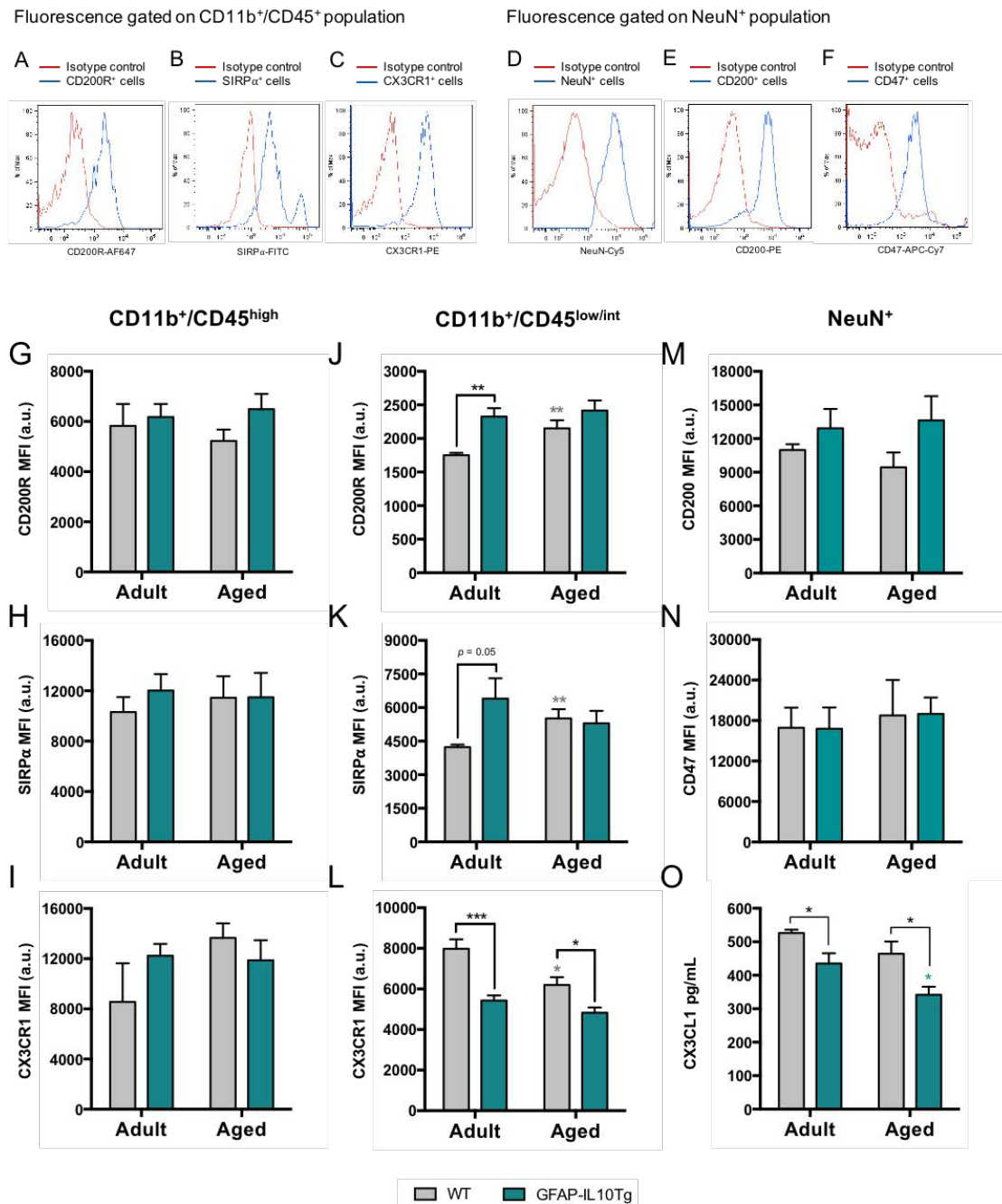
Figure 7. Altered homeostatic receptors in CD11b⁺/CD45ˡᵒʷ/ⁱⁿᵗ cells of GFAP-IL10Tg mice. Histograms representing isotype control and positive staining of CD200R-AlexaFluor-647 (A), SIRPα-FITC (B), CX3CR1-PE (C), NeuN-Cy5 (D), CD200-PE (E), CD47-APC-Cy7 (F) isotypes/antibodies. Cell expression of CD200R (G, J), SIRPα (H, K) and CX3CR1 (I, L) is represented by the mean fluorescence intensity in CD11b⁺/CD45ʰⁱᵍʰ (G-I) and CD11b⁺/CD45ˡᵒʷ/ⁱⁿᵗ (J-L) hippocampal cells. CD200 (M) and CD47 (N) cell expression is represented by the mean fluorescence intensity in hippocampal NeuN⁺ cells, whereas CX3CL1 (O) expression is showed by Luminex assay in hippocampal lysates. Grey and cyan asterisks are referred to significant differences by age between WT or GFAP-IL10Tg mice, respectively. $*p < 0.05$, $**p < 0.01$, $***p < 0.001$. Data are represented as the mean $\pm$ SEM. MFI: mean fluorescence intensity, a.u.: arbitrary units.

Regarding neurons, our data showed a similar number of NeuN⁺ cells in all the studied groups (data not shown). Expression of CD200, CD47 and CX3CL1, the neuronal ligands of CD200R, SIRPα and CX3CR1, respectively, was also studied. No

significant differences in CD200 or CD47 expression by age or genotype were detected in the neuronal population **(Figure 7M,N)**. Total CX3CL1 levels were unchanged with the aging. However, animals with IL-10 overproduction presented lower levels than WT animals at both ages **(Figure 7O)**. Additionally, transgenic animals underwent a reduction of this molecule upon aging **(Figure 7O)**.

4. DISCUSSION

The present study shows that chronic transgenic IL-10 overproduction in the CNS induces a hippocampal microglial phenotype in adults very similar to the observed in the physiological aging, which could be anticipating the aged-related decreased neurogenesis and cognitive deficits. To the best of our knowledge, this work is the first showing a negative effect of chronic IL-10 overproduction on hippocampal neurogenesis of the adult and the aged brain under physiological conditions *in vivo*.

During aging, the brain microenvironment has been reported to be modified upon a pro-inflammatory status characterized by high oxidative stress, pro-inflammatory cytokines, and microglial activation (Nakanishi and Wu, 2009; Sierra et al., 2007; Udeochu et al., 2016). Specifically, hippocampus is one of the most affected brain areas by age (Barrientos et al., 2015; Mattson and Magnus, 2006; Ojo et al., 2015). In this area, neurogenesis decreases dramatically with normal aging, impacting cognitive functions (Drapeau et al., 2003; Klempin and Kempermann, 2007; Villeda et al., 2011). Since neurogenic niches are intimately associated with the microenvironment, and it is known that inflammation is detrimental to the process of neurogenesis, it is plausible to think that the neuroinflammation of the aged brain is a critical factor for the decreased process of neurons generation in aging. In this context, we analyzed adult and aged hippocampal neurogenesis in transgenic animals with an anti-inflammatory microenvironment generated by the astrocyte-targeted overproduction of IL-10.

Our observations showing both fewer DCX$^+$ and BrdU$^+$ cells in aged animals are consistent with the lower hippocampal neurogenesis reported during aging (Klempin and Kempermann, 2007; Kuhn et al., 1996; Kuipers et al., 2015). Moreover, in these animals, we also report spatial memory impairment as principal feature of hippocampal affectation. Surprisingly, our results demonstrate that transgenic animals with overexpression of the anti-inflammatory IL-10 cytokine present lower hippocampal neurogenesis than WT mice during both adulthood and aging. In concordance with the decrease of newly neurons formation, IL-10 overproduction impaired hippocampal-dependent spatial learning and memory, as was determined by the T-maze and the

Morris water maze. These cognitive deficits also corroborate the lower excitability of hippocampal synapses and the absence of long-term potentiation, previously described in GFAP-IL10Tg animals (Almolda et al., 2015). In line with our observations, it has been reported that adeno-associated virus-mediated IL-10 expression exacerbates hippocampal-dependent memory impairment (Chakrabarty et al., 2015), whereas IL-10 deficiency partially restores this cognitive deficit (Guillot-Sestier et al., 2015) in Alzheimer's disease transgenic mouse models.

The negative effect of chronic IL-10 overexpression on hippocampal neurogenesis here reported, is consistent with a previous study reporting that IL-10 administration decreases the number of DCX^{+} cells in the SVZ, while in IL-10-KO mice DCX expression is increased (Perez-Asensio et al., 2013). On the contrary, another study reports that IL-10 gene delivery by adeno-associated virus enhances hippocampal neurogenesis and improves cognitive function in an Alzheimer's murine model (Kiyota et al., 2012). As possible cause of the different IL-10 effects, in Kiyota et al. (2012) study, the IL-10 was punctually administered at three months of age, while in our work, a chronic astrocyte-dependent IL-10 production exists since the birth. Moreover, unlike our study, neurogenesis is enhanced by IL-10 injections in a pathological situation. To study modifications in neuronal precursor proliferation as a possible explication of reduced neurogenesis in GFAP-IL10Tg mice, the number of cells incorporating the synthetic nucleotide BrdU was quantified before the apoptosis period. At this time, no differences in the number of proliferating BrdU^{+} cells were detected by IL-10 overexpression. Interestingly, our data showing a significant reduction in the number of BrdU^{+} cells after the apoptosis period in transgenic mice with respect to WT mice, demonstrate that IL-10 overexpression is negatively affecting the survival of hippocampal NSCs leading to a decreased neurogenesis since adulthood. However, no differences in the expression of hippocampal BDNF, which promotes neural survival/differentiation (Goldman et al., 1997; Lee et al., 2002; Taliaz et al., 2010), were detected between WT and GFAP-IL10Tg mice discarding this factor as the putative aspect affected by IL-10. Thus, this data demonstrates that BDNF is not the only factor required for neural survival.

Our results showing greater IL-10 levels in the hippocampus and serum of transgenic mice compared to WT, point to IL-10 as a key regulator of hippocampal neurogenesis. IL-10 intraventricular administration has been shown to maintain NSCs in an undifferentiated transition state by a direct effect of this cytokine on the NSCs allocated in the SVZ niche (Pereira et a., 2015; Perez-Asensio et al., 2013). However, as previously reported Perez-Asensio and collaborators (2013), our work demonstrates that neither WT nor GFAP-IL10Tg animals express IL-10 receptor in NSCs of the

hippocampal SGZ niche, and therefore, IL-10 must be indirectly acting on the neurogenesis regulation. In this way, immune cells, and especially microglial cells, are highly dependent on environmental signals (Bennett et al., 2018; Gosselin et al., 2014; Lavin et al., 2014) and play an important role in the process of neurogenesis (Carpentier and Palmer, 2009; Kokaia et al., 2012; Ziv and Schwartz, 2008). Here, we observed that transgenic animals present microglial modifications in markers of general activation (CD45 and CD11b) and markers involved in neuronal communication (CD200R, SIRPα and CX3CR1). Curiously, the specific microglial phenotype acquired by IL-10 overexpression in both ages was very similar to the observed in normal aging. This similar phenotype between adult GFAP-IL10Tg and aged WT microglia was already found in our previous study, where we showed an increased microglial cell density, high IBA1 expression and upregulation of phagocytic markers in GFAP-IL10Tg mice (Sanchez-Molina et al., 2021).

In concordance with our results, microglial pro-inflammatory activation has been reported specifically to affect hippocampal survival of newborn cells rather than cell proliferation or differentiation (Bastos et al., 2008; Ekdahl et al., 2003). Specifically, the present work shows CD200R and SIRPα increase as well as CX3CR1 decrease in transgenic mice and during physiological aging. Generally, CD200R-CD200 (Manich et al., 2018), SIRPα-CD47 (Zhang et al., 2015) and CX3CR1-CX3CL1 (Cardona et al., 2006) interactions maintain microglia in a homeostatic state characterized by anti-inflammatory signaling pathways (Biber et al., 2007; Hu et al., 2014; Linnartz and Neumann, 2013). Disruption of these interactions upon aging and its association with age-related microglial activation has been previously described by several studies (Jurgens and Johnson, 2012). Specifically, decreased levels of CD200 (Cox et al., 2012; Frank et al., 2006; Lyons et al., 2007) and CX3CL1 (Bachstetter et al., 2011; Lyons et al., 2009; Vukovic et al., 2012; Wynne et al., 2010) neuronal ligands have been reported in aged rodents. However, to the best of our knowledge, our findings demonstrate for first time different expression of CD200R, SIRPα and CX3CR1 microglial receptors with normal aging. Interestingly, research developed in the last decade has demonstrated that microglia-neuron communication is involved in hippocampal neurogenesis. As an example, administration of the neuronal ligand CD200 restores neurogenesis in a mouse model of Alzheimer's disease coinciding with an anti-inflammatory microglial status, however, CD200 overexpression did not enhance neurogenesis in WT mice (Varnum et al., 2015). Considering this data, the higher CD200R expression that we report in aged and transgenic animals could be trying to compensate the lower neurogenesis observed in these animals. On the other

hand, disruption of CX3CR1-CX3CL1 dialogue negatively regulates hippocampal neurogenesis by increased production of IL-1β leading to a pro-inflammatory scenario (Bachstetter et al., 2011). Thus, our findings showing decrease of CX3CR1 and CX3CL1 expression in GFAP-IL10Tg mice are in concordance with previous studies reporting their correlation with neurogenesis decline (Bachstetter et al., 2011; Reshef et al., 2017; Vukovic et al., 2012). Moreover, we provide evidence of SIRPα increase in aged mice as well as in GFAP-IL10Tg mice, suggesting that SIRPα-CD47 disruption also contributes to the neurogenesis process. In general, alterations of "do-not-eat-me" signaling result in a pro-inflammatory microenvironment shift affecting the production of new neurons. Here, we identify that homeostatic microglial receptors are altered by both IL-10 overexpression and normal aging. However, the levels of the main pro-inflammatory cytokines negatively involved in the process of neurogenesis, such as IL-6, IL-1β and TNF-α, were very low without differences between WT and GFAP-IL10Tg mice. Likewise, no differences in BDNF expression were detected by aging or IL-10 overproduction.

Taken together, our results suggest that IL-10 effect on neurogenesis could be mediated by a cell-to-cell contact between microglia and neurons. In this line, Kiyota and colleagues (2012) demonstrated that microglia pretreated with IL-10 enhances NSCs proliferation and survival in direct co-cultures. However, microglial conditioned medium through indirect (transwell) co-cultures with IL-10-treated microglia had no effects on neural population (Kiyota et al., 2012). These findings support the need for direct microglia-neuron contact for a correct neurogenesis promotion.

Although IL-10 has been usually described as an anti-inflammatory cytokine with neuroprotective functions (Burmeister and Marriott, 2018; Lobo-Silva et al., 2016), its temporal expression is critical for its effect. Moreover, IL-10 effect has been recently described as dual, including anti- and pro-inflammatory properties depending on the binding affinity for IL-10 receptor and its intracellular signaling (Saxton et al., 2021). Thus, here we report a microglial shift toward a more activated phenotype similar to that of aged microglia, with a detrimental effect on hippocampal neurogenesis in animals chronically overexpressing IL-10 since postnatal development.

5. CONCLUSIONS

This work shows the importance of the microenvironment on microglial cells and their relationship with neurogenesis. Interestingly, we demonstrated that chronic anti-inflammatory IL-10 overproduction has a similar effect to physiological aging on the hippocampus. Specifically, in transgenic animals and wildtype with normal aging,

hippocampal neurogenesis and memory are impaired together with alterations in the microglia-neuron communication. Likely, IL-10 overexpression modifies microglial receptors involved in neuronal communication resulting in reduced neurogenesis. This study emphasizes the variety of possibilities that a specific cytokine can exert depending on the moment and the time in which is expressed. Thus, we describe new properties of IL-10 in hippocampal neurogenesis *in vivo*.

REFERENCES

Aharoni, R., Arnon, R., Eilam, R., 2005. Neurogenesis and neuroprotection induced by peripheral immunomodulatory treatment of experimental autoimmune encephalomyelitis. J Neurosci. 25(36), 8217–8228. https://doi.org/10.1523/JNEUROSCI.1859-05.2005

Akkermann, R., Beyer, F., Küry, P., 2017. Heterogeneous populations of neural stem cells contribute to myelin repair. Neural Regen Res. 12(4), 509–517. https://doi.org/10.4103/1673-5374.204999

Almolda, B., de Labra, C., Barrera, I., Gruart, A., Delgado-Garcia, J.M., Villacampa, N., Vilella, A., Hofer, M.J., Hidalgo, J., Campbell, I.L., González, B., Castellano, B., 2015. Alterations in microglial phenotype and hippocampal neuronal function in transgenic mice with astrocyte-targeted production of interleukin-10. Brain Behav Immun. 45, 80–97. https://doi.org/10.1016/j.bbi.2014.10.015

Altman, J., Das, G.D., 1965. Autoradiographic and histological evidence of postnatal hippocampal neurogenesis in rats. J Comp Neurol. 124(3), 319–335. https://doi.org/10.1002/cne.901240303

Bachstetter, A.D., Morganti, J.M., Jernberg, J., Schlunk, A., Mitchell, S.H., Brewster, K.W., Hudson, C.E., Cole, M.J., Harrison, J.K., Bickford, P.C., Gemma, C., 2011. Fractalkine and CX 3 CR1 regulate hippocampal neurogenesis in adult and aged rats. Neurobiol Aging. 32(11), 2030–2044. https://doi.org/10.1016/j.neurobiolaging.2009.11.022

Barrientos, R.M., Kitt, M.M., Watkins, L.R., Maier, S.F., 2015. Neuroinflammation in the normal aging hippocampus. Neuroscience. 309, 84–99. https://doi.org/10.1016/j.neuroscience.2015.03.007

Bastos, G.N., Moriya, T., Inui, F., Katura, T., Nakahata, N., 2008. Involvement of cyclooxygenase-2 in lipopolysaccharide-induced impairment of the newborn cell survival in the adult mouse dentate gyrus. Neuroscience. 155(2), 454–462. https://doi.org/10.1016/j.neuroscience.2008.06.020

Battista, D., Ferrari, C.C., Gage, F.H., Pitossi, F.J., 2006. Neurogenic niche modulation by activated microglia: transforming growth factor beta increases neurogenesis in the adult dentate gyrus. Eur J Neurosci. 23(1), 83–93. https://doi.org/10.1111/j.1460-9568.2005.04539.x

Bennett, F.C., Bennett, M.L., Yaqoob, F., Mulinyawe, S.B., Grant, G.A., Hayden Gephart, M., Plowey, E.D., Barres, B.A., 2018. A Combination of Ontogeny and CNS Environment Establishes Microglial Identity. Neuron. 98(6), 1170–1183.e8. https://doi.org/10.1016/j.neuron.2018.05.014

Biber, K., Neumann, H., Inoue, K., Boddeke, H.W., 2007. Neuronal 'On' and 'Off' signals control microglia. Trends Neurosci. 30(11), 596–602. https://doi.org/10.1016/j.tins.2007.08.007

Bond, A.M., Berg, D.A., Lee, S., Garcia-Epelboim, A.S., Adusumilli, V.S., Ming, G.L., Song, H., 2020. Differential Timing and Coordination of Neurogenesis and Astrogenesis in Developing Mouse Hippocampal Subregions. Brain Sci. 10(12), 909. https://doi.org/10.3390/brainsci10120909

Bondolfi, L., Ermini, F., Long, J.M., Ingram, D.K., Jucker, M., 2004. Impact of age and caloric restriction on neurogenesis in the dentate gyrus of C57BL/6 mice. Neurobiol Aging. 25(3), 333–340. https://doi.org/10.1016/S0197-4580(03)00083-6

Borsini, A., Zunszain, P.A., Thuret, S., Pariante, C.M., 2015. The role of inflammatory cytokines as key modulators of neurogenesis. Trends Neurosci. 38(3), 145–157. https://doi.org/10.1016/j.tins.2014.12.006

Burmeister, A.R., Marriott, I., 2018. The Interleukin-10 Family of Cytokines and Their Role in the CNS. Front Cell Neurosci. 12, 458. https://doi.org/10.3389/fncel.2018.00458

Butovsky, O., Ziv, Y., Schwartz, A., Landa, G., Talpalar, A.E., Pluchino, S., Martino, G., Schwartz, M., 2006. Microglia activated by IL-4 or IFN-gamma differentially induce neurogenesis and oligodendrogenesis from adult stem/progenitor cells. Mol Cell Neurosci. 31(1), 149–160. https://doi.org/10.1016/j.mcn.2005.10.006

Cacci, E., Claasen, J.H., Kokaia, Z., 2005. Microglia-derived tumor necrosis factor-alpha exaggerates death of newborn hippocampal progenitor cells in vitro. J Neurosci Res. 80(6), 789–797. https://doi.org/10.1002/jnr.20531

Cardona, A.E., Pioro, E.P., Sasse, M.E., Kostenko, V., Cardona, S.M., Dijkstra, I.M., Huang, D., Kidd, G., Dombrowski, S., Dutta, R., Lee, J.C., Cook, D.N., Jung, S., Lira, S.A., Littman, D.R., Ransohoff, R.M., 2006. Control of microglial neurotoxicity by the fractalkine receptor. Nat Neurosci. 9(7), 917–924. https://doi.org/10.1038/nn1715

Carpentier, P.A., Palmer, T.D., 2009. Immune influence on adult neural stem cell regulation and function. Neuron. 64(1), 79–92. https://doi.org/10.1016/j.neuron.2009.08.038

Chakrabarty, P., Li, A., Ceballos-Diaz, C., Eddy, J.A., Funk, C.C., Moore, B., DiNunno, N., Rosario, A.M., Cruz, P.E., Verbeeck, C., Sacino, A., Nix, S., Janus, C., Price, N.D., Das, P., Golde, T.E., 2015. IL-10 alters immunoproteostasis in APP mice, increasing plaque burden and worsening cognitive behavior. Neuron. 85(3), 519–533. https://doi.org/10.1016/j.neuron.2014.11.020

Cornejo, F., von Bernhardi, R., 2016. Age-Dependent Changes in the Activation and Regulation of Microglia. Adv Exp Med Biol. 949, 205–226. https://doi.org/10.1007/978-3-319-40764-7_10

Cox, F.F., Carney, D., Miller, A.M., Lynch, M.A., 2012. CD200 fusion protein decreases microglial activation in the hippocampus of aged rats. Brain Behav Immun. 26(5), 789–796. https://doi.org/10.1016/j.bbi.2011.10.004

Drapeau, E., Mayo, W., Aurousseau, C., Le Moal, M., Piazza, P.V., Abrous, D.N., 2003. Spatial memory performances of aged rats in the water maze predict levels of hippocampal neurogenesis. Proc Natl Acad Sci U S A. 100(24), 14385–14390. https://doi.org/10.1073/pnas.2334169100

Ekdahl, C.T., Claasen, J.H., Bonde, S., Kokaia, Z., Lindvall, O., 2003. Inflammation is detrimental for neurogenesis in adult brain. Proc Natl Acad Sci U S A. 100(23), 13632–13637. https://doi.org/10.1073/pnas.2234031100

Encinas, J.M., Michurina, T.V., Peunova, N., Park, J.H., Tordo, J., Peterson, D.A., Fishell, G., Koulakov, A., Enikolopov, G., 2011. Division-coupled astrocytic differentiation and age-related depletion of neural stem cells in the adult hippocampus. Cell stem cell. 8(5), 566–579. https://doi.org/10.1016/j.stem.2011.03.010

Eriksson, P.S., Perfilieva, E., Björk-Eriksson, T., Alborn, A.M., Nordborg, C., Peterson, D.A., Gage, F.H., 1998. Neurogenesis in the adult human hippocampus. Nat. Med. 4(11), 1313–1317. https://doi.org/10.1038/3305

Frank, M.G., Barrientos, R.M., Biedenkapp, J.C., Rudy, J.W., Watkins, L.R., Maier, S.F., 2006. mRNA up-regulation of MHC II and pivotal pro-inflammatory genes in normal brain aging. Neurobiol Aging. 27(5), 717–722. https://doi.org/10.1016/j.neurobiolaging.2005.03.013

Goldman, S.A., Kirschenbaum, B., Harrison-Restelli, C., Thaler, H.T., 1997. Neuronal precursors of the adult rat subependymal zone persist into senescence, with no decline in spatial extent or response to BDNF. J Neurobiol. 32(6), 554–566. https://doi.org/10.1002/(sici)1097-4695(19970605)32:6<554::aid-neu2>3.0.co;2-z

Goshen, I., Kreisel, T., Ben-Menachem-Zidon, O., Licht, T., Weidenfeld, J., Ben-Hur, T., Yirmiya, R., 2008. Brain interleukin-1 mediates chronic stress-induced depression in mice via adrenocortical activation and hippocampal neurogenesis suppression. Mol Psychiatry. 13(7), 717–728. https://doi.org/10.1038/sj.mp.4002055

Gosselin, D., Link, V.M., Romanoski, C.E., Fonseca, G.J., Eichenfield, D.Z., Spann, N.J., Stender, J.D., Chun, H.B., Garner, H., Geissmann, F., Glass, C.K., 2014. Environment drives selection and function of enhancers controlling tissue-specific macrophage identities. Cell. 159(6), 1327–1340. https://doi.org/10.1016/j.cell.2014.11.023

Guillot-Sestier, M.V., Doty, K.R., Gate, D., Rodriguez, J., Jr, Leung, B.P., Rezai-Zadeh, K., Town, T., 2015. Il10 deficiency rebalances innate immunity to mitigate Alzheimer-like pathology. Neuron. 85(3), 534–548. https://doi.org/10.1016/j.neuron.2014.12.068

Hirabayashi, Y., Gotoh, Y., 2005. Stage-dependent fate determination of neural precursor cells in mouse forebrain. Neurosci Res. 51(4), 331–336. https://doi.org/10.1016/j.neures.2005.01.004

Hu, X., Liou, A.K., Leak, R.K., Xu, M., An, C., Suenaga, J., Shi, Y., Gao, Y., Zheng, P., Chen, J., 2014. Neurobiology of microglial action in CNS injuries: receptor-mediated signaling mechanisms and functional roles. Prog Neurobiol. 119-120, 60–84. https://doi.org/10.1016/j.pneurobio.2014.06.002

Imayoshi, I., Sakamoto, M., Ohtsuka, T., Kageyama, R., 2009. Continuous neurogenesis in the adult brain. Dev Growth Differ. 51(3), 379–386. https://doi.org/10.1111/j.1440-169X.2009.01094.x

Jurgens, H.A., Johnson, R.W., 2012. Dysregulated neuronal-microglial cross-talk during aging, stress and inflammation. Exp Neurol. 233(1), 40–48. https://doi.org/10.1016/j.expneurol.2010.11.014

Kaplan, M.S., Hinds, J.W., 1977. Neurogenesis in the adult rat: electron microscopic analysis of light radioautographs. Science. 197(4308), 1092–1094. https://doi.org/10.1126/science.887941

Kiyota, T., Ingraham, K.L., Swan, R.J., Jacobsen, M.T., Andrews, S.J., Ikezu, T., 2012. AAV serotype 2/1-mediated gene delivery of anti-inflammatory interleukin-10 enhances neurogenesis and cognitive function in APP+PS1 mice. Gene Ther. 19(7), 724–733. https://doi.org/10.1038/gt.2011.126

Kiyota, T., Okuyama, S., Swan, R.J., Jacobsen, M.T., Gendelman, H.E., Ikezu, T., 2010. CNS expression of anti-inflammatory cytokine interleukin-4 attenuates Alzheimer's disease-like pathogenesis in APP+PS1 bigenic mice. FASEB J. 24(8), 3093–3102. https://doi.org/10.1096/fj.10-155317

Klempin, F., Kempermann, G., 2007. Adult hippocampal neurogenesis and aging. Eur Arch Psychiatry Clin Neurosci. 257(5), 271–280. https://doi.org/10.1007/s00406-007-0731-5

Kokaia, Z., Martino, G., Schwartz, M., Lindvall, O., 2012. Cross-talk between neural stem cells and immune cells: the key to better brain repair?. Nat Neurosci. 15(8), 1078–1087. https://doi.org/10.1038/nn.3163

Koo, J.W., Duman, R.S., 2008. IL-1beta is an essential mediator of the antineurogenic and anhedonic effects of stress. Proc Natl Acad Sci U S A. 105(2), 751–756. https://doi.org/10.1073/pnas.0708092105

Kuhn, H.G., Dickinson-Anson, H., Gage, F.H., 1996. Neurogenesis in the dentate gyrus of the adult rat: age-related decrease of neuronal progenitor proliferation. J Neurosci. 16(6), 2027–2033. https://doi.org/10.1523/JNEUROSCI.16-06-02027.1996

Kuipers, S.D., Schroeder, J.E., Trentani, A., 2015. Changes in hippocampal neurogenesis throughout early development. Neurobiol Aging. 36(1), 365–379. https://doi.org/10.1016/j.neurobiolaging.2014.07.033

Lavin, Y., Winter, D., Blecher-Gonen, R., David, E., Keren-Shaul, H., Merad, M., Jung, S., Amit, I., 2014. Tissue-resident macrophage enhancer landscapes are shaped by the local microenvironment. Cell. 159(6), 1312–1326. https://doi.org/10.1016/j.cell.2014.11.018

Lee, J., Duan, W., Mattson, M.P., 2002. Evidence that brain-derived neurotrophic factor is required for basal neurogenesis and mediates, in part, the enhancement of neurogenesis by dietary restriction in the hippocampus of adult mice. J Neurochem. 82(6), 1367–1375. https://doi.org/10.1046/j.1471-4159.2002.01085.x

Lichtenwalner, R.J., Forbes, M.E., Bennett, S.A., Lynch, C.D., Sonntag, W.E., Riddle, D.R., 2001. Intracerebroventricular infusion of insulin-like growth factor-I ameliorates the age-related decline in hippocampal neurogenesis. Neuroscience. 107(4), 603–613. https://doi.org/10.1016/s0306-4522(01)00378-5

Linnartz, B., Neumann, H., 2013. Microglial activatory (immunoreceptor tyrosine-based activation motif)- and inhibitory (immunoreceptor tyrosine-based inhibition motif)-signaling receptors for recognition of the neuronal glycocalyx. Glia. 61(1), 37–46. https://doi.org/10.1002/glia.22359

Lobo-Silva, D., Carriche, G.M., Castro, A.G., Roque, S., Saraiva, M., 2016. Balancing the immune response in the brain: IL-10 and its regulation. J Neuroinflammation. 13(1), 297. https://doi.org/10.1186/s12974-016-0763-8

Lucin, K.M., Wyss-Coray, T., 2009. Immune activation in brain aging and neurodegeneration: too much or too little?. Neuron. 64(1), 110–122. https://doi.org/10.1016/j.neuron.2009.08.039

Lyons, A., Downer, E.J., Crotty, S., Nolan, Y.M., Mills, K.H., Lynch, M.A., 2007. CD200 ligand receptor interaction modulates microglial activation in vivo and in vitro: a role for IL-4. J Neurosci. 27(31), 8309–8313. https://doi.org/10.1523/JNEUROSCI.1781-07.2007

Lyons, A., Lynch, A.M., Downer, E.J., Hanley, R., O'Sullivan, J.B., Smith, A., Lynch, M.A., 2009. Fractalkine-induced activation of the phosphatidylinositol-3 kinase pathway attenuates microglial activation in vivo and in vitro. J Neurochem. 110(5), 1547–1556. https://doi.org/10.1111/j.1471-4159.2009.06253.x

Manich, G., Recasens, M., Valente, T., Almolda, B., González, B., Castellano, B., 2019. Role of the CD200-CD200R Axis During Homeostasis and Neuroinflammation. Neuroscience. 405, 118–136. https://doi.org/10.1016/j.neuroscience.2018.10.030

Mattson, M.P., Magnus, T., 2006. Ageing and neuronal vulnerability. Nat Rev Neurosci. 7(4), 278–294. https://doi.org/10.1038/nrn1886

Ming, G.L., Song, H., 2005. Adult neurogenesis in the mammalian central nervous system. Annu Rev Neurosci. 28, 223–250. https://doi.org/10.1146/annurev.neuro.28.051804.101459

Mira, H., Morante, J., 2020. Neurogenesis From Embryo to Adult - Lessons From Flies and Mice. Front Cell Dev Biol. 8, 533. https://doi.org/10.3389/fcell.2020.00533

Monje, M.L., Toda, H., Palmer, T.D., 2003. Inflammatory blockade restores adult hippocampal neurogenesis. Science. 302(5651), 1760–1765. https://doi.org/10.1126/science.1088417

Nakanishi, M., Niidome, T., Matsuda, S., Akaike, A., Kihara, T., Sugimoto, H., 2007. Microglia-derived interleukin-6 and leukaemia inhibitory factor promote astrocytic differentiation of neural stem/progenitor cells. Eur J Neurosci. 25(3), 649–658. https://doi.org/10.1111/j.1460-9568.2007.05309.x

Nakanishi, H., Wu, Z., 2009. Microglia-aging: roles of microglial lysosome- and mitochondria-derived reactive oxygen species in brain aging. Behav Brain Res. 201(1), 1–7. https://doi.org/10.1016/j.bbr.2009.02.001

Ojo, J.O., Rezaie, P., Gabbott, P.L., Stewart, M.G., 2015. Impact of age-related neuroglial cell responses on hippocampal deterioration. Front Aging Neurosci. 7, 57. https://doi.org/10.3389/fnagi.2015.00057

Packer, M.A., Stasiv, Y., Benraiss, A., Chmielnicki, E., Grinberg, A., Westphal, H., Goldman, S.A., Enikolopov, G., 2003. Nitric oxide negatively regulates mammalian adult neurogenesis. Proc Natl Acad Sci U S A. 100(16), 9566–9571. https://doi.org/10.1073/pnas.1633579100

Palmer, T.D., Willhoite, A.R., Gage, F.H., 2000. Vascular niche for adult hippocampal neurogenesis. J Comp Neurol. 425(4), 479–494. https://doi.org/10.1002/1096-9861(20001002)425:4<479::aid-cne2>3.0.co;2-3

Pereira, L., Font-Nieves, M., Van den Haute, C., Baekelandt, V., Planas, A.M., Pozas, E., 2015. IL-10 regulates adult neurogenesis by modulating ERK and STAT3 activity. Front Cell Neurosci. 9, 57. https://doi.org/10.3389/fncel.2015.00057

Perez-Asensio, F.J., Perpiñá, U., Planas, A.M., Pozas, E., 2013. Interleukin-10 regulates progenitor differentiation and modulates neurogenesis in adult brain. J Cell Sci. 126(Pt 18), 4208–4219. https://doi.org/10.1242/jcs.127803

Reshef, R., Kudryavitskaya, E., Shani-Narkiss, H., Isaacson, B., Rimmerman, N., Mizrahi, A., Yirmiya, R., 2017. The role of microglia and their CX3CR1 signaling in adult neurogenesis in the olfactory bulb. Elife. 6, e30809. https://doi.org/10.7554/eLife.30809

Ryan, S.M., O'Keeffe, G.W., O'Connor, C., Keeshan, K., Nolan, Y.M., 2013. Negative regulation of TLX by IL-1β correlates with an inhibition of adult hippocampal neural precursor cell proliferation. Brain Behav Immun. 33, 7–13. https://doi.org/10.1016/j.bbi.2013.03.005

Sanchez-Molina, P., Almolda, B., Benseny-Cases, N., González, B., Perálvarez-Marín, A., Castellano, B., 2021. Specific microglial phagocytic phenotype and decrease of lipid oxidation in white matter areas during aging: implications of different microenvironments. Neurobiol Aging. https://doi.org/10.1016/j.neurobiolaging.2021.03.015

Saxe, M.D., Battaglia, F., Wang, J.W., Malleret, G., David, D.J., Monckton, J.E., Garcia, A.D., Sofroniew, M.V., Kandel, E.R., Santarelli, L., Hen, R., Drew, M.R., 2006. Ablation of hippocampal neurogenesis impairs contextual fear conditioning and synaptic plasticity in the dentate gyrus. Proc Natl Acad Sci U S A. 103(46), 17501–17506. https://doi.org/10.1073/pnas.0607207103

Saxton, R.A., Tsutsumi, N., Su, L.L., Abhiraman, G.C., Mohan, K., Henneberg, L.T., Aduri, N.G., Gati, C., Garcia, K.C., 2021. Structure-based decoupling of the pro- and anti-inflammatory functions of interleukin-10. Science. 371(6535), eabc8433. https://doi.org/10.1126/science.abc8433

Scharfman, H., Goodman, J., Macleod, A., Phani, S., Antonelli, C., Croll, S., 2005. Increased neurogenesis and the ectopic granule cells after intrahippocampal BDNF infusion in adult rats. Exp Neurol. 192(2), 348–356. https://doi.org/10.1016/j.expneurol.2004.11.016

Sheng, W.S., Hu, S., Ni, H.T., Rowen, T.N., Lokensgard, J.R., Peterson, P.K., 2005. TNF-alpha-induced chemokine production and apoptosis in human neural precursor cells. J Leukoc Biol. 78(6), 1233–1241. https://doi.org/10.1189/jlb.0405221

Sierra, A., Encinas, J.M., Deudero, J.J., Chancey, J.H., Enikolopov, G., Overstreet-Wadiche, L.S., Tsirka, S.E., Maletic-Savatic, M., 2010. Microglia shape adult hippocampal neurogenesis through apoptosis-coupled phagocytosis. Cell stem cell. 7(4), 483–495. https://doi.org/10.1016/j.stem.2010.08.014

Sierra, A., Gottfried-Blackmore, A.C., McEwen, B.S., Bulloch, K., 2007. Microglia derived from aging mice exhibit an altered inflammatory profile. Glia. 55(4), 412–424. https://doi.org/10.1002/glia.20468

Snyder, J.S., Hong, N.S., McDonald, R.J., Wojtowicz, J.M., 2005. A role for adult neurogenesis in spatial long-term memory. Neuroscience, 130(4), 843–852. https://doi.org/10.1016/j.neuroscience.2004.10.009

Stanfield, B. B., Trice, J. E., 1988. Evidence that granule cells generated in the dentate gyrus of adult rats extend axonal projections. Exp Brain Res. 72(2), 399–406. https://doi.org/10.1007/BF00250261

Taliaz, D., Stall, N., Dar, D.E., Zangen, A., 2010. Knockdown of brain-derived neurotrophic factor in specific brain sites precipitates behaviors associated with depression and reduces neurogenesis. Mol Psychiatry. 15(1), 80–92. https://doi.org/10.1038/mp.2009.67

Taupin, P., Gage, F.H., 2002. Adult neurogenesis and neural stem cells of the central nervous system in mammals. J Neurosci Res. 69(6), 745–749. https://doi.org/10.1002/jnr.10378

Udeochu, J.C., Shea, J.M., Villeda, S.A., 2016. Microglia communication: Parallels between aging and Alzheimer's disease. Clin Exp Neuroimmunol. 7(2), 114–125. https://doi.org/10.1111/cen3.12307

Vallières, L., Campbell, I.L., Gage, F.H., Sawchenko, P.E., 2002. Reduced hippocampal neurogenesis in adult transgenic mice with chronic astrocytic production of interleukin-6. J Neurosci. 22(2), 486–492. https://doi.org/10.1523/JNEUROSCI.22-02-00486.2002

van Praag, H., Shubert, T., Zhao, C., Gage, F.H., 2005. Exercise enhances learning and hippocampal neurogenesis in aged mice. J Neurosci. 25(38), 8680–8685. https://doi.org/10.1523/JNEUROSCI.1731-05.2005

Varnum, M.M., Kiyota, T., Ingraham, K.L., Ikezu, S., Ikezu, T., 2015. The anti-inflammatory glycoprotein, CD200, restores neurogenesis and enhances amyloid phagocytosis in a mouse model of Alzheimer's disease. Neurobiol Aging. 36(11), 2995–3007. https://doi.org/10.1016/j.neurobiolaging.2015.07.027

Villeda, S.A., Luo, J., Mosher, K.I., Zou, B., Britschgi, M., Bieri, G., Stan, T.M., Fainberg, N., Ding, Z., Eggel, A., Lucin, K.M., Czirr, E., Park, J.S., Couillard-Després, S., Aigner, L., Li, G., Peskind, E.R., Kaye, J.A., Quinn, J.F., Galasko, D.R., Xie, X.S., Rando, T.A., Wyss-Coray, T., 2011. The ageing systemic milieu negatively regulates neurogenesis and cognitive function. Nature. 477(7362), 90–94. https://doi.org/10.1038/nature10357

Vukovic, J., Colditz, M.J., Blackmore, D.G., Ruitenberg, M.J., Bartlett, P.F., 2012. Microglia modulate hippocampal neural precursor activity in response to exercise and aging. J Neurosci. 32(19), 6435–6443. https://doi.org/10.1523/JNEUROSCI.5925-11.2012

Wagner, J.P., Black, I.B., DiCicco-Bloom, E., 1999. Stimulation of neonatal and adult brain neurogenesis by subcutaneous injection of basic fibroblast growth factor. J Neurosci. 19(14), 6006–6016. https://doi.org/10.1523/JNEUROSCI.19-14-06006.1999

Wolf, S.A., Steiner, B., Akpinarli, A., Kammertoens, T., Nassenstein, C., Braun, A., Blankenstein, T., Kempermann, G., 2009. CD4-positive T lymphocytes provide a neuroimmunological link in the control of adult hippocampal neurogenesis. J Immunol. 182(7), 3979–3984. https://doi.org/10.4049/jimmunol.0801218

Wynne, A.M., Henry, C.J., Huang, Y., Cleland, A., Godbout, J.P., 2010. Protracted downregulation of CX3CR1 on microglia of aged mice after lipopolysaccharide challenge. Brain Behav Immun. 24(7), 1190–1201. https://doi.org/10.1016/j.bbi.2010.05.011

Zhang, H., Li, F., Yang, Y., Chen, J., Hu, X., 2015. SIRP/CD47 signaling in neurological disorders. Brain Res. 1623, 74–80. https://doi.org/10.1016/j.brainres.2015.03.012

Zigova, T., Pencea, V., Wiegand, S.J., Luskin, M.B., 1998. Intraventricular administration of BDNF increases the number of newly generated neurons in the adult olfactory bulb. Mol Cell Neurosci. 11(4), 234–245. https://doi.org/10.1006/mcne.1998.0684

Ziv, Y., Schwartz, M., 2008. Immune-based regulation of adult neurogenesis: implications for learning and memory. Brain Behav Immun. 22(2), 167–176. https://doi.org/10.1016/j.bbi.2007.08.006

# ANNEX II. SUPPLEMENTARY FIGURES
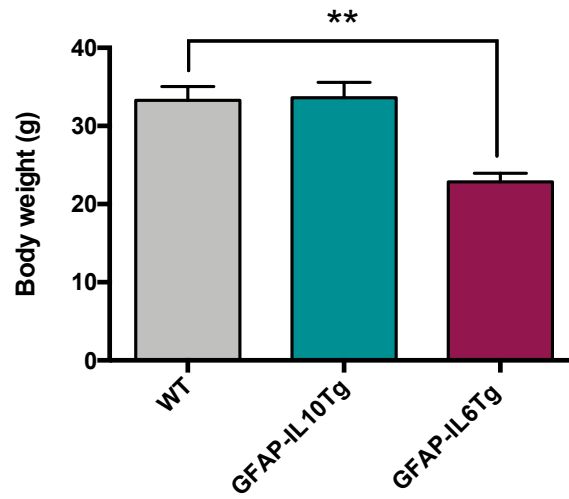
Supp. Figure 1. Body weight of aged WT, GFAP-IL10Tg and GFAP-IL6Tg mice. Data are represented as the mean $\pm$ SEM. **$p < 0.01$.
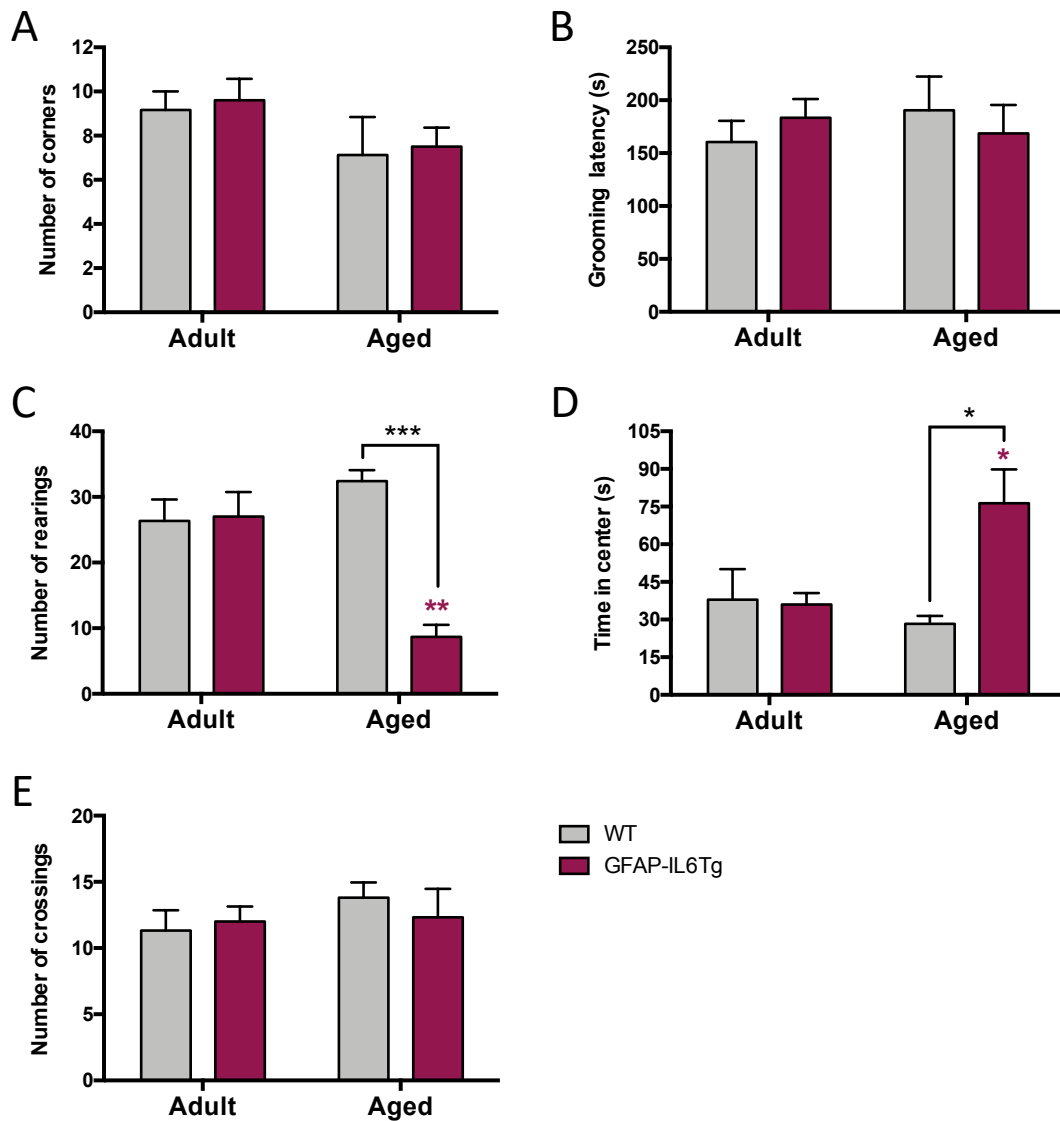
Supp. Figure 2. General locomotion and anxiety-like behavior measured in WT and GFAP-IL6Tg mice during adulthood and aging. **A)** Number of corners visited during 30 seconds in a new standard home-cage. **B)** Grooming latency (s), **C)** number of total rearings, **D)** time spent in the center of the apparatus (s) and **E)** number of crossings during 5 minutes in the open field test. Data are represented as the mean ± SEM. Magenta asterisks are referred to significant differences by age in GFAP-IL6Tg mice. *$p < 0.05$; **$p < 0.01$, ***$p < 0.001$.
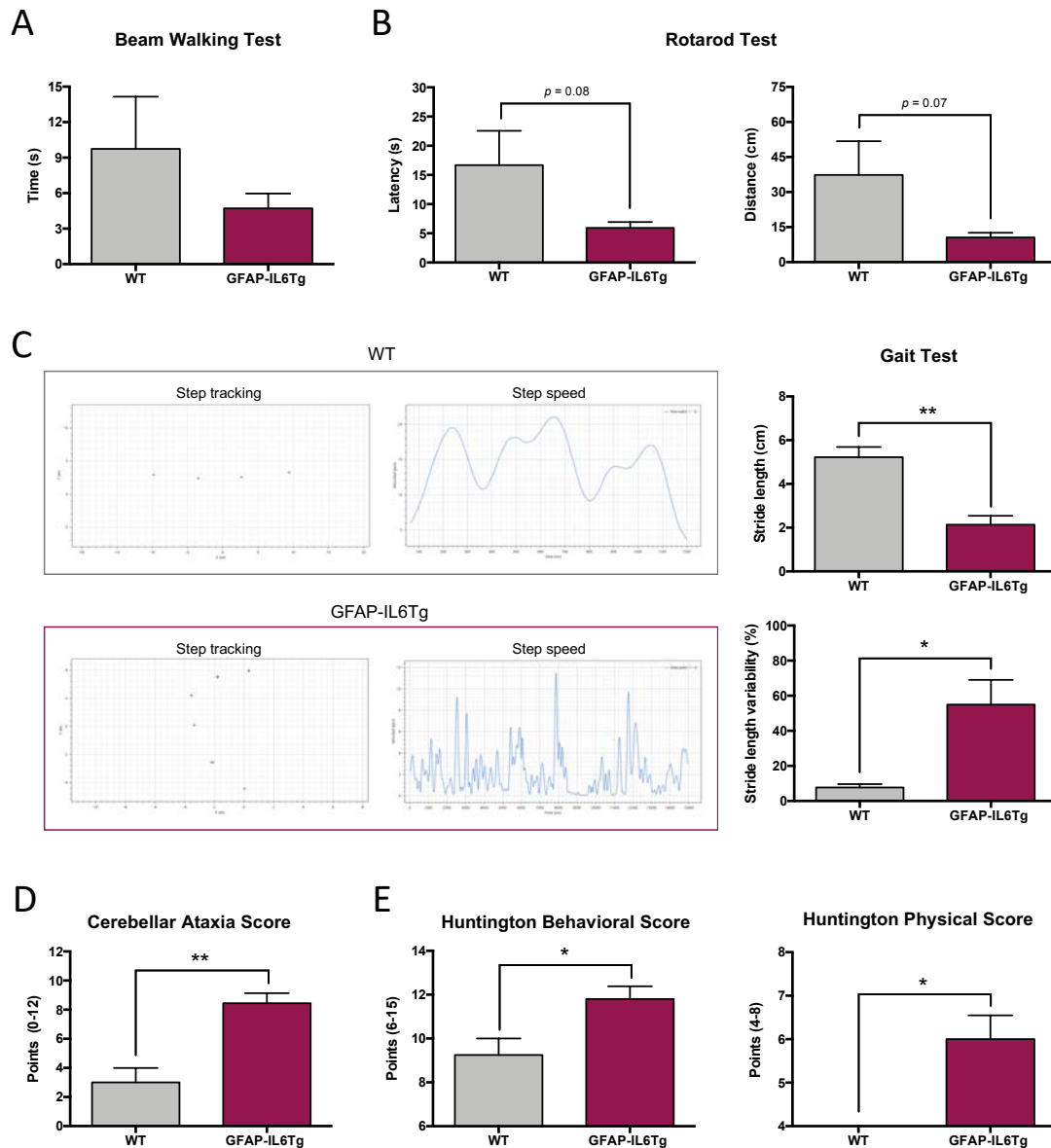
Supp. Figure 3. Locomotor study in aged WT and GFAP-IL6Tg mice. **A)** Latency (s) in the beam walking test. **B)** Graphs showing latency (s) and distance traveled (cm) in the rotarod test performed in accelerated mode (0-48 rpm). **C)** Left panel: Gait test showing footprint ("+") from one mouse hindlimb (step tracking) and the speed of the steps (step speed) in WT (upper) and GFAP-IL6Tg (lower) mice. Note the repetitive steps in GFAP-IL6Tg mice. Right panel: Quantification of stride length (cm) and its variability (%) in the gait test. **D)** Semi-quantitative scoring for cerebellar ataxia phenotype measured by ledge test, hindlimb clasping test, gait test and kyphosis. All measures were scored using 0-3 points and summed, being the total maximum scoring of 12. **E)** Left panel: Semi-quantitative neurobehavioral assessment for Huntington's disease phenotype measured by clasping (1-2 points), grooming (1-2 points), spontaneous motor activity (1-3 points), tremor (1-2), locomotor activity in the periphery (1-3) and rotarod latency (1-3). All measures were scored and summed, being the total maximum scoring of 15. Right panel: Semi-quantitative physical assessment for Huntington's disease phenotype measured by body position, palpebral closure, piloerection and tail position. All measures were scored using 1-2 points and summed, being the total maximum scoring of 8. Data are represented as the mean $\pm$ SEM. *$p < 0.05$; **$p < 0.01$.
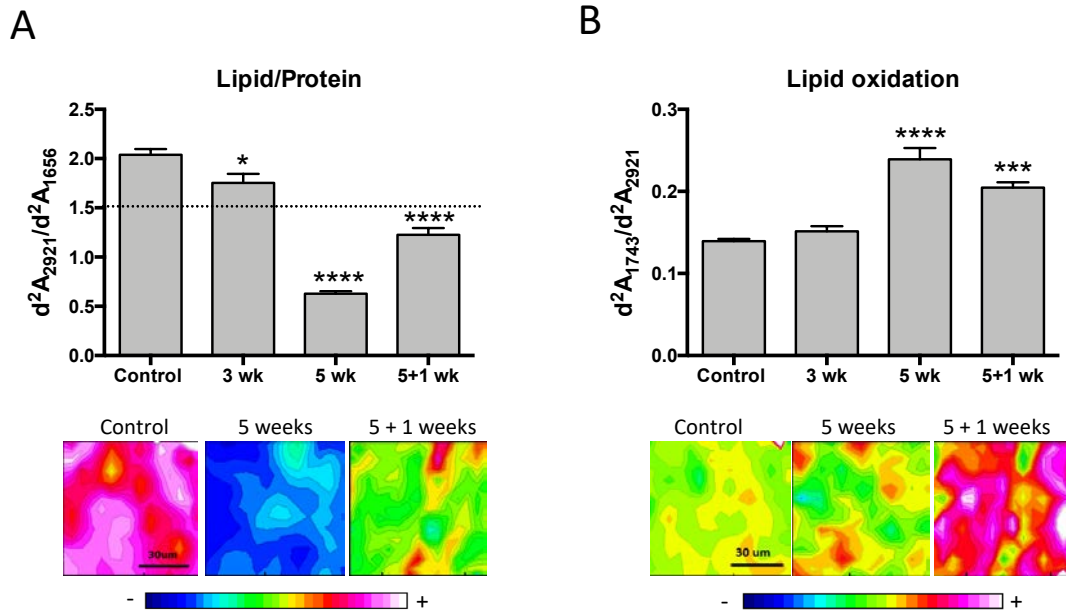
Supp. Figure 4. Synchrotron-based Fourier-transform infrared microspectroscopy (μFTIR) analysis in the corpus callosum of WT mice fed with normal chow (control) and with 0.2% (w/w) cuprizone mixed into normal chow for 3 and 5 weeks to induce demyelination, and for 5 weeks plus 1 week of control chow (5+1) to induce remyelination. **A)** Lipid and protein relative amount determined by CH_2/Amide I ratio (d^2A_{2921}/d^2A_{1656}) with their respective heatmaps. **B)** Lipid oxidation determined by $C=O/CH_2$ ratio (d^2A_{1743}/d^2A_{2921}) with their respective heatmaps. Abbreviations: wk (weeks), d^2 (second derivative). Data are represented as the mean $\pm$ SEM. *p < 0.05; ***p < 0.001; ****p < 0.0001.
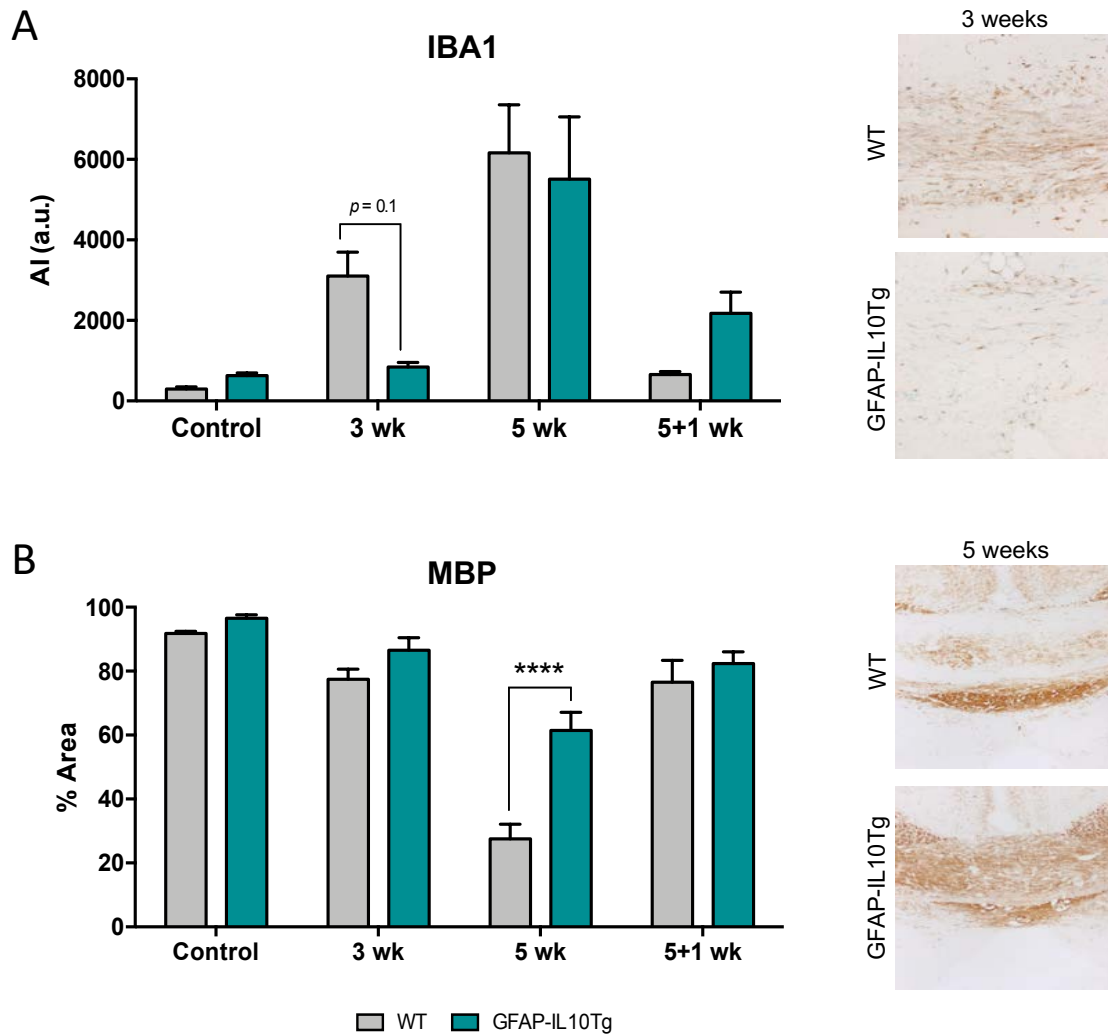
Supp. Figure 5. Microglial activation and demyelination in the corpus callosum of WT and GFAP-IL10Tg mice fed with normal chow (control) and with 0.2% (w/w) cuprizone mixed into normal chow for 3 and 5 weeks to induce demyelination, and for 5 weeks plus 1 week of control chow (5+1) to induce remyelination. **A)** Quantification of IBA1 immunohistochemistry and representative histological images after 3 weeks of treatment with cuprizone. **B)** Quantification of myelin basic protein (MBP) immunohistochemistry and representative histological images after 5 weeks of treatment with cuprizone. Abbreviations: AI (area x intensity), a.u. (arbitrary units), wk (weeks). Data are represented as the mean $\pm$ SEM. ****$p < 0.0001$.
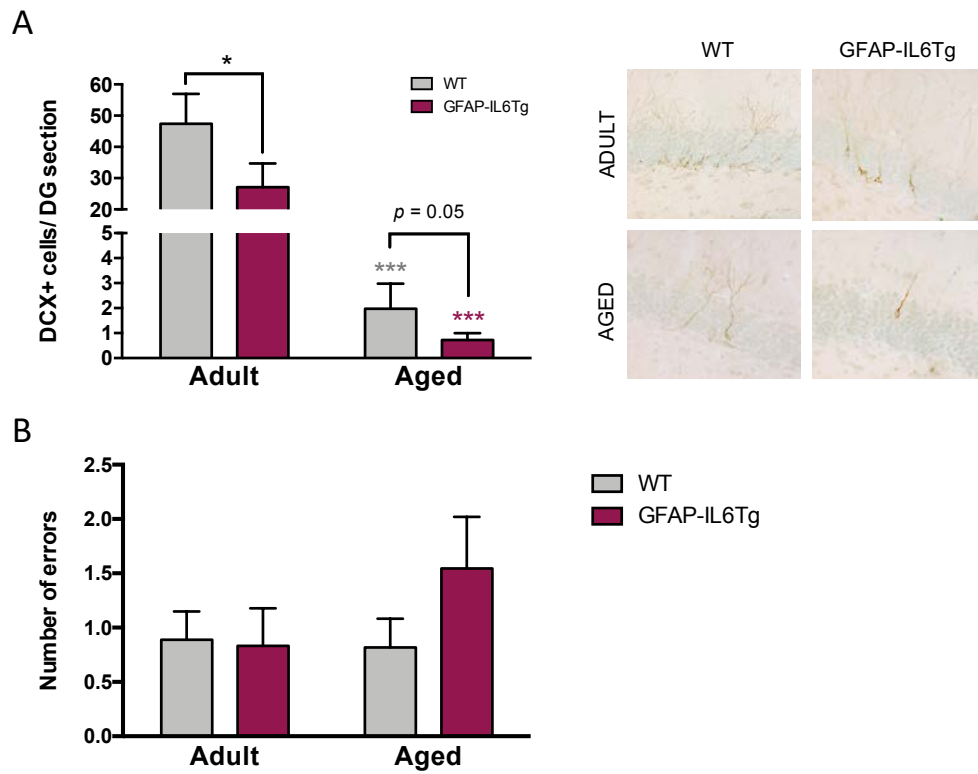
Supp. Figure 6. Hippocampal neurogenesis and spatial memory in WT and GFAP-IL6Tg mice during adulthood and aging. **A)** Quantification of the number of doublecortin (DCX) positive cells in the granular cell layer of the dentate gyrus (DG) and representative histological images. **B)** Quantification of the number of errors (exploration of an already explored arm) performed in the T-maze test as measure of working memory. Data are represented as the mean $\pm$ SEM. Grey and magenta asterisks are referred to significant differences by age in WT and GFAP-IL6Tg mice, respectively. *$p < 0.05$; ***$p < 0.001$.

ANNEX III. PARTICIPATION IN SCIENTIFIC MEETINGS

NATIONAL CONGRESSES

Sanchez-Molina, P; Almolda, B; González, B; Castellano, B.
Production of Interleukin-10 and Interleukin-6 in the Central Nervous System Modifies Glial Cell Response Associated to Physiological Aging
17 Congreso Nacional de la Sociedad Española de Neurociencia (SENC)
IX Reunión de la Red Glial Española (RGE)
Alicante (Spain), September 2017

Sanchez-Molina, P; Almolda, B; Giménez-Llort, L; González, B; Castellano, B.
Implications of Local IL-10 Overexpression in the Neuron-Microglia Communication and Hippocampal Neurogenesis during Aging
VI INc Scientific Conferences
Girona (Spain), October 2018
REV NEUROL 2018;67:311-319. doi:10.33588/rn.6708.2018358

Sanchez-Molina, P; Almolda, B; González, B; Castellano, B
Transgenic IL-6 and IL-10 Modify the Expression of Microglial Phagocytic Receptors Involved in Myelin Recognition during Aging
XI Simposi de Neurobiologia
Barcelona (Spain), November 2018

INTERNATIONAL CONGRESSES

Sanchez-Molina, P; Almolda, B; González, B; Castellano B
Astrocyte-targeted production of Interleukin-10 and Interleukin-6 alter the physiological microglial and astroglial responses associated to aging
XIII European Meeting on Glial Cells in Health and Disease
Edinburgh (UK), July 2017
GLIA 65:E103–E578 (2017). doi:10.1002/glia.23157

Sanchez-Molina, P; Almolda, B; González, B; Castellano, B
Transgenic IL-6 and IL-10 modify the expression of microglial phagocytic receptors involved in myelin recognition during aging
14th International Congress of Neuroimmunology (ISNI)
Brisbane (Australia), August 2018

Sanchez-Molina, P; Almolda, B; Giménez-Llort, L; González, B; Castellano, B
Chronic IL-10 overexpression induces alterations in microglia-neuron communication and neurogenesis during aging
XIV European Meeting on Glial Cells in Health and Disease
Porto (Portugal), July 2019
GLIA 67:E125–E766 (2019). doi:10.1002/glia.23675

Sanchez-Molina, P; Benseny-Cases, N; González, B; Castellano, B; Perálvarez-Marín, A; Almolda, B
Differential effects of age and cytokines between brain areas: When histology meets biophysics
International Society for Neurochemistry: 2019 ISN-ASN Meeting
Montreal (Canada), August 2019
J. Neurochem. (2019) 150 (Suppl. 1), 73-161. doi:10.1111/jnc.14776

Sanchez-Molina, P; Benseny-Cases, N; González, B; Castellano, B; Perálvarez-Marín, A; Almolda, B
Differential effects of age and cytokines between brain areas: When Histology Meets Biophysics

100 Years of Microglia International Symposium
Lausanne (Switzerland), December 2019

<u>Sanchez-Molina, P</u>; Benseny-Cases, N; González, B; Castellano, B; Perálvarez-Marín, A;
Almolda, B
Study of microglial phagocytic capacity in different brain areas and microenvironments during
aging
Symposium on neuro-immune interactions
Conte Center (Virtual), March 2021

Evans, F; Alí, D; Lago, N; Rego, N; Negro, L; <u>Sanchez-Molina, P</u>; Cawen, A; Pannunzio, B;
Reyes, L; Paolino, A; Bresque, M; Savio, E; Escande, C; Peluffo, H
CD300f immune receptor contributes to healthy aging by regulating inflammaging, metabolism
and cognitive decline
Keystone symposia: Neuro-immune interactions in health and disease
Keystone (Virtual), June 2021